Economics

CORSO DI DOTTORATO DI RICERCA

XXXVIII

CICLO DEL CORSO DI DOTTORATO

PhD in Economics in Roma Tre: Three essays on climate change, green investments and ecological transition

TITOLO DELLA TESI

Alessio Ferraro

Nome e Cognome del Dottorando

Firma

Francesco Giuli

Docente Guida: Prof

Firma

Silvia Nenci

Coordinatrice: Prof.

Firma

PhD in Economics

XXXVIII Cycle

PhD Thesis

PhD in Economics in Roma Tre: Three essays on climate change, green investments and ecological transition

PhD Candidate: Alessio Ferraro

Supervisor: Francesco Giuli
University Roma Tre

Co-Supervisor: Antonio Afonso
ISEG Lisbon School Economics

Introduction

The purpose of this thesis is to analyze how climate change and the transition towards low-emission technologies are reshaping the European macroeconomic landscape through the interaction of three key dimensions: physical climate shocks, fiscal policy, and demographic dynamics. The central premise is that the ecological transition is not merely an environmental challenge, but a deeply macroeconomic and macro-financial process, capable of affecting economic growth, macroeconomic stability, and distributive outcomes in a non-neutral way. In this perspective, understanding the transmission channels through which climate-related disturbances and policy responses affect economic activity, public finances, and population well-being becomes essential for the design of effective and sustainable policy interventions over the medium and long run.

To structure the analysis, the thesis adopts a unified conceptual framework in which climate-related disturbances propagate through three interconnected transmission channels. First, physical climate shocks, such as heat stress, affect labor supply, productivity, and price-setting behavior, thereby influencing output dynamics and inflationary pressures. Second, fiscal policy, and in particular the composition and effectiveness of public expenditure, shapes aggregate demand, investment, and macroeconomic stabilization during the transition. Third, demographic dynamics interact with both environmental shocks and policy responses, influencing labor market conditions, health outcomes, public finances, and long-run macro-fiscal sustainability. These three dimensions are analytically distinct, but empirically interdependent, and together define the broader macroeconomic architecture of the climate transition.

This thesis is submitted in fulfilment of the requirements of the PhD Program in Economics (XXXVIII cycle) at the Department of Economics, University of Roma Tre. It consists of three original and self-contained empirical essays. Although each essay addresses a distinct research question and relies on a different empirical methodology, they are jointly conceived as complementary contributions to a coherent research agenda on the macroeconomic implications of climate change and the low-carbon transition in Europe.

To reinforce the internal coherence of the thesis, the three essays can be mapped along three common dimensions: research questions, empirical strategies, and substantive contributions. In terms of research questions, the thesis investigates: first, how physical climate shocks affect macroeconomic outcomes through labor, productivity, and price channels; second, whether and under which conditions fiscal policy, especially green public expenditure, can support aggregate demand and macroeconomic stabilization; third, how climate policies interact with demographic dynamics and fiscal sustainability over the medium and long run. In methodological terms, the essays employ different empirical tools tailored to the nature of the question under investigation: Bayesian Local Projections and a non-linear VAR framework for the identification of physical climate shocks; a Smooth Transition Bayesian Panel VAR for the analysis of regime-dependent fiscal multipliers; and a Panel Bayesian Vector Error Correction Model for the study of long-run macro-fiscal and demographic adjustment. In terms of contribution, the three essays provide complementary evidence over different horizons, respectively addressing short-run supply-side effects, medium-run fiscal transmission, and long-run structural adjustment. Taken together, they offer an integrated perspective on the climate transition as a multidimensional macroeconomic process.

The first essay focuses on the role of physical climate shocks. It investigates the macroeconomic effects of Wet-Bulb Temperature (WBT) shocks in four Southern European economies. By combining Bayesian Local Projections with seasonal components and a non-linear VAR model with a temporal split of the sample, the analysis shows that the effects of heat stress are persistent and not confined to the summer season, but propagate beyond the hottest months, affecting labor supply and prices. The results also point to an increasing macroeconomic relevance of climate stress over time, together with substantial cross-country heterogeneity in the magnitude and persistence of responses. This essay provides the empirical foundation for the supply-side channel of the unified framework, showing how physical climate disturbances can generate macroeconomically relevant effects even in advanced European economies.

The second essay examines the role of fiscal policy in the green transition. It assesses the macroeconomic effectiveness of green public expenditure relative to non-green public spending using a Smooth Transition Bayesian Panel VAR applied to European regional blocs and to an aggregate panel of European Union countries. The results show that multipliers associated with green public expenditure are systematically larger and often exceed unity, particularly under specific public debt regimes, whereas non-green expenditure is associated with weak or negligible macroeconomic effects. These findings highlight the importance of expenditure composition for aggregate demand activation, fiscal policy credibility, and the effectiveness of macroeconomic stabilization in the context of de-carbonization. This essay contributes to the demand-side and policy transmission channel of the framework.

The third essay integrates climate policy, demographic dynamics, and macro-fiscal sustainability over the medium and long run. Using a Panel Bayesian Vector Error Correction Model (VECM), the analysis distinguishes between regressive environmental shocks, proxied by increases in carbon intensity, and mitigation shocks associated with changes in the OECD Environmental Policy Stringency (EPS) index. The results show that regressive shocks are associated with a deterioration in health indicators, contractions in economic activity, and worsening fiscal outcomes. By contrast, mitigation shocks produce relatively modest short-run effects, while their macro-fiscal benefits emerge more gradually through medium- to long-run structural adjustment processes. This essay captures the long-run adjustment channel linking climate policy, demographic change, and fiscal sustainability, thereby extending the analysis beyond short-run macroeconomic responses.

Taken together, the three essays provide a coherent analytical narrative in which physical shocks, fiscal policy, and demographic dynamics are not treated in isolation, but as mutually reinforcing components of the climate transition process. Despite their methodological heterogeneity, the contributions converge in showing that the management of the green transition requires coordinated and forward-looking policy design, attentive to regional, temporal, and institutional heterogeneity, and aware of the non-neutral role of macroeconomic choices with respect to growth, stabilization, and distributive outcomes. The thesis therefore contributes to a broader understanding of climate transition as an intrinsically macroeconomic and macro-financial phenomenon, requiring integrated analytical tools and multidimensional policy responses.

Macroeconomic Effects of Wet-Bulb Temperature Shocks.

Alessio Ferraro[1]

[1]Department of Economics, Roma Tre

Abstract

This paper analyzes the macroeconomic effects of wet-bulb temperature (WBT) shocks in Italy, Spain, Portugal, and Greece, focusing on supply-side transmission channels. Unlike standard 2-meter air temperature, WBT combines heat and humidity and provides a more accurate measure of thermal stress relevant for labor, productivity, and sectoral activity. We employ two complementary Bayesian strategies. In a Bayesian VAR estimated over two subsamples (pre-2012 and post-2012), impulse responses show that in the past decade WBT shocks generate more pronounced contractions in hours worked and industrial production. Forecast error variance decompositions further indicate that the share of macroeconomic variation explained by thermal shocks has increased, underscoring the growing relevance of humid-heat stress in these dynamics. Seasonal Bayesian Local Projections, based on seven sectoral indicators (four price sub-indices and three activity measures), reveal marked intra-annual heterogeneity: responses are strongest in summer, autumn, and also spring, with price increases and reductions in economic activity across major productive sectors. Overall, the results point to an increasingly important and strongly seasonal role of thermal stress in shaping the economic performance of Southern European countries, with significant implications for labor, production, and price dynamics.

Keywords: Climate change; Heat stress; Wet-bulb temperature; Macroeconomic effects; Temperature shocks; Local projections; Bayesian econometrics.

JEL Codes: Q54; E32; C32; C55.

Contents

1 1 Introduction

In recent decades, the frequency, intensity, and duration of extreme heatwaves have increased markedly, particularly in mid-latitude regions, with growing economic, social, and health implications (Horton et al. 2016; Russo et al. 2014). Climate projections suggest a further intensification of these events due to anthropogenic global warming (Coffel et al. 2017; Fischer and Knutti 2013). In this context, Wet-Bulb Temperature (WBT)—a metric combining temperature and humidity—has emerged as a critical indicator of heat-stress risk, being directly linked to the human body's ability to dissipate heat through perspiration (Lin and Yuan 2022; Raymond et al. 2020). Despite its relevance in climatology and human physiology (Raymond et al. 2020; Sherwood and Huber 2010), WBT remains almost entirely absent from empirical economic research, which has so far focused predominantly on dry air temperature. This omission is particularly significant given the vulnerability of Southern European economies to extreme weather events.

This study provides, to our knowledge, the first systematic empirical analysis of the macroeconomic effects of WBT in Southern Europe.We examine how WBT shocks affect labor supply, labor productivity, and consumer prices, allowing for sectoral and geographic heterogeneity as well as potential non-linear and seasonal dynamics.

We adopt two complementary econometric strategies. To guide the empirical analysis, we conceptualize the transmission of wet-bulb temperature shocks through three main channels. First, a labor supply and productivity channel: heat stress reduces effective labor input, particularly in heat-exposed sectors, leading to lower output and weaker sectoral performance. Second, a cost and price-setting channel: lower productivity and higher energy demand, especially for cooling, raise firms' marginal costs and may generate inflationary pressures under standard mark-up pricing. Third, a sectoral reallocation channel: climate stress may induce heterogeneous responses across sectors, shifting labor and production away from more exposed activities. These mechanisms provide the conceptual framework for interpreting the empirical evidence.First, we estimate a *seasonal Bayesian Local Projection* (BLP) model, which allows us to capture cyclical and seasonally differentiated responses to thermal stress. Second, we implement a *non-linear VAR* with a subsample split (2000–2012 vs. 2012–2022), designed to accommodate structural shifts in the macroeconomic effects of WBT, in line with the intensification of heat anomalies observed in the last decade (Ma et al. 2024).

The results reveal a heterogeneous yet statistically meaningful picture. In the non-linear VAR, the forecast error variance decomposition indicates that, during 2012–2022, the share of variance explained by WBT shocks increases across macroeconomic variables, signalling a stronger macroeconomic influence of heat stress in the most recent period. Moreover, impulse responses show that *both hours worked and industrial production contract in the post-2012 subsample across all four countries*, with the decline particularly pronounced in Italy. This pattern is consistent with tighter supply-side constraints induced by rising heat stress, as well as reduced aggregate demand under extreme climatic conditions as highlighted in the literature (Kim et al. 2021). These results are consistent with a transmission mechanism in which humid-heat stress compresses effective labor supply and productivity, thereby tightening supply-side constraints.

In the seasonal BLP model, sectoral prices rise in spring, summer, and autumn, with positive pass-through to differente prices: processed food, unprocessed food, energy, and services (Ciccarelli, Kuik, and Hernández 2024; Lucidi et al. 2024) . Hours worked in agriculture decline during the warm seasons, while responses in services and industry hours are less clear-cut. This pattern is consistent with the idea that heat stress affects sectors asymmetrically, with stronger labor-supply effects in more climate-exposed activities and possible reallocation toward less exposed sectors. The agricultural production index increases in winter and spring, whereas movements in other production indices are weaker and less well defined.

Robustness exercises further reinforce these findings. By restricting the sample to 2000–2019 to remove distortions introduced by the Covid-19 pandemic and the war in Ukraine, the macroeconomic responses become more stable and economically interpretable. The contraction in hours worked and the decline in production indices—both in industry and services—emerge more clearly in the trimmed sample, suggesting that recent shocks have masked part of the underlying transmission mechanism of heat-stress shocks.

A *linear* BLP specification, abstracting from seasonal heterogeneity, provides complementary evidence. While it detects partially deflationary dynamics consistent with the existing literature, it also uncovers inflationary pressures, particularly for processed food in Italy, unprocessed food in Spain and energy prices in Greece. This mixed evidence suggests that the aggregate price response depends on the balance between supply-side cost pressures and demand-side contraction, as well as on the sectoral composition of the shock. The linear model also reveals a mild reduction in hours worked following a WBT shock, aligning with broader evidence on heat-induced labour-supply constraints.

Overall, the results show that WBT shocks—an indicator that is more physiologically and climatologically informative than dry temperature—have significant macroeconomic implications for Southern Europe. The contraction in labor supply emerges as a key channel through which wet-bulb temperature shocks may generate recessionary pressures, with consequences for price dynamics, sectoral reallocation, and the broader macroeconomic adjustment process.

The remainder of the paper is structured as follows: Section 1 reviews the related literature; Section 2 describes the construction of the WBT indicator and its main features; Section 3 presents the non-linear VAR results; Section 4 discusses the seasonal and linear BLP estimates; and Section 5 concludes with policy implications and avenues for future research.

1.1 Literature Review

The existing literature on the economic impact of climate change has primarily focused on extreme weather events—such as hurricanes, floods, and droughts. Comparatively less attention has been given to the macroeconomic effects of extreme temperatures, particularly in advanced economies. Several studies have examined the relationship between temperature and economic activity, especially in emerging and low-income countries.

A seminal contribution is provided by Dell et al. 2012, who demonstrate that rising temperatures can reduce not only output levels but also long-term economic growth rates. The paper highlights the wide-ranging impacts of temperature increases, including reduced agricultural yields, lower industrial output, and even diminished political stability. More recently, Colacito et al. 2019 extend this analysis to advanced economies, showing that seasonal temperatures exert significant and systemic effects on the U.S. economy. Specifically, a 1°F increase in average summer temperature is associated with a 0.15–0.25 percentage point reduction in state-level annual GDP growth, implying that projected warming could lower U.S. economic growth by up to one-third.

Nath et al. 2024 challenge the assumption that rising temperatures permanently affect growth rates. By analyzing the dynamic effects of temperature shocks on GDP, they find that while global warming has persistent economic consequences, it does not lead to permanent divergence in growth rates—thanks in part to global technological diffusion.

Beyond aggregate GDP effects, other studies explore the transmission channels through which rising temperatures affect the economy. Schlenker and Roberts 2009 find that corn and soybean yields in the U.S.—which account for a significant share of global agriculture production—decline rapidly above certain temperature thresholds (29°C for corn, 30°C for soybeans), with yield losses projected to reach 36–40 percent under moderate warming and 63–82 percent under accelerated scenarios.

These agricultural effects have broader implications. De Winne and Peersman 2018 show that falling yields can lead to global food price inflation, disproportionately affecting food security and consumption patterns. Peersman 2022 further argue that advanced economies are not immune; the effects of climate change on agriculture are more severe than previously thought, even in high-income countries where food comprises a smaller share of household spending.

On the production side, Acevedo et al. 2020 find that higher temperatures depress investment, labor productivity, and output, particularly in warmer, low-income countries. A 1°C increase in annual temperature leads to a 2 percent decline in output and a 10 percent drop in investment over seven years in these economies. Economic development appears to offer some protection, with wealthier countries experiencing less damage.

The labor supply channel is also crucial. Dasgupta et al. 2021 document a non-linear, concave relationship between temperature and job offers. Their panel analysis shows that labor supply peaks at 16.2°C for low-exposure occupations and 14.7°C for high-exposure ones, declining sharply beyond these thresholds.

Kim et al. 2021 employ a Smooth Transition VAR (ST-VAR) to analyze macroeconomic responses to extreme weather shocks—such as temperature spikes, heavy rainfall, and drought—using time as a transition variable. They observe that after 1991, temperature extremes have increasingly negative effects on industrial production, inflation, and unemployment.

The body of research on climate change and inflation remains in its early stages, yet it is steadily expanding. Faccia et al. 2021 use local projections for a panel of 48 countries to show that hot summers cause short-term food price inflation, particularly in emerging markets. However, long-run effects tend to be weaker or even negative. Similarly, Mukherjee and Ouattara 2021 find persistent inflationary effects in both developing and developed countries, suggesting that central banks should consider climate variables in their forecasting models and policy frameworks.

A growing body of research explores the seasonal and sectoral dimensions of temperature effects. Ciccarelli and Marotta 2024 use a Bayesian VARX with seasonal meteorological data and consumer price indices for the euro area, finding that temperature shocks drive up food, energy, and service prices in summer—especially in hotter countries. Lucidi et al. 2024 focus on energy consumption, showing that warming increases cooling demand (raising electricity prices) but reduces heating needs (lowering gas demand).

Recent studies have begun to examine demand-side responses to temperature shocks. Natoli 2022 analyze how expectations of rising temperatures affect U.S. macroeconomic aggregates. They find that positive temperature expectation shocks reduce GDP and prices, primarily due to demand contraction. Sectoral decomposition reveals that food prices rise, while energy prices align with overall CPI trends.

A different perspective is offered by Mumtaz and Alessandri 2021, who explore the macroeconomic consequences of temperature volatility rather than level. Using a time-varying panel VAR for 133 countries, they find that a one-degree increase in temperature uncertainty reduces GDP growth by 0.3 percentage points and increases GDP volatility by 0.7 points. Importantly, these effects are observed across both rich and poor countries, suggesting that climate uncertainty has a broad economic cost—even before climate conditions materially change. In this paper, we contribute to the growing climate–economy literature by introducing a novel dimension: the role of wet-bulb temperature (WBT) in shaping labor supply and productivity outcomes. Unlike dry temperature metrics, WBT integrates heat and humidity, offering a more accurate proxy for human-experienced thermal stress. We focus on WBT's effects on the real economy—particularly labor input and productivity—across four Southern European countries (Italy, Spain, Portugal, and Greece), regions that are highly exposed to climate change.

By emphasizing the physical limits imposed by heat stress on human labor, our work highlights a key transmission channel of climate risk—one that is especially relevant for outdoor and low-skill labor-intensive sectors. We show that heatwaves can significantly reduce hours worked and individual productivity, especially under high exposure conditions. Our findings aim to complement the existing literature by offering new evidence on how WBT-driven thermal stress affects core components of economic activity. Taken together, the literature suggests that climate shocks may propagate through a combination of labor-supply effects, productivity losses, energy-demand pressures, and sectorally heterogeneous price adjustments. In this paper, these insights motivate an empirical framework that focuses on the supply-side transmission of wet-bulb temperature shocks and on the role of seasonal and sectoral heterogeneity in shaping macroeconomic responses.

1.2 What is the WBT and how to estimate it

The Wet Bulb Globe Temperature (WBGT) is an internationally recognized composite heat index, widely used across health, industrial, athletic, and climate science domains to assess thermal stress under extreme heat conditions. Among the indices developed to quantify heat-related health risks, the Wet Bulb Temperature (WBT) stands out as a particularly effective and accessible measure (Rogers et al. 2021; Wang, Leung, et al. 2019).

Theoretical studies have established a physiological tolerance threshold of approximately 35°C for WBT, beyond which sustained human exposure can lead to potentially fatal heat stress, even in well-adapted individuals (Buzan and Huber 2020; Sherwood and Huber 2010). Empirical evidence suggests that this critical threshold has already been reached, albeit briefly, in some subtropical coastal regions, and is likely to be exceeded more frequently under future warming scenarios (Raymond et al. 2020). Moreover, the observed upward trend in both WBT values and the frequency of extreme heat events is expected to continue across global regions, driven by anthropogenic climate change (Bekris et al. 2023; Buzan and Huber 2020; Coffel et al. 2017; Li et al. 2017; Raymond et al. 2020; Wang, Yang, et al. 2021).

This makes the study of WBT not only essential for improving climate forecasting and impact assessment, but also critical for informing policy responses to enhance adaptation and resilience, particularly in vulnerable regions. Nevertheless, the empirical use of WBT in large-scale analyses is limited by data availability, especially with regard to its components—namely, the globe temperature and natural wet bulb temperature—which are not systematically monitored across observational networks (Budd 2008; d'Ambrosio Alfano et al. 2014).

WBT is formally defined as a weighted average of three environmental parameters, as follows (Minard 1961):

WBT $= 0.7T_w + 0.2T_g + 0.1T_a$

T_W: natural wet bulb temperature, T_G: globe thermometer temperature, T_a: dry bulb (air) temperature measured at 2 meters

Due to the scarcity of direct observations of T_w and T_g , empirical applications typically rely on model-based approximations. Two widely used methods include:The ACSM approximation proposed by the American College of Sports Medicine (1987),

The Liljegren model, a physics-based heat transfer approach (Liljegren et al. 2008).

The ACSM approximation expresses WBT as a function of air temperature and water vapor pressure:

$$\text{WBT}_{\text{ACSM87}} = 0.567T_a + 0.393e + 3.94 \tag{1}$$

Where T_a denote the 2 meter air temperature and e is the saturation water vapor pressure (in kPa). This formulation follows the approximation proposed by the American College of Sports Medicine (1987).Using this formula, we compute daily wet bulb temperature anomalies (WBTA) at the grid level. The construction proceeds as follows:

We collect gridded daily data on T_a and at 2-meter height, interpolated onto a 25x25 km grid for each country.These grids are matched to administrative provinces. For temporal aggregation and alignment with macroeconomic variables, we compute monthly averages of WBT, obtaining $WBT_{p,t}(m)$,where p indexes provinces and m months. We define the WBT anomaly as the deviation from the $1981 - 2010$ historical monthly climatology for each province:

$$WBTA_{p,t(m)} = WBT_{p,t(m)} - \overline{WBT}_{p,m} \tag{2}$$

Where $WBT_{p,t}(m)$ is the wet-bulb temperature observed in province p at time t in month m, while $\overline{WBT}_{p,m}$ denotes the climatological mean monthly (1981-2010), commonly used in the climate literature, wet-bulb temperature for the same province and month.

To obtain the country-level measure, we compute a population-weighted average across provinces:

$$WBTA_y = \sum_{p=1}^{N} \bar{P}_{p,y} \cdot WBTA_{p,y} \tag{3}$$

This variable, constructed at the monthly frequency, serves as the principal climate shock input in our econometric analysis, enabling us to isolate the macroeconomic effects of heat stress as proxied by WBT anomalies.

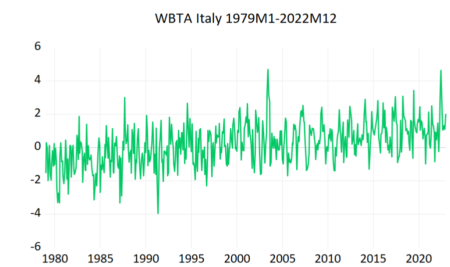

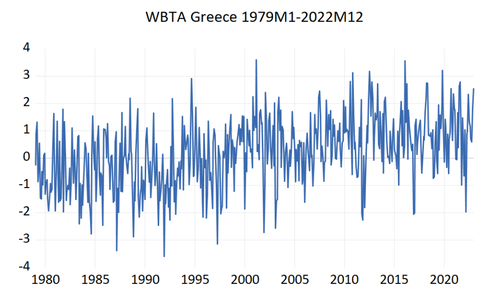

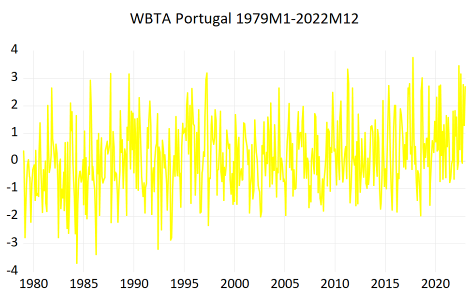

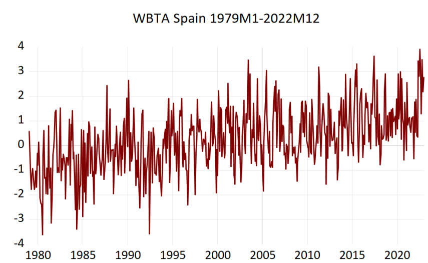

A positive deviation indicates a higher temperature than the historical average temperature for that month. The figures indicate a clear upward trend in WBTA events across all countries, highlighting episodes that generated severe socioeconomic consequences and unprecedented temperature–humidity anomalies. The year 2003 stands out as an extreme benchmark, with record heat contributing to an estimated 70,000 excess deaths and substantial agricultural losses in Southern Europe, resulting in approximately USD 9.5 billion dollars in economic damages (EEA, 2010). The trend of anomalies does not have an entirely similar excursus among the four countries.Portugal and Spain record positive anomalies in the winter and fall months, as does Greece to some extent. The latter reaches a summer heat peak in 2010 that corresponds to the heat wave that hit Russia. As for Italy the positive anomaly of wet bulb temperature corresponds with the summer months. Both Italy and Spain in recent years show a significant decrease in negative anomalies, while for Portugal and Greece negative anomalies always become episodic. As we shall see the anomaly of wet bulb temperatures has a heterogeneous impact on the economy in different countries and through different channels.

2 Non-linear Model Estimation by Subsample and Data Description

3 Methodological Overview and Identification Strategy

This section outlines the empirical strategy used to estimate the macroeconomic effects of wet-bulb temperature anomalies (WBTA) within a structural VAR (SVAR) framework. It summarizes the identification assumptions and estimation steps that guide the analysis.

Identification. WBTA shocks are identified using a recursive (Cholesky) ordering, which assumes that climate variables are predetermined within the period and do not respond contemporaneously to macroeconomic conditions. WBTA is therefore treated as an exogenous supply-side shock, consistent with the slow-moving nature of climate dynamics.

Variables are ordered as follows: (1) expected wet-bulb temperature $E(WBT)$, (2) WBTA, (3) industrial production, (4) hours worked, (5) CPI, and (6) energy CPI. This structure allows expected conditions to be controlled for while isolating unexpected thermal shocks.

Estimation. The empirical analysis proceeds in four steps: (i) specification of the VAR model; (ii) estimation of the reduced-form VAR with p lags; (iii) identification of structural shocks via Cholesky decomposition; and (iv) computation of impulse response functions.

WBTA is defined relative to a five-year moving average (Lucidi et al. 2024) to capture unexpected deviations from recent climate conditions and account for adaptive expectations.

3.1 SVAR split into two subsamples

We estimate the impact of the wet-bulb temperature anomaly (WBTA) using a structural VAR model. The reference specification is:

$$Y_t = \alpha\tau_t + \sum_{j=1}^{p} \beta_j Y_{t-j} + u_t, \tag{4}$$

where Y_t is an $N \times 1$ vector of endogenous variables, β_j is an $N \times N$ matrix of coefficients on lags Y_{t-i}, and τ_t is a matrix $K \times 1$ of exogenous variables with associated coefficients α (Mumtaz and Theodoridis 2020).

The covariance matrix of the reduced-form residuals is:

$$\Sigma = (Aq)(Aq)', \tag{5}$$

where A is the lower-triangular Cholesky factor of Σ, and q is an N-dimensional orthogonal matrix satisfying $q'q = I_N$. Structural shocks are defined as:

$$\varepsilon_t = A_0' u_t, \qquad \varepsilon_t \sim \mathcal{N}(0, I_N), \tag{6}$$

with $A_0 = Aq$. The choice $q = I_N$ corresponds to the standard recursive identification scheme. Following Auerbach and Gorodnichenko (2012) and Mumtaz and Theodoridis (2020), we adopt a recursive ordering to identify the WBTA shock.

The VAR includes six variables ordered as follows: (1) expected wet-bulb temperature $E(WBT)$; (2) WBTA; (3) industrial production index; (4) hours worked; (5) CPI; (6) energy CPI.

WBTA is treated as an exogenous shock, assuming no contemporaneous feedback from economic conditions. From an economic perspective, an unexpected increase in WBTA is interpreted as a supply-side climate shock that primarily affects the level of production and labor productivity, before translating into adjustments in labor input and production costs, and ultimately transmitting to output and prices. This exclusion restriction aligns with recent contributions in climate–macro modelling (Ciccarelli, Kuik, and Hernández 2024; Faccia et al. 2021; Lucidi et al. 2024), reflecting the slow-moving nature of anthropogenic climate dynamics relative to monthly economic fluctuations.

Expectations and adaptive behaviour. Agents may anticipate thermal conditions and adjust their behaviour accordingly. Short- and medium-term weather forecasts are widely used in agriculture (Lemos et al. 2012; Lucidi et al. 2024), in energy production and consumption planning (Agüera-Pérez et al. 2018), and across several European sectors exposed to rising climate variability (Marengo et al. 2018). To capture adaptive behaviour, we employ an adaptive definition of WBTA, following Lucidi et al. (2024):

$$WBTA'_{r,t}(m) = \frac{1}{w} \sum_{j=0}^{w-1} WBT_{r,t}(y - j, m), \tag{7}$$

with $w = 5$ years. This definition captures unexpected deviations relative to a narrow, recent-history reference window.

Under this definition and ordering, the WBTA shock represents an unexpected heat shock, while $E(WBT)$ controls for expected thermal conditions, consistent with the use of expectation variables as controls in Mumtaz and Theodoridis (2020) and Ramey (2011).

Motivation for the 2012 structural break. We estimate impulse responses separately for the pre- and post-2012 periods. This choice follows the climate-science literature, which documents a marked intensification of wet-bulb temperature levels after 2012 (Ma et al. 2024). Across the periods 1958–1989, 1990–2021, and 2012–2021, summer WBT increasingly shifts toward the upper tail, with pronounced warming in Southern and Central Europe and milder increases in high-latitude regions such as Fennoscandia (Ma et al. 2024). Figures 3 and 4 document these distributional shifts.

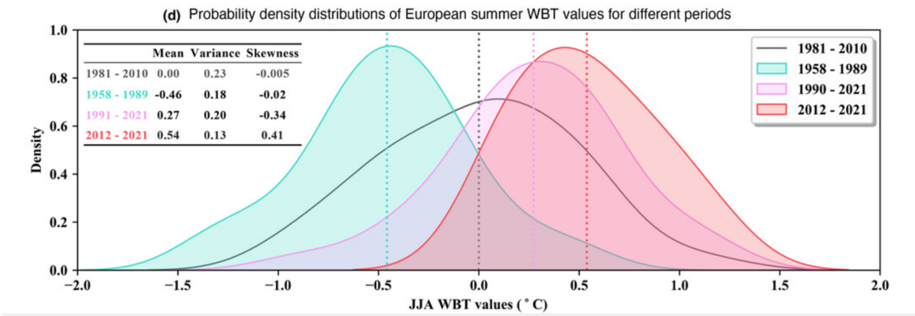

Figure 3: Distribution of WBT PDFs across three periods: 1958–1989, 1990–2021, 2012–2022.

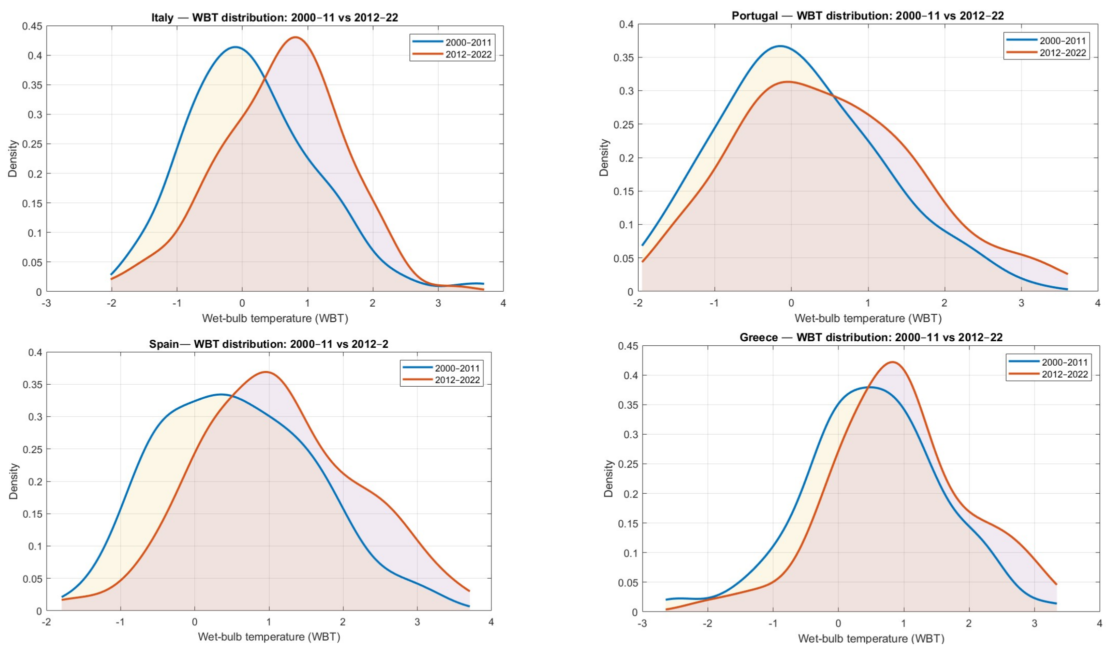

Figure 4: Kernel density of WBT for Italy, Portugal, Spain, and Greece, 2000–2011 vs. 2012–2022.

Comparing the PDFs for 1958–1989 and 1990–2021, the mean WBT increases by approximately 0.73°C, shifting the density toward warmer values and inducing more negative skewness (Kodra and Ganguly 2014; Ma et al. 2024). Country-level PDFs confirm the general warming trend and also reveal heterogeneous increases in skewness and kurtosis, indicating rising exposure to asymmetric heat extremes.

3.2 VAR with structural break.

To allow for time variation, we estimate the model separately for the two subsamples using:

$$Y_t = \alpha_s \tau_t + \sum_{j=1}^{p} \beta_{s,j} Y_{t-j} + u_t, \tag{8}$$

with corresponding covariance and structural shocks:

$$\Sigma_s = (A_s q)(A_s q)', \tag{9}$$

$$\varepsilon_{t,s} = A'_{0,s} u_t, \qquad \varepsilon_{t,s} \sim \mathcal{N}(0, I_N), \tag{10}$$

where A_s is the Cholesky factor for each subsample and $A_{0,s} = A_s q$.

Bayesian estimation. We estimate the SVAR using a conjugate Normal–Inverse Wishart and Minnesota prior (Bańbura et al. 2010). The prior includes: (i) an overall tightness parameter λ; (ii) a sum-of-coefficients prior τ encouraging persistence; (iii) an intercept prior ϵ.

Dummy observations implement these priors, ensuring stability and avoiding over-fitting. The covariance matrix follows an Inverse Wishart prior. Gibbs sampling (500,000 iterations, 350,000 burn-in) approximates the posterior. All macroeconomic variables are in logs except CPI and CPI-Energy, expressed in rates of change, for the lags see Appendix B.The choice of a parsimonious lag structure (L = 2) follows the evidence in Carriero et al. 2015, who show that for monthly macroeconomic indicators such as industrial production and hours worked, Bayesian VARs benefit little from long lag specifications. Their results indicate that while very high lag orders (e.g. p = 12) can improve forecasting for a few variables, optimal lag selection based on marginal likelihood overwhelmingly favours p = 1–2 and yields more robust performance across variables. Consistent with this evidence, we adopt a reduced lag length to balance model flexibility and estimation stability in our monthly setup (see Appendix for AIC and BIC test).

3.3 Macroeconomic Data

For our analysis, we use high-frequency macroeconomic series from various official sources. The Industrial Production Index (IPI), the headline Consumer Price Index (CPI), and the energy sub-component (CPI energy) are obtained from the Federal Reserve Bank of St. Louis' FRED database, which compiles and harmonizes data from national and international statistical agencies. Total hours worked are taken from the International Labour Organization (ILO), whose coverage is limited to annual or quarterly frequencies for many countries. To make this variable comparable with the other series, we interpolate it to a monthly frequency using the Denton method, which preserves the long-term trend while minimizing distortions in short-term dynamics. All high-frequency series are seasonally adjusted, where necessary, according to the official procedures provided by the original sources.

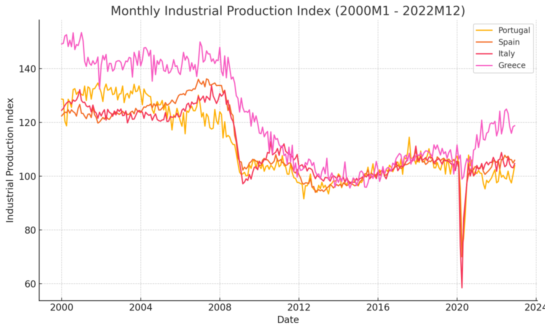

(a) Industrial Production Index

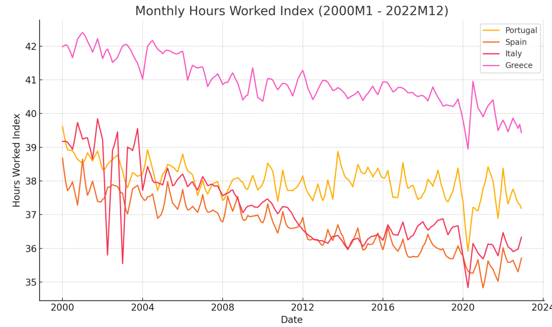

(b) Hours Worked

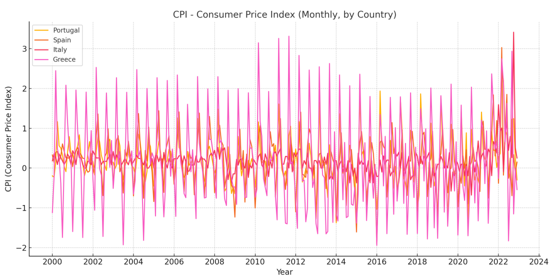

(c) Headline CPI

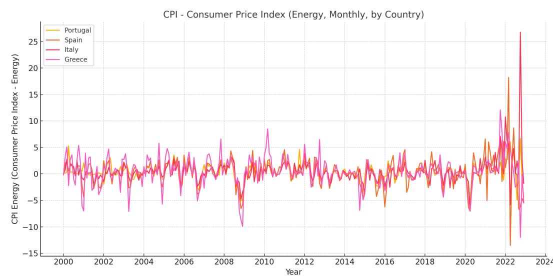

(d) CPI Energy

Figure 5: Time series for the four variables.

Our approach is closely related to Kim et al. 2021, who estimate a structural threshold VAR (STVAR) to model the dynamic effects of climate shocks on the U.S. economy across different time periods. While their analysis focuses on a single national economy and employs a composite climate risk indicator (AIC) as the shock variable, we instead estimate separate standard VAR models for four Southern European economies—Spain, Italy, Greece, and Portugal—and split the sample into subsamples to capture potential changes in shock propagation over time. Moreover, we use wet-bulb temperature (WBT) as our shock measure, which directly captures the combined effects of heat and humidity on human and economic activity.

The use of WBT allows us to capture climate shocks that may have more pronounced microeconomic effects, particularly in warmer regions. For example, within the countries we study, a WBT shock is likely to have larger and more immediate impacts in hotter areas (e.g., southern Spain, southern Italy, Greek islands, southern Portugal) compared to more temperate regions, due to both physiological stress and sectoral vulnerabilities (e.g., agriculture, tourism, construction). By focusing on macroeconomic variables, our VAR framework is designed to capture both the aggregate economic consequences and the broader spillover effects of such shocks, while recognizing that their local intensity and transmission mechanisms may vary substantially across regions within each country.

3.4 Results and Comments

In the full sample in Portugal (figure 6), industrial production (Ip) registers a mild immediate contraction following a WBT shock, with no marked persistence. In the pre-2012 period, IP shows no immediate reaction and turns moderately positive at medium horizons, indicating an attenuated and partly compensatory adjustment. After 2012, this pattern reverses: the response becomes clearly negative and persistent, signalling heightened vulnerability of real activity to thermo-hygrometric shocks.

Hours worked exhibit a slight contraction in the full sample. In the pre-2012 period the decline is more pronounced, while in the post-2012 period it remains negative but is comparatively smaller.A plausible interpretation is that the stronger contraction in hours worked during the pre-2012 period reflects lower adaptive capacity in a labor market more exposed to heat-sensitive sectors and weaker institutional and technological adjustments. In the post-2012 period, the negative response persists but is comparatively smaller, suggesting improved adaptation margins and a partial shift of the adjustment mechanism from labor input to output losses. CPI-energy appears largely insignificant in the full sample and before 2012, whereas in the post-2012 period it declines more visibly, consistent with a dis-inflationary adjustment.

The behaviour of the CPI is particularly notable: in the post-2012 period its decline is not only stronger but also highly persistent, with dis-inflationary effects extending throughout the entire horizon of the response. This stands in contrast to the pre-2012 period, where the CPI shows a mildly positive and only marginally significant response at longer horizons.In the post-2012 period, the sharper and more persistent decline in the CPI can also be interpreted through the dynamics of the energy market. Rising temperatures reduce the demand for heating energy, while the progressive improvement in energy efficiency and the growing share of solar and wind power contribute to lowering overall supply costs (Sareen and Nordholm 2021) . This context limits upward pressure on prices and supports a more prolonged dis-inflationary adjustment. Consequently, the impact of wet-bulb temperature shocks manifests primarily through a slowdown in prices rather than through immediate adjustments in output or hours worked.

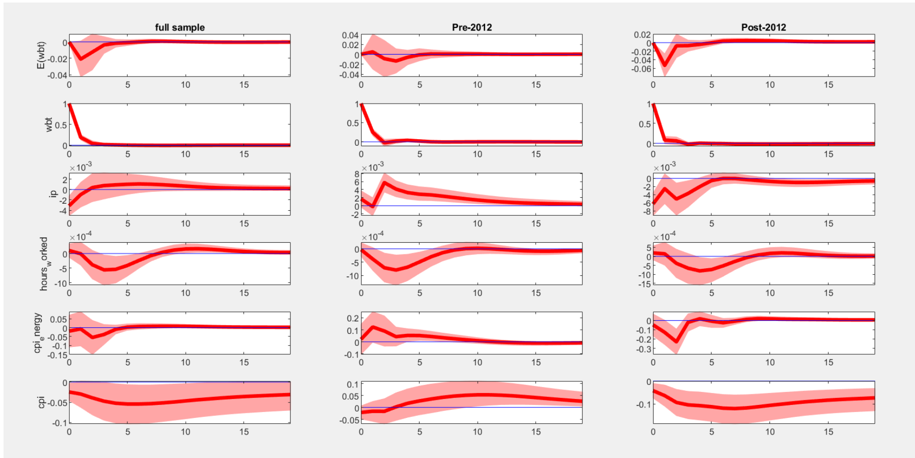

Figure 6: Impulse response functions for Portugal: pre-2012 vs post-2012

Table 1: Forecast Error Variance Decomposition (FEVD) for Portugal, pre-2012

Variable	**h=1**	**h=4**	**h=8**	**h=12**	**h=20**
E(wbt)	0.00	1.49	1.69	1.73	1.76
wbt	97.36	81.04	78.26	77.43	76.71
ip	1.22	7.20	8.63	8.96	8.99
hours_worked	0.88	3.51	4.80	4.71	4.81
cpi_energy	0.92	3.25	3.62	3.67	3.74
cpi	1.13	1.68	2.61	3.61	4.56

Table 2: Forecast Error Variance Decomposition (FEVD) for Portugal Post 2012

Variable	**h=1**	**h=4**	**h=8**	**h=12**	**h=20**
E(wbt)	0.00	4.44	4.56	4.67	4.74
wbt	95.18	81.13	78.90	77.71	76.51
ip	4.61	5.89	6.12	6.18	6.41
hours_worked	0.99	2.41	4.08	4.23	4.42
cpi_energy	0.90	4.59	4.76	4.82	4.89
cpi	2.10	6.17	8.66	9.89	10.59

Before 2012 (Table 1 and 2), WBT shocks account for a modest share of the variability of real and price indicators in Portugal, with industrial production and hours worked explaining around 9 percent and 5 percent of the long-run variance, respectively. Price variables contribute even less, reflecting a relatively mild and diffuse transmission of climatic stress. After 2012, the decomposition changes substantially: the contribution of WBT shocks to CPI-energy nearly doubles, and the share explained in headline CPI increases sharply to more than 10 percent at long horizons. These results confirm a marked rise in the climate sensitivity of the Portuguese economy after 2012, particularly through the price channel

For Spain (figure 7), the full-sample impulse responses reveal very limited macroeconomic sensitivity to WBT shocks. Industrial production and hours worked display no statistically significant adjustments at any horizon, while CPI-energy is the only variable exhibiting a brief but clearly identifiable decline immediately after the shock. The response of headline CPI is small and not persistent.

Before 2012, the responses remain muted for all variables except industrial production, which shows a positive and persistent reaction across horizons. This pattern suggests that, in the earlier part of the sample, WBT shocks were not associated with meaningful real or nominal adjustments, with the sole exception of a modest but sustained increase in industrial activity. Hours worked and both price measures remain statistically indistinguishable from zero throughout.

After 2012, real variables continue to display no significant responses, indicating that WBT shocks do not exert robust effects on industrial production or labor input. By contrast, the price block becomes more reactive: both CPI-energy and headline CPI register a statistically significant decline lasting roughly three to four months. This pattern is consistent with a mild dis-inflationary effect of WBT shocks in the post-2012 period.

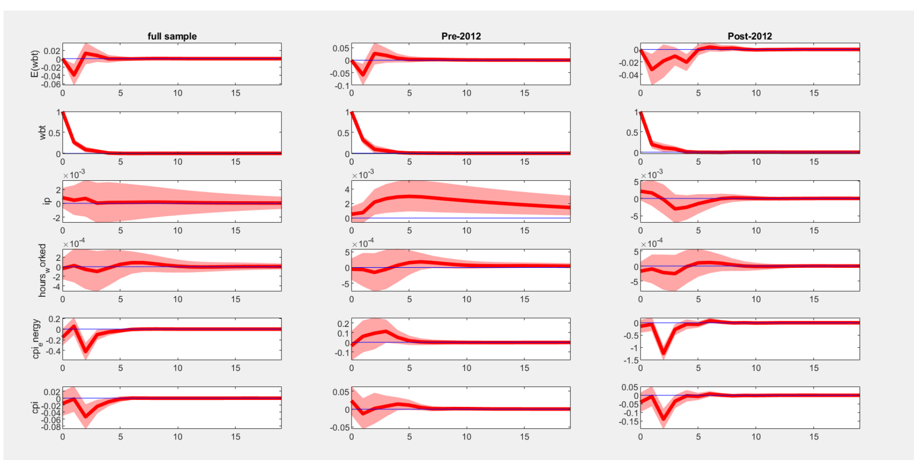

Figure 7: Impulse response functions for Spain: pre-2012 vs post-2012

For Spain (table 3 and 4), the pre-2012 FEVDs indicate that WBT shocks account for only a limited share of the variability in real and price variables. At longer horizons, industrial production explains roughly 7 percent of the forecast error variance attributable to the shock, while hours worked, CPI-energy, and headline CPI remain below 4 percent. Most of the variance continues to be driven directly by the climatic indicators themselves (E(wbt) and wbt), suggesting a relatively weak macroeconomic transmission of thermo-hygrometric shocks in the early part of the sample.

Table 3: Forecast Error Variance Decomposition (FEVD) for Spain, pre-2012

Variable	$h = 1$	$h = 4$	$h = 8$	$h = 12$	$h = 20$
E(wbt)	0.00	3.05	3.22	3.26	3.29
wbt	99.07	89.79	88.35	87.96	87.56
ip	0.94	3.72	6.10	6.89	7.41
hours worked	0.74	1.98	2.79	2.93	3.03
cpi energy	0.77	2.84	3.09	3.12	3.15
cpi	0.95	2.33	2.62	2.64	2.67

Table 4: Forecast Error Variance Decomposition (FEVD) for Spain, post-2012

Variable	$h = 1$	$h = 4$	$h = 8$	$h = 12$	$h = 20$
E(wbt)	0.00	3.32	4.00	4.03	4.04
wbt	97.05	86.81	84.36	84.06	83.99
ip	1.27	2.69	3.73	3.79	3.80
hours worked	1.05	2.23	3.20	3.31	3.33
cpi energy	1.03	15.08	14.97	14.96	14.95
cpi	1.22	6.80	6.97	6.98	6.98

In the post-2012 period, the contribution of WBT shocks to real activity remains modest: both industrial production and hours worked display slightly lower shares of variance explained, consistent with the absence of statistically significant responses in the IRFs. The most notable change concerns price dynamics. The variance share explained by WBT shocks increases sharply for CPI-energy, rising from about 3 percent to nearly 15 percent at short and medium horizons, while headline CPI increases from roughly 2.5 percent to almost 7 percent. This pattern reflects a pronounced rise in the sensitivity of energy prices and overall inflation to WBT shocks, which in the post-2012 period generate clearly disinflationary adjustments, as documented in the IRFs.

Overall, the FEVD evidence for Spain points to an essentially unchanged transmission of WBT shocks to real variables, but a substantial increase in the sensitivity of the price block after 2012, with effects that consistently take a disinflationary direction.

For Greece (figure 8), the full-sample responses to WBT shocks are generally weak. Real variables do not display statistically significant adjustments, and the only clear reaction concerns CPI-energy, which shows a short-lived contraction on impact followed by an immediate return toward zero.

In the pre-2012 period, some clearer dynamics emerge. Industrial production exhibits a positive and statistically significant response in the first two horizons before reverting to zero; hours worked show a moderate contraction, with significance concentrated in the middle horizons; price variables do not display any meaningful reaction to the shock.

In the post-2012 period, the stronger transmission of WBT shocks to industrial production and hours worked can be interpreted as evidence of a shift in adjustment mechanisms.A brief contraction in the industrial production index emerges on impact, while the other variables remain essentially unchanged.

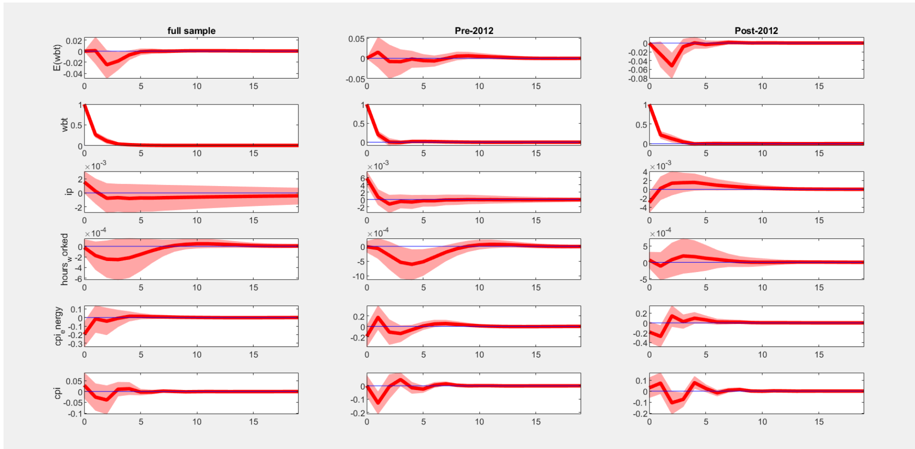

Figure 8: Impulse response functions for Greece: pre-2012 vs post-2012

Table 5: Forecast Error Variance Decomposition (FEVD), Greece pre-2012

Variable	$h = 1$	$h = 4$	$h = 8$	$h = 12$	$h = 20$
E(wbt)	0.00	1.83	2.13	2.24	2.28
wbt	97.28	89.02	85.91	85.20	84.73
ip	7.16	6.13	5.45	5.24	5.13
hours worked	0.74	2.65	4.78	4.83	4.85
cpi energy	1.35	3.56	3.77	3.85	3.86
cpi	0.70	3.74	3.98	3.99	4.00

Table 6: Forecast Error Variance Decomposition (FEVD), Greece post-2012

Variable	$h = 1$	$h = 4$	$h = 8$	$h = 12$	$h = 20$
E(wbt)	0.00	4.02	4.15	4.16	4.17
wbt	95.80	84.27	78.68	78.06	77.88
ip	2.09	3.17	3.83	3.93	3.96
hours worked	0.85	1.85	2.70	2.77	2.78
cpi energy	1.40	3.93	4.30	4.33	4.33
cpi	0.88	3.39	3.95	3.98	3.98

For Greece (table 5 and 6), the pre-2012 FEVDs show that WBT shocks explain a modest but non-negligible share of the variance of real and price variables. At longer horizons, industrial production accounts for about 5 percent of the forecast error variance attributable to the shock, while hours worked rise to almost 5 percent. CPI-energy and headline CPI remain in the range of 3.5–4 percent. As in the other countries, most of the variance is absorbed by the climatic indicators themselves (E(wbt) and wbt), indicating a limited overall transmission of WBT shocks in the earlier period.

In the post-2012 period, the variance shares attributed to WBT shocks decrease for all real variables. Industrial production falls from roughly 5 percent to around 4 percent at long horizons, and hours worked drop from nearly 5 percent to below 3 percent. These patterns are consistent with the IRFs, which show weaker and mostly insignificant real responses after 2012. Price variables display only minor changes: CPI-energy increases slightly from about 3.8 percent to 4.3 percent, while headline CPI remains broadly stable at around 4 percent across horizons.

Overall, the FEVD evidence suggests that the transmission of WBT shocks to Greek macroeconomic variables was modest already before 2012 and became even weaker afterwards, particularly on the real side. The price block shows only a marginal increase in sensitivity, corroborating the view that Greece exhibits comparatively muted macroeconomic reactions to heat-humidity shocks in both periods.

For Italy, the full-sample impulse responses indicate a clear and persistent contraction in industrial production following a WBT shock. Hours worked exhibit a similarly persistent decline, while CPI-energy and headline CPI display a short-lived but statistically significant reduction immediately after the shock.

In the pre-2012 subsample, the response of industrial production becomes statistically insignificant and hours worked contract less intensely, suggesting a milder real adjustment to WBT shocks. The price block behaves similarly to the full sample: both CPI-energy and headline CPI show a brief and significant decline at short horizons, followed by a rapid return toward zero.

In the post-2012 period, the transmission of WBT shocks strengthens considerably on the real side. Industrial production displays a negative and persistent reaction over several months, and hours worked follow a similar pattern, with persistence matching or even exceeding that observed in the full sample. By contrast, the price variables do not exhibit statistically significant responses, indicating that the disinflationary effects identified in the earlier period do not reappear in the more recent subsample.In the Italian context—identified in the literature as a European climatic hot spot (Lazoglou et al. 2024), with temperature increases exceeding the regional average—heat-related disruptions tend to materialize more forcefully on real activity. Higher sectoral exposure to physically intensive tasks, limited short-run productivity adaptation, and the reallocation of labor away from heat-sensitive activities amplify the impact on real inputs.

Regarding price variables, the available evidence does not allow for definitive conclusions. Factors such as higher energy efficiency and the rising share of renewables in the electricity mix may have contributed to attenuating the transmission to price indices, although this interpretation remains indicative rather than causal. Consequently, the adjustment appears to occur predominantly through quantities—output and labour input—while price effects seem more contained and less clearly identified.

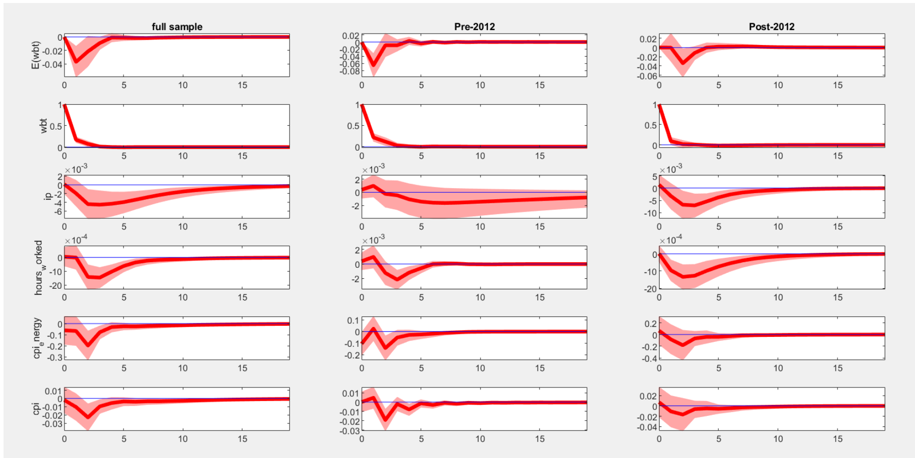

Figure 9: Impulse response functions for Italy: pre-2012 vs post-2012

Table 7: Forecast Error Variance Decomposition (FEVD), Italy — Pre-2012

Variable	**h=1**	**h=4**	**h=8**	**h=12**	**h=20**
E(wbt)	0.00	4.58	4.70	4.71	4.71
wbt	97.64	86.63	85.65	85.38	85.08
ip	0.75	1.81	2.91	3.47	3.83
hours_worked	0.81	4.15	4.94	4.95	4.96
cpi_energy	1.60	4.46	4.80	4.81	4.82
cpi	0.63	3.78	4.26	4.29	4.31

Table 8: Forecast Error Variance Decomposition (FEVD), Italy — Post-2012

Variable	**h=1**	**h=4**	**h=8**	**h=12**	**h=20**
E(wbt)	0.00	2.37	2.52	2.55	2.56
wbt	98.58	86.23	84.13	83.80	83.66
ip	0.92	3.99	5.52	5.72	5.78
hours_worked	0.93	6.78	8.44	8.65	8.71
cpi_energy	0.85	2.93	3.20	3.24	3.26
cpi	0.87	2.85	3.15	3.23	3.26

For Italy, the pre-2012 FEVDs indicate a moderate transmission of WBT shocks to real and price variables. At longer horizons, industrial production accounts for around 3–4 percent of the variance attributable to the shock, while hours worked reach nearly 5 percent. CPI-energy and headline CPI display variance shares of roughly 4.8 and 4.3 percent, respectively. Most of the variance continues to be explained by the climatic components themselves (E(wbt) and wbt), reflecting a relatively contained influence of WBT shocks during the earlier period.

In the post-2012 subsample, the contribution of WBT shocks to real variables increases noticeably. The variance share explained in industrial production rises to almost 6 percent, and hours worked exhibit an even stronger increase, reaching 8–9 percent across horizons. These patterns align with the IRFs, which show more persistent and pronounced contractions in real activity after 2012. By contrast, the variance explained in CPI-energy and headline CPI decreases relative to the pre-2012 period, with long-horizon shares remaining close to 3 percent. This reduction mirrors the lack of significant price responses in the IRFs for the post-2012 period.

Overall, the FEVD evidence for Italy points to a shift in the transmission of WBT shocks: real variables become substantially more sensitive after 2012, while price variables exhibit a smaller and more muted contribution. This contrasts with the pre-2012 period, where both real activity and prices absorbed a comparable share of the shock, and highlights a post-2012 strengthening of the real-side channel relative to the price channel. A cross-country comparison of the level-based IRFs reveals marked asymmetries in the response to WBT shocks across Southern Europe. Italy stands out as the only country displaying a pronounced contraction in both industrial production and hours worked in the post-2012 period. This pattern is consistent with the pre-/post-2012 PDFs, which identify Italy as a clear climatic hot spot, exposed to more intense thermo-hygrometric stress.

Portugal shows a more visible decline in industrial production in the post-2012 sample, alongside a notable contraction in consumer prices, particularly energy components. Spain exhibits a similar price adjustment: both energy prices and the overall CPI fall significantly after the shock in the post-2012 period . In contrast, Greece offers only weak and largely insignificant responses, with no consistent adjustment across real or price variables.

Overall, the evidence points to substantial heterogeneity in how Southern European economies react to heat-humidity stress, with Italy experiencing the strongest real-side deterioration, Portugal and Spain showing more prominent price-level adjustments, and Greece displaying limited and statistically weak responses.

3.5 Subsample Analysis of Growth Effects: Pre-2012 vs Post-2012

To further investigate whether the macroeconomic effects of WBT shocks differ when focusing on growth rates rather than levels, we re-estimate the VAR models for each country using the logarithmic differences of real activity variables Ip industrial production and hours worked instead of their natural logarithms. This transformation allows us to capture the short- and medium-term responses of economic growth to climate-related thermal stress, rather than changes in the levels of output and labor input. The approach follows that adopted by Kim et al. 2021 and in particular, by Nath et al. 2024 , who use a log-difference specification to assess how temperature shocks affect economic growth and whether their impact is short-lived or displays persistence over several horizons, with potential implications for the long-run level of economic activity.

The analysis is carried out separately for the pre-2012 and post-2012 subsample, as in the baseline specification, to assess whether the transmission of WBT shocks to growth has undergone structural changes over time. This exercise provides a complementary perspective to the level-based estimates: if growth responses to WBT shocks are short-lived and revert quickly to zero, this is consistent with only temporary deviations from trend and limited long-run effects on the level of activity; by contrast, more persistent growth responses would be indicative of more sizeable and lasting effects on output and labour input levels.

Figure 10 for Portugal shows that, in log-difference terms, industrial production exhibits no significant response to WBT shocks in either the pre-2012 or the post-2012 period. Hours worked display a mild contraction on impact only in the pre-2012 subsample, while in the post-2012 period the responses are essentially not significant.

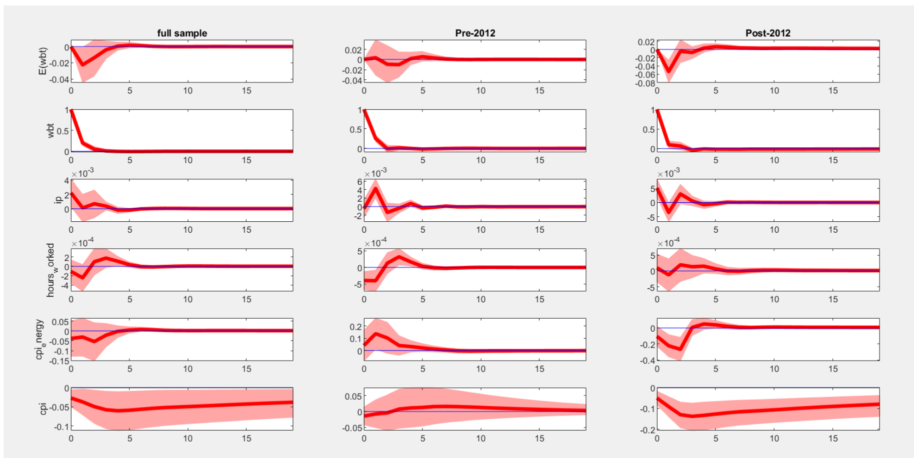

Figure 10: Impulse response functions for Portugal: pre-2012 vs post-2012

For Greece (figure 11), the log-level VAR results point to a very limited macroeconomic response to WBT shocks. The only discernible adjustment occurs in the post-2012 period, where hours worked register a mild contraction on impact. Beyond this immediate effect, the impulse responses display little statistical significance, with both industrial production and price variables remaining essentially unresponsive. This pattern suggests that, in the Greek case, heat-humidity shocks do not translate into systematic or persistent macroeconomic adjustments, in contrast with the stronger and more heterogeneous responses observed in the other Southern European economies.

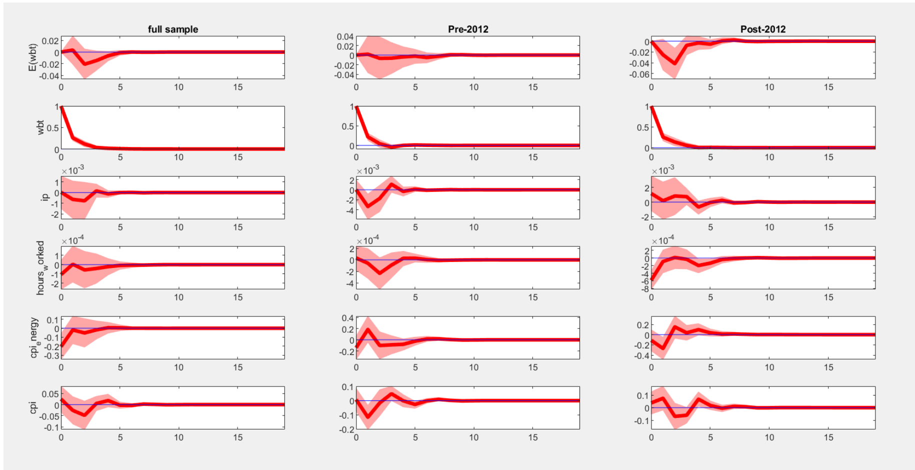

Figure 11: Impulse response functions for Greece: pre-2012 vs post-2012

For Italy (figure 12), the log-level VAR reveals a clear and relatively robust pattern. Hours worked contract in the full sample as well as in both the pre-2012 and post-2012 subsamples, with the decline being noticeably stronger and more persistent in the post-2012 period. Industrial production also shows a significant and prolonged reduction after the shock, again with a more marked adjustment in the post-2012 years. Although these responses are less pronounced and somewhat less persistent than those found in the level-based specification, they nonetheless indicate that Italy exhibits a comparatively stronger macroeconomic sensitivity to WBT shocks relative to the other Southern European economies.

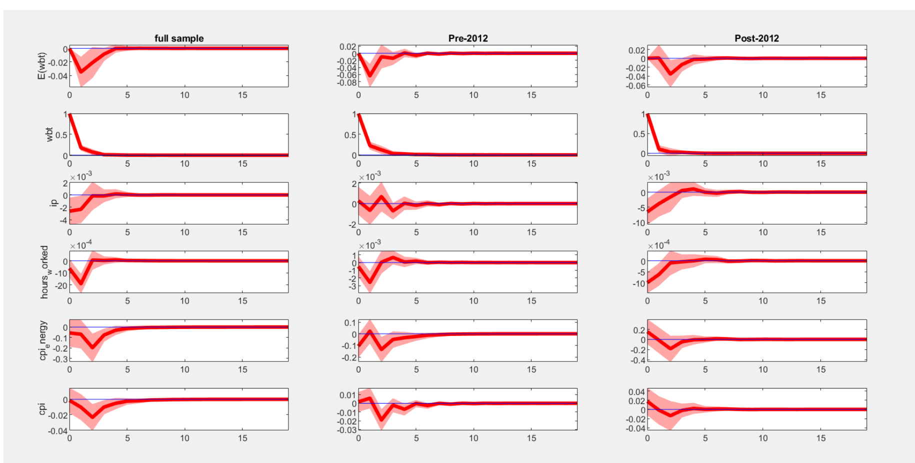

Figure 12: Impulse response functions for Italy: pre-2012 vs post-2012

Spain (figure 13) shows a pattern broadly similar to that of Greece. The macroeconomic variables display only weak or short-lived responses to WBT shocks, with significance—when present—limited to a single horizon. Overall, the evidence points to a very modest transmission of heat-humidity shocks to real activity and prices, with no meaningful persistence.

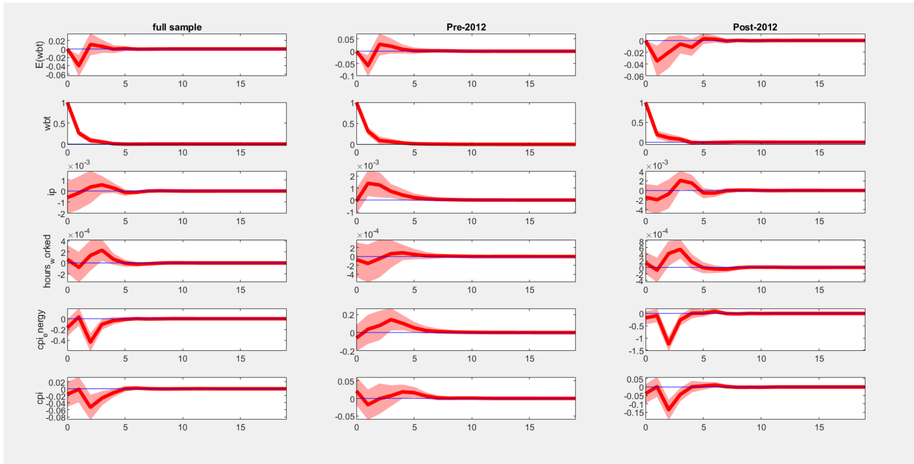

Figure 13: Impulse response functions for Spain: pre-2012 vs post-2012

Log-level specifications capture changes in the levels of real variables, producing more persistent responses to WBT shocks and reflecting the gradual adjustment of the economy. By contrast, log-difference specifications measure changes in growth rates, generating more immediate and transitory responses, as the effects of the shocks are quickly reabsorbed. As a result, thermal shocks may appear more macroeconomically relevant and persistent in level specifications, whereas in growth rate specifications they tend to manifest as temporary fluctuations with no lasting impact on output or labour input.A useful way to interpret our evidence is in light of the distinction emphasized by Nath et al. 2024 between level effects and growth effects of climatic shocks. In their framework, temperature shocks may generate persistent reductions in the level of economic activity, while their impact on growth rates tends to be short-lived and eventually fades. Our results align closely with this mechanism.

In the log-level specifications, WBT shocks produce clearer and more persistent adjustments in real variables, particularly in Italy, indicating that heat-humidity stress can shift the long-run level of output and labour input. By contrast, in log-difference specifications the responses of activity growth are weak, short-lived, or statistically insignificant in most countries. This pattern suggests either that growth effects dissipate rapidly—as proposed in Nath et al. 2024 interpretation—or that WBT shocks capture level adjustments more effectively than changes in growth dynamics.

Overall, the evidence indicates that WBT shocks exert macroeconomic effects primarily through level adjustments rather than through sustained changes in GDP or labour input growth.

3.6 Seasonality of WBT Shocks

3.6.1 Methodological Overview: Bayesian Local Projections

This section estimates the dynamic effects of wet-bulb temperature anomalies (WBTA) using a Bayesian Local Projection (BLP) framework.

Identification. The WBTA shock is defined as an unexpected deviation of wet-bulb temperature from its historical norm and is treated as an exogenous climate shock. The identification relies on the assumption that short-run economic conditions do not affect temperature realizations.

To account for seasonality, the contemporaneous WBTA shock is interacted with seasonal dummies (Winter, Spring, Summer, Autumn), allowing its impact to differ across periods of the year. Lagged values of WBTA are included to capture persistence in temperature dynamics and to separate temporary fluctuations from prolonged heat stress.

Lagged dependent variables and other macroeconomic controls are included to isolate the effect of the WBTA shock from endogenous dynamics.

Estimation. For each horizon h, the local projection is estimated through a separate regression. Each specification includes: (i) the contemporaneous WBTA shock interacted with seasonal dummies, (ii) lags of WBTA, (iii) lags of the dependent variable, and (iv) lags of other macroeconomic controls.

A Bayesian approach is used to stabilize estimation. Coefficients are estimated using a Gaussian ridge prior, while the error variance follows an Inverse-Gamma prior. Posterior distributions are obtained via MCMC methods.

Impulse responses are computed from the posterior distribution of the coefficients associated with the contemporaneous WBTA shock. Point estimates correspond to posterior medians, and uncertainty is summarized by 68% credible intervals.

3.7 Local Projection Bayesian

We estimate the dynamic effects of wet-bulb temperature anomalies using a Bayesian Local Projection (BLP) framework in the spirit of Jordà 2005, following recent methodological contributions such as L. N. Ferreira et al. 2025. For each country i and each macroeconomic variable $y_{i,t}$, the horizon-specific regression is specified as:

$$\Delta y_{i,t+h} = \alpha_h + \sum_{s\in\{W,Sp,Su,A\}} \beta_{h,s}\, S_{i,t} D_t^{(s)} + \sum_{\ell=1}^{q_S} \gamma_{h,\ell}\, S_{i,t-\ell} + \sum_{\ell=1}^{p} \phi_{h,\ell}\, \Delta y_{i,t-\ell} + \sum_{k\neq y} \sum_{\ell=1}^{p} \theta_{h,k,\ell}\, \Delta x_{i,k,t-\ell} + u_{i,t+h}. \tag{11}$$

The wet-bulb temperature anomaly $S_{i,t}$ is constructed consistently with the definition adopted in the VAR model. Monthly WBT is expressed as the deviation from its 1981–2010 climatological mean. The anomaly is expressed at the country level so that the shock as a one–standard-deviation relative to the national climatic distribution. Seasonal dummies $D_t^{(s)}$ for Winter, Spring, Summer, and Autumn allow the contemporaneous effect of the shock to vary across the four thermo-hygrometric regimes that characterize Southern European climate patterns. The term $\sum_{\ell=1}^{q_S} \gamma_{h,\ell} S_{i,t-\ell}$ includes q_S lags of the climate shock, accounting for the high serial correlation of WBT anomalies and ensuring that seasonal interactions do not mechanically absorb delayed thermal effects. Including these lags helps distinguish short-lived anomalies from persistent heat-stress conditions and avoids identification based solely on autocorrelated temperature dynamics. $\Delta x_{i,k,t-\ell}$ denotes the set of control variables included in the local projection specification.

The parameter p denotes the number of autoregressive lags in the projection equation. Based on AIC and BIC criteria obtained from auxiliary autoregressive models, we set $p = 6$. The specification also includes p lags of all other macroeconomic variables (prices, production indices, hours worked, and sectoral indicators), which enter as controls to isolate the dynamic effect of the climate shock and avoid attributing endogenous co-movements to WBT anomalies.

A further motivation for adopting Local Projections relates to the intrinsic characteristics of WBT shocks. A linear VAR implicitly assumes that shocks affect the economy uniformly across the year, while heat–humidity stress is strongly seasonal and reaches its maximum intensity in specific months. The LP framework allows us to capture these intra-annual differences explicitly, identifying the horizons and seasons in which WBT exerts its strongest macroeconomic influence. Moreover, LPs offer greater flexibility than VAR models when the underlying data-generating process is only partially understood—a relevant consideration given the still limited macroeconometrics literature on WBT and heat-stress dynamics. By imposing fewer parametric restrictions, Local Projections reduce the risk of misspecification and provide a transparent representation of how climatic anomalies propagate over time.

3.7.1 Bayesian implementation of the Local Projections

In the Local Projection framework, each horizon h is estimated by means of a separate linear regression. For each country, macroeconomic variable, and season, the specification in equation (11) can therefore be written as:

$$y_{t+h} = X_t \beta_h + \varepsilon_{t,h}, \qquad \varepsilon_{t,h} \sim \mathcal{N}(0, \sigma_h^2 I_T), \tag{12}$$

where y_{t+h} is the $T \times 1$ vector of future realizations of the dependent variable, X_t is the $T \times K$ matrix of regressor (including the contemporaneous seasonal WBT shock, its lags, lags of the dependent variable, and lags of all remaining macroeconomic controls), and β_h is the $K \times 1$ vector of coefficients associated with horizon h.

Prior on coefficients. Since each regression is estimated in a finite sample and includes highly persistent regressor, we impose a Gaussian ridge prior on the coefficients:

$$\beta_h \sim \mathcal{N}(0, \lambda^{-1} I_K), \tag{13}$$

where $\lambda > 0$ is a shrinkage hyperparameter. This prior shrinks the coefficients mildly towards zero and stabilizes inference without imposing any restriction across horizons, fully preserving the logic of the Local Projection framework. In practice, the ridge prior is implemented by augmenting the design matrix with pseudo-observations:

$$X_h^* = \begin{bmatrix} X_t \\ \sqrt{\lambda} I_K \end{bmatrix}, \qquad y_h^* = \begin{bmatrix} y_{t+h} \\ 0_K \end{bmatrix},$$

so that the posterior mode of β_h corresponds to a ridge-penalized estimator. Following the Bayesian VAR literature, we set λ proportional to $1/T$, ensuring mild shrinkage that decreases with sample size (Miranda-Agrippino and Ricco 2021; Tanaka 2020).

Prior on the error variance. The variance of the regression errors is assigned a weakly informative Inverse-Gamma prior,

$$\sigma_h^2 \sim IG(a_0, b_0), \tag{14}$$

with (a_0, b_0) set to small values ($a_0 = b_0 = 0.01$), a standard choice that produces a proper but diffuse prior equivalent to the Jeffreys prior in the limit.

Posterior inference. Posterior inference for (β_h, σ_h^2) is conducted using Markov Chain Monte Carlo (MCMC) methods. For each variable, country, and horizon we generate $M = 4000$ posterior draws and discard the first 1000 as burn-in. Convergence diagnostics (trace plots and stability of posterior moments) are monitored to ensure stationarity of the chains.

Impulse responses. The impulse responses are obtained from the posterior distribution of the coefficients on the contemporaneous seasonal WBT shock. For each horizon h and season $s \in \{\text{Winter}, \text{Spring}, \text{Summer}, \text{Autumn}\}$ we collect the posterior draws of the corresponding element $\beta_{h,s}$. The median of these draws is used as the point estimate of the impulse response, while uncertainty is summarized by the 16th and 84th posterior percentiles, yielding approximate 68% Bayesian credible intervals around the median response.

This Bayesian implementation provides a flexible and robust way to estimate Local Projections in the presence of seasonal climatic shocks, stabilizing the coefficients while avoiding parametric restrictions across horizons.

3.7.2 Data

In our BLP exercise we use a consistent set of macroeconomic and sectoral variables for the four Southern European countries most exposed to heat-stress episodes: **Portugal, Greece, Italy, and Spain**. The monthly dataset includes:

- harmonized consumer price indices (HICP) for processed food ($PROC_FOOD$), unprocessed food ($UNPROC_FOOD$), non-energy industrial goods ($GOODS$), energy ($ENERGY$), and services ($SERVICES$);
- hours worked in agriculture ($HOURS_A$), manufacturing ($HOURS_M$), and services ($HOURS_S$);
- industrial production indices for manufacturing (IP_M), agriculture (IP_A), and utilities (IP_U);

- a monthly indicator of labor productivity ($LABOR_PRODU$).

All series are harmonized and transformed into year-on-year growth rates or logarithmic differences, depending on the nature of the variable (see Appendix A). These transformed variables enter as Δy_{t+h} in the Local Projection regressions, which we estimate separately for each country.

The model specification is kept identical across countries.

The climate shock is constructed as a monthly wet-bulb temperature anomaly relative to the 1981–2010 climatology and globally standardized. Seasonal heterogeneity enters only through the contemporaneous interaction between the shock and the four seasonal dummies (Winter, Spring, Summer, Autumn), while lagged shocks serve exclusively as persistence controls.

3.8 Transmission Mechanisms and Theoretical Framework

To guide the interpretation of the empirical results, this section outlines the main transmission mechanisms through which wet-bulb temperature (WBT) shocks affect the economy.

Heat stress can be interpreted as a physiological constraint that reduces effective labor supply and productivity. In a standard production framework, this can be captured by a temperature-dependent productivity term, such that output is given by

$$Y = A(T) \cdot F(K, L),$$

with $A'(T) < 0$. As temperature increases beyond critical thresholds, labor efficiency declines, leading to lower output and higher unit labor costs.

From a price-setting perspective, multiple channels coexist. On the one hand, reduced productivity and increased energy demand generate cost-push inflationary pressures. On the other hand, declining labor income and working hours dampen aggregate demand, exerting downward pressure on prices. In addition, firms may adjust prices based on expectations of persistent climate shocks. The interaction of these opposing forces implies that the net inflationary effect of WBT shocks is theoretically ambiguous and must be determined empirically.

Finally, the strength of these mechanisms varies across sectors depending on exposure to heat and technological adaptability. Sectors relying on outdoor labor or characterized by limited capital intensity are more vulnerable, leading to heterogeneous responses across countries and industries.

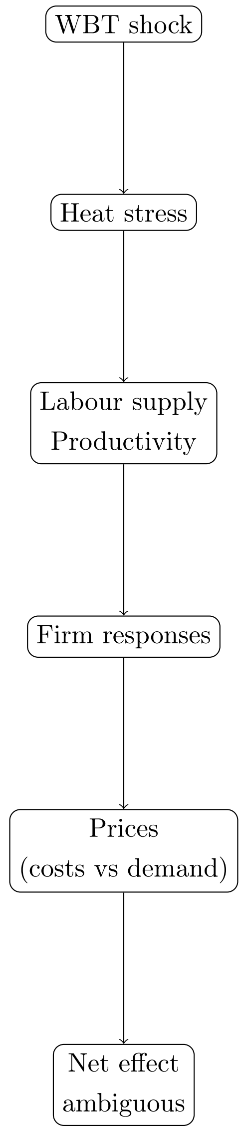

Figure 14: Transmission mechanisms of WBT shocks

3.9 Results and Comments

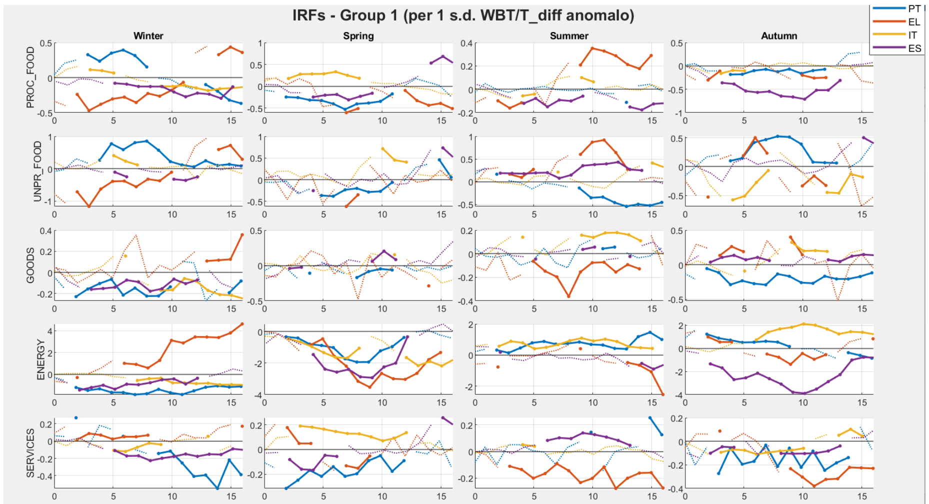

Figure 15: IRFs Seasonal BLP SUB-Index Prices

The BLP estimates reveal clear and economically coherent seasonal responses to WBT anomalies across the four Southern European countries, solid lines are found where the IRFs are significant, dashed lines where they are not.

Summer. Upward pressures are most evident during the summer months (figure 14). Prices of unprocessed food rise sharply in Greece (EL), while both Spain (ES) and Greece display significant increases in non-processed food items. Energy prices register substantial growth in Italy (IT) and Portugal (PT) (Ciccarelli, Kuik, and Hernández 2024; Lucidi et al. 2024) , and industrial goods rise appreciably in Italy. As for services, a notable positive response emerges only in Spain.

Winter. Winter dynamics are more heterogeneous (figure 13) but remain well defined. In Portugal, the only categories that increase in winter are unprocessed food and, marginally, processed food. For energy, the winter response is negative in all countries, including Portugal, as expected: with lower temperatures and the absence of cold waves, heating demand declines and energy prices follow (Ciccarelli, Kuik, and Hernández 2024; Lucidi et al. 2024) .It is noteworthy that energy prices in Greece increase even under a positive winter WBT anomaly, reflecting mild and humid conditions that raise electricity needs for ventilation and dehumidification in a relatively inelastic energy market system (Makrygiorgou et al. 2023).

Spring and autumn. In the spring months, processed-food prices rise in Italy, while unprocessed food increases in Portugal and, more mildly, in Greece. In Italy, a modest uptick re-emerges in autumn. Industrial goods display a positive autumn response in Spain, whereas energy prices continue to rise in both Italy and Portugal during the same season. Service prices show a moderate increase in Italy already in spring.

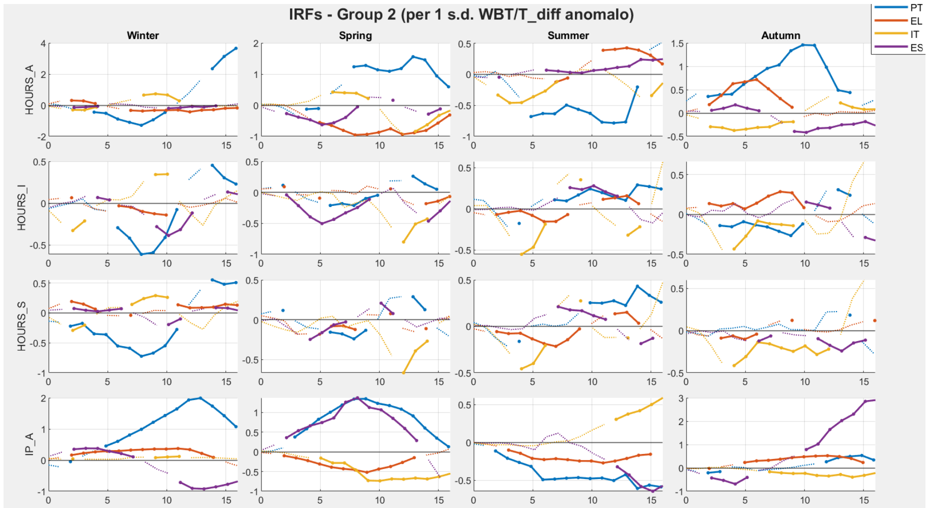

Figure 16: IRFs Seasonal BLP Hours worked

The impulse responses of hours worked and agricultural production display a marked seasonal structure (Figure 15), with substantial heterogeneity across countries and sectors. Overall, heat-stress shocks generate highly asymmetric within-year dynamics, rather than uniform contractions or expansions.

In winter,Portugal displays a distinct pattern: after a mild initial contraction, agricultural hours worked rise sharply at longer horizons. This increase is large and persistent, and it is accompanied by a rise in the agricultural production index (Auffhammer and Mansur 2014; Hristov et al. 2020), indicating that winter shocks induce an operational realignment in Portuguese agriculture rather than a downturn. By contrast, service- and manufacturing-sector responses in Portugal remain weakly negative or close to zero, and the other countries exhibit only mild or statistically insignificant adjustments across most sectors during winter.

In spring, Adjustments in the agricultural sector display substantial heterogeneity. Greece experiences a decline in hours worked, whereas Spain and Portugal record an increase in the agricultural production index. By contrast, both Italy and Greece show a contraction in output, indicating a greater vulnerability of crop production to thermo-hygrometric anomalies. In the industrial sector, Spain exhibits a reduction in hours worked, suggesting a stronger exposure of manufacturing activities to anomalous conditions.

In summer, The most pronounced effect emerges in the Greek service sector, where hours worked decline sharply, consistent with the greater physical strain associated with hot and humid conditions. Italy shows a more complex pattern: hours worked in services and manufacturing contract initially but recover at longer horizons, indicating a transitory rather than a persistent shock effect. In agriculture, hours worked decrease in the early horizons in both Italy and Portugal. In the industrial sector, hours worked fall slightly in Italy and more markedly in Greece. On the production side, agricultural output contracts in Greece and Portugal, increases in Italy at later horizons, and declines in Spain.

In autumn, Agricultural activity strengthens in Spain and Greece, with increases in both hours worked and agricultural output. Portugal also records an expansion in agricultural hours, confirming that seasonal adjustments in the sector are not limited to winter. Italy, by contrast, experiences a contraction in hours worked in agriculture and services, accompanied by a decline in agricultural output. Across other sectors, Italy and Portugal display relatively limited movements during this season.

Taken together, these results indicate that anomalous wet-bulb temperature shocks influence labour markets and agricultural production in a strongly seasonal and highly country-specific manner. In particular: (i) Portugal shows pronounced agricultural reactivity in both winter and autumn; (ii) Greece experiences strong summer contractions in services and agricultural declines in summer; (iii) Italy exhibits initial contractions followed by recoveries, with a spring decline in agriculture; and (iv) Spain shows positive agricultural responses in spring and autumn.

Overall, the evidence suggests that thermo-hygrometric shocks generate complex, within-year adjustments that extend beyond the peak heat season, reflecting cross-country differences in productive structure, climatic exposure, and seasonal patterns of activity. Direct evidence on the interaction between humidity, winter conditions and hours worked in Portugal is scarce. However, several studies document that indoor temperature–humidity combinations in Portuguese buildings are associated with substantial thermal discomfort and adverse health or well-being outcomes (Delgado et al. 2022; Felgueiras et al. 2024; Guedes et al. 2009). Evidence for teleworkers further indicates that deviations of indoor temperature and relative humidity from recommended ranges are linked to worse self-reported productivity and health (A. Ferreira and Barros 2022). These findings are consistent with the broader climate–labour literature, which shows that humid heat stress, typically measured using WBGT or wet-bulb-based indices, reduces labour productivity in Southern Europe, including Portugal (García-León et al. 2021; Gosling et al. 2018).

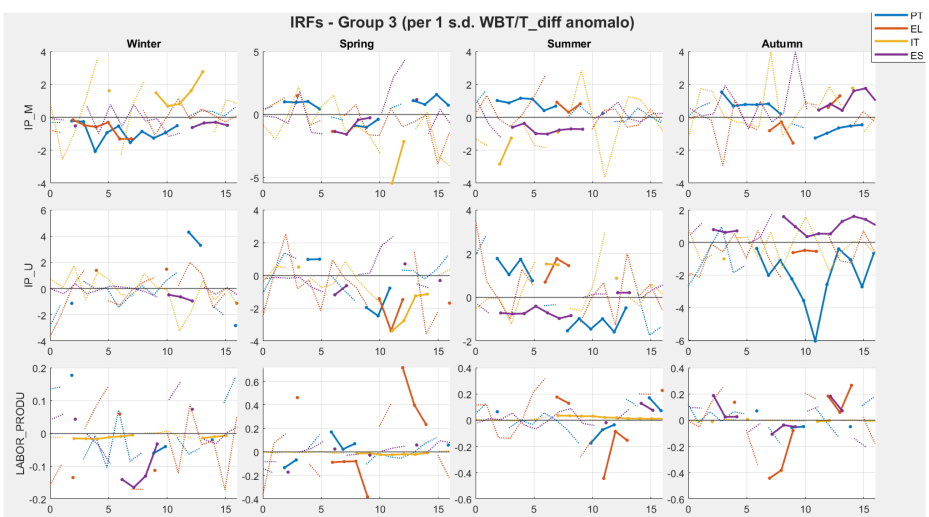

Figure 17: IRFs Seasonal BLP SUB-Index production and Labor Productivity

The impulse responses of manufacturing output (figure 16), utilities, and labor productivity display only weak and largely non-robust seasonal patterns, with few genuinely significant effects and marked heterogeneity across countries.

Overall, and abstracting from high-frequency noise, only Portugal and Spain exhibit clearly positive responses in the manufacturing index, respectively in summer (Portugal) and in autumn (Spain). These increases remain short-lived and do not display strong persistence.

For the utilities sector, a more orderly pattern emerges only in Spain, which records moderate positive responses in spring and summer. Italy shows a mild contraction in spring, but also a short-lived *positive* response in summer; however, significance is restricted to very few horizons and does not suggest a persistent adjustment. No interpretable effects arise for Greece or Portugal.

Labour productivity exhibits essentially no meaningful response across the four seasons. Impulse responses fluctuate around zero and lack persistent significance, a result consistent with the notion that thermo-hygrometric shocks affect labor inputs and sectoral activity rather than productivity measured at monthly frequency.

Taken together, the evidence suggests that anomalous wet-bulb temperature shocks generate only modest industrial and production-side adjustments, with a few seasonal and country-specific exceptions (notably Portugal and Spain), but no systematic or sizeable effects on labor productivity. The results are very similar to those found so far in the literature (Lucidi et al. 2024) . It is interesting to note that these variables exhibit the same path also in the 2000–2019 sample.

3.10 Test WALD

The relevance and the seasonal structure of wet-bulb temperature shocks are assessed through Wald tests based on linear restrictions of the form

$$H_0 : R\beta = r, \qquad W = (R\hat{\beta} - r)'\big(R\hat{\Sigma}_{\beta}R'\big)^{-1}(R\hat{\beta} - r), \quad W \sim \chi^2_q,$$

where $\hat{\beta}$ and $\hat{\Sigma}_{\beta}$ denote the posterior mean of the coefficients and their covariance matrix, and q is the number of imposed restrictions.

Three sets of restrictions are tested. (i) *Seasons all = 0*: all four contemporaneous seasonal coefficients of the shock are jointly equal to zero, $H_0 : \beta_{W,h} = \beta_{Sp,h} = \beta_{Su,h} = \beta_{A,h} = 0$. (ii) *Winter = Summer*: the effects in the cold and warm seasons coincide, $H_0 : \beta_{W,h} - \beta_{Su,h} = 0$. (iii) *Lag shock = 0*: all q_S lags of the shock are irrelevant, $H_0 : \phi_{1,h} = \cdots = \phi_{q_S,h} = 0$.

Frequent rejection of these hypotheses indicates that WBT shocks generate statistically relevant, seasonally differentiated, and dynamically persistent macroeconomic responses (see Appendix).

3.11 Robustness Checks

As a first robustness check, we re-estimate the model on a restricted sample (2000-2019), thereby excluding the COVID-19 period, the subsequent supply-chain disruptions, and the energy-price spike associated with the war in Ukraine. As a second robustness exercise, we estimate a linear version of the Bayesian Local Projection (BLP) model in which the wet-bulb temperature shock enters without seasonal interactions, i.e. without Winter, Spring, Summer and Autumn dummies. This specification removes the seasonal heterogeneity and treats temperature shocks as purely linear drivers.

3.11.1 Estimate IRFs without Covid-19 shock and WAR Ukraine

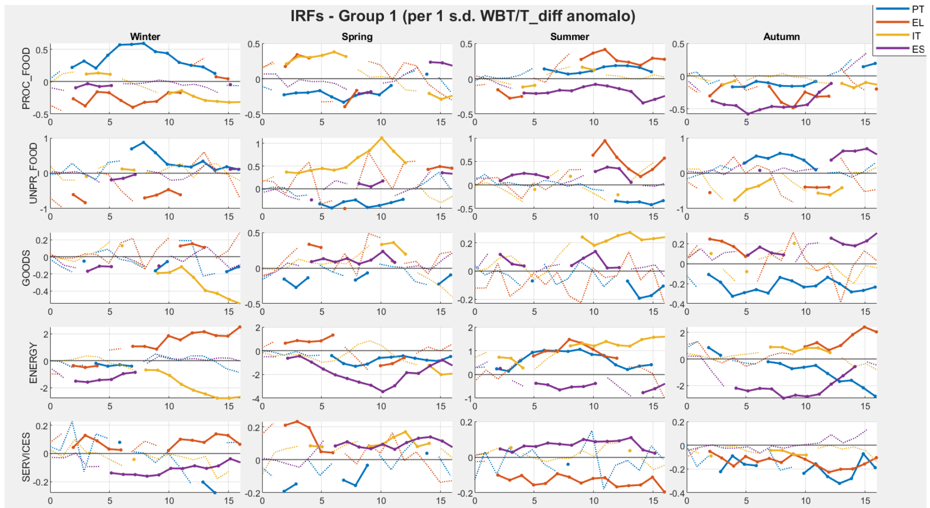

Figure 18: IRFs Seasonal BLP SUB-Index Prices 2000-2019

The shock reveals (figure 17) that the sign of the price responses remains consistent with the baseline. In several cases, however, the magnitude is larger in the 2000–2019 sample. This indicates that, during the COVID-19 period, a concurrent contraction in demand likely dampened the effects of the temperature shock.

In winter, prices of both processed and unprocessed food increase in Portugal, while energy prices in Greece display effects consistent with the baseline. The remaining price sub-indices generally show negative or only weakly significant responses across the other countries, with no evidence of systematic inflationary pressures during the winter period.

The positive response of food prices in Portugal during winter may reflect structural vulnerabilities in the country's agro-food supply chain. The literature documents that anomalous thermo-hygrometric conditions can increase spoilage, storage costs and food-price volatility (Burke et al. 2015). Portugal also exhibits a stronger seasonal dependence on food imports and a less resilient logistics network (Igwe et al. 2024), which amplifies the pass-through of cost shocks compared with other Southern European countries. **In sping**, prices of both processed and unprocessed food increase in Italy, with larger magnitudes and stronger persistence compared with the baseline. Industrial goods rise in Spain, while energy prices increase in Greece. Service prices also rise in Spain and Greece, in contrast with the baseline where service-price increases were observed only in Italy. **In summer**, processed-food prices rise not only in Greece but also in Portugal, while energy prices increase in Greece and Portugal, in addition to Italy, relative to the baseline. **In autumn**, unprocessed food prices increase in Portugal and Spain; industrial goods rise in Spain and Greece; and energy prices grow in Italy and Greece, with a more moderate increase in Portugal. This pattern differs from the baseline, where these effects were more limited or distributed less uniformly across countries.

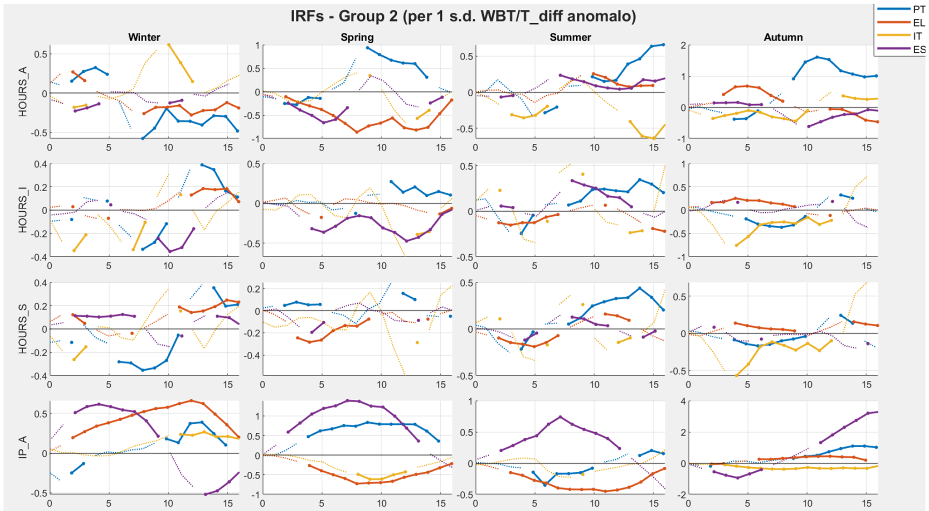

Figure 19: IRFs Seasonal BLP SUB-Index Hours-worked 2000-2019

The dynamics of hours worked (figure 18) exhibit a partial discontinuity relative to the baseline estimates. In the 2000–2019 sample, hours worked increase more strongly in services, particularly in Spain and Greece in winter. By contrast, the negative winter effects observed for Portugal and Spain are noticeably attenuated compared with the baseline, suggesting that the pandemic-related shutdowns had induced a sharper contraction in labor supply than the wet-bulb temperature shock itself. In this sense, the pre-COVID sample restores a labor-hours response more consistent with expected economic behavior.

The response of agricultural hours worked is highly heterogeneous across countries and seasons. In Portugal and Greece, hours decline in winter, in contrast with the baseline, while in Portugal they increase during the other seasons. In Greece, the spring effects display stronger persistence. In Italy, compared with the baseline, the summer contraction in agricultural hours is more muted. It is plausible that the final years of the full sample, which were among the warmest of the century, influenced the behaviour of agricultural hours relative to the pre-Covid period. Overall, the observed dynamics suggest that the WBT shock did not fully capture the evolution of the variables in a context still affected by the pandemic.

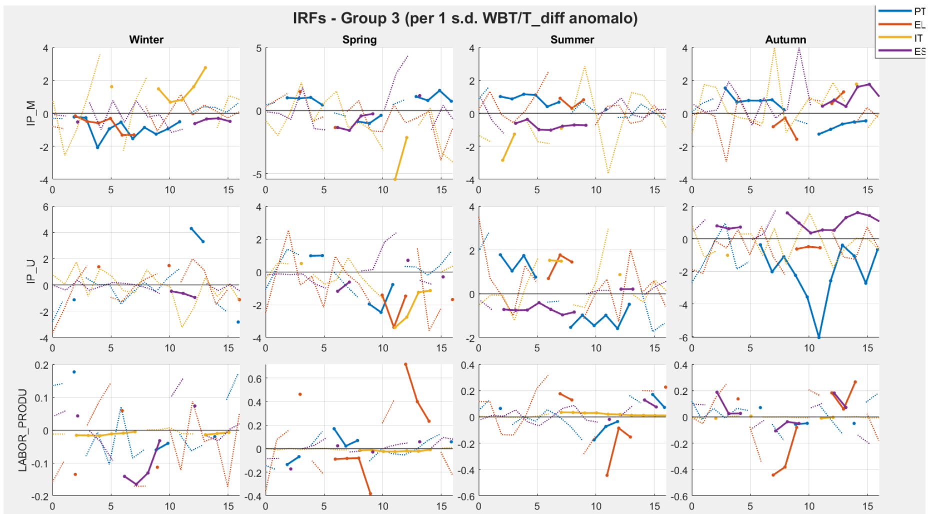

Figure 20: IRFs Seasonal BLP Sub-Index Production and Labor Productivity 2000-2019

The responses of industrial production (figure 19), utilities output, and labor productivity are weak, heterogeneous, and non-persistent across countries and seasons. Manufacturing output exhibits only short-lived fluctuations with no systematic pattern. Utilities respond in an equally irregular manner, with isolated increases in Italy during winter and Greece in autumn, but no consistent cross-country dynamics. Labor productivity displays only small and statistically fragile adjustments. Overall, Group 3 variables do not show a robust transmission channel from the WBT shock, suggesting that climate-related thermo-hygrometric anomalies have limited short-term effects on these macroeconomic aggregates once controls and seasonal interactions are accounted for, the results are similar with finding in literature (Ciccarelli, Kuik, and Hernández 2024; Lucidi et al. 2024). Only a strong decrease in utilities production is observed in Portugal during autumn; this result warrants further investigation in future work.

3.11.2 Bayesian Local Projections: Linear Specification

We estimate a linear Bayesian Local Projections (BLP) model for each country and macroeconomic variable according to:

$$\Delta y_{t+h} = \alpha_h + \beta_h S_t + \sum_{\ell=1}^{q_S} \gamma_{h,\ell} S_{t-\ell} + \sum_{\ell=1}^{p} \phi_{h,\ell} \Delta y_{t-\ell} + \sum_{k \neq y} \sum_{\ell=1}^{p} \theta_{h,k,\ell} \Delta x_{k,t-\ell} + \varepsilon_{t+h}. \tag{15}$$

The shock S_t is the globally standardized temperature anomaly. The specification is fully linear, with lagged shocks included only as controls. All variables are expressed as annual growth rates or log-differences, and we use six lags for both the dependent variable and all additional macroeconomic controls.

Estimation relies on a ridge-regularized Bayesian likelihood, and impulse responses are summarized by posterior medians and 16–84 percent credible intervals. The sample period is 2000–2022.

Transformations (log-differences or year-on-year rates) follow the data appendix, and lag orders are guided by univariate AIC/BIC diagnostics.

Coefficients are estimated horizon-by-horizon using a Gaussian pseudo-likelihood with a mild ridge prior to stabilize inference and avoid erratic dynamics (see BLP seasonal). Posterior medians deliver the impulse responses, while percentile bands report uncertainty. Joint Wald tests on the contemporaneous and lagged shock terms assess the statistical relevance and persistence of WBT shocks in the linear setting (see Appendix).

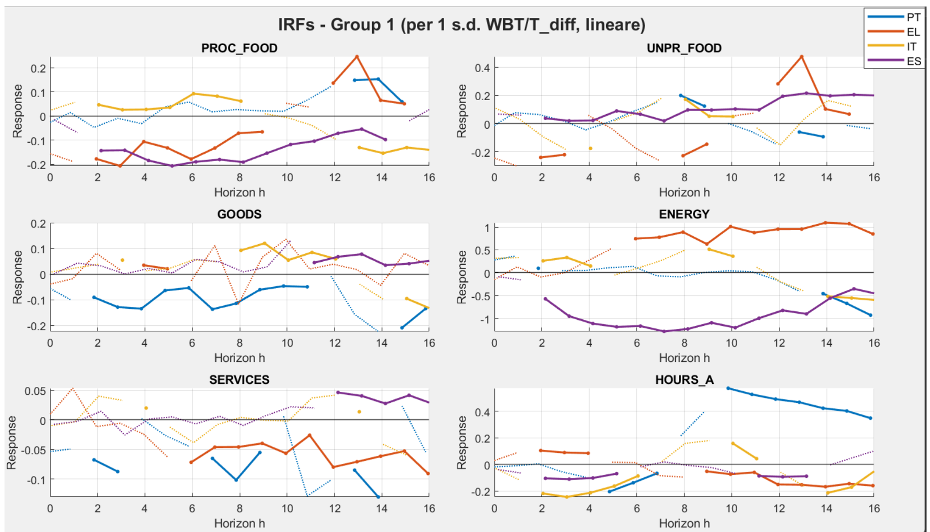

Figure 21: IRFs BPL Linear Model - SUB-Index prices

Overall, the linear BLP estimates show heterogeneous and generally mild responses of prices and hours worked to a one–standard–deviation wet-bulb temperature shock. Processed and unprocessed food prices display no common pattern, with short-run fluctuations that differ in sign across countries. Industrial goods and services also exhibit weak and unsystematic adjustments, without a consistent cross-country profile.

Energy prices constitute the only category with more pronounced reactions, driven mainly by Greece and, to a lesser extent, Italy, where the shock is associated with persistent increases at medium horizons. Portugal and Spain display only modest or temporary effects.

Labour-input responses are irregular: agricultural hours decline in Portugal and Spain, rise slightly and briefly in Greece, and show no clear pattern in Italy. Overall, labor-market effects appear country-specific, with no shared propagation mechanism.

In contrast to Ciccarelli, Kuik, and Hernández 2024 linear model—where shocks based on 2-meters air temperature produced largely deflationary or insignificant effects—here we find weak but noticeable inflationary pressures, especially in energy prices. This suggests that a wet-bulb temperature shock captures a form of climatic stress more tightly linked to thermo-hygrometric conditions, with different economic implications than shocks based solely on surface air temperature.

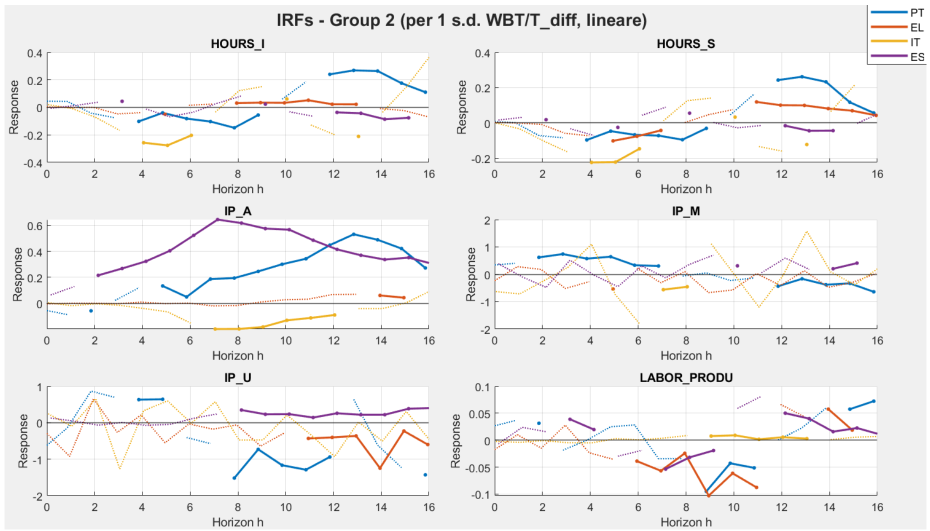

Figure 22: IRFs BPL Linear Model - SUB-Index production

In the second group of variables, the linear BLP estimates reveal modest and strongly country-specific dynamics in response to a one-standard-deviation wet-bulb temperature shock. Hours worked in industry and services remain volatile but unsystematic, with small and short-lived fluctuations that do not indicate any common propagation mechanism.

Agricultural production (IP_A) shows clear and persistent increases in Spain and Portugal, while Italy exhibits a slight contraction and Greece remains essentially flat. This pattern is consistent with the idea that milder and more humid conditions can favour agricultural output in climates such as Spain and Portugal, whereas Italy has experienced marked temperature increases in recent decades, especially in the South, which may offset the potentially beneficial role of higher humidity.

Manufacturing production (IP_m) does not display an interpretable profile, fluctuating around zero across all countries. Utilities production (IP_U) shows large but irregular movements, with no consistent pattern. Labor productivity ($LABOR_PRODU$) also remains essentially flat, with no indication of systematic adjustment.

Overall, the linear wet-bulb temperature shock produces moderate effects and no clear transmission channel outside agriculture, with responses that remain strongly dependent on each country's climatic and production context. Overall, the empirical evidence does not identify a single, unified transmission channel, but rather suggests heterogeneous and weak effects that vary significantly across countries and sectors.

4 Conclusions

The combined evidence from the two empirical approaches outlines a coherent picture of the macroeconomic effects of wet-bulb temperature (WBT) shocks in Southern Europe. The Bayesian VAR estimated on the pre-2012 and post-2012 subsample shows that, compared with the earlier period, the last decade features a larger share of explained variance (FEVD) and more pronounced responses: hours worked decline, and price indicators display persistent adjustments. In parallel, the seasonal-shock analysis reveals marked intra-annual heterogeneity: inflationary pressures do not arise exclusively in the summer months but, in several cases, extend into spring and autumn, accompanied by reductions in labor supply, whereas colder seasons tend to show moderately deflationary dynamics.

Robustness checks indicate that the pandemic and the war in Ukraine have influenced the responses to WBT shocks, making them less clearly identifiable in the most recent years. In particular, the responses of production indicators remain very similar to those observed in the period encompassing the pandemic and the war, while price indicators exhibit clearer variations in the 2000–2019 sample, making this interval more coherent and interpretable, although not exhaustive.

Overall, the results show that WBT shocks generate persistent, seasonally asymmetric and country-specific economic effects, both across decades and within the annual cycle. Moreover, the responses are not fully symmetric even across countries with similar climatic and economic profiles, suggesting that thermal shocks associated with climate change complicate macroeconomic policy-making and pose additional challenges for central banks seeking to maintain stability. These findings also have direct implications for labor market policies. The estimated decline in hours worked associated with WBT shocks suggests that heat stress operates primarily through reductions in effective labor supply and productivity. This mechanism points to the need for targeted adaptation measures in the workplace.

In particular, heat-related workplace regulations, such as maximum temperature thresholds, mandatory breaks, and safety protocols in exposed sectors, become increasingly relevant. At the same time, greater working-time flexibility, including the reallocation of working hours toward cooler periods of the day, may help mitigate productivity losses.

Sector-specific strategies are equally important. Activities with high exposure to outdoor conditions or limited technological adaptability—such as construction, agriculture, and certain services—are likely to require more intensive policy support, including investment in protective technologies and organizational adjustments (Costa et al. 2024; Morabito et al. 2021) .

Overall, these results suggest that labor market institutions will play a key role in shaping the economic resilience to climate-related thermal shocks, complementing broader macroeconomic stabilization policies.

4.1 Description Data

Table 9 reports the data sources used in both the BVAR model and the Bayesian Local Projections (BLP) exercises. All series are monthly. In the BVAR, macroeconomic variables are transformed into natural logarithms and subsequently into monthly log differences, in line with the model specification. The only exceptions are the headline CPI and CPI Energy series, for which we use the monthly growth rates provided directly by FRED.

In the BLP exercises, all macroeconomic variables are instead converted into annual growth rates according to

$$y_{i,t} = 100 \times \frac{Y_{i,t} - Y_{i,t-12}}{Y_{i,t-12}},$$

where $Y_{i,t}$ denotes the series in levels. The only exception is labour productivity, which is expressed in logarithmic growth rates, consistent with its definition and standard practice in the literature.

Most series are obtained from Eurostat (HICP components, industrial p

Table 9: Macroeconomic variables and sources

Variable	**Description**	**Source**
HICP components		
Processed food	HICP – Processed food incl. alcohol and tobacco, Monthly Index, NSA	Eurostat
Unprocessed food	HICP – Unprocessed food, Monthly Index, NSA	Eurostat
Goods	HICP – Industrial goods excluding energy, Monthly Index, NSA	Eurostat
Services	HICP – Services, Monthly Index, NSA	Eurostat
Consumer prices (FRED)		
CPI	Consumer Price Index, all items, Monthly Index	FRED
CPI Energy	Consumer Price Index, energy component, Monthly Index	FRED
Labour input (hours worked)		
Hours worked (Agriculture)	Total hours worked in agriculture	ILO
Hours worked (Industry)	Total hours worked in industry	ILO
Hours worked (Services)	Total hours worked in services	ILO
Industrial production		
IP – Manufacturing	Industrial Production Index, Manufacturing; WSA	Eurostat
IP – Agriculture	Agricultural production index	FAOSTATA
IP – Utilities	Industrial Production Index, Utilities; WSA	Eurostat
Labor productivity	Output/Hours worked ;	Eurostat

4.2 Climate Data

The 2-meter air temperature used to compute wet-bulb temperature (WBT) is obtained from the JRC's reanalysis-based dataset, which provides spatially consistent monthly temperature fields across Europe. Water vapor pressure is not directly available and is reconstructed using the Magnus–Tetens formulation applied to 2-meter temperature and relative humidity, following standard climatological practice.

$$e_s(T) = 0.6108 \exp\left(\frac{17.27\,T}{T + 237.3}\right), \tag{16}$$

4.3 Bayesian VAR

The fiscal model of Mumtaz and Theodoridis 2020 is adapted to study wet-bulb temperature (WBT) shocks, but we do *not* use any external instrument or proxy-SVAR structure in this application. The WBT shock is treated as a standard structural innovation identified within a Bayesian VAR.

We assume a natural-conjugate prior for the VAR parameters $\mathbf{b} = \text{vec}(B)$ and the covariance matrix Σ, implemented via dummy observations in the spirit of Bańbura et al. 2010. Let Y_t denote the vector of endogenous variables and X_t the corresponding lagged regressor. The prior is equivalent to augmenting the sample with artificial observations (Y_D, X_D) that encode: (i) shrinkage of lag coefficients toward univariate AR(1) dynamics, (ii) a sum-of-coefficients restriction, and (iii) a weak prior on the intercept.

In the implementation, overall lag tightness is governed by $\lambda = 10$, the prior on the sum of lagged coefficients by $\tau = 10\lambda$, and the prior on the constant by $c = 1/1000$. Scaling across variables is based on the residual standard deviations from preliminary AR(1) regressions for each series. Conditional on Σ, the VAR coefficients are Gaussian; the covariance matrix itself follows an inverse-Wishart prior. No additional prior is specified for an instrument equation, since no external proxy is used in the WBT application.

Table 10: Information criteria for lag-length selection (Italy)

	Full sample		Pre-2012		Post-2012	
Lag	AIC	BIC	AIC	BIC	AIC	BIC
1	-609.23	-435.63*	-707.14*	-564.92*	-374.51	-253.75*
2	-616.93	-313.42	-686.01	-437.72	-383.51	-159.85
3	-616.01	-182.87	-655.99	-302.14	-360.03	-34.01
4	-652.03	-89.53	-654.51	-195.61	-363.45	64.36
5	-647.26	44.35	-641.48	-78.06	-349.29	179.73
6	-629.37	191.07	-616.28	51.13	-365.66	263.99
7	-727.81*	221.20	-658.37	112.51	-379.13	350.58
8	-705.76	371.53	-634.72	239.08	-397.21*	431.95

Note: l'asterisco indica il valore minimo per ogni colonna/criterio.

For Italy, lag–length selection based on AIC and BIC shows substantial divergence across criteria and subsample. AIC favours higher lag orders (p = 7 in the full sample and p = 8 post-2012), while BIC consistently selects p = 1. Given the short length of the subsample and the need for model comparability in the pre- and post-2012 windows, we adopt a lag order of L = 2, which provides a standard compromise between goodness-of-fit and parameter parsimony and is widely used in small-sample VAR applications.

As shown in Table 10, the information criteria do not converge on a single optimal lag length. The AIC consistently selects L = 2 across the full, pre-2012, and post-2012 samples, while the BIC favours either L = 1 or L = 2 depending on the subsample. We therefore adopt L = 2 as a parsimonious and robust compromise: it is supported by the AIC in all specifications, remains close to the BIC minima, and avoids over-parameterization in the shorter subsample. The main results are unchanged when estimating the models with L = 1 or, for the full sample, L = 5.

Table 11: Information criteria for lag-length selection (Portugal)

Lag	Full sample AIC	Full sample BIC	Pre-2012 AIC	Pre-2012 BIC	Post-2012 AIC	Post-2012 BIC
1	-944.05	-770.45*	-675.67	-533.46*	-334.32	-213.57*
2	-1027.00	-723.54*	-717.84*	-469.55	-365.41*	-141.74
3	-999.35	-566.21	-689.80	-335.95	-339.08	-13.06
4	-1026.20	-463.73	-702.48	-243.58	-323.61	104.19
5	-1045.60*	-353.97	-693.35	-129.93	-318.37	210.65
6	-1017.00	-196.55	-673.17	-5.76	-328.73	300.93
7	-1006.60	-57.55	-666.01	104.87	-296.25	433.45
8	-982.28	95.02	-649.05	224.75	-261.57	567.59

Note: L'asterisco indica il valore minimo per ciascuna colonna (criterio).

Table 12: Information criteria for VAR lag length selection (Spain)

Lag	AIC_full	BIC_full	AIC_pre	BIC_pre	AIC_post	BIC_post
1	-523.52	-349.92	-526.51	-384.30*	-196.08	-75.32
2	-587.71	-284.21	-538.29	-290.00	-245.42	-21.76
3	-853.55	-420.41*	-677.27	-323.42	-362.87	-36.85*
4	-922.27	-359.77	-702.94	-244.04	-408.60	19.20
5	-891.32	-199.71	-715.21	-151.79	-378.77	150.25
6	-1018.20	-197.80	-753.20	-85.79	-435.38	194.27
7	-1014.60	-65.59	-770.23	0.65	-446.23	283.47
8	-1025.40*	51.87	-800.84*	72.96	-452.57*	376.59

Note: Asterisks mark the lowest value in each column.

A suitable lag length for the Spanish VAR can be justified by inspecting the information criteria in Table 12. Although the criteria do not converge on a single optimal value, they offer a clear rationale for adopting $L = 2$. The AIC systematically favours higher lag orders across all samples (often up to $L = 8$), whereas the BIC strongly penalizes over-parameterization and selects either $L = 1$ or $L = 3$ depending on the subsample. Setting $L = 2$ therefore provides a parsimonious compromise: it lies close to the BIC minima in all columns, avoids the overfitting risk implied by the AIC-preferred high-lag models, and maintains consistency with the lag structure used for the other countries. Robustness checks confirm that the main impulse-response patterns remain stable when estimating the models with $L = 1$ or $L = 3$, supporting $L = 2$ as an appropriate baseline specification.

For Greece, the information criteria reported in Table 13 do not identify a single dominant lag order. The AIC selects relatively high lag lengths in all samples (up to $L = 8$), while the BIC consistently favours very parsimonious specifications, selecting $L = 1$ in each column. Choosing $L = 2$ therefore represents a balanced compromise between fit and parsimony. It avoids the over-parameterization implied by the AIC-preferred models, remains close to the BIC minima across all

Table 13: Information criteria for VAR lag length selection (Greece)

Lag	AIC_full	BIC_full	AIC_pre	BIC_pre	AIC_post	BIC_post
1	-156.36	17.249*	-77.475	64.741*	-150.47	-29.707*
2	-326.03	-22.523	-175.73	72.563	-212.18	11.487
3	-308.58	124.56	-160.40	193.46	-190.21	135.81
4	-441.32	121.19	-200.13	258.77	-254.51	173.29
5	-493.68	197.92	-239.12	324.30	-270.28	258.74
6	-697.45	122.99	-324.46	342.95	-422.15	207.50
7	-724.43	224.58	-332.18*	438.70	-432.44	297.26
8	-757.34*	319.96	-327.70	546.10	-448.40*	380.76

Note: Asterisks mark the lowest value in each column.

subsample, and ensures comparability with the lag structure used for the other countries. Robustness checks indicate that impulse-response patterns obtained with $L = 1$ and $L = 3$ are qualitatively similar, confirming $L = 2$ as a stable and appropriate baseline specification.

4.4 TEST WALD, BIC and AIC

The Wald tests provide systematic evidence of seasonal heterogeneity in the response of all macroeconomic variables to WBT anomalies. The joint test "All seasons = 0" is rejected at conventional levels for virtually all countries and variables, confirming the relevance of the seasonal structure embedded in the LP specification. The restriction "Winter = Summer" is often rejected, especially for energy-intensive variables and labor outcomes, indicating asymmetric thermal sensitivity between cold and warm seasons. The test on the lagged shock terms (qS = 2) is frequently significant: dynamic components of WBT anomalies contribute to the overall adjustment process beyond the contemporaneous seasonal effect. Although the AIC criterion favors relatively high lag orders (5–8), the BIC consistently pushes toward more compact specifications (2–6). To preserve comparability across countries and ensure stable estimation at all horizons, a uniform AR lag length of $p = 6$ is adopted. This value balances flexibility and parsimony and avoids the horizon–specific overfitting that may arise from country-specific AIC-optimal choices.

The number of shock lags is set to $q_S = 2$. Empirically, WBT anomalies exhibit short persistence and their predictive content beyond two months sharply decays. Including two lags captures the relevant dynamics while preventing variance inflation and instability in the posterior draws. This choice is validated by Wald tests, which frequently reject the null that lagged shocks are jointly irrelevant.

Table 14: Wald tests for seasonal BLP (h = 16), price variables

Country	Variable	All seasons = 0	Winter = Summer	Lag shock = 0
PT	PROC_FOOD	0.0000***	0.1185	0.0000***
PT	UNPR_FOOD	0.0000***	0.0000***	0.0000***
PT	GOODS	0.0000***	0.0000***	0.0001***
PT	ENERGY	0.0000***	0.0000***	0.0000***
PT	SERVICES	0.0000***	0.0000***	0.0000***
EL	PROC_FOOD	0.0000***	0.0000***	0.0000***
EL	UNPR_FOOD	0.0000***	0.0000***	0.0000***
EL	GOODS	0.0000***	0.0132**	0.0000***
EL	ENERGY	0.0000***	0.0000***	0.0220**
EL	SERVICES	0.0000***	0.0000***	0.0000***
IT	PROC_FOOD	0.0000***	0.0000***	0.0000***
IT	UNPR_FOOD	0.0000***	0.0000***	0.0000***
IT	GOODS	0.0000***	0.0000***	0.0000***
IT	ENERGY	0.0000***	0.0000***	0.0000***
IT	SERVICES	0.0000***	0.0000***	0.0000***
ES	PROC_FOOD	0.0000***	0.5493	0.0000***
ES	UNPR_FOOD	0.0000***	0.0012***	0.0000***
ES	GOODS	0.0000***	0.0000***	0.0000***
ES	ENERGY	0.0000***	0.1492	0.0046***
ES	SERVICES	0.0000***	0.6976	0.0000***

Notes: p-values reported. *** $p < 0.01$, ** $p < 0.05$, * $p < 0.10$.

Table 15: Auxiliary AR Lag Selection for LP Specification

Country	T_{eff}	p(AIC)	p(BIC)
PT	259	6	4
EL	263	8	6
IT	251	5	4
ES	262	5	2

Notes. Lag order p governs the autoregressive structure imposed on the dependent variable within the Local Projection. Although AIC typically selects higher lag orders (between 5 and 8), the BIC favors more parsimonious values (2–6). A common lag order of $p = 6$ is therefore adopted to ensure homogeneous dynamics across countries, avoid horizon-dependent overfitting, and retain sufficient flexibility to capture medium-run persistence. The choice $q_S = 2$ for shock lags follows the same rationale: it captures the short persistence in WBT anomalies without introducing instability or inflating credible intervals.

Table 16: Wald Tests (Sample 2000–2019) – Summary by Country

Country	All seasons = 0	Winter = Summer	Lag shock = 0
PT	Significant for 12/12 vars	Significant for 9/12	Significant for 10/12
EL	Significant for 12/12 vars	Significant for 10/12	Significant for 11/12
IT	Significant for 12/12 vars	Significant for 12/12	Significant for 12/12
ES	Significant for 12/12 vars	Significant for 10/12	Significant for 12/12

Table 17: Auxiliary AR Lag Selection (Sample 2000–2019)

Country	p(AIC)	p(BIC)
PT	5	5
EL	12	6
IT	5	4
ES	2	2

The robustness exercise on the 2000–2019 sample confirms the baseline findings. Wald tests continue to reject the null hypotheses for nearly all countries and variables, indicating stable seasonal patterns and significant dynamic components of WBT shocks. AIC and BIC remain broadly consistent with the baseline, supporting the choice of a uniform AR lag length of $p = 6$ in the main specification.

Table 18: Lag order selection and joint Wald tests (linear BLP with WBT shock)

Country	p_{AIC}	p_{BIC}	Wald (shock + lags)[a]
Portugal (PT)	6	4	All variables: $p < 0.01$ at $h = 0, 4, 8, 12, 16$
Greece (EL)	8	6	All variables: $p < 0.01$ at $h = 0, 4, 8, 12, 16$
Italy (IT)	5	4	All variables: $p < 0.01$ at $h = 0, 4, 8, 12, 16$, except `LABOR_PRODU` at $h = 16$ ($p \approx 0.12$)
Spain (ES)	5	2	All variables: $p < 0.01$ at $h = 0, 4, 8, 12, 16$, except `HOURS_I` at $h = 8$ ($p \approx 0.17$)

Notes: p_{AIC} and p_{BIC} denote the lag order selected by univariate AR diagnostics on a representative macro variable. The Wald column summarises joint tests of the null that the WBT shock and its lags are jointly zero in the linear Bayesian Local Projections specification for prices, hours and industrial production at horizons $h \in \{0, 4, 8, 12, 16\}$.

References

Acevedo, S., Mrkaic, M., Novta, N., Pugacheva, E., & Topalova, P. (2020). The effects of weather shocks on economic activity: What are the channels of impact? *Journal of Macroeconomics*, *65*, 103207.

Agüera-Pérez, A., Palomares-Salas, J. C., De La Rosa, J. J. G., & Florencias-Oliveros, O. (2018). Weather forecasts for microgrid energy management: Review, discussion and recommendations. *Applied energy*, *228*, 265–278.

Auerbach, A. J., & Gorodnichenko, Y. (2012). Measuring the output responses to fiscal policy. *American Economic Journal: Economic Policy*, *4*(2), 1–27.

Auffhammer, M., & Mansur, E. T. (2014). Measuring climatic impacts on energy consumption: A review of the empirical literature. *Energy Economics*, *46*, 522–530.

Bańbura, M., Giannone, D., & Reichlin, L. (2010). Large bayesian vector auto regressions. *Journal of applied Econometrics*, *25*(1), 71–92.

Bekris, Y., Loikith, P. C., & Neelin, J. D. (2023). Short warm distribution tails accelerate the increase of humid-heat extremes under global warming. *Geophysical Research Letters*, *50*(11), e2022GL102164.

Budd, G. M. (2008). Wet-bulb globe temperature (wbgt)—its history and its limitations. *Journal of science and medicine in sport*, *11*(1), 20–32.

Burke, M., Hsiang, S. M., & Miguel, E. (2015). Global non-linear effect of temperature on economic production. *Nature*, *527*(7577), 235–239.

Buzan, J. R., & Huber, M. (2020). Moist heat stress on a hotter earth. *Annual Review of Earth and Planetary Sciences*, *48*(1), 623–655.

Carriero, A., Clark, T. E., & Marcellino, M. (2015). Bayesian vars: Specification choices and forecast accuracy. *Journal of Applied Econometrics*, *30*(1), 46–73.

Ciccarelli, M., Kuik, F., & Hernández, C. M. (2024). The asymmetric effects of temperature shocks on inflation in the largest euro area countries. *European Economic Review*, *168*, 104805.

Ciccarelli, M., & Marotta, F. (2024). Demand or supply? an empirical exploration of the effects of climate change on the macroeconomy. *Energy Economics*, *129*, 107163.

Coffel, E. D., Horton, R. M., & De Sherbinin, A. (2017). Temperature and humidity based projections of a rapid rise in global heat stress exposure during the 21st century. *Environmental Research Letters*, *13*(1), 014001.

Colacito, R., Hoffmann, B., & Phan, T. (2019). Temperature and growth: A panel analysis of the united states. *Journal of Money, Credit and Banking*, *51*(2-3), 313–368.

Costa, H., Franco, G., Unsal, D. F., & Sarath-Chandra, M. (2024). The heat is on: Heat stress, productivity and adaptation among firms. *Available at SSRN 5556799*.

d'Ambrosio Alfano, F. R., Malchaire, J., Palella, B. I., & Riccio, G. (2014). Wbgt index revisited after 60 years of use. *Annals of occupational Hygiene*, *58*(8), 955–970.

Dasgupta, S., van Maanen, N., Gosling, S. N., Piontek, F., Otto, C., & Schleussner, C.-F. (2021). Effects of climate change on combined labour productivity and supply: An empirical, multi-model study. *The Lancet Planetary Health*, *5*(7), e455–e465.

De Winne, J., & Peersman, G. (2018). *Agricultural price shocks and business cycles-a global warning for advanced economies* (tech. rep.). CESifo Working Paper.

Delgado, J., Matos, A. M., & Guimarães, A. S. (2022). Linking indoor thermal comfort with climate, energy, housing, and living conditions: Portuguese case in european context. *Energies*, *15*(16), 6028.

Dell, M., Jones, B. F., & Olken, B. A. (2012). Temperature shocks and economic growth: Evidence from the last half century. *American Economic Journal: Macroeconomics*, *4*(3), 66–95.

Faccia, D., Parker, M., & Stracca, L. (2021). Feeling the heat: Extreme temperatures and price stability.

Felgueiras, F., Mourão, Z., Moreira, A., & Gabriel, M. F. (2024). Indoor environmental quality in portuguese office buildings: Influencing factors and impact of an intervention study. *Sustainability*, *16*(21), 9160.

Ferreira, A., & Barros, N. (2022). Covid-19 and lockdown: The potential impact of residential indoor air quality on the health of teleworkers. *International Journal of Environmental Research and Public Health*, *19*(10), 6079.

Ferreira, L. N., Miranda-Agrippino, S., & Ricco, G. (2025). Bayesian local projections. *Review of Economics and Statistics*, *107*(5), 1424–1438.

Fischer, E. M., & Knutti, R. (2013). Robust projections of combined humidity and temperature extremes. *Nature Climate Change*, *3*(2), 126–130.

García-León, D., Casanueva, A., Standardi, G., Burgstall, A., Flouris, A. D., & Nybo, L. (2021). Current and projected regional economic impacts of heatwaves in europe. *Nature communications*, *12*(1), 5807.

Gosling, S. N., Zaherpour, J., Ibarreta, D., et al. (2018). *Peseta iii: Climate change impacts on labour productivity*. Publications Office of the European Union Luxembourg.

Guedes, M. C., Matias, L., & Santos, C. P. (2009). Thermal comfort criteria and building design: Field work in portugal. *Renewable Energy*, *34*(11), 2357–2361.

Horton, R. M., Mankin, J. S., Lesk, C., Coffel, E., & Raymond, C. (2016). A review of recent advances in research on extreme heat events. *Current Climate Change Reports*, *2*, 242–259.

Hristov, J., Toreti, A., Pérez Domínguez, I., Dentener, F., Fellmann, T., Elleby, C., Ceglar, A., Fumagalli, D., Niemeyer, S., Cerrani, I., et al. (2020). Analysis of climate change impacts on eu agriculture by 2050. *Publications Office of the European Union, Luxembourg, Luxembourg*, 2020–05.

Igwe, A. N., Eyo-Udo, N. L., & Stephen, A. (2024). Strategies for mitigating food pricing volatility: Enhancing cost affordability through sustainable supply chain practices. *Strategies*, *13*(9), 151–163.

Jordà, Ò. (2005). Estimation and inference of impulse responses by local projections. *American economic review*, *95*(1), 161–182.

Kim, H. S., Matthes, C., & Phan, T. (2021). Extreme weather and the macroeconomy. *Available at SSRN 3918533*.

Kodra, E., & Ganguly, A. R. (2014). Asymmetry of projected increases in extreme temperature distributions. *Scientific reports*, *4*(1), 5884.

Lazoglou, G., Papadopoulos-Zachos, A., Georgiades, P., Zittis, G., Velikou, K., Manios, E. M., & Anagnostopoulou, C. (2024). Identification of climate change hotspots in the mediterranean. *Scientific reports*, *14*(1), 29817.

Lemos, M. C., Kirchhoff, C. J., & Ramprasad, V. (2012). Narrowing the climate information usability gap. *Nature climate change*, *2*(11), 789–794.

Li, C., Zhang, X., Zwiers, F., Fang, Y., & Michalak, A. M. (2017). Recent very hot summers in northern hemispheric land areas measured by wet bulb globe temperature will be the norm within 20 years. *Earth's Future*, *5*(12), 1203–1216.

Liljegren, J. C., Carhart, R. A., Lawday, P., Tschopp, S., & Sharp, R. (2008). Modeling the wet bulb globe temperature using standard meteorological measurements. *Journal of occupational and environmental hygiene*, *5*(10), 645–655.

Lin, Q., & Yuan, J. (2022). Linkages between amplified quasi-stationary waves and humid heat extremes in northern hemisphere midlatitudes. *Journal of Climate*, *35*(24), 8245–8258.

Lucidi, F. S., Pisa, M. M., & Tancioni, M. (2024). The effects of temperature shocks on energy prices and inflation in the euro area. *European Economic Review*, *166*, 104771.

Ma, Q., Chen, Y., & Ionita, M. (2024). European summer wet-bulb temperature: Spatiotemporal variations and potential drivers. *Journal of Climate*, *37*(6), 2059–2080.

Makrygiorgou, J. J., Karavas, C.-S., Dikaiakos, C., & Moraitis, I. P. (2023). The electricity market in greece: Current status, identified challenges, and arranged reforms. *Sustainability*, *15*(4), 3767.

Marengo, J. A., Souza Jr, C. M., Thonicke, K., Burton, C., Halladay, K., Betts, R. A., Alves, L. M., & Soares, W. R. (2018). Changes in climate and land use over the amazon region: Current and future variability and trends. *Frontiers in Earth Science*, *6*, 228.

Minard, D. (1961). Prevention of heat casualties in marine corps recruits: Period of 1955–60, with comparative incidence rates and climatic heat stresses in other training categories. *Military medicine*, *126*(4), 261–272.

Miranda-Agrippino, S., & Ricco, G. (2021). Bayesian local projections.

Morabito, M., Messeri, A., Crisci, A., Bao, J., Ma, R., Orlandini, S., Huang, C., & Kjellstrom, T. (2021). Heat-related productivity loss: Benefits derived by working in the shade or work-time shifting. *International Journal of Productivity and Performance Management*, *70*(3), 507–525.

Mukherjee, K., & Ouattara, B. (2021). Climate and monetary policy: Do temperature shocks lead to inflationary pressures? *Climatic change*, *167*(3), 32.

Mumtaz, H., & Alessandri, P. (2021). The macroeconomic cost of climate volatility. *Available at SSRN 3895032*.

Mumtaz, H., & Theodoridis, K. (2020). Fiscal policy shocks and stock prices in the united states. *European Economic Review*, *129*, 103562.

Nath, I. B., Ramey, V. A., & Klenow, P. J. (2024). *How much will global warming cool global growth?* (Tech. rep.). National Bureau of Economic Research.

Natoli, F. (2022). Temperature surprise shocks.

Peersman, G. (2022). International food commodity prices and missing (dis) inflation in the euro area. *Review of Economics and Statistics*, *104*(1), 85–100.

Ramey, V. A. (2011). Can government purchases stimulate the economy? *Journal of Economic Literature*, *49*(3), 673–685.

Raymond, C., Matthews, T., & Horton, R. M. (2020). The emergence of heat and humidity too severe for human tolerance. *Science Advances*, *6*(19), eaaw1838.

Rogers, C. D., Ting, M., Li, C., Kornhuber, K., Coffel, E. D., Horton, R. M., Raymond, C., & Singh, D. (2021). Recent increases in exposure to extreme humid-heat events disproportionately affect populated regions. *Geophysical Research Letters*, *48*(19), e2021GL094183.

Russo, S., Dosio, A., Graversen, R. G., Sillmann, J., Carrao, H., Dunbar, M. B., Singleton, A., Montagna, P., Barbola, P., & Vogt, J. V. (2014). Magnitude of extreme heat waves in present climate and their projection in a warming world. *Journal of Geophysical Research: Atmospheres*, *119*(22), 12–500.

Sareen, S., & Nordholm, A. J. (2021). Sustainable development goal interactions for a just transition: Multi-scalar solar energy rollout in portugal. *Energy Sources, Part B: Economics, Planning, and Policy*, *16*(11-12), 1048–1063.

Schlenker, W., & Roberts, M. J. (2009). Nonlinear temperature effects indicate severe damages to us crop yields under climate change. *Proceedings of the National Academy of sciences*, *106*(37), 15594–15598.

Sherwood, S. C., & Huber, M. (2010). An adaptability limit to climate change due to heat stress. *Proceedings of the National Academy of Sciences*, *107*(21), 9552–9555.

Tanaka, M. (2020). Bayesian inference of local projections with roughness penalty priors. *Computational Economics*, *55*(2), 629–651.

Wang, P., Leung, L. R., Lu, J., Song, F., & Tang, J. (2019). Extreme wet-bulb temperatures in china: The significant role of moisture. *Journal of Geophysical Research: Atmospheres*, *124*(22), 11944–11960.

Wang, P., Yang, Y., Tang, J., Leung, L. R., & Liao, H. (2021). Intensified humid heat events under global warming. *Geophysical Research Letters*, *48*(2), e2020GL091462.

Green Fiscal Multipliers with Different Sovereign Debt Trajectories in EU Countries.

Alessio Ferraro[1]

[1]Department of Economics, Roma Tre

Abstract

This paper estimates the GDP and private-investment multipliers of green public spending using Bayesian Smooth-Transition VARs for EU member states over 1995–2022. Nonlinear fiscal transmission is captured through low- and high-debt regimes. The analysis covers three regional panels (Southern, Eastern and Northern Europe) and a full-EU aggregate. Generally across all samples, green-spending multipliers on GDP exceed one and are systematically larger than those associated with conventional public expenditure, indicating more favourable expectations, lower perceived risk and intertemporal redistribution linked to the climate transition. Private investment responds less to green public spending because such spending does not primarily stimulate short-run demand, but instead induces processes of productive reorganization and adjustment that materialize mainly over the medium term. When public debt is high, the composition of public spending becomes crucial: green spending proves more effective than traditional spending, especially in Southern European countries, where fiscal constraints are more binding. In Northern Europe, green shocks are more effective in high-debt phases, consistent with countercyclical slack. Overall, green spending is perceived differently from undifferentiated fiscal expansions and delivers macroeconomic multipliers above unity without triggering destabilising financial reactions.

Keywords:green fiscal multipliers; debt trajectories; interest rates; Bayesian Panel Vector Autoregression (BVAR)
JEL codes:C23; E44; E62; G15; H62; H63

Contents

1 Introduction

To meet the goals of the Paris Agreement, the International Energy Agency estimates that global investment in green infrastructure will need to increase by around 2 percent of world GDP per year. A substantial share of this effort is expected to come from the public sector, forcing governments to reconcile the need to restore post-pandemic fiscal positions with the urgency of expanding green public expenditure. This trade-off is particularly salient in the European Union, where public investment is projected to rise by approximately 0.6 percent of annual GDP throughout this decade, and potentially more if the green transition accelerates in response to geopolitical shocks such as Russia's invasion of Ukraine.

Against this backdrop, a central policy question is whether green public spending can operate as an effective fiscal instrument when public-debt constraints are binding. While a growing literature documents sizable output effects of green investment, considerably less is known about how these effects vary across debt regimes, regions, and transmission channels, particularly in a multi-country European setting characterized by strong fiscal heterogeneity.

This paper assesses the macroeconomic effects of green public spending under different debt conditions, with a focus on output, investment, and financial variables. Using quarterly data for the period 1995–2022, we estimate Smooth Transition Bayesian panel VAR models for three European blocs and for an aggregate EU panel of 18 countries. The regional blocs comprise Southern Europe (Italy, Spain, Portugal, Greece, France, Belgium), Eastern Europe (Poland, Hungary, Czech Republic, Slovenia, Slovakia, Romania), and Northern Europe (Germany, Austria, Netherlands, Denmark, Sweden, Finland). In addition to standard fiscal and macroeconomic variables, the empirical framework includes sovereign spreads and an indicator of household and firm expectations, allowing us to capture financial conditions and economic sentiment. Fiscal shocks are identified through a recursive Cholesky ordering, with green spending placed first.

The results reveal pronounced regional and regime-dependent heterogeneity. In Southern Europe, where fiscal space is structurally constrained, shocks to non-green public spending generate negative output multipliers, whereas green-spending shocks produce multipliers well above one, indicating a clear macroeconomic advantage of targeted climate-related interventions. In Northern Europe, green multipliers exceed unity only under high-debt conditions, consistent with recession-type environments characterized by ample economic slack, while financial variables react only mildly. In Eastern Europe, by contrast, green spending displays weak macroeconomic effects across regimes: output multipliers remain below one and expectations show limited adjustment, pointing to a muted aggregate-demand channel.

Evidence from the aggregate EU panel reinforces these patterns. Under low-debt conditions, green-spending shocks generate GDP multipliers well above one, while conventional spending shocks remain markedly weaker. Under high-debt conditions, non-green multipliers increase slightly but remain well below unity. Overall, within the EU-wide sample, green public spending is the only configuration that consistently delivers output multipliers above one, whereas non-green expenditure never crosses this threshold.

Private investment responses further qualify these findings. A systematic differential reaction between green and non-green spending shocks emerges only in the aggregate EU panel. In this setting, non-green spending shocks generate larger and more responsive investment multipliers, suggesting that firms interpret conventional expenditure primarily as a short-run cyclical stimulus. By contrast, increases in green public spending do not trigger a statistically significant private-investment response in terms of multipliers, indicating that the private channel remains largely inactive in the short run. Importantly, this pattern does not generalize to the regional blocs, where investment responses to both green and non-green shocks are weak or statistically indistinguishable from zero. As a result, the heterogeneity observed in output multipliers across regions reflects differences in aggregate-demand conditions and fiscal transmission mechanisms rather than investment-driven dynamics.

Although regulatory instruments remain essential, the transition to a low-emissions economy cannot rely exclusively on them. As emphasized by Darvas and Wolff (2021), fiscal policy plays a crucial complementary role. Our results indicate that an effective climate strategy requires sustained fiscal support, whose macroeconomic returns depend critically on public debt conditions, regional heterogeneity, and private sector expectations.

In this context, a central fiscal design question emerges: how to reconcile the expansion of green public spending with the preservation of debt sustainability and fiscal credibility. On the one hand, our findings suggest that the composition of spending is a key determinant of macroeconomic effectiveness. On the other hand, they indicate that strategies relying exclusively on expenditure-side instruments may generate significant pressures on public finances in the absence of adequate revenue-side measures. This implies that the design of fiscal policy for the climate transition should be based on a balance between expenditure composition, financing instruments, and medium-term anchors, rather than on a simple expansion of spending or on automatic exemptions from fiscal rules, which could undermine credibility.The recent literature on fiscal multipliers highlights the strong state dependence of fiscal effectiveness.Romer and Romer (2010) andAuerbach and Gorodnichenko (2012) show that multipliers tend to be larger during recessions, while Afonso and Sousa (2012) and Ilzetzki et al. (2013) emphasize that high levels of public debt can weaken the impact of fiscal stimulus. A growing strand of research focuses specifically on green public investment and spending, analyzing their potential to deliver both expansionary and sustainable outcomes. Batini et al. (2022) find that green fiscal interventions can yield high multipliers, particularly when economic slack is present, while Ciaffi (2025) shows that environmental spending can foster growth, innovation, and social cohesion, contributing to an effective ecological transition.

Given the extraordinary nature of the fiscal and macroeconomic shocks observed in 2020, Appendices D and E provide a set of robustness exercises in which the impulse–response functions of both green spending shocks and non-green (total net-of-green) expenditure shocks are re-estimated over the pre-pandemic sample 1995–2019. This allows us to assess the stability of the estimated transmission mechanisms and to verify that our baseline results are not driven by the COVID-19 episode.

The remainder of the paper is organized as follows. Section 2 reviews the literature on fiscal multipliers, with a focus on green public spending. Section 3 describes the data. Section 4 presents the empirical strategy and discusses the results from the Smooth Transition Bayesian panel VAR on green-spending shocks and fiscal multipliers. Section 5 reports the corresponding results for non-green spending shocks. Section 6 concludes.

2 Literature

The literature on fiscal multipliers has grown substantially since the 2008–2009 Global Financial Crisis (GFC), with a central focus on identifying the macroeconomic conditions under which fiscal policy is most effective. A key finding from this body of work is that fiscal multipliers are not constant: they vary depending on the state of the economy, the type of fiscal intervention, the level of public debt, and expectations about future policy.

Auerbach and Gorodnichenko (2012) provide evidence that multipliers are significantly higher during recessions than expansions, using a regime-switching model that captures the state-dependence of fiscal effects. Their results suggest that fiscal stimulus can be particularly effective when output is below potential and monetary policy is constrained. However, this view is challenged by Ramey and Zubairy (2018), who, using historical U.S. data, find that multipliers do not systematically increase during periods of high unemployment. These contrasting results highlight the sensitivity of fiscal multiplier estimates to model specification and identification strategy.

Another important strand of the literature examines how fiscal multipliers vary with public debt levels.Ilzetzki et al. (2013) and Huidrom et al. (2020) find that high debt levels tend to reduce the effectiveness of fiscal policy, due to expectations of future consolidation (the Ricardian channel) and increases in sovereign risk premiums.Auerbach and Gorodnichenko (2017) argue, however, that even under high debt, fiscal stimulus can still be effective, especially when real interest rates are low. These findings underscore the importance of fiscal space as a constraint on discretionary fiscal action.

More recent research has shifted attention to the composition of fiscal spending. Several studies—including Deleidi et al. (2020) and Saccone et al. (2022)—highlight that public investment, especially in infrastructure and human capital, tends to produce larger and more persistent output effects than current or transfer spending. This has led to renewed interest in investment-led fiscal policy, particularly in the context of the post-pandemic recovery and climate transition.

Within this broader framework, a growing body of literature focuses on the macroeconomic effects of green public spending. Batini et al. (2022) offer one of the first systematic evaluations of green fiscal multipliers, showing that investments in low-carbon infrastructure, renewable energy, and biodiversity yield multipliers ranging between 1.1 and 1.7—substantially higher than those associated with fossil fuel-intensive projects. Their findings are based on cross-country data and highlight that green investments are not only environmentally necessary but also economically efficient, particularly in times of economic slack.

Similarly, Ciaffi (2025) analyze the impact of green public spending in Europe, emphasizing the North-South divide. Using a Local Projections framework applied to 30 European countries from 1995 to 2020, they show that green investment spending produces more favorable macroeconomic outcomes than green current expenditures. The expansionary effects are more pronounced in high-income countries, and the study documents positive spillovers on productivity and private investment, supporting the hypothesis that green public investment can initiate self-sustaining growth dynamics. However, the literature still lacks systematic evaluations of how green multipliers interact with fiscal conditions such as public debt levels.

At the subnational level.Ficarra (2024) investigates the heterogeneity of green and non-green spending effects across Italian provinces. By constructing a new dataset of public works between 2013 and 2021, and employing a Local Projections approach, the study shows that green investment tends to have a more positive impact on output than non-green spending, although the effects vary significantly by region and institutional quality. For example, green investment in Northern Italy generates modest but persistent growth, whereas in the South, the initial response is strong but fades quickly. The paper also highlights a surprising result: in contexts of high regulatory burden, corruption may paradoxically increase the fiscal multiplier by circumventing bureaucratic inefficiencies.

Taken together, this literature points to several gaps that our work seeks to address. First, while the macroeconomic effectiveness of green public investment is increasingly recognized, little is known about how this effectiveness varies under different public debt regimes. Second, most studies estimate average multipliers without accounting for nonlinearities induced by fiscal space constraints or shifts in debt dynamics. Third, the identification of exogenous green fiscal shocks remains challenging, with few studies employing narrative or structural approaches.

Our study contributes to the limited literature on green fiscal multipliers by examining how public debt levels influence their magnitude and how debt and interest rates respond to green fiscal shocks. Unlike studies relying on narrative identification or local projections, our empirical strategy is based on a Bayesian Panel VAR model, where fiscal shocks are identified using a Cholesky decomposition, ordering green spending first. This allows us to isolate the exogenous impact of green public spending on the economy.

3 Data

This study uses data from the Environmental Protection Expenditure Accounts (EPEA) of the European Commission, which measure the economic resources allocated by households, firms, and governments to environmental protection activities—such as pollution abatement, waste and wastewater management, biodiversity conservation, *RD*, and education. Structured by institutional sector and environmental domain (based on the CEPA 2000 classification), the EPEA captures both public and private environmental services provision.

Environmental protection expenditure reflects the total resources used within a country to safeguard the environment, and includes current and capital spending, as well as net transfers abroad. According to Eurostat, total EU environmental protection expenditure—measured by National Expenditure on Environmental Protection (NEEP)—rose by 27 percent between 2018 and 2023 (see figures Appendix A), though its share of GDP remained relatively stable, fluctuating between 2 percent and 2.2 percent. Over the same period, investment in environmental protection rose by 28 percent, with a 22 percent increase recorded between 2020 and 2023, after the temporary drop caused by the COVID-19 crisis.

In 2023, NEEP reached €357 billion in the EU, tracking GDP growth and keeping the NEEP-to-GDP ratio stable at around 2.1–2.2 percent. The business sector accounted for 52 percent of NEEP, including both specialist producers and firms managing environmental activities in-house. Between 2018 and 2023, business-related environmental spending increased by 33 percent. Public administrations and non-profits contributed 31 percent, and households 17 percent, with public/non-profit spending growing by 33 percent and household spending rising by 6 percent.

There is wide variation in NEEP-to-GDP ratios across EU countries. In 2021, values ranged from 0.9 percent in Ireland and Luxembourg to 3.6 percent in Austria. Eight countries—including Italy, Germany, and Poland—exceeded the EU average of 2.2 percent. The European Green Deal identifies investment as key to delivering environmental goals. In 2023, the EU invested €67 billion in environmental services, mainly in wastewater (41.6 percent) and waste management (26.6 percent), followed by air protection (10.4 percent), biodiversity (6.4 percent), soil protection (5.6 percent), and *RD*, education, and other activities (8.4

Public investment in environmental protection varies substantially across member states—from 0.1 percent to 9.6 percent of total spending—reflecting different institutional arrangements (e.g., public vs. market provision of waste services). Our dataset follows the COFOG classification (Division 5), which includes waste, wastewater, pollution abatement, biodiversity, and related activities. In 2023, total government spending on environmental protection in the EU was 0.8 percent of GDP, with 0.4 percent allocated to waste, and 0.1 percent each to wastewater, pollution, biodiversity, and unclassified services.

Greece and the Netherlands had the highest public green spending (1.5 percent of GDP), followed by Malta and Belgium (1.2 percent) and Luxembourg (1.1 percent). Waste management represented the highest shares in Greece, Netherlands, Bulgaria, and Malta (up to 0.9 percent of GDP), while wastewater management was particularly relevant in Luxembourg, Slovenia, Netherlands, and Cyprus. Greece also led the EU in pollution abatement (0.6 percent of GDP), ahead of Belgium (0.4 percent). Spending on biodiversity remains low across the EU, peaking at 0.2 percent of GDP in Malta, Czechia, Denmark, and Iceland. Public *RD* in environmental protection remains marginal, typically below 0.1 percent of GDP (see Appendix A).

Between 1995 and 2023, general government spending on environmental protection fluctuated between 0.7 percent and 0.8 percent of GDP, and between 1.5 percent and 1.7 percent of total public expenditure. From 2022 to 2023, environmental protection spending rose by €14 billion (+11 percent), from €127 billion to €142 billion, with its GDP share stable at 0.8 percent.

To match the quarterly frequency of the rest of the dataset, annual series on green public expenditure, total government expenditure, tax revenues, nominal GDP, and real GDP were interpolated using the Denton method, which preserves annual totals while smoothing high-frequency fluctuations. The analysis covers the period 1995–2002 (see Appendix A) and is conducted using quarterly data. Since information on these variables is only available at an annual frequency, interpolation ensures consistency with officially reported aggregates and improves the temporal resolution of the empirical analysis.

Long-term interest rates (10-year government bond yields), sovereign spreads, and the Economic Sentiment Indicator (ESI)—financial variables already available at higher frequencies—were converted or aggregated to quarterly frequency in order to track developments in market conditions and household and firm expectations. In particular, sovereign spreads capture changes in perceived sovereign risk and financing conditions, which are central to the transmission of fiscal and green-spending shocks, especially in high-debt environments. The ESI provides a timely proxy for confidence and expectations of households and firms, allowing the analysis to account for expectation-driven channels that may amplify or dampen real economic responses.

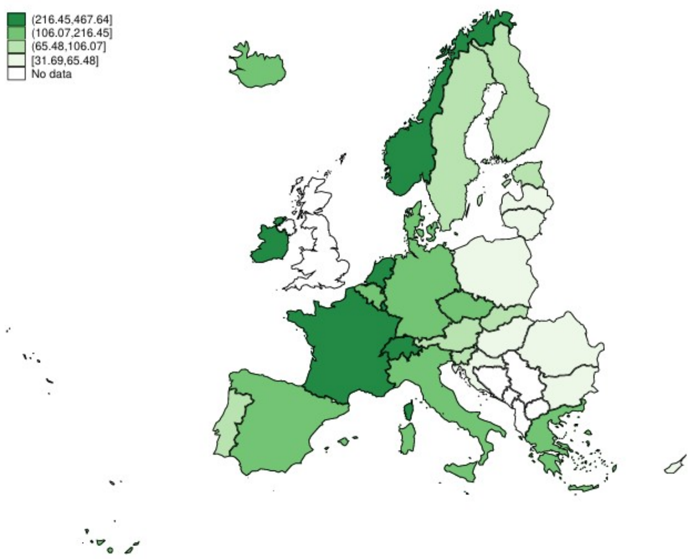

Figure 1: Public Green Spending 1995-2023

In our dataset, the debt-to-GDP ratio from 1995 to 2022 captures the effects of major macroeconomic shocks, notably the 2008 global financial crisis — followed by the sovereign debt crisis within the euro area — and the 2020 COVID-19 pandemic. These events led to significant increases in public debt levels, the trajectory of which is illustrated in the figures presented.As shown in Figure 2,3 and 4, public debt levels in EU countries rose sharply following the 2008 financial crisis, then either stabilized or declined in some cases during the following decade. However, a renewed increase is observed in response to the COVID-19 shock. Debt levels remain structurally higher in Southern European countries, highlighting greater fiscal space constraints in these economies—particularly in the face of green public spending initiatives. Public debt was normalized to account for the considerable heterogeneity in debt levels across countries, which would otherwise hinder meaningful cross-country comparisons.Specifically, for each country i and time t, the normalized debt variable is computed as:

$$z\text{-score}_{i,t} = \frac{\text{debt}_{i,t} - \mu_{\text{EU}}}{\sigma_{\text{EU}}} \tag{1}$$

where μ_{eu} and σ_{eu} denote, respectively, the cross-country mean and standard deviation of public debt within the European Union. This normalization accounts for large cross-sectional differences in debt levels and allows for more meaningful comparisons across countries and over time.

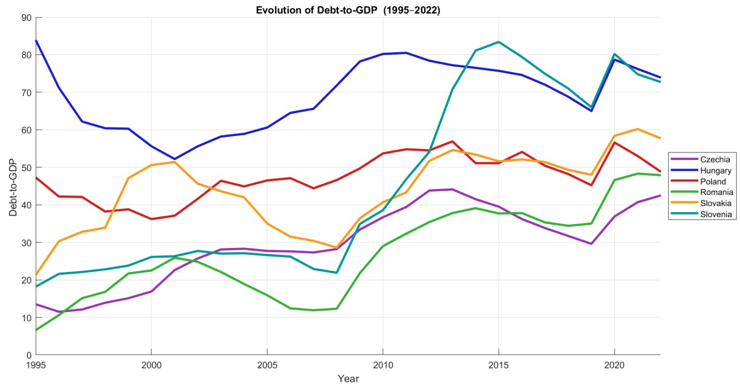

Figure 2: Debt to GDP East European Countries

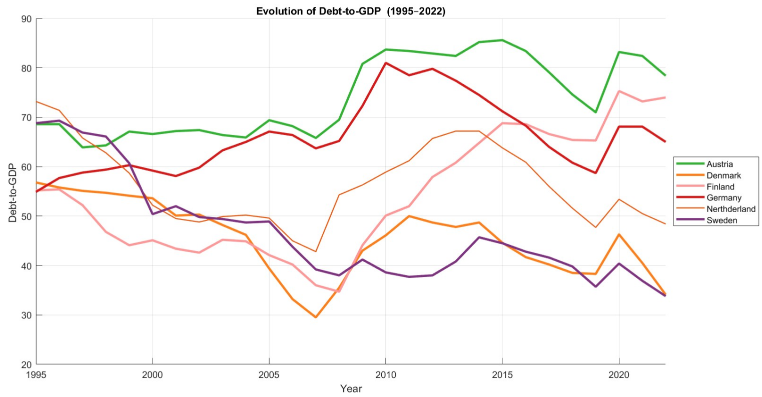

Figure 3: Debt to GDP North European Countries

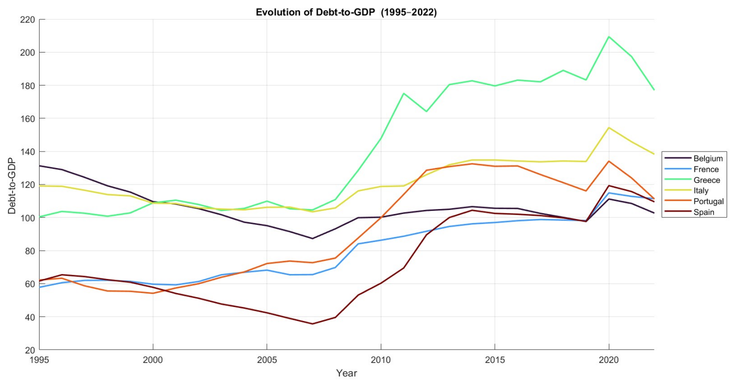

Figure 4: Debt to GDP South European Countries

4 Empirical Strategy

4.1 Empirical strategy and identification overview

This section outlines the empirical strategy used to estimate the macroeconomic effects of fiscal shocks, with a particular focus on green public expenditure and its interaction with public debt conditions.

The analysis is conducted within a panel Smooth-Transition Bayesian VAR (ST-BVAR) framework, which allows the transmission of fiscal shocks to vary across regimes defined by the level of public debt. The objective is to assess whether fiscal multipliers depend on fiscal space, expenditure composition, and regional heterogeneity.

Identification of fiscal shocks relies on a recursive ordering of the variables. This implies that public expenditure does not respond contemporaneously to other macroeconomic shocks within the quarter, allowing innovations in green and non-green spending to be interpreted as unanticipated fiscal shocks.

More specifically, the identification strategy is based on the following assumptions:

A1 Public expenditure is predetermined within the quarter with respect to other macroeconomic innovations.

A2 Identified shocks capture unexpected fiscal variation rather than endogenous policy responses.

A3 Green and non-green spending are defined as mutually exclusive components, ensuring a clean identification of composition effects.

A4 Regime dependence arises from public debt conditions, which affect the propagation of fiscal shocks.

The estimation proceeds by constructing a quarterly panel dataset, estimating the ST-BVAR model with Bayesian methods, identifying structural shocks via Cholesky decomposition, and computing regime-dependent impulse responses and cumulative multipliers.

The following section presents the formal model specification.

4.2 Panel Smooth-Transition Bayesian VAR

We estimate a Panel Smooth-Transition Bayesian VAR (ST-BVAR) to study the regime-dependent transmission of green-spending shocks across European economies(Auerbach and Gorodnichenko, 2012) . The model is defined on a balanced quarterly panel of country-level macroeconomic variables including public green expenditure, total public spending is defined net of green public expenditure (GREEN) (so that the two series are mutually exclusive by construction. This prevents mechanical overlap between green and non-green spending and ensures a clean identification of composition effects) , tax revenues, public debt, business sentiment, sovereign spreads, long-term interest rates, investment, and real GDP.In the model, all fiscal and macroeconomic variables are included in levels (natural logarithms), in line with standard practice in quarterly BVAR applications. This specification preserves the interpretability of coefficients in percentage terms and allows for the construction of cumulative multipliers without imposing stationarity through pre-filtering. Let $y_{i,t}$ denote a $K \times 1$ vector of the endogenous variables for country $i = 1, \ldots, N$ and period $t = 1, \ldots, T$. The system follows a VAR(4) specification with country and year fixed effects:

$$y_{i,t} = B^{(r_{i,t})} X_{i,t} + \alpha_i + \tau_t + \varepsilon_{i,t}^{(r_{i,t})},$$

where $X_{i,t} = (y'_{i,t-1}, \ldots, y'_{i,t-4})'$ is vector of the lagged endogenous variables, α_i and τ_t capture country and year fixed effects, and $r_{i,t} \in \{\text{low}, \text{high}\}$ denotes the prevailing regime.

The regime indicator evolves smoothly as a function of a standardised transition variable $z_{i,t}$ measuring public-debt pressure:

$$G(z_{i,t}) = \frac{1}{1 + \exp[-\gamma(z_{i,t} - c)]}.$$

Following standard practice in the smooth-transition VAR literature, the transition function is calibrated with $\gamma = 3$, ensuring a reasonably fast yet continuous shift across regimes, while the location parameter c is set to the empirical median of $z_{i,t}$, producing two states that approximate low- and high-debt configurations without imposing discrete sample splits. Bayesian estimation follows a Normal–Inverse Wishart setup in which Minnesota-type shrinkage is imposed on the autoregressive coefficients, with own lags shrunk toward persistent dynamics and cross-variable lags penalized more aggressively, and with tightness decreasing in lag order and scaled by relative innovation variances. Country- and year-specific effects are treated as unrestricted coefficients with diffuse variance. The regime-specific innovation covariance matrices Σ_{low} and Σ_{high} are assigned independent inverse-Wishart priors. This estimation strategy is consistent with established Bayesian VAR contributions relying on Normal–Inverse Wishart conjugacy and Minnesota shrinkage (Kadiyala and Karlsson, 1997; Sims and Zha, 1998; Bańbura et al., 2010), and with recent applications of Bayesian smooth-transition VARs and regime-weighting schemes (Bruns and Piffer, 2024).

Posterior simulation is carried out through a Gibbs sampling algorithm. We generate 20,000 draws and discard the first 8,000 iterations as burn-in, retaining only parameter realizations that satisfy standard VAR stability conditions in both regimes (see Appendix B). We use 4 lags.

The identification of green-spending shocks relies on a recursive ordering of the variables and a Cholesky factorization of the pooled covariance matrix of innovations, in line with the standard approach adopted in the fiscal VAR literature (Blanchard and Perotti, 2002; Mountford and Uhlig, 2009). This strategy implies that public green expenditure does not respond contemporaneously to other macroeconomic shocks within the period, while it can affect their dynamic evolution in subsequent periods. Although restrictive, this assumption ensures a transparent and easily interpretable identification scheme, which is particularly well suited to a multi-country panel setting.

The resulting framework is a regime-dependent smooth-transition panel VAR, in which the transmission of green-spending shocks varies as a function of the level of public debt, following the non-linear fiscal modelling literature that emphasizes the role of debt sustainability conditions (Auerbach and Gorodnichenko, 2012, 2013; Ilzetzki et al., 2013; Huidrom et al., 2020). In this setting, the degree of indebtedness governs the probability of operating in regimes characterized by distinct macro-fiscal dynamics, allowing an assessment of how the effectiveness of green spending depends on the available fiscal space. The smooth-transition structure avoids discrete sample splits and allows the effects to vary gradually along the distribution of public debt.

The panel structure of the model further accounts for unobserved heterogeneity across countries and over time, preventing the estimates from being driven by idiosyncratic dynamics in individual economies and exploiting the cross-country dimension to identify common patterns in the transmission of fiscal shocks. Consistent with this framework, the same identification strategy and regime-dependence mechanism are also applied to non-green public spending shocks, defined as the residual component of total public expenditure net of green spending, thereby enabling a direct comparison between the two types of fiscal interventions within a homogeneous empirical setting.

4.3 Eastern Europe: ST-BVAR Results

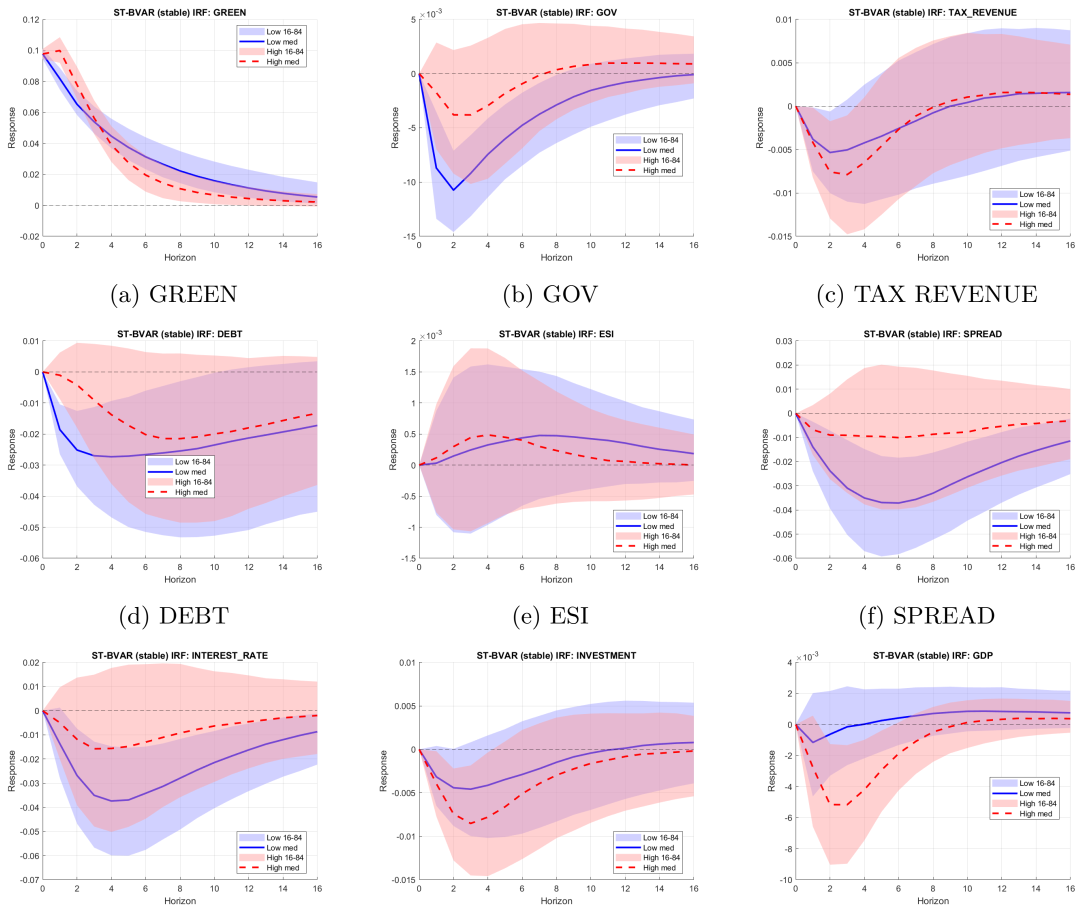

(a) GREEN (b) GOV (c) TAX REVENUE

(d) DEBT (e) ESI (f) SPREAD

(g) INTEREST RATE (h) INVESTMENT (i) GDP

Figure 5: Impulse responses to a green-spending shock: Eastern Europe ST-BVAR (low vs high debt regimes).

In the high-debt regime in Eastern Europe (Figure 5), the impulse response functions indicate that a green-spending shock generates short-run contractionary effects on real activity. Following a positive innovation in green expenditure, non-green government spending declines persistently, suggesting that the increase in the green component occurs through an internal budget reallocation rather than through a net fiscal expansion. Tax revenues initially decrease, consistent with the contraction in economic activity.

Public debt does not display a statistically significant response, indicating that the adjustment operates primarily through changes in expenditure composition rather than through variations in borrowing.

On the real side, both GDP and investment react negatively in the short run. Output remains below zero for approximately six quarters, while investment contracts more sharply and persistently. This pattern is consistent with a transmission mechanism whereby, under tight fiscal constraints, an increase in green spending compresses other components of public demand, generating net restrictive effects in the short term. Moreover, in economies characterized by shallower financial markets and higher perceived sovereign risk, expenditure reallocation may generate uncertainty regarding fiscal priorities, thereby discouraging private investment.

From an economic perspective, green spending in a high-debt regime does not operate as a

Keynesian stimulus, but rather as expenditure substitution, with temporarily recessionary effects before any potential structural benefits can materialize. In the low-debt regime, the green-spending shock does not generate statistically significant macroeconomic effects on GDP or private investment. As in the high-debt case, non-green expenditure declines following the innovation, indicating an internal reallocation of the public budget rather than an overall fiscal expansion.

However, unlike in the high-debt regime, public debt, interest rates, and sovereign spreads decrease, signalling an improvement in financial conditions and a reduction in perceived risk. This suggests that, in the presence of fiscal space, markets interpret green spending as consistent with debt sustainability and a credible fiscal trajectory.

Despite the improvement in financial conditions, these adjustments do not translate into an expansion of real activity. Neither output nor private capital formation exhibits statistically significant responses. This result indicates that, in the absence of a net expansion in public demand, green spending primarily operates as a budget-rebalancing and financial-stabilization measure, without activating a demand-driven multiplier or generating crowding-in effects on private investment in the short run.

In summary, for Eastern Europe green spending does not operate as an automatic expansionary stimulus: what matters is the composition of expenditure rather than its overall level. In the absence of a net fiscal expansion, and especially when financed through internal reallocation, green spending does not generate large multipliers. Debt constraints shape the transmission of the shock, but they do not, in themselves, guarantee positive macroeconomic effects.

4.4 Southern Europe: ST-VAR Results

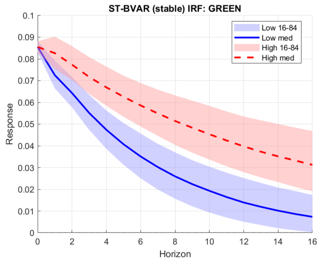

(a) GREEN

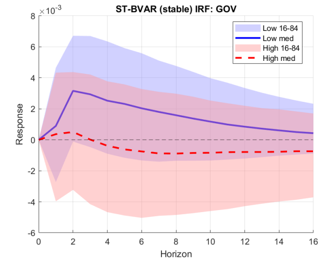

(b) GOV

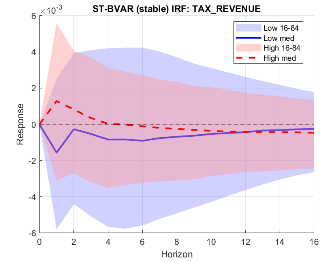

(c) TAX REVENUE

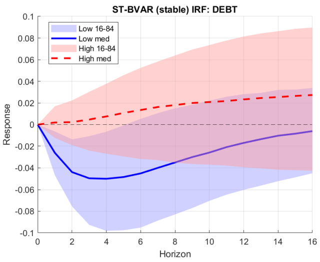

(d) DEBT

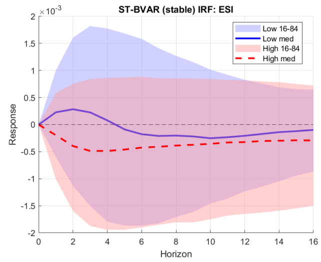

(e) ESI

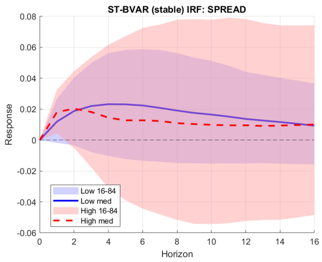

(f) SPREAD

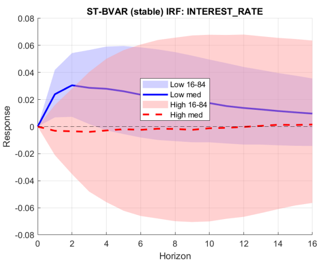

(g) INTEREST RATE

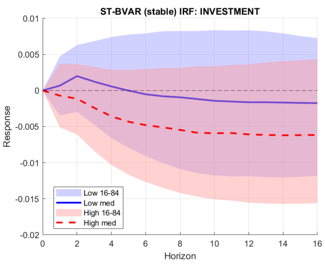

(h) INVESTMENT

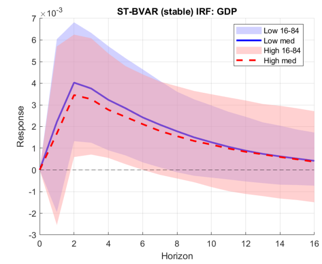

(i) GDP

Figure 6: Impulse responses to a green-spending shock: Southern Europe ST-BVAR (low vs high debt regimes).

In the high-debt regime, the transmission of the green-spending shock operates primarily through a demand-driven mechanism, with a brief activation of the financial channel. The initial increase in sovereign spreads signals a temporary tightening of financing conditions, consistent with precautionary market reactions in a context of elevated public debt. However, the rapid normalization of spreads indicates that the shock does not generate persistent concerns about fiscal sustainability.

On the real side, GDP turns positive with a one-period delay and remains above baseline for several quarters. This suggests that green spending functions as an aggregate-demand stimulus, likely through direct public demand effects and their multiplier impact on consumption and related services. The absence of a systematic response in private investment indicates that the transmission does not operate through an expansion of productive capacity or crowding-in effects, but remains largely confined to the demand side.

Overall, in a high-debt environment, green expenditure does not appear as a reallocation–consolidation device. Instead, it acts as a targeted expansionary intervention that markets tolerate, albeit with an initial temporary risk premium. Under the low-debt regime, the real transmission channel is clearer and more persistent. The increase in GDP is larger and more sustained than in the high-debt regime, indicating that fiscal space amplifies the effectiveness of the shock.

The temporary rise in short-term interest rates may reflect a monetary or financial adjustment to stronger economic activity. At the same time, the decline in public debt over multiple horizons suggests that the expansion is not financed through additional borrowing, but rather supported by favorable growth dynamics relative to financing costs.

Once again, private investment does not exhibit a significant response, indicating that the expansion is primarily driven by public-demand channels rather than by an acceleration of private capital formation. Overall, in the low-debt regime, green spending generates a sustained output expansion without triggering leverage-driven mechanisms or persistent financial stress. The transmission is consistent with a traditional fiscal multiplier operating in a context of fiscal credibility. For Southern Europe, green public spending behaves primarily as an aggregate-demand stimulus rather than as a reallocation–consolidation mechanism. Its effectiveness is stronger in the presence of fiscal space, but even under high-debt conditions the expansionary effects are not offset by persistent financial tensions. The absence of a significant investment channel suggests that the short-run effects are mainly cyclical rather than driven by supply-side capacity expansion.

4.5 Northern Europe: ST-VAR Results

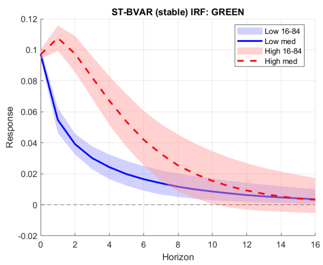

(a) GREEN

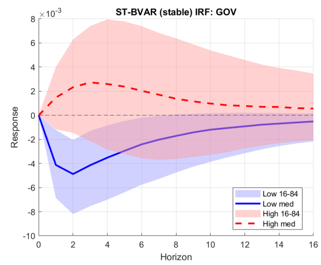

(b) GOV

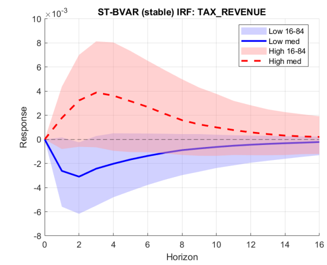

(c) TAX REVENUE

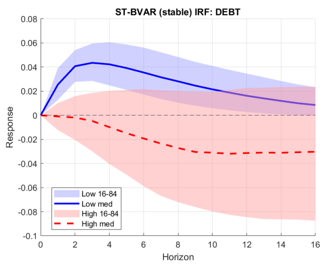

(d) DEBT

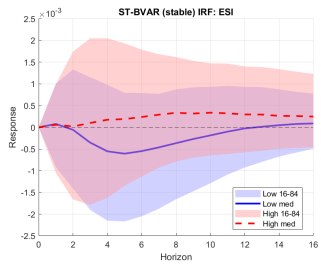

(e) ESI

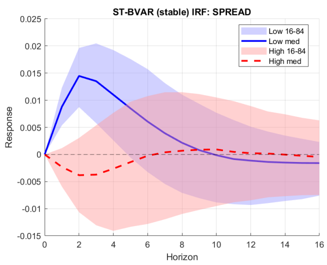

(f) SPREAD

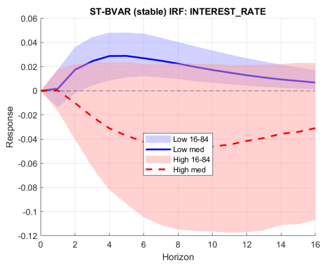

(g) INTEREST RATE

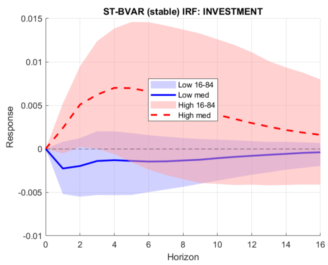

(h) INVESTMENT

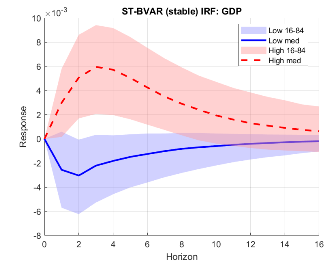

(i) GDP

Figure 7: Impulse responses to a green-spending shock: Northern Europe ST-BVAR (low vs high debt regimes).

In the high-debt regime, Northern European economies display a clearly expansionary transmission mechanism, primarily driven by the aggregate-demand channel. Real GDP turns positive from the second period onwards and remains above baseline for several quarters, indicating a stable short-run multiplier.

The investment channel is only temporarily activated: private investment responds positively on impact but the effect fades quickly. This suggests that the transmission does not operate through a persistent expansion of productive capacity, but rather through a direct demand impulse that propagates to income and consumption.

The financial channel remains largely neutral: sovereign spreads do not exhibit significant tensions and no persistent tightening in financing conditions is observed. This is crucial. It implies that in Northern European economies even relatively high levels of debt are not perceived as a sustainability risk. In other words, the "high-debt regime" does not represent a binding fiscal constraint, but rather reflects cyclical conditions.

From an economic perspective, green spending in this context behaves as a traditional Keynesian stabilizer, supported by strong fiscal credibility and the absence of financial frictions.

Under the low-debt regime, the transmission mechanism changes substantially.

Here, the shock does not primarily operate through the real economy, but rather through financial and debt-accumulation channels. Public debt increases persistently and long-term interest rates rise for several periods, indicating that the expansion is financed through additional borrowing and incorporated into bond pricing.

The decline in non-green expenditure suggests a partial internal budget reallocation. However, this compositional adjustment does not translate into a robust real expansion. GDP does not display a strong or persistent response, and other macroeconomic variables fluctuate around zero.

The transmission mechanism therefore differs from the high-debt regime:

- it is not driven by a demand multiplier;
- it does not operate through a sustained investment channel;
- it primarily reflects financial pricing and debt accumulation.

In economies characterized by ample fiscal space and an already relatively high share of green expenditure, additional increases tend to crowd out other components or generate diminishing marginal effects. From a macroeconomic perspective, the multiplier is lower because the economy does not exhibit significant slack.

In Northern Europe, public debt levels do not constitute a binding credibility constraint. The difference between regimes reflects cyclical conditions and structural characteristics rather than sustainability concerns:

- Under high debt (likely associated with weaker cyclical conditions), green spending operates as a demand-side stabilizer.
- Under low debt (a context of solid economic conditions and strong public finances), the shock mainly feeds into debt accumulation and interest rate adjustments, without producing significant real effects.

In sum, the macroeconomic effectiveness of green spending in Northern Europe depends more on cyclical slack than on debt levels per se. Fiscal constraints are not the dominant transmission channel; rather, the presence or absence of unused capacity and the composition of expenditure shape the response.

4.6 European Union : ST-VAR Results

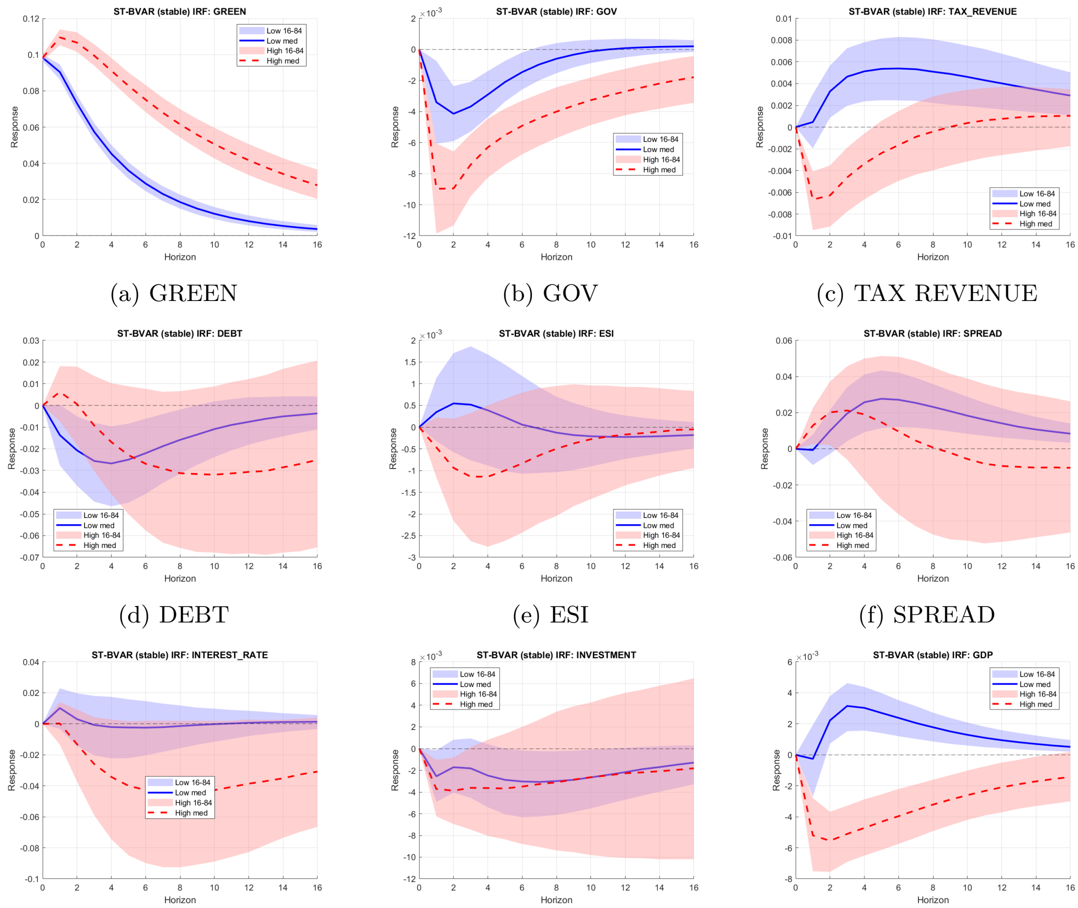

(a) GREEN (b) GOV (c) TAX REVENUE

(d) DEBT (e) ESI (f) SPREAD

(g) INTEREST RATE (h) INVESTMENT (i) GDP

Figure 8: Impulse responses to a green-spending shock: European Union ST-BVAR (low vs high debt regimes).

In the aggregate EU panel, under the high-debt regime, the transmission of the green-spending shock assumes a predominantly contractionary configuration in the short and medium run. Real GDP is significantly negative throughout the entire horizon considered, indicating a persistent decline in aggregate activity.

The dominant mechanism is that of internal budget reallocation: non-green expenditure contracts systematically and persistently, suggesting that the increase in the green component occurs through substitution across spending categories rather than through a net fiscal expansion. In the absence of an overall increase in public demand, the direct impulse from green spending is offset by the compression of other expenditure components.

The decline in private investment during the initial periods signals short-run crowding-out effects, likely linked to weaker aggregate demand or uncertainty regarding fiscal priorities. The reduction in tax revenues over the first horizons is consistent with the contraction in GDP and indicates a temporary weakening of the fiscal base.

The initial increase in sovereign spreads suggests a short-lived tightening in financial conditions, which may have amplified the restrictive dynamics, although without generating persistent financial stress.

Overall, under high-debt conditions, green spending in the EU panel does not translate into an expansion of aggregate demand. The net effect reflects the interaction between internal budget reallocation and adverse macroeconomic dynamics, which dominate the direct expansionary impulse.

Under the low-debt regime, the transmission mechanism changes significantly and assumes an expansionary configuration.

Real GDP increases persistently across the entire horizon considered, indicating a stable and positive multiplier. At the same time, tax revenues rise significantly and continuously, signaling a strengthening of the fiscal base.

Public debt declines systematically despite the increase in green expenditure. This suggests that the expansion is not accommodated through additional borrowing but is instead supported by favorable growth dynamics and improvements in tax revenues.

Non-green expenditure contracts persistently, indicating systematic reallocation toward the green component. However, unlike the high-debt regime, this compositional shift does not generate contractionary effects; instead, it is accompanied by an expansion in economic activity.

The persistent increase in sovereign spreads does not appear consistent with sustainability concerns, but rather with financial repricing in a context of stronger economic performance. The absence of a significant private investment response suggests that transmission operates primarily through income and aggregate-demand effects rather than through an immediate expansion of productive capacity. In the EU panel, the level of public debt shapes the way the shock is transmitted to the real economy.

- Under high debt, binding fiscal conditions induce internal budget reallocation that does not translate into net aggregate-demand expansion. The substitution effect dominates the direct spending impulse, producing contractionary outcomes.
- Under low debt, the availability of fiscal space allows green spending to support output and strengthen the tax base, leading to a reduction in the debt-to-GDP ratio through growth effects.

From a macroeconomic perspective, the effectiveness of green spending depends on the fiscal environment in which it is implemented. When fiscal space is available, compositional effects and the expansion of the tax base can dominate potential crowding-out effects. When debt levels are elevated, internal reallocation and financial conditions may attenuate or reverse the initial expansionary impulse.

4.7 Measuring Green Fiscal Multipliers

In the empirical fiscal policy literature, a central step for assessing the macroeconomic effects of government spending shocks is the construction of *fiscal multipliers*, which measure the variation in output generated by a one–unit variation in public expenditure. The multiplier therefore summarises the dynamic transmission from an exogenous fiscal shock to real activity.

An important distinction concerns how multipliers are computed. Studies adopting a narrative identification typically implement an ex ante normalisation, ensuring that GDP and government spending are measured in the same units before estimation. Following Hall (2009) and Barro and Redlick (2011), Ramey and Zubairy (2018) rescales percentage changes in output and spending using the current G/Y ratio, so that VAR coefficients can be directly interpreted in levels.

By contrast, the dominant tradition in structural VARs and in local–projection methods defines multipliers *ex post* as the ratio between the cumulative impulse responses of output and government spending. This approach originates with Blanchard and Perotti (2002) and is widely used in subsequent applications, including Mountford and Uhlig (2009) and the state–dependent estimates of Auerbach and Gorodnichenko (2012, 2013). In this framework, the multiplier at horizon h is given by:

$$M(h) = \frac{\sum_{j=0}^{h} \mathrm{IRF}_Y(j)}{\sum_{j=0}^{h} \mathrm{IRF}_G(j)} \times \frac{\overline{Y}}{\overline{G}}, \tag{2}$$

where $\sum_{j=0}^{h} \mathrm{IRF}_Y(j)$ and $\sum_{j=0}^{h} \mathrm{IRF}_G(j)$ denote the cumulative responses of output and spending, and $\overline{Y}/\overline{G}$ is the sample mean ratio between GDP and government expenditure.

In our analysis, we adopt this *ex post* definition, computing multipliers from cumulative IRFs identified through the ST–BVAR model. This choice is consistent with structural multiplier estimation in the existing literature and allows a transparent interpretation of the short–run effects of green fiscal expansions in terms of realised output responses.

Table 1: Cumulative multipliers of a green spending shock (Eastern Europe, by debt regime)

	GDP		**Private investment**	
Years after shock	**Low debt**	**High debt**	**Low debt**	**High debt**
0	0.000	0.000	0.000	0.000
1	-0.325	**-2.713**	-2.763	**-4.349**
2	0.004	**-3.110**	-3.333	-6.088
3	0.377	**-2.874**	-3.093	-6.505
4	0.693	-2.620	-2.660	-6.535

In Eastern European countries, green-spending shocks do not generate positive or statistically significant cumulative multipliers on GDP. Under the low-debt regime, the effects remain weak and fluctuate around zero, without consolidating into an expansionary dynamic. Under the high-debt regime, multipliers are systematically negative, consistent with a restrictive transmission driven by budgetary reallocation rather than aggregate-demand stimulus. In both regimes, private-investment multipliers remain negative, indicating the absence of a credible crowding-in mechanism and a limited reaction of the private sector to green fiscal interventions (see Appendix C).

Table 2: Cumulative multipliers of a green spending shock (Southern Europe, by debt regime)

	GDP		**Private investment**	
Years after shock	**Low debt**	**High debt**	**Low debt**	**High debt**
0	**0.00**	0.000	0.000	0.000
1	**4.687**	**3.347**	**1.57**	**-2.32**
2	**5.683**	**3.590**	**0.55**	**-5.13**
3	**5.895**	**3.420**	**-0.77**	**-7.43**
4	**5.966**	3.184	**-2.08**	-9.443

In Southern European economies, cumulative GDP multipliers are positive and statistically significant in both the low-debt and high-debt regimes. The expansionary effect is considerably stronger under low debt: after four years the cumulative multiplier approaches a value around six, signalling a persistent and sizeable boost to aggregate activity following a green-spending shock. Under high debt, the cumulative multiplier stabilises around three, indicating that fiscal stimulus is attenuated but remains clearly expansionary. Overall, the evidence contradicts the notion of non-Keynesian effects in high-debt environments and suggests that green public spending supports demand even when debt burdens are elevated.This suggests that such expenditure may be perceived differently from conventional fiscal expansions. Rather than being interpreted as a deterioration of fiscal sustainability, green spending appears to be priced as growth-enhancing or investment-type expenditure, capable of supporting medium-term output prospects and stabilising debt dynamics. This differentiated perception may explain why adverse expectation effects do not materialise in high-debt Southern economies.

For private investment, the evidence points to a more nuanced pattern consistent with nonlinear fiscal transmission. In the low-debt regime, multipliers are positive and statistically significant in the first and second year, indicating an initial phase of crowding-in. However, they turn negative in the third and fourth year and are no longer statistically distinguishable from zero, suggesting that the effect fades out and may even reverse in the medium run. In the high-debt regime, multipliers remain negative throughout the entire horizon, with statistically significant effects in the second and third year and non-significance in the fourth, pointing to a form of attenuated crowding-out that does not generate lasting reactions but reflects tighter financial and budgetary conditions.

In sum, the green spending expansion in Southern Europe activates a robust and persistent GDP multiplier, whereas the investment channel is conditional on fiscal space: initially supportive under low debt, and quickly fragile or negative under high debt (see Appendix C).

Table 3: Cumulative multipliers of a green spending shock (Northern Europe, by debt regime)

	GDP		**Private investment**	
Years after shock	**Low debt**	**High debt**	**Low debt**	**High debt**
0	0.000	0.000	0.000	0.000
1	-4.75	**5.29**	-4.13	6.69
2	-5.59	**7.08**	-5.97	10.97
3	-5.83	**7.81**	-7.15	13.32
4	-5.89	**8.18**	-7.66	14.68

In Northern European economies, cumulative GDP multipliers exhibit a strong regime dependence. In the low-debt regime, multipliers are sizeable and persistently negative, pointing to contractionary effects of green spending over the four-year horizon. By contrast, in the high-debt regime the multipliers are large and positive, suggesting an expansionary response of output when public debt is elevated. This pattern is consistent with a regime-switching environment in which the macroeconomic impact of green fiscal shocks crucially depends on the underlying debt conditions.

For private investment, cumulative multipliers are negative under low debt and positive under high debt. Only the first two years of the high-debt investment multipliers are statistically significant, while longer-horizon responses become imprecisely estimated. As a result, the evidence points to short-run crowding-in of private investment in high-debt episodes, but does not support strong conclusions about longer-term capital-formation dynamics (see Appendix C).

Table 4: Cumulative multipliers of a green spending shock (18 European countries, annual horizons, by debt regime)

	GDP		**Private investment**	
Years after shock	**Low debt**	**High debt**	**Low debt**	**High debt**
0	0.000	0.000	0.000	0.000
1	**2.309**	**-4.28**	-2.476	**-3.10**
2	**3.792**	**-4.77**	-4.597	-3.778
3	**4.50**	**-4.86**	**-6.261**	-4.128
4	**4.868**	**-4.90**	**-7.277**	-4.405

Cumulative GDP multipliers across the full European sample display a stark debt-regime asymmetry. In the low-debt regime, the annualised multipliers turn positive and grow steadily over time, approaching a value close to five after four years. This trajectory suggests a persistent expansionary impact of green-spending shocks when fiscal space is available.

In the high-debt regime, the cumulative GDP multipliers are persistently negative and increasingly large in absolute value, reaching roughly –5 after four years. The pattern indicates contractionary dynamics in high-debt environments, consistent with tighter macro-financial constraints and limited stimulus transmission. Overall, the multipliers associated with green public expenditure appear relatively large, in line with recent empirical evidence (Batini et al., 2022; Ciaffi, 2025; Shah and Wu, 2025).

The investment multipliers are negative in both high-debt and low-debt regimes. However, in the low-debt regime they are statistically significant across the entire four-year horizon, whereas in the high-debt regime significance is limited to the first two years. This points to an evident absence of crowding-in: the private sector does not respond to the green stimulus in a way that reinforces public spending, and in high-debt environments the reaction deteriorates rapidly (see Appendix C).

5 Conventional spending shock.

To complement the analysis of green fiscal shocks, we construct a conventional spending shock obtained by excluding climate–related expenditure from total government spending. The purpose is to disentangle the macroeconomic transmission of environmental spending from the broader dynamics generated by standard fiscal interventions. We therefore isolate a conventional component of government expenditure, defined as total public spending net of explicitly green allocations, and estimate its associated structural shock following the same identification strategy used for the green series.

This conventional shock serves two analytical objectives. First, it allows us to assess whether the macroeconomic responses attributed to environmental spending merely reflect ordinary fiscal demand effects. Second, it provides a counterfactual measure to evaluate whether green expenditure produces stronger or weaker multipliers than traditional government spending. The resulting comparison isolates the climate–policy transmission channel from generic fiscal stimulus and helps clarify the heterogeneous debt–regime responses documented in the paper.

5.1 Total Government shock Eastern Europe: ST-VAR Results

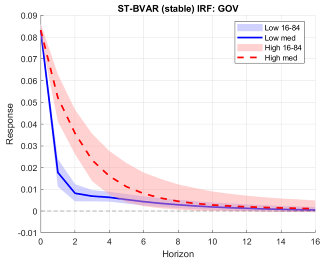

(a) GOV

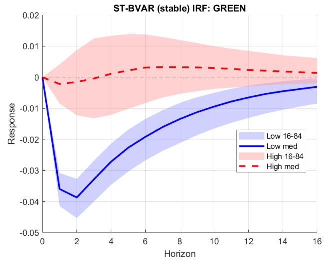

(b) GREEN

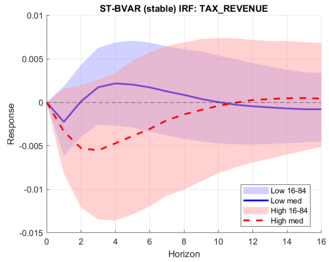

(c) TAX REVENUE

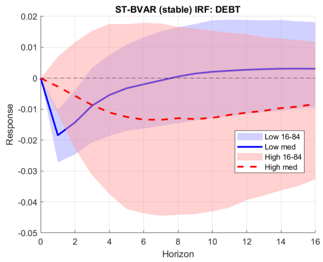

(d) DEBT

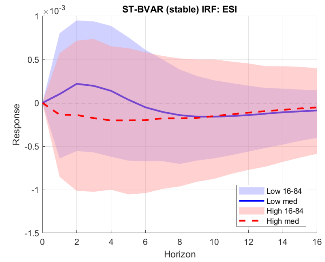

(e) ESI

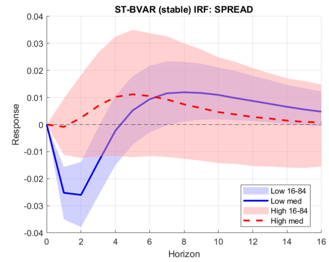

(f) SPREAD

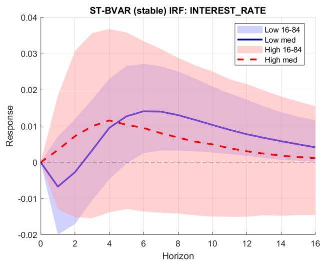

(g) INTEREST RATE

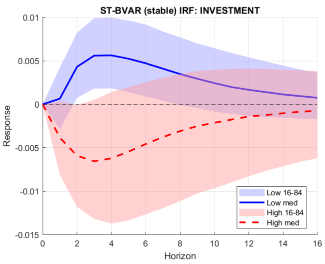

(h) INVESTMENT

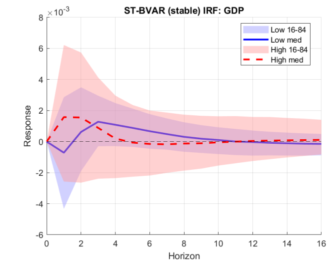

(i) GDP

Figure 9: Impulse responses to a Total Government Shock: Eastern Europe ST-BVAR (low vs high debt regimes).

The impulse–response functions (Figure 9) show that, for the East European panel, a non-green public spending shock generates limited macroeconomic effects that depend critically on the public-debt regime, activating primarily financial and budget-composition channels rather than a traditional expansionary aggregate-demand channel.

In the high-debt regime, the shock leads to an increase in public debt that is statistically significant for about six periods, accompanied by a rise in interest rates, while sovereign spreads do not display statistically significant responses. This configuration indicates that markets do not revise sovereign risk premia upward, but react to higher public financing needs through a general increase in yields. As a result, financial conditions tighten, constraining the real transmission of the shock: GDP does not exhibit significant responses and the overall macroeconomic impact remains weak. In this regime, non-green spending operates mainly through an interest-rate channel, generating macro-restrictive effects despite the absence of overt financial stress.

In the low-debt regime, responses are more articulated. While GDP displays a contraction that is not statistically significant over the entire horizon, private investment increases significantly between the second and eighth periods. On the financial side, sovereign spreads compress significantly from the early horizons and throughout the response window, whereas interest rates decline only temporarily, with statistically significant effects concentrated in the intermediate periods. Public debt shows a temporary initial improvement, consistent with ample fiscal space. Overall, the low-debt regime is characterised by an easing of financial conditions that supports private investment, without translating into a statistically significant expansion of aggregate economic activity.

The apparent divergence between investment and output dynamics in the low-debt regime can be explained by the nature of the activated transmission channels. The compression of sovereign spreads reflects a reduction in perceived risk and an immediate improvement in financing conditions, stimulating capital accumulation through a risk-premium channel rather than through aggregate-demand expansion. The response of interest rates is slower and more limited in magnitude, indicating that investment decisions are driven primarily by lower risk rather than by direct monetary accommodation. At the same time, the absence of a net fiscal expansion and the contraction of green expenditure weakens the pass-through from investment to output. As a result, higher investment does not translate into statistically significant GDP growth in the short to medium run.

Overall, the IRF evidence suggests that non-green public spending fails to activate a Keynesian demand channel under either debt regime. When public debt is high, the shock tightens financial conditions through higher interest rates; when fiscal conditions are more favourable, it generates financial easing that supports investment but remains disconnected from real economic activity. These findings point to weak and selective fiscal transmission, consistent with the emergence of fiscal multipliers below unity even in low-debt environments.

5.2 Total Government Shock Southern Europe : ST-VAR Results

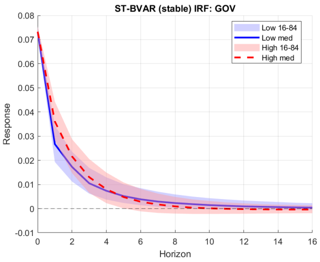

(a) GOV

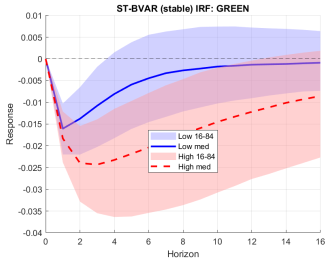

(b) GREEN

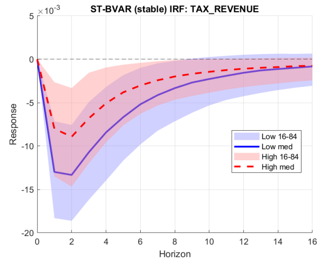

(c) TAX REVENUE

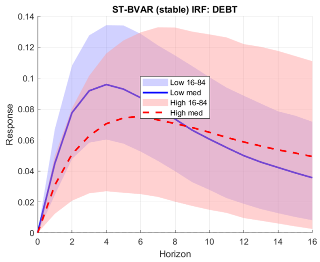

(d) DEBT

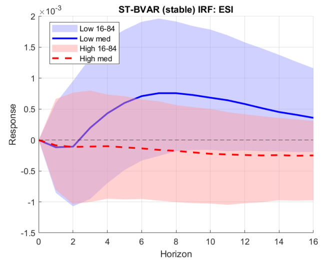

(e) ESI

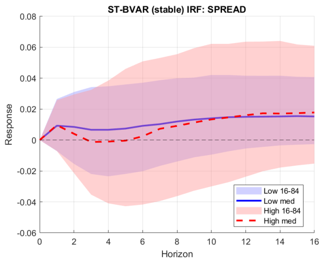

(f) SPREAD

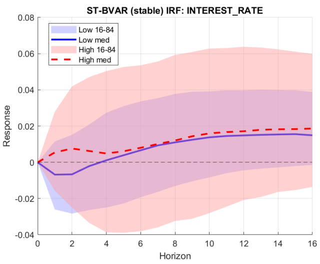

(g) INTEREST RATE

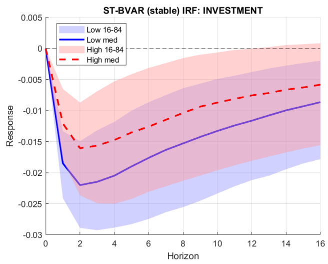

(h) INVESTMENT

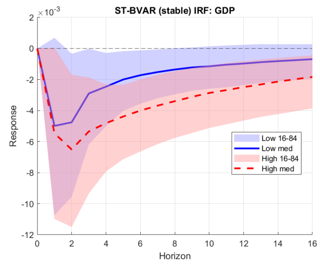

(i) GDP

Figure 10: Impulse responses to a Total Government Shock: Southern Europe ST-BVAR (low vs high debt regimes).

The impulse responses indicate that a non-green government spending shock in South European Countries (figure 10) does not stimulate economic activity in high-debt environments. Public liabilities rise immediately and display strong persistence over the medium term, in the absence of any compensating fiscal adjustment on the revenue side. Private investment reacts negatively over the first eight horizons, consistent with crowding-out effects driven by tighter financial conditions. Output remains below baseline throughout the twelve-period window, suggesting that higher public expenditure financed through costly debt issuance fails to support aggregate demand. Notably, neither sovereign spreads nor long-term interest rates exhibit statistically significant responses, indicating that the weak macroeconomic performance does not stem from an immediate deterioration in market financing conditions. Overall, the evidence points to a low-efficiency fiscal intervention, in which additional spending primarily raises sovereign risk without generating meaningful real activity gains. The results for the low-debt regime closely mirror the dynamics observed under high-debt conditions in terms of fiscal, financial, and investment responses: public liabilities rise persistently, taxation does not provide compensating adjustment, and private investment records statistically significant crowding-out effects in the short and medium run. However, in contrast with the high-debt case, the output response is not statistically distinguishable from zero at any horizon. This indicates that, when debt sustainability is not a binding constraint, non-green spending shocks fail to generate real activity gains but also do not induce the contractionary outcomes observed in high-debt environments,for the behavior of the gdp in two regimes the same results are found in the literature (Ilzetzki et al., 2013; Huidrom et al., 2020).

5.3 Total Government Shock Northern Europe : ST-VAR Results

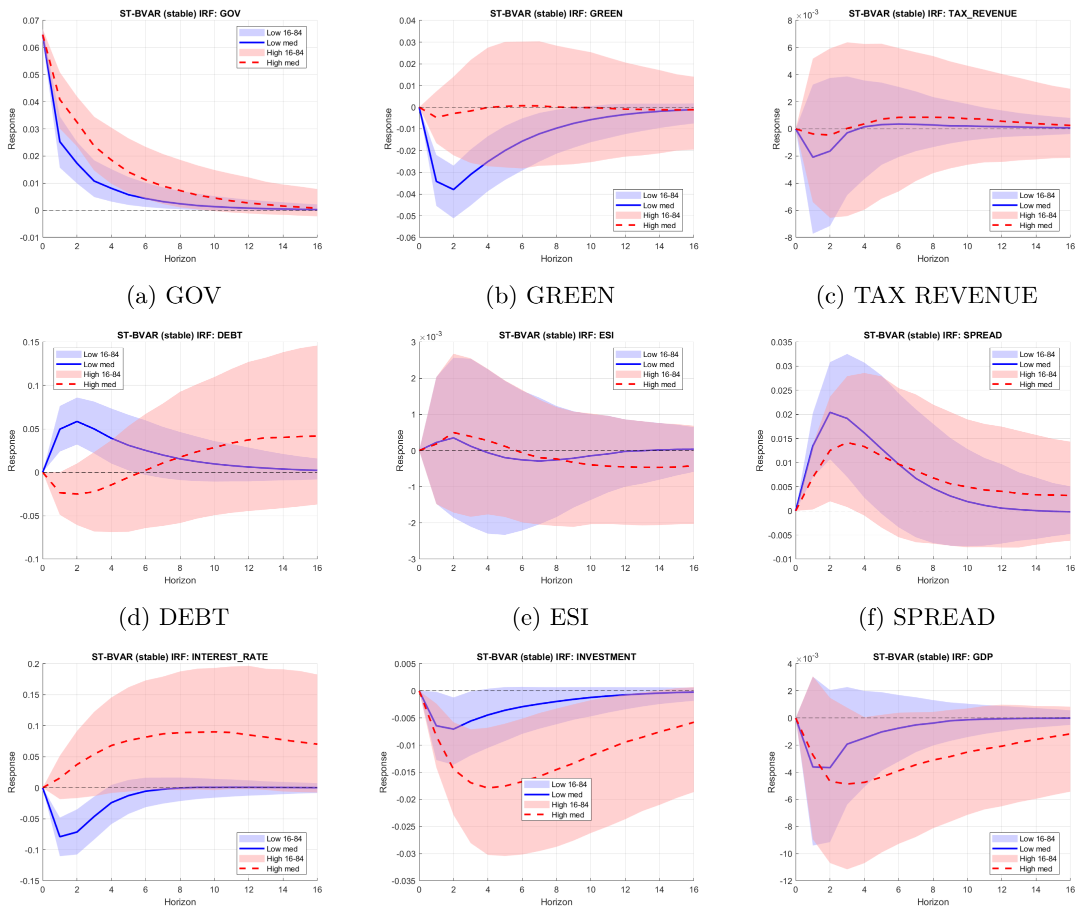

(a) GOV (b) GREEN (c) TAX REVENUE

(d) DEBT (e) ESI (f) SPREAD

(g) INTEREST RATE (h) INVESTMENT (i) GDP

Figure 11: Impulse responses to a Total Government Shock: Northern Europe ST-BVAR (low vs high debt regimes).

The impulse–response functions indicate that, in Northern European economies (figure 11), a non-green public spending shock does not propagate primarily through a Keynesian aggregate-demand channel. Instead, it activates fiscal, financial, and budget-composition mechanisms, whose strength crucially depends on the prevailing public-debt regime.

In the high-debt regime, the shock generates a persistent and statistically significant contraction in private investment, while no meaningful responses emerge for GDP or other real macroeconomic variables. This pattern is consistent with the activation of an intertemporal crowding-out channel, whereby the increase in public financing needs and expectations of future fiscal adjustment worsen private-sector investment conditions. Sovereign spreads rise only in the very short run, indicating an immediate but transitory market reaction that does not evolve into a sustained loss of fiscal credibility, yet is sufficient to reinforce the contractionary effects on investment. Overall, under high-debt conditions, the shock operates as macro-restrictive, despite the absence of prolonged financial stress.

In the low-debt regime, the transmission of the shock takes a qualitatively different form but remains weak overall. Green expenditure contracts significantly, pointing to the activation of a fiscal reallocation channel rather than a net budgetary expansion. Public debt increases temporarily, while sovereign spreads and long-term interest rates move in opposite directions in the short run, reflecting an adjustment in financial conditions in which fiscal tensions are partially offset by an accommodative monetary-financial response. However, this easing does not translate into real economic effects, as none of the main macroeconomic variables displays persistent responses.

Taken together, the IRF evidence suggests that, in Northern European economies, non-green public spending shocks fail to activate an expansionary aggregate-demand channel under either debt regime. When public debt is high, such shocks mainly trigger investment crowding-out; when fiscal conditions are more favourable, they lead to temporary adjustments in spending composition and financial conditions, without generating durable macroeconomic effects.

5.4 Total Government Shock European Union : ST-VAR Results

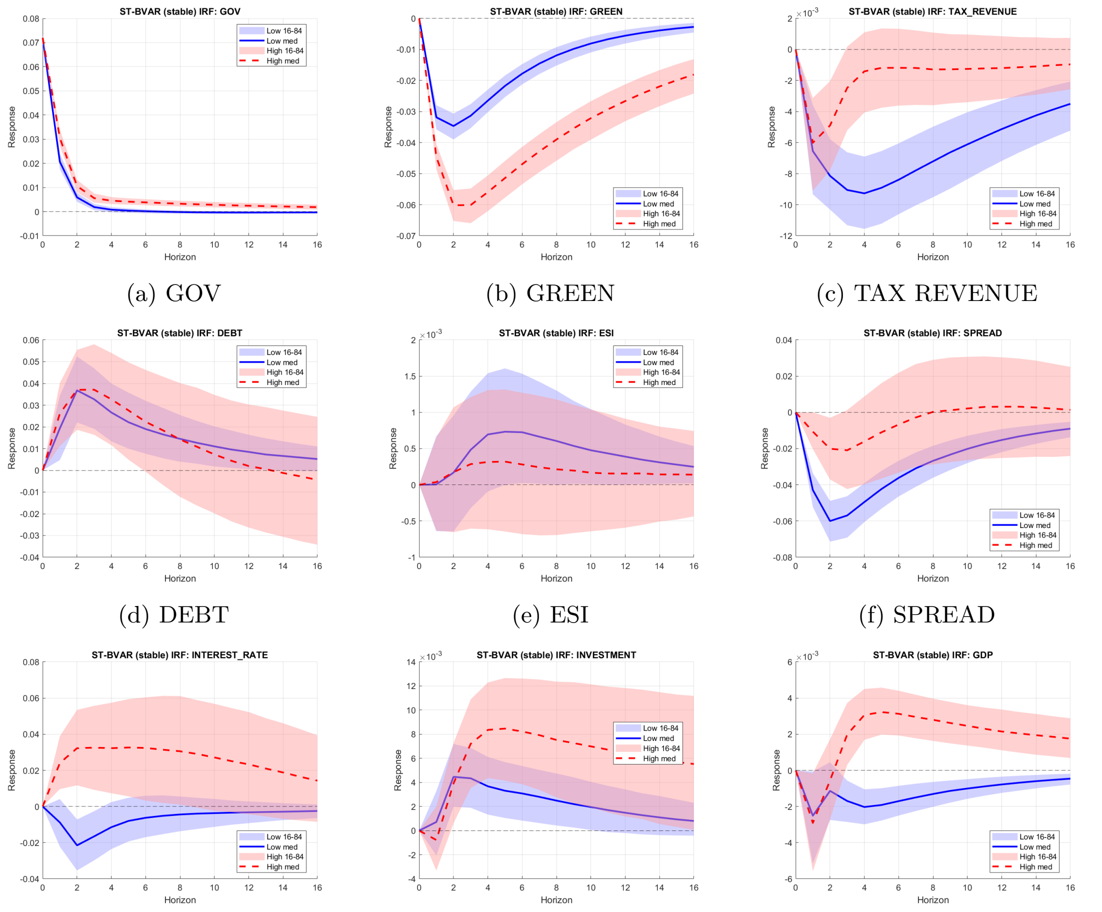

(a) GOV (b) GREEN (c) TAX REVENUE

(d) DEBT (e) ESI (f) SPREAD

(g) INTEREST RATE (h) INVESTMENT (i) GDP

Figure 12: Impulse responses to a Total Government Shock: European Union ST-BVAR (low vs high debt regimes).

In the high-debt regime in the European Union (Figure 12), the non-green spending shock deteriorates the fiscal position (lower green expenditure, reduced revenues, higher public debt, and rising interest rates), yet GDP and private investment increase persistently. This pattern suggests a reaction driven by expectations rather than by financing conditions. Financial transmission remains weak, while real-side propagation is active.

The absence of a persistent increase in sovereign spreads indicates that the shock is not interpreted as a structural deterioration of fiscal sustainability. Forward-looking agents may therefore perceive the fiscal loosening as temporary or embedded within a credible macro-fiscal framework, mitigating expectations of future restrictive adjustment. In this context, private investment expands despite worsening fiscal indicators, pointing to an expectations-based transmission mechanism rather than to a conventional interest-rate or credit channel.

An additional plausible interpretation is that high-debt regimes may coincide with adverse cyclical conditions. If the shock occurs during a negative phase of the business cycle, characterised by economic slack and weak private demand, the observed expansion may reflect the countercyclical effects of fiscal policy rather than an improvement in fiscal fundamentals. In such circumstances, the absence of persistent financial stress allows the fiscal impulse to operate despite deteriorating budget indicators. While the present analysis does not directly identify the cyclical position of the economy at the time of the shock, this mechanism is consistent with the stabilising role of fiscal policy during downturns documented in the literature (Auerbach and Gorodnichenko, 2012) .

In the low-debt regime, the shock generates the opposite configuration: investment rises, supported by improved financial conditions (declining spreads and lower interest rates), but GDP falls persistently, indicating that the expansion of private capital does not translate into an aggregate-demand impulse. This dynamic is consistent with an internal reallocation of expenditure that does not produce a net fiscal expansion.

In this regime, the dominant transmission mechanism operates through a risk-premium channel: declining spreads reduce the perceived cost of capital and stimulate investment. However, the absence of an overall fiscal expansion and the contraction in green expenditure suggest that the shock primarily induces a shift in the composition of public spending rather than a demand stimulus. As a result, improved financing conditions lead to higher capital accumulation without activating a self-sustaining multiplier process, explaining the negative GDP dynamics despite stronger investment.

Overall, at the aggregate EU level, non-green spending shocks operate through regime-dependent channels: in the high-debt regime, expectations-driven transmission, potentially reinforced by adverse cyclical conditions; in the low-debt regime, financial and compositional mechanisms that fail to activate aggregate demand. In neither case does the evidence support the emergence of a standard, self-sustaining Keynesian multiplier.

5.5 Total Government Fiscal Multipliers

To assess the effectiveness of the shock, this section reports government spending multipliers for the different areas considered. This allows us to evaluate the extent to which the responses identified in the IRFs translate into cumulative and comparable effects across regimes.

Table 5: Government spending multipliers on GDP and private investment Eastern Europe

	GDP		Private investment	
Horizon	Low debt	High debt	Low debt	High debt
Impact	0.000	0.000	0.000	0.000
1 year	0.045	0.048	**0.32**	-0.259
2 years	0.081	0.037	**0.59**	-0.397
3 years	0.081	0.035	**0.71**	-0.456
4 years	0.072	0.037	0.770	-0.482

The multipliers confirm a very weak aggregate-demand channel in Eastern European economies: output responses remain well below 0.1 across all horizons and are statistically insignificant in both regimes, indicating that non-green expenditure does not translate into meaningful GDP gains. By contrast, private investment reacts positively and monotonically only in low-debt environments, with long-term multipliers approaching 0.8, while remaining negative in high-debt regimes, consistent with crowding-out effects. Overall, fiscal space governs the sign of capital accumulation, but even under favourable conditions magnitudes stay far below unity. These results suggest that in Eastern Europe non-green public spending non substantial real activity effects (see Appendix C).

Table 6: Government spending multipliers on GDP and private investment in Southern Europe

	GDP		Private investment	
Horizon	Low debt	High debt	Low debt	High debt
Impact	0.000	0.000	0.000	0.000
1 year	**-0.22**	**-0.29**	**-1.22**	**-0.77**
2 years	**-0.29**	**-0.46**	**-2.02**	**-1.31**
3 years	**-0.33**	**-0.6**	**-2.61**	**-1.72**
4 years	**-0.37**	**-0.709**	**-3.073**	**-2.06**

In Southern Europe, the multipliers indicate contractionary dynamics: GDP responses are negative and statistically significant in both regimes, pointing to a widespread sensitivity to fiscal stress. Private investment exhibits large and persistent negative multipliers across regimes, consistent with crowding-out and risk-pricing mechanisms. The deterioration is stronger in low-debt environments, suggesting that additional public spending neither anchors expectations nor complements private capital. Overall, non-green fiscal expansions increase macro-financial fragility rather than stimulating economic activity in Southern Europe (see Appendix C).

Table 7: Government spending multipliers on GDP and private investment in Northern Europe

	GDP		Private investment	
Horizon	Low debt	High debt	Low debt	High debt
Impact	0.000	0.000	0.000	0.000
1 year	-0.172	-0.192	**-0.37**	**-0.64**
2 years	-0.191	-0.29	**-0.49**	**-1.11**
3 years	-0.191	-0.354	-0.536	**-1.42**
4 years	-0.190	-0.395	-0.551	**-1.63**

In Northern Europe, fiscal multipliers do not generate expansionary effects. Output responses remain negative and statistically insignificant in both debt regimes, indicating the absence of a demand channel. Private investment also displays negative multipliers, but statistical significance emerges only in high-debt environments, where values deteriorate to roughly -1.6 at longer horizons. Overall, non-green fiscal expansions appear to reinforce financial tightening rather than capital accumulation in Northern Europe (see Appendix C).

Table 8: Government spending multipliers on GDP and private investment in the full EU panel

	GDP		Private investment	
Horizon	Low debt	High debt	Low debt	High debt
Impact	0.000	0.000	0.000	0.000
1 year	**-0.14**	**0.02**	**0.26**	**0.31**
2 years	**-0.27**	**0.20**	**0.50**	**0.75**
3 years	**-0.35**	**0.31**	**0.65**	**1.07**
4 years	**-0.41**	**0.40**	**0.75**	**1.32**

In the full EU panel, non-green fiscal expansions generate systematically weak real effects. Output multipliers are positive in high-debt clusters and negative in low-debt clusters, yet in both cases remain well below unity, indicating that additional public expenditure does not translate into proportionate GDP gains. Private investment displays a clear regime asymmetry: in low-debt environments multipliers stay below one, consistent with financial crowding-out, whereas in high-debt environments they exceed one over medium horizons, suggesting a crowding-in mechanism. This pattern confirms what has emerged in the literature: under conditions of economic slack, higher fiscal multipliers can be observed, with more pronounced effects than in phases where productive capacity is closer to full utilization. Overall, even where capital formation reacts favourably, the magnitudes remain modest, underscoring the limited aggregate-demand role of non-green expenditure in the EU (see Appendix C).

6 Conclusions

Across the European sample, the empirical evidence reveals pronounced heterogeneity in fiscal transmission. Southern, Northern and Eastern Europe display distinct output–investment configurations, with debt regimes either amplifying or dampening the aggregate-demand channel in a non-uniform manner. The comparison across spending types reinforces this fragmentation: green expenditure delivers systematically higher multipliers than total spending, indicating that agents attach different expectations and risk assessments to climate-related interventions. This mechanism is particularly evident in Southern Europe, where tighter fiscal space magnifies the contrast between green and non-green shocks. In Northern Europe, by contrast, the green shock becomes more powerful under high-debt conditions, suggesting that climate measures gain traction primarily during recessionary phases when economic slack is substantial and expectations of future consolidation support private responses; however, this result requires further scrutiny to assess robustness and to isolate the underlying channels. Finally, although green spending produces high GDP multipliers, the behaviour of private investment indicates that part of the transmission does not rely solely on an immediate cyclical boost, but also reflects expectations of technological adjustment and future profitability associated with the climate transition.

Overall, the results carry relevant implications for fiscal design. First, expenditure composition matters more than aggregate size: green spending generates systematically higher multipliers than non-green expenditure, suggesting that climate-related investment can perform both an environmental function and a macroeconomic stabilization role. By contrast, non-green expansions tend to produce weak effects that are strongly dependent on the prevailing debt regime. This is consistent with the broader evidence showing that fiscal multipliers vary significantly with the composition of expenditure (Ramey, 2019; Blanchard and Leigh, 2013). At the same time, these findings do not imply that climate-related expenditure should be mechanically exempted from fiscal constraints. As emphasized in the recent policy debate, strategies relying predominantly on spending-based instruments may put significant pressure on fiscal balances and debt dynamics in the absence of compensatory measures on the revenue side. This suggests that the effectiveness of green fiscal policy depends not only on expenditure composition but also on the broader policy mix and on the credibility of the fiscal framework in which it is embedded.

Second, debt sustainability conditions modify the transmission channel of fiscal policy. In high-debt environments, economic responses are shaped by expectations and the credibility of the fiscal framework; in low-debt settings, financial and expenditure-reallocation mechanisms tend to dominate. This implies that credible medium-term fiscal frameworks are essential to preserve policy effectiveness, in line with recent contributions emphasizing the role of expectations in debt sustainability (Blanchard, 2019). In this respect, a key policy implication is that climate-related fiscal strategies should be integrated within medium-term fiscal frameworks that explicitly account for the macroeconomic and fiscal effects of climate policies, rather than relying on simple rule-based exemptions. Such frameworks can help identify an appropriate balance between green spending, revenue mobilization, and debt stabilization objectives, while preserving fiscal credibility.

More generally, these results suggest that fiscal frameworks should move beyond a neutral treatment of expenditure composition and explicitly account for the heterogeneous macroeconomic effects of different spending categories. In particular, green public investment should be prioritized within constrained fiscal environments, either through expenditure reallocation or through dedicated budgetary provisions, rather than being treated as fully interchangeable with other forms of public spending. This does not necessarily imply a relaxation of fiscal discipline, but rather a more efficient allocation of limited fiscal space toward components with higher macroeconomic and structural returns.

These findings also have implications for the design of fiscal rules. Standard deficit- or expenditure-based rules may be too blunt to accommodate the dual stabilization and structural role of green spending, as they do not differentiate across expenditure categories with markedly different macroeconomic effects. At the same time, simple "green" exemptions from fiscal rules may undermine fiscal discipline and create incentives for reclassification, potentially weakening the credibility of the fiscal framework and leading to adverse debt dynamics. A more effective approach would involve embedding climate considerations within a broader medium-term fiscal framework, allowing for a differentiated but disciplined treatment of green investment, supported by clear classification criteria, transparent governance, and consistency with debt sustainability objectives.

With regard to financing strategies, the results suggest that the choice between debt-financed expansion and expenditure reallocation should depend on the prevailing fiscal conditions. In low-debt environments, debt-financed green spending can play a countercyclical role while supporting structural transformation. In high-debt contexts, however, the effectiveness of fiscal policy is more tightly linked to expectations and credibility, implying that green expenditure should be embedded within a well-defined medium-term fiscal path, potentially relying more on compositional shifts or targeted revenue measures, such as carbon pricing, to safeguard fiscal sustainability.

Finally, the evidence highlights that automatic stabilizers, while essential for income smoothing, may be insufficient to address the specific nature of climate-related downturns. These episodes often combine demand contraction with supply-side disruptions, physical damages, and sectoral reallocation pressures, which are not fully captured by standard cyclical mechanisms. In this context, fiscal transmission becomes inherently state-dependent, as documented in the literature on nonlinear fiscal multipliers (Auerbach and Gorodnichenko, 2012; Caselli et al., 2024), implying that the effectiveness of passive fiscal instruments may vary substantially across economic conditions. In particular, when downturns are associated with structural or climate-related shocks, automatic stabilizers may fail to generate a sufficiently strong or targeted response, as they primarily operate through income smoothing rather than through sectoral reallocation or investment support. As a result, discretionary and well-targeted green measures appear better suited to support both aggregate demand and the reconfiguration of the production structure. Importantly, however, such interventions should be embedded within a credible and sustainable fiscal framework, to avoid undermining expectations and debt sustainability.

Taken together, these results highlight the importance of designing fiscal frameworks that are not only counter-cyclical but also structurally oriented toward supporting the green transition, particularly in heterogeneous and debt-constrained environments such as the European Union.

A Data Sources and Variable Definitions

Table 9: Data Sources and Definitions of Key Variables

Variable	Description	Source
Green Public Spending	Environmental protection expenditure (e.g. waste management, wastewater, biodiversity, R&D)	Eurostat (EPEA, COFOG)
Total Government Spending	General government expenditure by function (COFOG classification)	Eurostat (COFOG)
Public Debt-to-GDP	Government consolidated gross debt as percentage of GDP	Eurostat
Long-Term Interest Rate	10-year government bond yields	Eurostat
Sovereign Spread	Difference between national 10-year government bond yields and the German Bund yield	ECB Statistical Data Warehouse
Economic Sentiment Indicator	Composite indicator of business and consumer confidence, aggregating sentiment in manufacturing, services, construction, retail trade and households	European Commission (AMECO)
Nominal GDP	Gross domestic product at current prices	FRED (OECD Quarterly National Accounts)
GDP Deflator	Implicit price deflator for GDP	FRED
Population	Total population (national estimate)	Eurostat

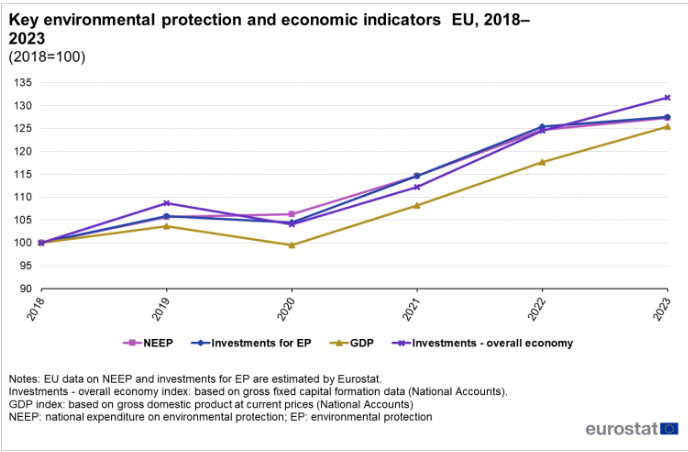

Figure 13: EU green expenditure indicators

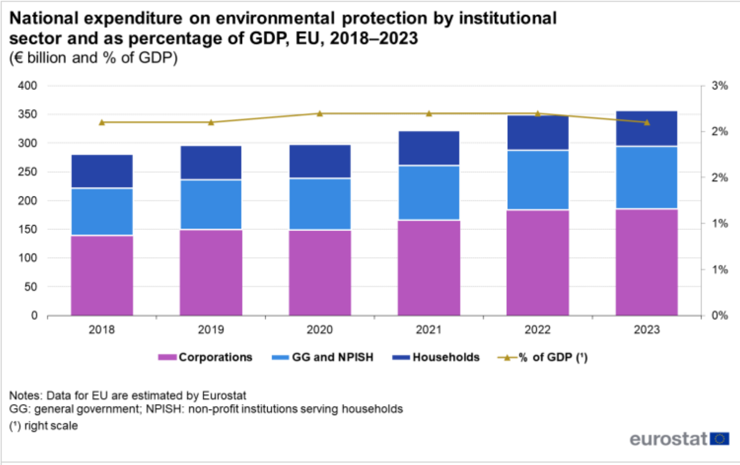

Figure 14: Share green expenditure for sector

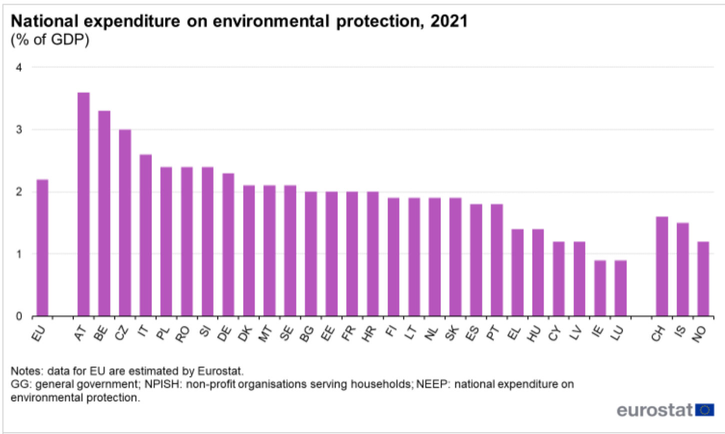

Figure 15: Green Public Spending

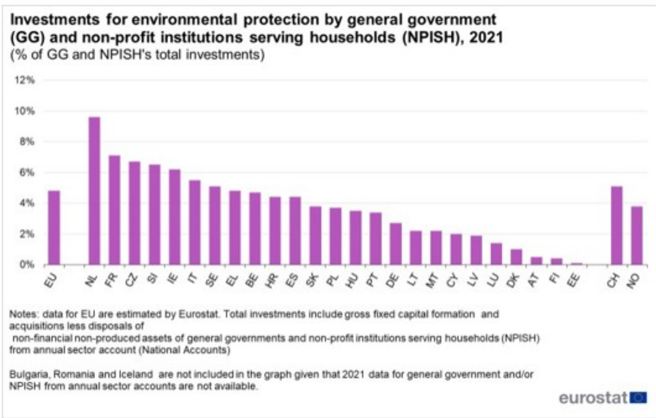

Figure 16: Green Public Spending

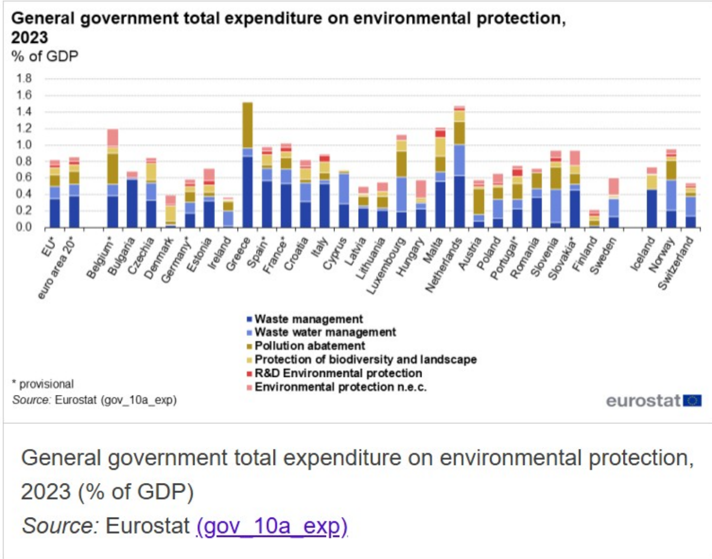

Figure 17: Share Public Spending

B Bayesian Inference for the ST-BVAR

Let y_t denote the $K \times 1$ vector of endogenous variables and let X_t collect the Kp lags and deterministic components. After stacking observations and reshaping coefficients, the panel VAR in each regime $r \in \{\text{low}, \text{high}\}$ can be written as

$$Y_r = X_r B_r + E_r,$$

where

$$\text{vec}(E_r) \sim \mathcal{N}(0, \Sigma_r \otimes I_{T_r}), \qquad \text{vec}(B_r) \equiv b_r \in R^{MK}.$$

B.1 Minnesota Prior for B_r

We impose a Normal prior on the stacked coefficient vector

$$b_r \sim \mathcal{N}(b_0, V_0), \qquad b_0 = 0,$$

where $V_0 = \text{diag}(v_{jj})$ is diagonal. Let $v_{i,j,\ell}$ denote the prior variance of the coefficient on variable j at lag ℓ in equation i. Three hyperparameters regulate shrinkage: $\lambda > 0$ (overall tightness), $\theta \in (0, 1)$ (cross-variable tightness), and $\delta > 0$ (lag decay). Let $\sigma_i^2 = \text{Var}(y_i)$ denote the unconditional variance of variable i. Then

$$v_{i,j,\ell} = \begin{cases} \dfrac{\lambda^2 \sigma_i^2}{\ell^\delta}, & \text{if } i = j, \\[2ex] \dfrac{\theta^2 \lambda^2 \sigma_i^2}{\ell^\delta}, & \text{if } i \neq j, \end{cases}$$

which penalises distant lags and cross-effects more aggressively. Intercepts and fixed effects are treated as unrestricted coefficients, with a large diffuse variance $v_{jj} = \bar{v}$.

B.2 Posterior for B_r

Conditional on Σ_r, conjugacy implies

$$b_r \mid \Sigma_r, Y_r \sim \mathcal{N}\big(b_r^{\text{post}}, V_r^{\text{post}}\big),$$

with posterior precision and mean given by

$$\left(V_r^{\text{post}}\right)^{-1} = V_0^{-1} + \left(\Sigma_r^{-1} \otimes X_r' X_r\right),$$

$$b_r^{\text{post}} = V_r^{\text{post}} \Big[V_0^{-1} b_0 + \left(\Sigma_r^{-1} \otimes X_r'\right) \text{vec}(Y_r) \Big].$$

A posterior draw of B_r is obtained by reshaping a multivariate Normal random vector of dimension MK.

B.3 Inverse-Wishart Priors for Σ_r

Regime-specific covariance matrices follow independent inverse-Wishart priors:

$$\Sigma_r \sim \mathcal{IW}(\nu_0, S_0), \qquad r \in \{\text{low}, \text{high}\},$$

with degrees of freedom $\nu_0 = K + 25$ and scale $S_0 = I_K$.

B.4 Posterior for Σ_r

Let

$$E_r = Y_r - X_r B_r, \qquad S_r = S_0 + E_r' E_r, \qquad \nu_r = \nu_0 + T_r,$$

where T_r denotes the effective contribution of observations to regime r. Then

$$\Sigma_r \mid B_r, Y_r \sim \mathcal{IW}(\nu_r, S_r).$$

B.5 Sampling Algorithm

Posterior simulation alternates over the two blocks:

1. Draw b_r from $\mathcal{N}(b_r^{\text{post}}, V_r^{\text{post}})$.
2. Draw Σ_r from $\mathcal{IW}(\nu_r, S_r)$.
3. Reject parameter draws that violate VAR stability (spectral radius below unity).

This Gibbs scheme delivers joint posterior distributions for regime-specific coefficient matrices and innovation covariances, consistent with the smooth-transition structure of the model.

C Additional Results: Posterior Evidence on Multipliers

C.1 Posterior probability and significance criterion

For each horizon $h = 0, \ldots, H$, we summarize the posterior distribution of the GDP multiplier M_h separately for the low-debt and high-debt regimes. Let $\{M_h^{(s)}\}_{s=1}^S$ denote the S posterior draws of the multiplier at horizon h for a given regime. We report the posterior median and the 16th–84th percentiles, which form a 68% credible interval.

To assess whether the multiplier is more likely to be expansionary, we compute the posterior probability that the multiplier is positive:

$$\Pr(M_h > 0 \mid \mathcal{D}) \;=\; \frac{1}{S} \sum_{s=1}^{S} \mathbf{1}\Big(M_h^{(s)} > 0\Big), \tag{3}$$

where $\mathbf{1}(\cdot)$ is the indicator function and $\mathcal{D}$ denotes the observed data. This quantity is the share of posterior draws lying above zero and provides a direct Bayesian measure of the probability that the effect at horizon h is expansionary.

We additionally define an indicator of statistical relevance based on the 68% credible interval. Specifically, *Sig68* equals one when the 68% credible interval excludes zero, i.e. when either $p16_h > 0$ or $p84_h < 0$. Equivalently, this corresponds to $\Pr(M_h > 0 \mid \mathcal{D}) > 0.84$ (or $\Pr(M_h > 0 \mid \mathcal{D}) < 0.16$).

Table 10: GDP multipliers of a green spending shock: Eastern Europe (68% posterior)

h	M_L	L_{16}	L_{84}	Sig_L	$P(M_L > 0)$	M_H	H_{16}	H_{84}	Sig_H	$P(M_H > 0)$
0	0.00	0.00	0.00	0	0.00	0.00	0.00	0.00	0	0.00
1	-0.37	-1.51	0.65	0	0.37	-0.81	-1.94	0.17	0	0.21
2	-0.43	-1.70	0.81	0	0.37	-1.67	-3.12	-0.24	1	0.12
3	-0.38	-1.83	1.05	0	0.40	-2.30	-3.98	-0.55	1	0.09
4	-0.32	-1.90	1.22	0	0.42	-2.71	-4.71	-0.75	1	0.09
5	-0.25	-1.92	1.43	0	0.45	-2.96	-5.15	-0.79	1	0.09
6	-0.18	-1.91	1.61	0	0.48	-3.08	-5.42	-0.78	1	0.09
7	-0.09	-1.88	1.80	0	0.49	-3.12	-5.52	-0.72	1	0.10
8	0.00	-1.85	1.96	0	0.51	-3.11	-5.59	-0.66	1	0.11
9	0.10	-1.78	2.19	0	0.53	-3.07	-5.64	-0.58	1	0.12
10	0.20	-1.75	2.32	0	0.55	-3.01	-5.69	-0.44	1	0.13
11	0.29	-1.67	2.50	0	0.57	-2.94	-5.65	-0.28	1	0.14
12	0.38	-1.62	2.65	0	0.58	-2.87	-5.64	-0.19	1	0.15
13	0.46	-1.57	2.79	0	0.59	-2.80	-5.69	-0.02	1	0.16
14	0.54	-1.51	2.97	0	0.60	-2.74	-5.69	0.21	0	0.17
15	0.62	-1.51	3.12	0	0.61	-2.68	-5.72	0.37	0	0.19
16	0.69	-1.47	3.25	0	0.62	-2.62	-5.73	0.50	0	0.19

Note: No multipliers are credibly different from zero in the low-debt regime. Under high debt, negative multipliers are statistically significant from horizons 2 to roughly 13, but lose significance thereafter as credible intervals cross zero.

Table 11: Investment multipliers of a green spending shock: Eastern Europe (68% posterior)

h	M_L	L_{16}	L_{84}	Sig_L	$P(M_L > 0)$	M_H	H_{16}	H_{84}	Sig_H	$P(M_H > 0)$
0	0.00	0.00	0.00	0	0.00	0.00	0.00	0.00	0	0.00
1	-1.02	-2.12	0.13	0	0.19	-1.16	-2.28	-0.06	1	0.15
2	-1.80	-3.62	0.02	0	0.16	-2.41	-4.20	-0.54	1	0.10
3	-2.37	-4.86	0.12	0	0.17	-3.49	-6.04	-0.84	1	0.10
4	-2.76	-5.93	0.33	0	0.18	-4.35	-7.58	-0.94	1	0.11
5	-3.02	-6.76	0.63	0	0.20	-5.02	-8.95	-0.70	1	0.12
6	-3.20	-7.36	1.01	0	0.22	-5.49	-10.22	-0.42	1	0.14
7	-3.30	-8.09	1.36	0	0.24	-5.84	-11.13	-0.01	1	0.16
8	-3.33	-8.62	1.74	0	0.26	-6.09	-11.97	0.31	0	0.17
9	-3.31	-9.13	2.30	0	0.28	-6.27	-12.74	0.79	0	0.20
10	-3.25	-9.55	2.75	0	0.30	-6.38	-13.47	1.38	0	0.21
11	-3.18	-9.98	3.29	0	0.32	-6.46	-14.23	1.79	0	0.22
12	-3.09	-10.29	3.77	0	0.32	-6.50	-14.91	2.27	0	0.23
13	-2.99	-10.56	4.28	0	0.34	-6.52	-15.64	2.59	0	0.25
14	-2.88	-10.83	4.72	0	0.35	-6.54	-16.30	2.89	0	0.26
15	-2.77	-11.11	5.21	0	0.37	-6.54	-16.95	3.36	0	0.27
16	-2.66	-11.30	5.71	0	0.38	-6.53	-17.56	3.67	0	0.28

Note: M_L and M_H denote ex-post investment multipliers of a green spending shock in the low- and high-debt regimes. L_{16}–L_{84} and H_{16}–H_{84} report 68% posterior credible intervals. $\mathrm{Sig}_L/\mathrm{Sig}_H$ equal 1 when at least 84% of posterior mass lies strictly on one side of zero. $P(M_L > 0)$ and $P(M_H > 0)$ are the posterior probabilities that the multiplier is positive at horizon h in each regime.

Table 12: GDP multipliers of a green spending shock: Southern Europe (68% posterior)

h	M_L	L_{16}	L_{84}	Sig_L	$P(M_L > 0)$	M_H	H_{16}	H_{84}	Sig_H	$P(M_H > 0)$
0	0.00	0.00	0.00	0	0.00	0.00	0.00	0.00	0	0.00
1	1.60	-1.42	4.36	0	0.70	1.14	-1.73	3.86	0	0.66
2	3.21	0.25	6.14	1	0.86	2.39	-0.42	5.08	0	0.81
3	4.12	0.86	7.27	1	0.90	3.03	0.20	5.77	1	0.85
4	4.66	1.23	8.08	1	0.91	3.32	0.45	6.24	1	0.88
5	5.03	1.48	8.76	1	0.91	3.48	0.56	6.57	1	0.89
6	5.28	1.47	9.28	1	0.91	3.56	0.62	6.73	1	0.89
7	5.46	1.51	9.66	1	0.90	3.58	0.52	6.82	1	0.88
8	5.60	1.49	9.87	1	0.90	3.57	0.53	6.88	1	0.88
9	5.69	1.45	10.15	1	0.90	3.54	0.43	7.03	1	0.87
10	5.76	1.31	10.32	1	0.90	3.50	0.32	7.09	1	0.86
11	5.82	1.33	10.43	1	0.89	3.45	0.18	7.17	1	0.86
12	5.86	1.21	10.57	1	0.89	3.40	0.01	7.13	1	0.84
13	5.88	1.11	10.61	1	0.88	3.34	-0.06	7.15	0	0.83
14	5.90	0.99	10.78	1	0.87	3.28	-0.11	7.17	0	0.83
15	5.92	0.75	10.89	1	0.87	3.23	-0.30	7.21	0	0.82
16	5.93	0.65	10.96	1	0.87	3.16	-0.51	7.33	0	0.81

Note: M_L and M_H denote ex-post GDP multipliers of a green spending shock in the low- and high-debt regimes. L_{16}–L_{84} and H_{16}–H_{84} report 68% posterior credible intervals. $\text{Sig}_L/\text{Sig}_H$ equal 1 when at least 84% of posterior mass lies strictly on one side of zero. $P(M_L > 0)$ and $P(M_H > 0)$ are the posterior probabilities that the multiplier is positive at horizon h in each regime.

Table 13: Investment multipliers of a green spending shock: Southern Europe (68% posterior)

h	M_L	L_{16}	L_{84}	Sig_L	$P(M_L > 0)$	M_H	H_{16}	H_{84}	Sig_H	$P(M_H > 0)$
0	0.00	0.00	0.00	0	0.00	0.00	0.00	0.00	0	0.00
1	0.49	-1.42	4.36	0	0.70	-0.48	-1.73	3.86	0	0.66
2	1.37	0.25	6.14	1	0.86	-0.86	-0.42	5.08	0	0.81
3	1.61	0.86	7.27	1	0.90	-1.53	0.20	5.77	1	0.85
4	1.57	1.23	8.08	1	0.91	-2.33	0.45	6.24	1	0.88
5	1.39	1.48	8.76	1	0.91	-3.11	0.56	6.57	1	0.89
6	1.12	1.47	9.28	1	0.91	-3.83	0.62	6.73	1	0.89
7	0.83	1.51	9.66	1	0.90	-4.49	0.52	6.82	1	0.88
8	0.55	1.49	9.87	1	0.90	-5.13	0.53	6.88	1	0.88
9	0.24	1.45	10.15	1	0.90	-5.77	0.43	7.03	1	0.87
10	-0.10	1.31	10.32	1	0.90	-6.36	0.32	7.09	1	0.86
11	-0.43	1.33	10.43	1	0.89	-6.90	0.18	7.17	1	0.86
12	-0.77	1.21	10.57	1	0.89	-7.43	0.01	7.13	1	0.84
13	-1.10	1.11	10.61	1	0.88	-7.95	-0.06	7.15	0	0.83
14	-1.42	0.99	10.78	1	0.87	-8.45	-0.11	7.17	0	0.83
15	-1.75	0.75	10.89	1	0.87	-8.92	-0.30	7.21	0	0.82
16	-2.08	0.65	10.96	1	0.87	-9.38	-0.51	7.33	0	0.81

Note: M_L and M_H are ex-post investment multipliers of a green spending shock in the low- and high-debt regimes. L_{16}–L_{84} and H_{16}–H_{84} report 68% posterior credible intervals. $\text{Sig}_L/\text{Sig}_H$ equal 1 when at least 84% of posterior mass lies strictly on one side of zero. $P(M_L > 0)$ and $P(M_H > 0)$ are the posterior probabilities that the multiplier in each regime is positive at horizon h.

Table 14: Posterior cumulative GDP multipliers to a green spending shock – Northern Europe

Horizon	Low-debt regime			Sig68	$P(M > 0)$	High-debt regime			Sig68	$P(M > 0)$
	Median	P16	P84			Median	P16	P84		
0	0.000	0.000	0.000	No	0.0000	0.000	0.000	0.000	No	0.0000
1	-2.042	-4.644	0.474	No	0.2133	1.765	0.092	3.435	Yes	0.8508
2	-3.546	-7.420	-0.050	Yes	0.1550	3.228	0.938	5.637	Yes	0.9142
3	-4.275	-9.009	0.006	Yes	0.1600	4.416	1.466	7.304	Yes	0.9342
4	-4.750	-10.251	0.205	No	0.1683	5.293	1.916	8.689	Yes	0.9367
5	-5.075	-11.461	0.256	No	0.1675	5.942	2.228	9.621	Yes	0.9392
6	-5.313	-12.035	0.417	No	0.1767	6.427	2.348	10.454	Yes	0.9450
7	-5.477	-12.766	0.505	No	0.1792	6.793	2.487	11.163	Yes	0.9467
8	-5.592	-13.262	0.558	No	0.1800	7.089	2.584	11.767	Yes	0.9408
9	-5.681	-13.664	0.603	No	0.1825	7.330	2.633	12.304	Yes	0.9392
10	-5.752	-13.945	0.660	No	0.1875	7.520	2.652	12.726	Yes	0.9325
11	-5.803	-14.244	0.680	No	0.1858	7.680	2.487	13.228	Yes	0.9258
12	-5.839	-14.312	0.651	No	0.1892	7.810	2.380	13.685	Yes	0.9225
13	-5.867	-14.448	0.776	No	0.1917	7.926	2.298	13.978	Yes	0.9175
14	-5.884	-14.603	0.879	No	0.1942	8.027	2.217	14.200	Yes	0.9142
15	-5.893	-14.787	0.973	No	0.2000	8.113	2.092	14.320	Yes	0.9125
16	-5.898	-14.871	1.060	No	0.1992	8.187	1.976	14.509	Yes	0.9058

Notes: Posterior medians and 16–84 credible intervals for cumulative GDP multipliers. $P(M > 0)$ is the posterior probability of a positive multiplier. "Sig68" flags significance at a 68% posterior probability rule.

Table 15: Posterior distribution of cumulative investment multipliers – Northern Europe

Horizon	Low-debt regime			Sig68	$P(M>0)$	High-debt regime			Sig68	$P(M>0)$
	Median	P16	P84			Median	P16	P84		
0	0.000	0.000	0.000	No	0.0000	0.000	0.000	0.000	No	0.0000
1	-2.179	-5.138	0.762	No	0.2333	1.701	-0.363	3.735	No	0.7842
2	-3.242	-7.866	1.173	No	0.2367	3.610	-0.077	6.960	No	0.8333
3	-3.723	-10.150	2.184	No	0.2667	5.205	0.012	10.030	Yes	0.8408
4	-4.131	-12.330	2.924	No	0.2967	6.696	-0.152	12.758	No	0.8333
5	-4.588	-14.351	3.649	No	0.3000	8.001	-0.409	15.496	No	0.8275
6	-5.079	-16.293	4.168	No	0.3033	9.145	-0.820	17.924	No	0.8175
7	-5.550	-17.937	4.603	No	0.3025	10.127	-1.615	20.597	No	0.8033
8	-5.978	-19.654	4.833	No	0.2950	10.970	-2.376	22.395	No	0.7933
9	-6.367	-20.714	5.020	No	0.2933	11.694	-3.329	24.393	No	0.7850
10	-6.682	-22.018	5.342	No	0.2917	12.303	-3.790	26.521	No	0.7758
11	-6.941	-22.669	5.586	No	0.2892	12.847	-4.636	27.960	No	0.7683
12	-7.159	-23.533	6.057	No	0.2875	13.321	-5.501	29.642	No	0.7658
13	-7.336	-24.215	6.128	No	0.2883	13.734	-6.409	31.298	No	0.7617
14	-7.479	-24.667	6.306	No	0.2900	14.093	-7.425	32.882	No	0.7592
15	-7.583	-25.019	6.329	No	0.2900	14.409	-8.423	33.919	No	0.7575
16	-7.669	-25.651	6.639	No	0.2925	14.684	-9.285	34.811	No	0.7542

Notes: The table reports posterior medians and 16th–84th percentile credible intervals of cumulative investment multipliers for Northern European countries. "Sig68" indicates whether the 16–84 credible interval excludes zero. $P(M>0)$ denotes the posterior probability that the multiplier is positive in each regime.

Table 16: Posterior cumulative GDP multipliers to a green spending shock – Full European Union Sample

Horizon	Low-debt regime			Sig68	$P(M>0)$	High-debt regime			Sig68	$P(M>0)$
	Median	P16	P84			Median	P16	P84		
0	0.000	0.000	0.000	No	0.0000	0.000	0.000	0.000	No	0.0000
1	-0.146	-1.496	1.068	No	0.4492	-2.638	-3.848	-1.415	Yes	0.0167
2	0.791	-0.666	2.161	No	0.7108	-3.604	-4.973	-2.293	Yes	0.0050
3	1.691	0.181	3.083	Yes	0.8667	-4.038	-5.473	-2.654	Yes	0.0025
4	2.357	0.755	3.823	Yes	0.9208	-4.294	-5.793	-2.862	Yes	0.0017
5	2.857	1.156	4.457	Yes	0.9392	-4.464	-5.982	-2.956	Yes	0.0008
6	3.251	1.487	4.958	Yes	0.9458	-4.588	-6.105	-3.049	Yes	0.0017
7	3.564	1.689	5.382	Yes	0.9533	-4.677	-6.278	-3.060	Yes	0.0017
8	3.822	1.846	5.697	Yes	0.9608	-4.741	-6.427	-3.082	Yes	0.0017
9	4.032	1.992	6.021	Yes	0.9650	-4.789	-6.544	-3.057	Yes	0.0017
10	4.208	2.092	6.268	Yes	0.9683	-4.825	-6.623	-3.053	Yes	0.0033
11	4.354	2.154	6.487	Yes	0.9717	-4.851	-6.741	-2.984	Yes	0.0058
12	4.479	2.213	6.633	Yes	0.9717	-4.870	-6.846	-2.972	Yes	0.0058
13	4.587	2.270	6.801	Yes	0.9725	-4.885	-6.895	-2.940	Yes	0.0067
14	4.680	2.319	6.934	Yes	0.9725	-4.899	-6.967	-2.919	Yes	0.0067
15	4.759	2.377	7.044	Yes	0.9733	-4.911	-7.007	-2.877	Yes	0.0083
16	4.828	2.406	7.172	Yes	0.9742	-4.923	-7.100	-2.838	Yes	0.0125

Notes: Posterior medians and 16–84 credible intervals for cumulative GDP multipliers. $P(M>0)$ denotes the posterior probability of a positive multiplier. "Sig68" indicates significance under a 68% posterior sign-probability rule.

Table 17: Posterior cumulative investment multipliers to a green spending shock – Full European Union sample

Horizon	Low-debt regime					High-debt regime				
	Median	P16	P84	Sig68	$P(M > 0)$	Median	P16	P84	Sig68	$P(M > 0)$
0	0.000	0.000	0.000	No	0.000	0.000	0.000	0.000	No	0.000
1	-1.424	-2.765	-0.081	Yes	0.147	-1.889	-3.168	-0.515	Yes	0.080
2	-1.717	-3.559	0.179	No	0.190	-2.548	-4.379	-0.684	Yes	0.083
3	-2.008	-4.254	0.246	No	0.198	-2.856	-5.135	-0.534	Yes	0.101
4	-2.476	-5.250	0.250	No	0.193	-3.100	-5.805	-0.395	Yes	0.123
5	-3.012	-6.261	0.184	No	0.178	-3.322	-6.415	-0.151	Yes	0.147
6	-3.554	-7.322	0.005	No	0.161	-3.502	-7.010	0.134	No	0.167
7	-4.089	-8.354	-0.169	Yes	0.150	-3.648	-7.523	0.488	No	0.188
8	-4.597	-9.327	-0.219	Yes	0.148	-3.778	-8.108	0.776	No	0.203
9	-5.079	-10.274	-0.253	Yes	0.143	-3.885	-8.735	1.118	No	0.220
10	-5.516	-11.099	-0.316	Yes	0.143	-3.976	-9.340	1.574	No	0.233
11	-5.910	-11.820	-0.429	Yes	0.145	-4.058	-9.917	1.941	No	0.245
12	-6.261	-12.500	-0.490	Yes	0.143	-4.128	-10.529	2.356	No	0.258
13	-6.564	-13.231	-0.515	Yes	0.142	-4.202	-11.099	3.012	No	0.271
14	-6.836	-13.874	-0.498	Yes	0.140	-4.274	-11.699	3.454	No	0.281
15	-7.072	-14.472	-0.454	Yes	0.144	-4.342	-12.142	3.843	No	0.285
16	-7.277	-14.967	-0.374	Yes	0.145	-4.405	-12.746	4.218	No	0.294

Notes: Posterior medians and 16–84 credible intervals for cumulative investment multipliers following a green spending shock on the full European Union sample. "Sig68" indicates significance under a 68% posterior sign-probability rule based on the sign of the multiplier; $P(M > 0)$ reports the posterior probability that the multiplier is positive in each regime.

Table 18: Posterior cumulative GDP multipliers to a non-green expenditure shock (total expenditure net of green) – Eastern Europe

Horizon	Low-debt regime					High-debt regime				
	Median	P16	P84	Sig68	$P(M > 0)$	Median	P16	P84	Sig68	$P(M > 0)$
0	0.000	0.000	0.000	No	0.000	0.000	0.000	0.000	No	0.000
1	-0.017	-0.107	0.069	No	0.423	0.028	-0.048	0.109	No	0.649
2	-0.002	-0.115	0.109	No	0.489	0.044	-0.065	0.158	No	0.653
3	0.025	-0.098	0.154	No	0.578	0.050	-0.077	0.192	No	0.657
4	0.045	-0.087	0.180	No	0.628	0.048	-0.097	0.203	No	0.635
5	0.060	-0.085	0.208	No	0.658	0.045	-0.106	0.212	No	0.619
6	0.070	-0.085	0.227	No	0.673	0.042	-0.121	0.221	No	0.604
7	0.077	-0.089	0.241	No	0.681	0.039	-0.133	0.227	No	0.598
8	0.081	-0.096	0.250	No	0.679	0.037	-0.146	0.234	No	0.587
9	0.083	-0.103	0.256	No	0.674	0.036	-0.157	0.241	No	0.579
10	0.083	-0.111	0.262	No	0.669	0.035	-0.171	0.247	No	0.580
11	0.082	-0.118	0.270	No	0.662	0.034	-0.176	0.256	No	0.577
12	0.081	-0.127	0.271	No	0.658	0.034	-0.183	0.270	No	0.581
13	0.079	-0.137	0.273	No	0.653	0.035	-0.193	0.272	No	0.578
14	0.077	-0.146	0.277	No	0.642	0.035	-0.197	0.276	No	0.576
15	0.075	-0.160	0.279	No	0.638	0.036	-0.206	0.283	No	0.571
16	0.072	-0.172	0.280	No	0.631	0.037	-0.215	0.288	No	0.576

Notes: Posterior cumulative GDP multipliers following a non-green expenditure shock in Eastern Europe. Intervals are 16–84 posterior credible bands. Significance (Sig68) based on a 68% posterior sign rule; $P(M > 0)$ reports the posterior probability of a positive multiplier.

Table 19: Posterior cumulative investment multipliers to a non-green expenditure shock – Eastern Europe

Horizon	Low-debt regime					High-debt regime				
	Median	P16	P84	Sig68	$P(M>0)$	Median	P16	P84	Sig68	$P(M>0)$
0	0.00000	0.00000	0.00000	No	0.000	0.00000	0.00000	0.00000	No	0.000
1	0.01566	-0.06792	0.10187	No	0.580	-0.06854	-0.14816	0.00598	No	0.182
2	0.11019	-0.03361	0.26640	No	0.783	-0.13783	-0.28213	-0.00054	Yes	0.158
3	0.22053	0.01865	0.45177	Yes	0.863	-0.20264	-0.41466	0.00427	No	0.165
4	0.32063	0.06005	0.61761	Yes	0.888	-0.25856	-0.53976	0.01275	No	0.169
5	0.40691	0.09481	0.76030	Yes	0.896	-0.30485	-0.64378	0.03337	No	0.189
6	0.48028	0.10911	0.87998	Yes	0.902	-0.34226	-0.74572	0.05672	No	0.198
7	0.54113	0.11734	0.99607	Yes	0.900	-0.37228	-0.84055	0.07987	No	0.208
8	0.59082	0.11589	1.09535	Yes	0.898	-0.39636	-0.92030	0.11267	No	0.218
9	0.63176	0.11239	1.18203	Yes	0.890	-0.41560	-1.00330	0.14712	No	0.231
10	0.66489	0.10081	1.25638	Yes	0.886	-0.43171	-1.06123	0.17603	No	0.247
11	0.69122	0.08179	1.31860	Yes	0.875	-0.44473	-1.12696	0.21157	No	0.258
12	0.71322	0.06626	1.38479	Yes	0.873	-0.45475	-1.18560	0.24191	No	0.268
13	0.73171	0.05477	1.43393	Yes	0.861	-0.46351	-1.24387	0.27509	No	0.273
14	0.74655	0.03264	1.48316	Yes	0.853	-0.47067	-1.29779	0.30364	No	0.283
15	0.75892	0.00982	1.51664	Yes	0.845	-0.47643	-1.34897	0.33505	No	0.293
16	0.76875	-0.01395	1.55773	No	0.836	-0.48140	-1.39055	0.37503	No	0.301

Notes. Posterior cumulative investment multipliers following a non-green expenditure shock in Eastern Europe. Intervals are 16–84 posterior credible bands. Sig68 indicates significance under a 68% sign-probability rule.

Table 20: Posterior cumulative GDP multipliers to non-green expenditure shocks – Northern Europe

Horizon	Low-debt regime					High-debt regime				
	Median	P16	P84	Sig68	$P(M>0)$	Median	P16	P84	Sig68	$P(M>0)$
0	0.00000	0.00000	0.00000	No	0.000	0.00000	0.00000	0.00000	No	0.000
1	-0.08417	-0.22106	0.07149	No	0.286	-0.05422	-0.18093	0.06278	No	0.310
2	-0.14219	-0.33370	0.07545	No	0.248	-0.11258	-0.28129	0.05474	No	0.253
3	-0.16344	-0.41824	0.10216	No	0.268	-0.15927	-0.37456	0.04873	No	0.225
4	-0.17756	-0.46997	0.12105	No	0.275	-0.19819	-0.45522	0.03801	No	0.201
5	-0.18618	-0.50041	0.13851	No	0.288	-0.23086	-0.51425	0.02765	No	0.189
6	-0.19178	-0.51797	0.15678	No	0.293	-0.25796	-0.57754	0.02415	No	0.181
7	-0.19506	-0.53858	0.16822	No	0.293	-0.28098	-0.62729	0.01327	No	0.172
8	-0.19732	-0.55834	0.18515	No	0.298	-0.30109	-0.67007	0.01116	No	0.168
9	-0.19789	-0.56514	0.19480	No	0.306	-0.31992	-0.71143	0.00882	No	0.168
10	-0.19794	-0.57502	0.19965	No	0.309	-0.33638	-0.74836	0.01202	No	0.167
11	-0.19775	-0.58138	0.21280	No	0.309	-0.35177	-0.78162	0.01192	No	0.168
12	-0.19751	-0.58091	0.21862	No	0.311	-0.36611	-0.81755	0.01158	No	0.169
13	-0.19725	-0.58167	0.22614	No	0.314	-0.37869	-0.84716	0.01054	No	0.171
14	-0.19691	-0.58873	0.23466	No	0.314	-0.38998	-0.87308	0.01553	No	0.166
15	-0.19669	-0.59303	0.23980	No	0.313	-0.39998	-0.90875	0.01513	No	0.170
16	-0.19643	-0.59852	0.24343	No	0.316	-0.40876	-0.93955	0.01454	No	0.168

Notes. Negative and non-significant multipliers across both regimes. No horizon crosses the 68% sign rule. Markets apparently said "no grazie" to fiscal transmission.

Table 21: Posterior cumulative investment multipliers to non green expenditure shock – Northern Europe

Horizon	Low-debt regime					High-debt regime				
	Median	P16	P84	Sig68	$P(M>0)$	Median	P16	P84	Sig68	$P(M>0)$
0	0.000	0.000	0.000	No	0.000	0.000	0.000	0.000	No	0.000
1	-0.150	-0.300	-0.004	Yes	0.154	-0.166	-0.287	-0.046	Yes	0.079
2	-0.264	-0.495	-0.047	Yes	0.113	-0.347	-0.568	-0.139	Yes	0.048
3	-0.339	-0.645	-0.053	Yes	0.118	-0.516	-0.847	-0.217	Yes	0.047
4	-0.391	-0.755	-0.042	Yes	0.127	-0.671	-1.106	-0.286	Yes	0.043
5	-0.431	-0.851	-0.036	Yes	0.133	-0.812	-1.339	-0.344	Yes	0.047
6	-0.462	-0.926	-0.037	Yes	0.140	-0.939	-1.573	-0.378	Yes	0.049
7	-0.488	-0.995	-0.027	Yes	0.142	-1.054	-1.769	-0.406	Yes	0.051
8	-0.508	-1.044	-0.009	Yes	0.149	-1.156	-1.946	-0.436	Yes	0.055
9	-0.525	-1.092	-0.006	Yes	0.157	-1.251	-2.127	-0.457	Yes	0.061
10	-0.537	-1.133	-0.006	Yes	0.158	-1.335	-2.287	-0.486	Yes	0.068
11	-0.547	-1.173	0.001	Yes	0.160	-1.410	-2.434	-0.503	Yes	0.071
12	-0.555	-1.202	0.007	No	0.164	-1.477	-2.599	-0.518	Yes	0.075
13	-0.560	-1.222	0.016	No	0.169	-1.539	-2.752	-0.525	Yes	0.075
14	-0.565	-1.247	0.022	No	0.172	-1.595	-2.871	-0.537	Yes	0.078
15	-0.568	-1.270	0.029	No	0.178	-1.645	-2.966	-0.543	Yes	0.084
16	-0.570	-1.289	0.044	No	0.179	-1.689	-3.077	-0.549	Yes	0.084

Notes. Posterior medians and 16–84 credible intervals for cumulative investment multipliers. "Sig68" indicates significance under a 68% posterior sign-probability rule; $P(M>0)$ is the posterior probability that the multiplier is positive in each regime.

Table 22: Posterior cumulative GDP multipliers to non-green expenditure shocks – Southern Europe

Horizon	**Low-debt regime**				**High-debt regime**			
	Median	[P16; P84]	Sig68	$P(M>0)$	Median	[P16; P84]	Sig68	$P(M>0)$
0	0.0000	[0.000; 0.000]	No	0.000	0.0000	[0.000; 0.000]	No	0.000
1	-0.0998	[-0.2162; 0.0133]	No	0.186	-0.1000	[-0.2020; 0.0009]	No	0.163
2	-0.1663	[-0.3199;-0.0181]	Yes	0.129	-0.1829	[-0.3276;-0.0479]	Yes	0.095
3	-0.1980	[-0.3794;-0.0261]	Yes	0.126	-0.2406	[-0.4162;-0.0777]	Yes	0.073
4	-0.2237	[-0.4263;-0.0351]	Yes	0.115	-0.2912	[-0.4893;-0.1037]	Yes	0.0525
5	-0.2439	[-0.4585;-0.0439]	Yes	0.103	-0.3382	[-0.5561;-0.1409]	Yes	0.0367
6	-0.2613	[-0.4894;-0.0496]	Yes	0.103	-0.3823	[-0.6140;-0.1793]	Yes	0.0283
7	-0.2769	[-0.5182;-0.0539]	Yes	0.099	-0.4239	[-0.6760;-0.2063]	Yes	0.0225
8	-0.2908	[-0.5409;-0.0615]	Yes	0.0925	-0.4634	[-0.7378;-0.2407]	Yes	0.0175
9	-0.3034	[-0.5552;-0.0671]	Yes	0.0883	-0.5006	[-0.7950;-0.2692]	Yes	0.0142
10	-0.3156	[-0.5722;-0.0742]	Yes	0.0892	-0.5355	[-0.8553;-0.2889]	Yes	0.0133
11	-0.3268	[-0.5934;-0.0747]	Yes	0.0892	-0.5687	[-0.9203;-0.3171]	Yes	0.0133
12	-0.3374	[-0.6160;-0.0781]	Yes	0.0917	-0.6002	[-0.9769;-0.3358]	Yes	0.0100
13	-0.3471	[-0.6397;-0.0799]	Yes	0.0933	-0.6299	[-1.0440;-0.3478]	Yes	0.0092
14	-0.3561	[-0.6626;-0.0816]	Yes	0.0967	-0.6577	[-1.0977;-0.3624]	Yes	0.0083
15	-0.3647	[-0.6806;-0.0841]	Yes	0.0967	-0.6838	[-1.1466;-0.3703]	Yes	0.0083
16	-0.3725	[-0.6967;-0.0868]	Yes	0.0983	-0.7083	[-1.2002;-0.3771]	Yes	0.0092

Notes. All multipliers cumulative. "Sig68" indicates significance under a 68% posterior sign-confidence rule. Shock: total expenditure net of green spending.

Table 23: Posterior cumulative **investment** multipliers to non-green expenditure shocks – Southern Europe

Horizon	**Low-debt regime**				**High-debt regime**			
	Median	[P16; P84]	Sig68	$P(M>0)$	Median	[P16; P84]	Sig68	$P(M>0)$
0	0.0000	[0.000; 0.000]	No	0.000	0.0000	[0.000; 0.000]	No	0.000
1	-0.3701	[-0.4872;-0.2622]	Yes	0.000	-0.2212	[-0.3320;-0.1171]	Yes	0.0125
2	-0.6911	[-0.8970;-0.4942]	Yes	0.000	-0.4302	[-0.6426;-0.2452]	Yes	0.0133
3	-0.9706	[-1.2731;-0.6633]	Yes	0.000	-0.6087	[-0.9501;-0.3184]	Yes	0.0167
4	-1.2210	[-1.6355;-0.7945]	Yes	0.000	-0.7706	[-1.2536;-0.3731]	Yes	0.0183
5	-1.4468	[-1.9738;-0.9115]	Yes	0.0008	-0.9196	[-1.5381;-0.4035]	Yes	0.0233
6	-1.6528	[-2.2872;-1.0304]	Yes	0.0033	-1.0609	[-1.8280;-0.4365]	Yes	0.0292
7	-1.8423	[-2.5784;-1.1186]	Yes	0.0042	-1.1920	[-2.1137;-0.4645]	Yes	0.0392
8	-2.0188	[-2.8470;-1.1946]	Yes	0.0058	-1.3132	[-2.3904;-0.4779]	Yes	0.0433
9	-2.1826	[-3.1176;-1.2759]	Yes	0.0075	-1.4253	[-2.6451;-0.4897]	Yes	0.0500
10	-2.3360	[-3.3684;-1.3260]	Yes	0.0108	-1.5314	[-2.9108;-0.5074]	Yes	0.0550
11	-2.4796	[-3.6020;-1.3828]	Yes	0.0133	-1.6321	[-3.1455;-0.5229]	Yes	0.0650
12	-2.6152	[-3.8318;-1.4218]	Yes	0.0142	-1.7275	[-3.3877;-0.5124]	Yes	0.0717
13	-2.7410	[-4.0452;-1.4617]	Yes	0.0175	-1.8193	[-3.6420;-0.5154]	Yes	0.0758
14	-2.8576	[-4.2464;-1.4939]	Yes	0.0208	-1.9054	[-3.8975;-0.5183]	Yes	0.0783
15	-2.9675	[-4.4428;-1.5377]	Yes	0.0225	-1.9877	[-4.1162;-0.5297]	Yes	0.0808
16	-3.0701	[-4.6258;-1.5761]	Yes	0.0258	-2.0649	[-4.3571;-0.5367]	Yes	0.0867

Notes. All multipliers cumulative. "Sig68" = significance at 68% posterior sign rule. Very low $P(M>0)$ suggests contractionary investment response even in low-debt configurations.

Table 24: Posterior cumulative GDP multipliers to total (non-green) spending shocks – Full Sample EU

Horizon	**Low-debt regime**				**High-debt regime**			
	Median	[P16; P84]	Sig68	$P(M>0)$	Median	[P16; P84]	Sig68	$P(M>0)$
0	0.0000	[0.000; 0.000]	No	0.000	0.0000	[0.000; 0.000]	No	0.000
1	-0.0554	[-0.1149;-0.0014]	Yes	0.1558	-0.0580	[-0.1124;-0.0033]	Yes	0.1417
2	-0.0757	[-0.1480;-0.0067]	Yes	0.1342	-0.0628	[-0.1429; 0.0145]	No	0.2300
3	-0.1088	[-0.1985;-0.0264]	Yes	0.0908	-0.0257	[-0.1227; 0.0706]	No	0.4092
4	-0.1489	[-0.2504;-0.0536]	Yes	0.0525	0.0261	[-0.0792; 0.1343]	No	0.5925
5	-0.1869	[-0.3037;-0.0771]	Yes	0.0383	0.0771	[-0.0399; 0.1946]	No	0.7467
6	-0.2208	[-0.3483;-0.1012]	Yes	0.0308	0.1236	[-0.0029; 0.2497]	No	0.8342
7	-0.2511	[-0.3905;-0.1208]	Yes	0.0258	0.1652	[0.0297; 0.3032]	Yes	0.8917
8	-0.2778	[-0.4326;-0.1357]	Yes	0.0225	0.2028	[0.0593; 0.3494]	Yes	0.9225
9	-0.3016	[-0.4708;-0.1492]	Yes	0.0217	0.2365	[0.0849; 0.3889]	Yes	0.9392
10	-0.3230	[-0.5048;-0.1624]	Yes	0.0217	0.2669	[0.1098; 0.4264]	Yes	0.9525
11	-0.3423	[-0.5361;-0.1714]	Yes	0.0208	0.2942	[0.1317; 0.4603]	Yes	0.9600
12	-0.3595	[-0.5669;-0.1804]	Yes	0.0200	0.3190	[0.1491; 0.4918]	Yes	0.9633
13	-0.3749	[-0.5953;-0.1852]	Yes	0.0192	0.3419	[0.1657; 0.5209]	Yes	0.9658
14	-0.3886	[-0.6179;-0.1930]	Yes	0.0192	0.3631	[0.1799; 0.5486]	Yes	0.9642
15	-0.4008	[-0.6391;-0.2001]	Yes	0.0200	0.3829	[0.1940; 0.5718]	Yes	0.9650
16	-0.4117	[-0.6580;-0.2047]	Yes	0.0192	0.4013	[0.2077; 0.5962]	Yes	0.9667

Notes. Cumulative multipliers. "Sig68" flags 68% posterior sign significance. High-debt regime shows positive and increasing multipliers, unlike the low-debt regime where responses remain persistently negative.

Table 25: Posterior cumulative **investment** multipliers to total spending shocks – Full Sample EU

Horizon	**Low-debt regime**				**High-debt regime**			
	Median	[P16; P84]	Sig68	$P(M>0)$	Median	[P16; P84]	Sig68	$P(M>0)$
0	0.0000	[0.000;0.000]	No	0.000	0.0000	[0.000;0.000]	No	0.000
1	0.0157	[-0.0448;0.0709]	No	0.6108	-0.0156	[-0.0672;0.0398]	No	0.3792
2	0.1074	[0.0108;0.2027]	Yes	0.8642	0.0566	[-0.0431;0.1590]	No	0.7200
3	0.1938	[0.0647;0.3269]	Yes	0.9242	0.1781	[0.0262;0.3392]	Yes	0.8800
4	0.2665	[0.0978;0.4389]	Yes	0.9358	0.3104	[0.1063;0.5210]	Yes	0.9392
5	0.3320	[0.1213;0.5509]	Yes	0.9400	0.4363	[0.1806;0.6938]	Yes	0.9550
6	0.3934	[0.1362;0.6525]	Yes	0.9442	0.5519	[0.2337;0.8604]	Yes	0.9625
7	0.4499	[0.1496;0.7502]	Yes	0.9425	0.6578	[0.2849;1.0159]	Yes	0.9642
8	0.5008	[0.1592;0.8443]	Yes	0.9383	0.7538	[0.3311;1.1545]	Yes	0.9617
9	0.5467	[0.1799;0.9272]	Yes	0.9375	0.8431	[0.3612;1.2930]	Yes	0.9625
10	0.5882	[0.1920;1.0112]	Yes	0.9317	0.9260	[0.3929;1.4170]	Yes	0.9575
11	0.6249	[0.1926;1.0833]	Yes	0.9267	1.0033	[0.4228;1.5461]	Yes	0.9542
12	0.6575	[0.1911;1.1519]	Yes	0.9225	1.0746	[0.4299;1.6682]	Yes	0.9483
13	0.6861	[0.1916;1.2210]	Yes	0.9142	1.1422	[0.4428;1.7895]	Yes	0.9450
14	0.7111	[0.1939;1.2878]	Yes	0.9125	1.2059	[0.4426;1.8951]	Yes	0.9442
15	0.7328	[0.1984;1.3468]	Yes	0.9092	1.2657	[0.4469;2.0112]	Yes	0.9400
16	0.7518	[0.1926;1.3909]	Yes	0.9058	1.3229	[0.4435;2.1228]	Yes	0.9350

D Robustness Checks Green Shock 1995-2019 pre-Covid

We report robustness checks in which the estimation sample is restricted to the pre-pandemic period (1995–2019), thereby excluding the COVID-19 shock. The results indicate that the qualitative sign of the impulse–response functions to both green and non-green government spending shocks is preserved relative to the baseline specification. However, the magnitude and statistical significance of the estimated multipliers change in some cases across regions and debt regimes. In particular, in Southern European countries under high-debt conditions, output multipliers associated with green spending shocks become weaker and, in some specifications, statistically insignificant. Conversely, in Northern Europe, private investment responses under high-debt conditions become statistically significant in the restricted sample.

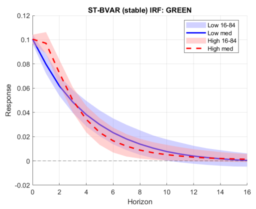

(a) GREEN

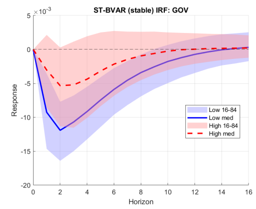

(b) GOV

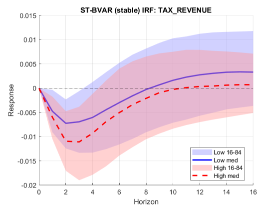

(c) TAX REVENUE

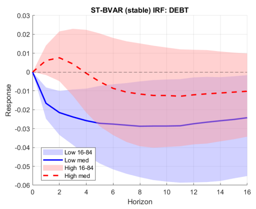

(d) DEBT

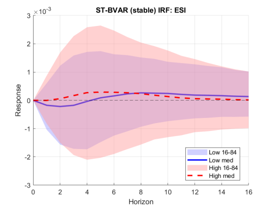

(e) ESI

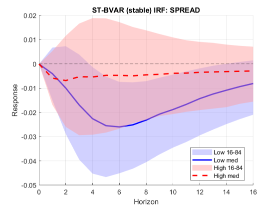

(f) SPREAD

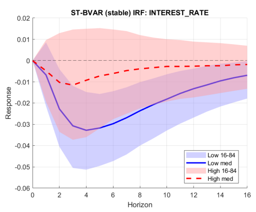

(g) INTEREST RATE

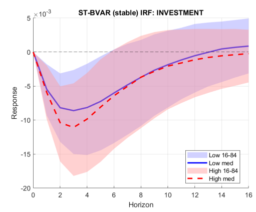

(h) INVESTMENT

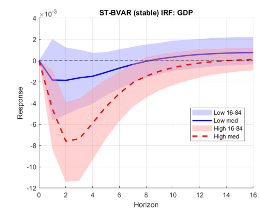

(i) GDP

Figure 18: Impulse responses to a green-spending shock: Eastern Europe 1995-2019 ST-BVAR (low vs high debt regimes).

Table 26: Eastern Europe: GDP and Investment IRFs at selected horizons (Low vs High debt regimes)

Variable	Regime	$h = 0$	$h = 4$	$h = 8$	$h = 12$	$h = 16$
GDP	Low	0.000 (0.000, 0.000)	-1.200* (-9.020, -1.872)	-1.267* (-13.979, -1.160)	-0.983 (-16.639, 0.294)	-0.600 (-18.141, 2.238)
GDP	High	0.000 (0.000, 0.000)	-4.167* (-10.103, -2.670)	-5.091* (-15.772, -1.940)	-5.175* (-19.106, -0.365)	-5.080 (-21.055, 0.916)
Investment	Low	0.000 (0.000, 0.000)	-5.378* (-9.020, -1.872)	-7.330* (-13.979, -1.160)	-7.684 (-16.639, 0.294)	-7.319 (-18.141, 2.238)
Investment	High	0.000 (0.000, 0.000)	-6.110* (-10.103, -2.670)	-8.461* (-15.772, -1.940)	-9.108* (-19.106, -0.365)	-9.208 (-21.055, 0.916)

Notes: Entries report posterior median M and 68% credible interval ($p16, p84$). An asterisk (*) denotes Sig68 = TRUE (the 68% credible interval excludes zero).

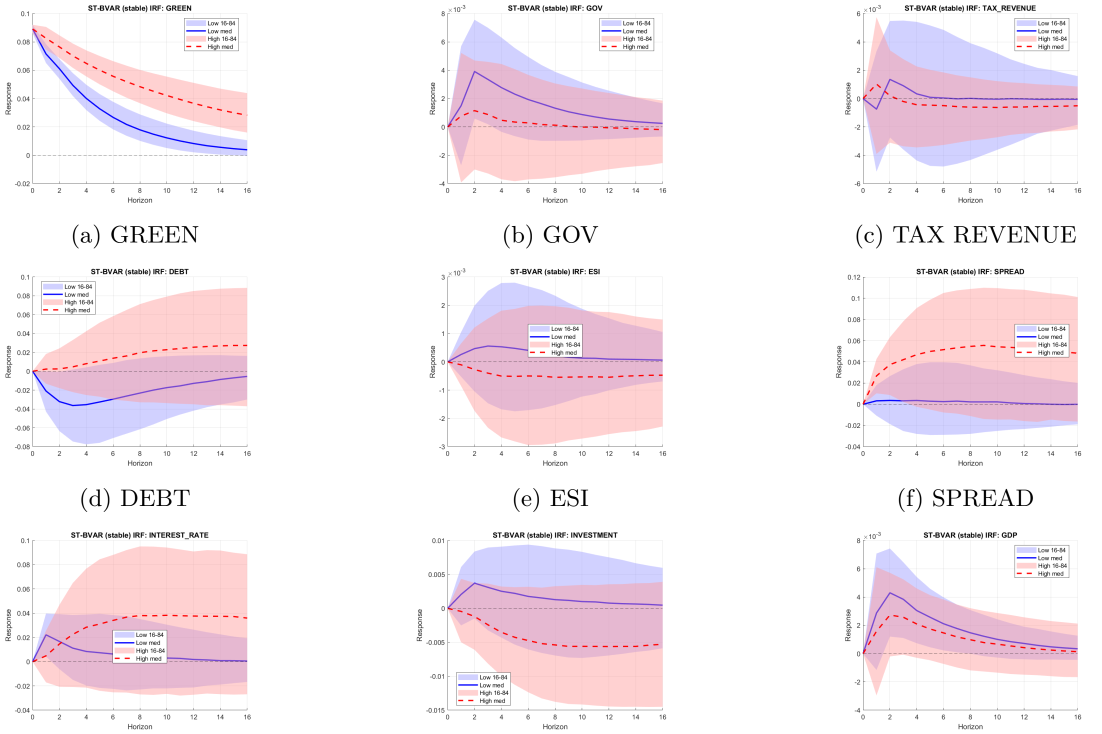

(a) GREEN (b) GOV (c) TAX REVENUE

(d) DEBT (e) ESI (f) SPREAD

(g) INTEREST RATE (h) INVESTMENT (i) GDP

Figure 19: Impulse responses to a green-spending shock: Southern Europe 1995-2019 ST-BVAR (low vs high debt regimes).

Table 27: Southern Europe: GDP and Investment IRFs at selected horizons (Low vs High debt regimes)

Variable	Regime	$h = 0$	$h = 4$	$h = 8$	$h = 12$	$h = 16$
GDP	Low	0.000 (,)	5.190 (-170.799, 350.058)	6.155 (-270.792, 423.545)	6.499 (-394.405, 501.016)	6.651 (-507.858, 536.770)
GDP	High	0.000 (,)	2.695 (-271.390, 301.630)	2.753 (-382.474, 463.243)	2.528 (-480.813, 578.533)	2.290 (-576.550, 722.744)
Investment	Low	0.000 (,)	4.206 (-170.799, 350.058)	5.091 (-270.792, 423.545)	5.568 (-394.405, 501.016)	5.901 (-507.858, 536.770)
Investment	High	0.000 (,)	-2.273 (-271.390, 301.630)	-5.207 (-382.474, 463.243)	-7.470 (-480.813, 578.533)	-9.259 (-576.550, 722.744)

Notes: Entries report posterior median M and 68% credible interval $(p16, p84)$. All Sig68 indicators are FALSE in this sample, hence no significance markers are displayed.

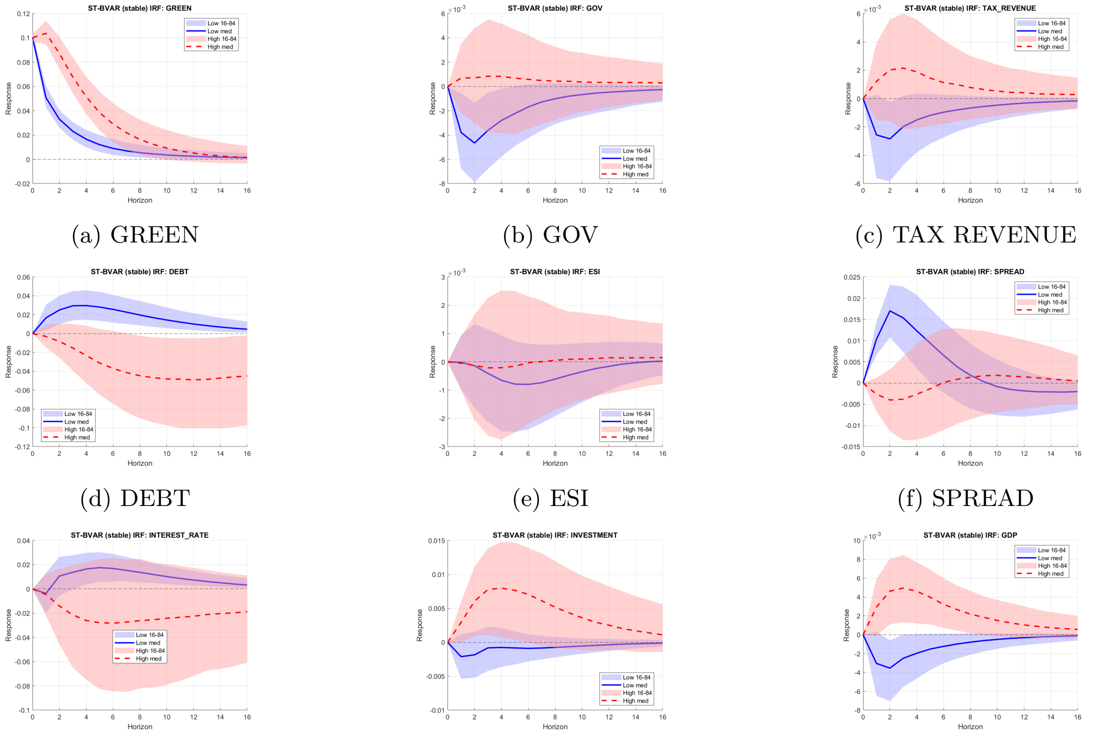

(a) GREEN (b) GOV (c) TAX REVENUE

(d) DEBT (e) ESI (f) SPREAD

(g) INTEREST RATE (h) INVESTMENT (i) GDP

Figure 20: Impulse responses to a green-spending shock: Northern Europe 1995-2019 ST-BVAR (low vs high debt regimes).

Table 28: Northern Europe: GDP and Investment IRFs at selected horizons (Low vs High debt regimes)

Variable	Regime	$h = 0$	$h = 4$	$h = 8$	$h = 12$	$h = 16$
GDP	Low	0.000 (0.000, 0.000)	-5.971* (-12.190, -0.724)	-7.319* (-15.329, -0.595)	-7.755* (-16.511, -0.666)	-7.856* (-16.848, -0.241)
GDP	High	0.000 (0.000, 0.000)	5.058* (1.538, 8.409)	6.856* (2.115, 11.659)	7.686* (2.317, 13.416)	8.167* (2.409, 14.446)
Investment	Low	0.000 (0.000, 0.000)	-2.995* (-12.190, -0.724)	-4.164* (-15.329, -0.595)	-4.854* (-16.511, -0.666)	-5.062* (-16.848, -0.241)
Investment	High	0.000 (0.000, 0.000)	7.310* (1.538, 8.409)	11.917* (2.115, 11.659)	14.156* (2.317, 13.416)	15.245* (2.409, 14.446)

Notes: Entries report posterior median M and 68% credible interval ($p16, p84$). An asterisk (*) denotes Sig68 = TRUE, i.e. the 68% credible interval excludes zero.

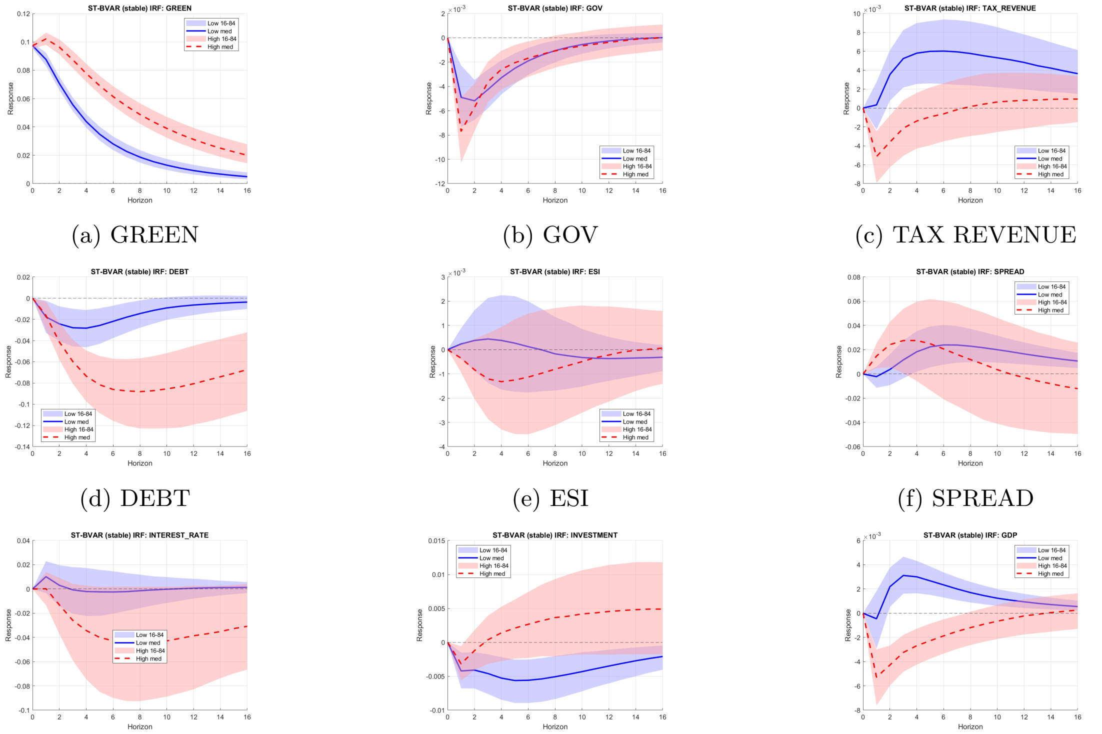

(a) GREEN (b) GOV (c) TAX REVENUE

(d) DEBT (e) ESI (f) SPREAD

(g) INTEREST RATE (h) INVESTMENT (i) GDP

Figure 21: Impulse responses to a green-spending shock: Full Panel European Union 1995-2019 ST-BVAR (low vs high debt regimes).

Table 29: European Union (18 countries): GDP and Investment IRFs at selected horizons (Low vs High debt regimes)

Variable	Regime	$h = 0$	$h = 4$	$h = 8$	$h = 12$	$h = 16$
GDP	Low	0.000 (0.000, 0.000)	2.335* (0.607, 3.916)	3.808* (1.839, 5.739)	4.424* (2.283, 6.698)	4.752* (2.501, 7.120)
GDP	High	0.000 (0.000, 0.000)	-3.538* (-4.907, -2.213)	-3.382* (-5.011, -1.851)	-3.065* (-4.949, -1.272)	-2.711* (-4.907, -0.577)
Investment	Low	0.000 (0.000, 0.000)	-5.404* (-8.485, -2.434)	-9.156* (-14.261, -4.256)	-11.688* (-18.278, -5.340)	-13.173* (-21.207, -5.677)
Investment	High	0.000 (0.000, 0.000)	-0.598 (-3.365, 2.183)	1.363 (-3.333, 5.890)	3.239 (-3.628, 9.968)	5.075 (-3.983, 14.296)

Notes: Entries report posterior median M and 68% credible interval ($p16, p84$). An asterisk (*) denotes Sig68 = TRUE (the 68% credible interval excludes zero).

Appendix E: Robustness Checks Total Government expenditure net green shock 1995-2019 pre-Covid

We report robustness checks for the total government spending shock net of green expenditure, using the pre-pandemic sample (1995–2019). As in the case of green spending shocks, restricting the sample does not alter the qualitative sign of the estimated impulse–response functions relative to the baseline specification. Differences emerge instead in terms of magnitude and statistical significance. In Eastern European countries and in the aggregate European Union panel, private investment responses under the low-debt regime become positive and larger in magnitude compared to the baseline, resulting in higher investment multipliers. By contrast, in Southern and Northern European countries, the contractionary response of private investment persists across regimes and gdp, consistent with a real crowding-out mechanism and behaviour consistent with Ricardian-type responses, as already observed in the baseline specification.

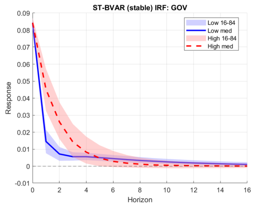

(a) GOV

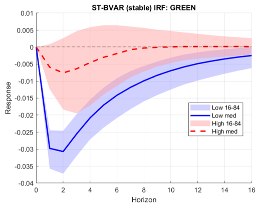

(b) GREEN

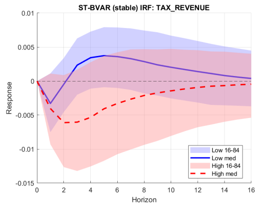

(c) TAX REVENUE

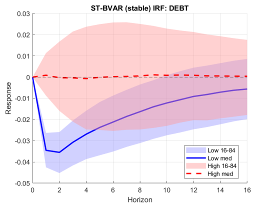

(d) DEBT

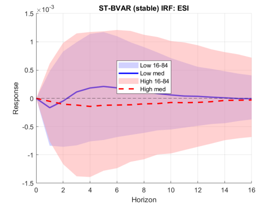

(e) ESI

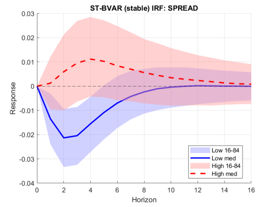

(f) SPREAD

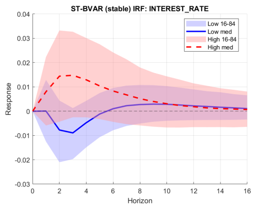

(g) INTEREST RATE

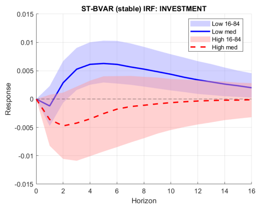

(h) INVESTMENT

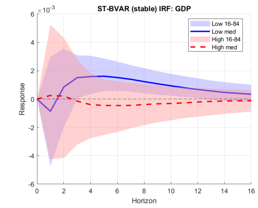

(i) GDP

Figure 22: Impulse responses to a Total government-spending net green shock : Eastern Europe 1995-2019 ST-BVAR (low vs high debt regimes).

Table 30: Eastern Europe: GDP and Investment IRFs to total government expenditure (net green), selected horizons

Variable	Regime	$h = 0$	$h = 4$	$h = 8$	$h = 12$	$h = 16$
GDP	Low	0.000 (0.000, 0.000)	0.064* (0.001, 0.550)	0.160* (0.234, 1.133)	0.209* (0.352, 1.517)	0.231* (0.398, 1.753)
GDP	High	0.000 (0.000, 0.000)	-0.001 (-0.545, 0.078)	-0.023 (-0.877, 0.269)	-0.037 (-1.117, 0.433)	-0.044 (-1.276, 0.554)
Investment	Low	0.000 (0.000, 0.000)	0.271* (0.001, 0.550)	0.660* (0.234, 1.133)	0.895* (0.352, 1.517)	1.028* (0.398, 1.753)
Investment	High	0.000 (0.000, 0.000)	-0.218 (-0.545, 0.078)	-0.293 (-0.877, 0.269)	-0.319 (-1.117, 0.433)	-0.328 (-1.276, 0.554)

Notes: Entries report posterior median M and 68% credible interval ($p16, p84$). An asterisk (*) denotes Sig68 = TRUE (the 68% credible interval excludes zero).

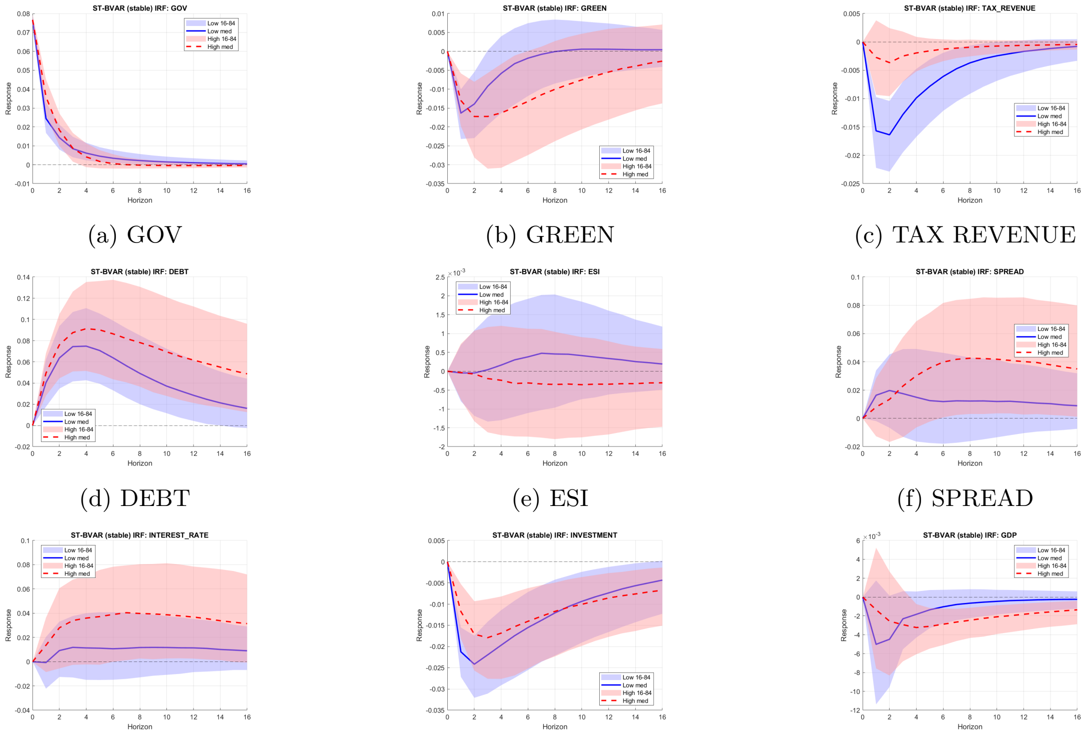

(a) GOV (b) GREEN (c) TAX REVENUE

(d) DEBT (e) ESI (f) SPREAD

(g) INTEREST RATE (h) INVESTMENT (i) GDP

Figure 23: Impulse responses to a Total government-spending net green shock : Southern Europe 1995-2019 ST-BVAR (low vs high debt regimes).

Table 31: Southern Europe: GDP and Investment IRFs to total government expenditure at selected horizons

Variable	Regime	$h = 0$	$h = 4$	$h = 8$	$h = 12$	$h = 16$
GDP	Low	0.000 (0.000, 0.000)	-0.209* (-1.773, -0.929)	-0.244* (-2.852, -1.243)	-0.258* (-3.589, -1.340)	-0.267* (-4.110, -1.360)
GDP	High	0.000 (0.000, 0.000)	-0.140* (-1.382, -0.462)	-0.290* (-2.623, -0.809)	-0.406* (-3.645, -1.037)	-0.496* (-4.550, -1.220)
Investment	Low	0.000 (0.000, 0.000)	-1.337* (-1.773, -0.929)	-2.040* (-2.852, -1.243)	-2.442* (-3.589, -1.340)	-2.684* (-4.110, -1.360)
Investment	High	0.000 (0.000, 0.000)	-0.884* (-1.382, -0.462)	-1.609* (-2.623, -0.809)	-2.163* (-3.645, -1.037)	-2.600* (-4.550, -1.220)

Notes: Entries report posterior median M and 68% credible interval $(p16, p84)$. An asterisk (*) denotes Sig68 = TRUE (the 68% credible interval excludes zero).

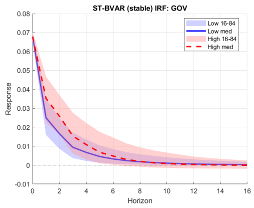

(a) GOV

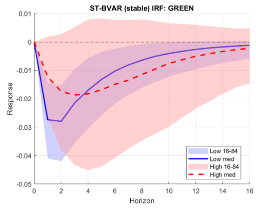

(b) GREEN

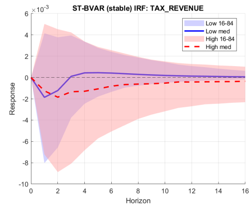

(c) TAX REVENUE

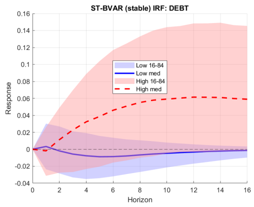

(d) DEBT

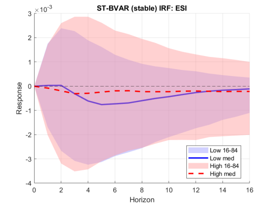

(e) ESI

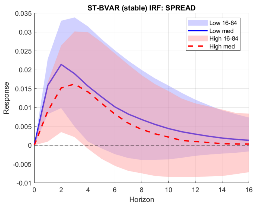

(f) SPREAD

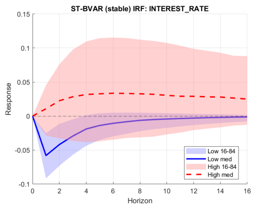

(g) INTEREST RATE

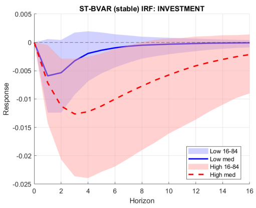

(h) INVESTMENT

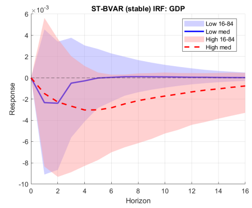

(i) GDP

Figure 24: Impulse responses to a Total government-spending net green shock : Northern Europe 1995-2019 ST-BVAR (low vs high debt regimes).

Table 32: Northern Europe: GDP and Investment IRFs to total government expenditure at selected horizons

Variable	Regime	$h = 0$	$h = 4$	$h = 8$	$h = 12$	$h = 16$
GDP	Low	0.000 (0.000, 0.000)	-0.294 (-0.674, 0.055)	-0.326 (-0.822, 0.124)	-0.335 (-0.871, 0.154)	-0.339 (-0.906, 0.165)
GDP	High	0.000 (0.000, 0.000)	-0.626* (-1.201, -0.163)	-1.060* (-2.091, -0.222)	-1.318* (-2.749, -0.194)	-1.460* (-3.179, -0.184)
Investment	Low	0.000 (0.000, 0.000)	-0.316* (-0.550, -0.088)	-0.391* (-0.780, -0.021)	-0.419 (-0.927, 0.072)	-0.431 (-1.036, 0.165)
Investment	High	0.000 (0.000, 0.000)	-0.389* (-0.669, -0.116)	-0.746* (-1.297, -0.166)	-1.039* (-1.897, -0.182)	-1.293* (-2.475, -0.137)

Notes: Entries report posterior median M and 68% credible interval ($p16, p84$). An asterisk (*) denotes Sig68 = TRUE.

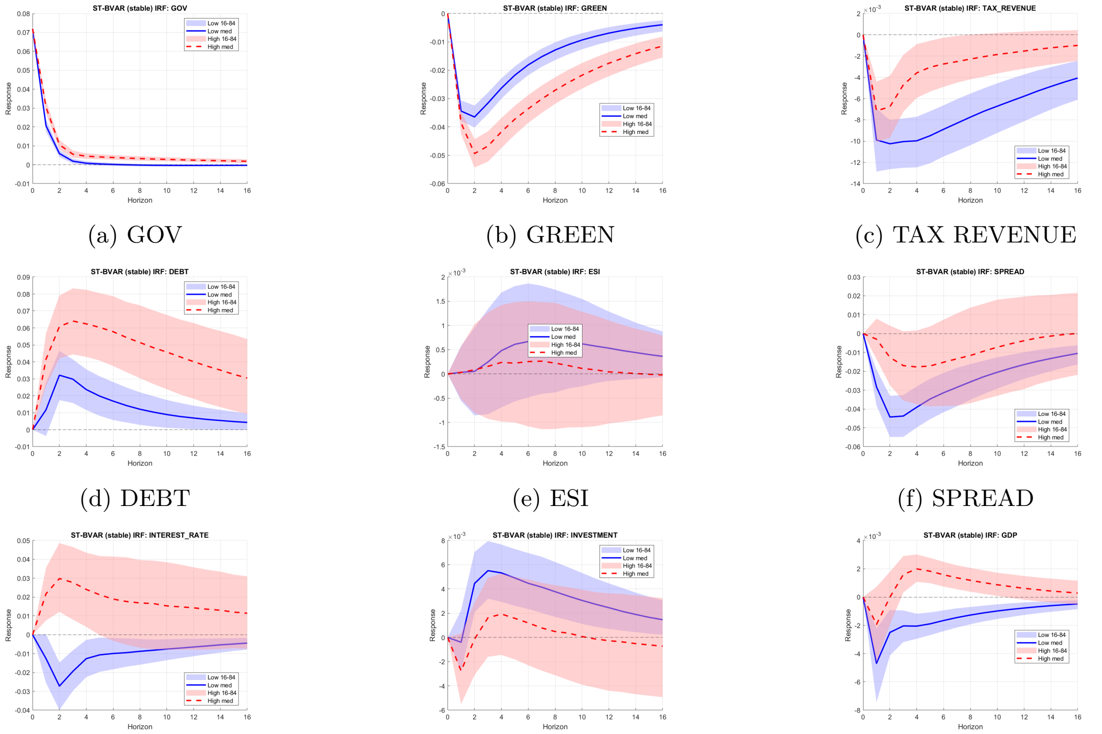

(a) GOV (b) GREEN (c) TAX REVENUE

(d) DEBT (e) ESI (f) SPREAD

(g) INTEREST RATE (h) INVESTMENT (i) GDP

Figure 25: Impulse responses to a Total government-spending net green shock : Full Panel European Union 1995-2019 ST-BVAR (low vs high debt regimes).

Table 33: Full EU: Responses to Total Government Expenditure Shock

	$h = 0$	$h = 4$	$h = 8$	$h = 12$	$h = 16$
Panel A: GDP					
Low debt	0.000	-0.256^{*} (0.152, 0.524)	-0.390^{*} (0.374, 1.093)	-0.474^{*} (0.495, 1.537)	-0.530^{*} (0.548, 1.845)
High debt	0.000	0.034 (–0.212, 0.232)	0.147 (–0.384, 0.537)	0.204 (–0.632, 0.770)	0.230 (–0.967, 0.962)
Panel B: Investment					
Low debt	0.000	0.338^{*} (0.111, 0.254)	0.715^{*} (0.117, 0.250)	0.975^{*} (0.121, 0.259)	1.144^{*} (0.124, 0.266)
High debt	0.000	0.013 (–0.077, 0.042)	0.091^{*} (–0.101, –0.002)	0.089^{*} (–0.110, –0.007)	0.047^{*} (–0.115, –0.001)

Notes: Cells report posterior median and 68% credible interval. Low (High) denotes the low- (high-) debt regime. * indicates significance at the 68% credible level (Sig68 = TRUE).

References

Afonso, A. and Sousa, R. M. (2012). The macroeconomic effects of fiscal policy. *Applied Economics*, 44(34):4439–4454.

Auerbach, A. J. and Gorodnichenko, Y. (2012). Measuring the output responses to fiscal policy. *American Economic Journal: Economic Policy*, 4(2):1–27.

Auerbach, A. J. and Gorodnichenko, Y. (2013). Output spillovers from fiscal policy. *American Economic Review*, 103(3):141–146.

Auerbach, A. J. and Gorodnichenko, Y. (2017). Fiscal stimulus and fiscal sustainability. Technical report, National Bureau of Economic Research.

Bańbura, M., Giannone, D., and Reichlin, L. (2010). Large bayesian vector auto regressions. *Journal of applied Econometrics*, 25(1):71–92.

Barro, R. J. and Redlick, C. J. (2011). Macroeconomic effects from government purchases and taxes. *The Quarterly Journal of Economics*, 126(1):51–102.

Batini, N., Di Serio, M., Fragetta, M., Melina, G., and Waldron, A. (2022). Building back better: How big are green spending multipliers? *Ecological Economics*, 193:107305.

Blanchard, O. (2019). Public debt and low interest rates. *American Economic Review*, 109(4):1197–1229.

Blanchard, O. and Perotti, R. (2002). An empirical characterization of the dynamic effects of changes in government spending and taxes on output. *the Quarterly Journal of economics*, 117(4):1329–1368.

Blanchard, O. J. and Leigh, D. (2013). Growth forecast errors and fiscal multipliers. *American Economic Review*, 103(3):117–120.

Bruns, M. and Piffer, M. (2024). Tractable bayesian estimation of smooth transition vector autoregressive models. *The Econometrics Journal*, 27(3):343–361.

Caselli, F., Lagerborg, A., and Medas, M. P. A. (2024). *Green fiscal rules? Challenges and policy alternatives*. International Monetary Fund.

Ciaffi, G. (2025). Green fiscal multipliers and the energy transition. Working Paper.

Deleidi, M., Iafrate, F., and Levrero, E. S. (2020). Public investment fiscal multipliers: An empirical assessment for european countries. *Structural Change and Economic Dynamics*, 52:354–365.

Ficarra, M. (2024). Public spending, green growth, and corruption: a local fiscal multiplier analysis for italian provinces. Technical report, Graduate Institute of International and Development Studies Working Paper.

Hall, R. E. (2009). By how much does gdp rise if the government buys more output? Technical report, National Bureau of Economic Research.

Huidrom, R., Kose, M. A., Lim, J. J., and Ohnsorge, F. L. (2020). Why do fiscal multipliers depend on fiscal positions? *Journal of Monetary Economics*, 114:109–125.

Ilzetzki, E., Mendoza, E. G., and Végh, C. A. (2013). How big (small?) are fiscal multipliers? *Journal of monetary economics*, 60(2):239–254.

Kadiyala, K. R. and Karlsson, S. (1997). Numerical methods for estimation and inference in bayesian var-models. *Journal of Applied Econometrics*, 12(2):99–132.

Mountford, A. and Uhlig, H. (2009). What are the effects of fiscal policy shocks? *Journal of applied econometrics*, 24(6):960–992.

Ramey, V. (2019). Fiscal policy: Tax and spending multipliers in the united states. *Evolution or Revolution?: Rethinking Macroeconomic Policy after the Great Recession*, pages 121–30.

Ramey, V. A. and Zubairy, S. (2018). Government spending multipliers in good times and in bad: evidence from us historical data. *Journal of political economy*, 126(2):850–901.

Romer, C. D. and Romer, D. H. (2010). The macroeconomic effects of tax changes. *American Economic Review*, 100(3):763–801.

Saccone, D., Della Posta, P., Marelli, E., and Signorelli, M. (2022). Public investment multipliers by functions of government: An empirical analysis for european countries. *Structural Change and Economic Dynamics*, 60:531–545.

Shah, S. S. A. and Wu, K. (2025). How effective are green spending multipliers? eco-friendly vs non-eco-friendly spending in oecd economies. *Energy Policy*, 204:114676.

Sims, C. A. and Zha, T. (1998). Bayesian methods for dynamic multivariate models. *International Economic Review*, pages 949–968.

Climate Policy Shocks, Demographics, and Fiscal Sustainability in European Countries

Alessio Ferraro[1]

[1]Roma Tre University, Department of Economics

Abstract

This paper analyzes the macroeconomic, fiscal, demographic, and health effects of emission and environmental policy shocks in Europe. Using a panel Bayesian VECM for 21 European countries over 1995–2019, we assess the joint responses to two types of shocks: a brown shock, defined as an increase in emissions due to a relaxation of mitigation policies, and a mitigation shock, representing a tightening of green measures. Results show that brown shocks raise mortality and morbidity, reduce transfer and pension expenditures over time, and lead to lower GDP, consumption, and wages. Mitigation shocks, instead, reduce emissions and—after an initial contraction—improve macroeconomic conditions. The macro-fiscal and demographic impacts of mitigation policies differ across shock types, depending on whether they are market-based, non-market-based, or technology-driven.

Keywords: Climate policy shocks; Carbon intensity; Environmental policy stringency; Demographic and health outcomes; Panel Bayesian VECM.
JEL Classification: C11; E32; Q54; J11; I15.

Contents

1 Introduction

The renewed debate over global population growth reflects a deeper ambivalence about its implications for sustainable development and climate change. On one hand, some scholars argue that slowing or reversing population growth is essential to prevent a socio-ecological collapse (Crist et al. 2022; P. R. Ehrlich and A. H. Ehrlich 2013) . On the other hand, a more optimistic perspective contends that the real issue lies in high-consumption lifestyles, economic inequality, and inefficient resource management rather than in population size itself (Coole 2013). From this viewpoint, demographic pressure can even foster innovation and productivity (Boserup 1965; Simon 2019).

Today, however, the focus of concern has shifted: global population growth is slowing sharply, and the debate no longer centers on the risk of overpopulation but rather on the opposite threat — population decline — and its potential economic and social implications (Dorling 2020).

Economic literature has so far analyzed climate change and demographic dynamics largely as separate phenomena or has focused on how population growth and structure influence the climate and, indirectly, the economy. However, recent studies highlight that these two forces are deeply interdependent and are likely to interact increasingly over the long term. On the one hand, population growth and aging affect productivity and macroeconomic sustainability; on the other, climate change reduces growth potential, increases uncertainty, and amplifies pressures on inflation, interest rates, and public finances.(Henderson et al. 2024; Thakoor and Kara 2022)

In this context, the aim of the present study is to identify the effects of climate policy shocks — both a relaxation of green measures (brown shock) and, conversely, a tightening of mitigation policies — on demographic dynamics and macro-fiscal outcomes. This approach allows us to capture the reverse channel relative to the existing literature, assessing how climate policy choices directly and indirectly influence population dynamics, public spending, and overall economic performance.

The possibility of a brown shock can be linked to political and institutional orientations that, in specific contexts, have reduced or questioned the commitment to the ecological transition. A relevant example is the stance taken by the Trump administration at the United Nations, which led to a temporary rollback of international climate commitments. In the European context, a similar debate emerged under President Von Der Leyen within the European Parliament, where proposals to relax certain Green Deal measures were discussed in order to balance environmental objectives with industrial competitiveness.

To address these issues, we employ a Panel Bayesian Vector Error Correction Model (VECM), which captures both short-term dynamics and long-term equilibrium relationships among variables across countries. The VECM framework allows for heterogeneous adjustments while maintaining a common long-run structure, making it particularly suitable for analyzing interconnected macroeconomic and demographic systems. Within this setting, we estimate an emissions shock — proxied by changes in carbon intensity — and assess its effects on health, demographic, and macro-fiscal variables. This approach enables us to quantify both the immediate and persistent impacts of climate policy shifts on demographic outcomes and economic performance.

The link between CO emissions — the main greenhouse gas responsible for climate change — and health problems has attracted the attention of many scholars. Epidemiological studies have demonstrated the effects of air pollution from combustion on four major categories of human diseases: cardiovascular diseases, diabetes mellitus, cancer, and chronic kidney diseases.(Rasoulinezhad et al. 2020)

Several empirical studies have also shown that the growth of more developed economies is closely correlated with CO emissions, suggesting the existence of a short-term feedback relationship between the two phenomena (Jia et al. 2023) . Our study contributes to this empirical literature by examining how transition shocks brown propagate through demographic and health dynamics before shaping macro-fiscal outcomes.

Moreover, mitigation policies — captured through shocks to the OECD Environmental Policy Stringency (EPS) indicator, which measures the degree of policy rigidity — provide insights into how such shocks affect both macroeconomic and demographic variables.

Emissions shock, interpreted as an increase in carbon intensity (brown shock), leads to a rise in climate-related morbidity and mortality among both individuals over and under 65 years of age. This, in turn, generates adverse effects on key macroeconomic components, including declines in GDP, wages, consumption, and employment. On the fiscal side, we estimate a contraction in pension and transfer expenditures, accompanied by an increase in public debt and interest rates. These results highlight how demographic dynamics capture novel aspects of the relationship between GDP and emissions, which becomes less cyclical over time.

By contrast, various types of mitigation policies — whether market-based, non-market-based, or technology-oriented — improve demographic and health outcomes while reducing emissions. Although macro-fiscal components initially respond negatively, hey gradually re-align with their medium-term path in the following years.

The paper is structured as follows. Section 1 provides a review of the existing literature, with particular attention to studies examining the interactions between demographic, health, and macroeconomic dynamics in relation to climate change and environmental policies. Section 2 describes the data employed, the variables of interest, and the main statistical sources. Section 3 outlines the empirical methodology — a Panel Bayesian Vector Error Correction Model (VECM) — section 4 discusses the main results in detail. Finally, Section 5 concludes by summarizing the key findings and outlining policy implications and avenues for future research.

2 Literature review

The relationship between demographic dynamics and economic growth has been debated since antiquity, from Platone and Malthus to modern economists. After the 20th-century concern over overpopulation (P. R. Ehrlich and A. H. Ehrlich 2009; Kuznets 1967), attention has shifted toward population slowdown and decline. Recent studies show that demographic decline does not necessarily imply stagnation: theoretical models (Elgin and Tumen 2012; Jones 2022; Strulik 2024) indicate that per capita income can continue to grow, driven by technological progress and human capital. Although much attention has been devoted to population aging, the decline in the working-age population also carries significant economic implications (Maestas et al. 2023). After decades of a "demographic dividend," a shrinking labor force may lead to lower productivity, requiring new strategies for employment, economic development, and social policy. This raises questions about policymakers' ability to manage such a profound demographic transition effectively.Conversely, population growth poses significant challenges for climate change dynamics, particularly in terms of resource consumption. Among the proposed strategies to mitigate the disruptions caused by climate change, one emphasizes that the human population "must be stabilized—and, ideally, gradually reduced—within a framework that ensures social integrity" (Ripple et al. 2020).Population is a key driver of resource consumption and waste generation, and thus a fundamental determinant of global change. Climate change, driven by rising greenhouse gas emissions, affects livelihoods, agricultural production, economic conditions, and human health, thereby influencing demographic processes—fertility, mortality, and migration—and consequently the structure and distribution of the population. The interaction among emissions, climate change, and health thus creates a potential feedback loop within human–environment systems, whereby human activities alter the climate, and climatic impacts, in turn, feed back onto the population.Climate research has shown that CO emissions—the main greenhouse gas responsible for climate change—have direct impacts on human health (Jacobson 2008). Pollution from the combustion of fossil fuels can disrupt hypothalamic regulation of appetite and metabolism, contribute to diabetes through oxidative stress, and promote the development of cancer and COPD via mitochondrial damage and inflammatory responses(Rasoulinezhad et al. 2020) . It is therefore widely recognized that fossil fuel consumption has negative effects on health . At the same time, the literature highlights a complex relationship between economic growth and health: while growth requires higher energy consumption and thus increases emissions, it can also enhance healthcare infrastructure and overall living conditions. Scientific evidence shows that rising CO_2 levels, beyond driving global warming, have indirect yet significant impacts on human health (Abdul-Nabi et al. 2025) . Higher temperatures and humidity resulting from increased CO_2 concentrations elevate ozone and particulate matter levels, worsening air pollution in already affected regions. According to high-resolution global models, each 1°C increase in CO_2-induced temperature may cause about 1,000 additional deaths per year in the United States and over 20,000 worldwide, mainly from ozone- and particle-related diseases (Jacobson 2008) . Although CO_2 does not directly affect respiration, its climatic effects alter meteorological conditions and amplify the impact of air pollution on human health.The macro-econometric literature examining the joint dynamics of emissions and the economy is extremely limited. Most studies have focused primarily on the impact of economic growth on emission levels. A notable contribution is provided by Skare et al. 2021, who employ vector autoregressive models to explore the relationship between economic shocks and emissions across 20 advanced economies from 1870 to 2016. Their results reveal a strong co-movement between emissions and economic activity, showing that approximately 40 percent of CO_2 fluctuations are explained by aggregate economic factors such as output, population, and oil prices.Recent macro-econometric literature has explored the relationship between economic growth and CO emissions, revealing heterogeneous results depending on methodology and context. Jia et al. 2023, using a mixed-frequency VAR, show that in G7 countries, growth rates are strongly correlated with CO_2 emissions. Earlier studies—based on both panel and single-country regressions—examined how economic expansion influences pollution, often finding a feedback relationship between growth and emissions (Friedl and Getzner 2003; Roca et al. 2001).

More recent evidence from both advanced and emerging economies (Bekun et al. 2022; Caglar et al. 2022) confirms that economic growth, energy consumption, and the exploitation of natural resources tend to increase emissions, whereas factors such as trade openness and economic complexity can enhance environmental quality. However, results vary considerably: some studies identify causality running from GDP to emissions, others find bidirectional or no causality at all, underscoring the complexity of the relationship between economic development, energy, and the environment (Cohen et al. 2018; Espoir et al. 2021).

In DSGE modeling, Lupi and Marsiglio 2021 analyze the two-way interaction between population growth and climate change: population increases drive carbon emissions, while climate change affects mortality and thus demographic dynamics. Incorporating these population–climate feedbacks into an integrated climate–economy model with endogenous fertility and temperature-dependent mortality, they show that accounting for demographic change raises the social cost of carbon, but population control policies can significantly reduce overall mitigation costs. This highlights the potential of demographic policy as a complementary tool to traditional climate strategies.

Another DSGE model Henderson et al. 2024 underscores that its findings must not be interpreted as justification for downplaying the centrality of climate change in favour of population growth considerations. While recognizing that population can be a key driver of environmental pressure, the authors stress that the damages caused by climate change remain severe and are largely the result of decisions made in developed countries. Moreover, their analysis does not address the costs or unintended consequences of policies aimed at reducing population growth, nor the ethical and welfare differences between mitigating global warming and curbing population growth.Thakoor and Kara 2022 develop a DSGE model integrating demographic dynamics and climate change, distinguishing between workers and retirees to capture heterogeneous responses to shocks. By modeling climate change as a negative productivity shock, the authors show that rising temperatures reduce output and increase inflation, while also generating indirect effects through greater uncertainty. Their results indicate that, without stronger mitigation and adaptation policies, economic and fiscal costs could rise rapidly, particularly in developing countries facing growing capital demands. The study concludes that fiscal and monetary frameworks must be revised to account for climate-related shocks, as climate change is expected to raise debt-to-GDP ratios, fuel inflationary pressures, and make monetary policy implementation more complex.As we have seen so far, the literature has mainly focused on the effects of population growth on climate change and on how emissions and economic growth interact. This study helps address this gap by analyzing how a brown shock affects demographic and health dynamics and, through these transmission channels, key macroeconomic and fiscal variables. Our approach reverses the prevailing perspective in the literature: rather than starting from economic activity to explain emissions, we take environmental shocks as the point of departure and examine their cascading effects on population trends, public health, and the macro-fiscal framework.

The literature on Environmental Policy Stringency (EPS) examines how the degree of environmental regulation affects emissions, innovation, and economic growth. Recent studies show that higher stringency reduces emissions and promotes green technologies, though it may entail short-term economic costs that vary depending on the type of policy and countries' level of development. Numerous studies have investigated the impact of environmental policies on economic growth at the national level, but the number of cross-country analyses remains limited (Bhattacharya et al. 2016; Halkos and Psarianos 2016; Rubashkina et al. 2015). Some studies estimating economic growth models report conflicting results regarding the effect of CO_2 emission reduction policies on economic performance (Ricci 2007; Soytas and Sari 2009). These inconsistencies have contributed to a widespread perception among policymakers that efforts to curb greenhouse gas emissions may harm economic growth, leading many countries to adopt minimal or negligible emission reduction trajectories(Nordhaus 2018). There is evidence suggesting that efforts to reduce greenhouse gas (GHG) emissions may be detrimental to GDP growth and employment in the short term (Le Quéré et al. 2018; Maji 2015), as such reductions often entail significant capital costs. However, environmental policy may yield long-term dividends in the form of sustained economic growth. For instance, Sweden, the first country to introduce a carbon tax in 1991—and currently the nation with the highest carbon tax in the world—has experienced GDP growth exceeding the European average (Aziz et al. 2022). Consistent with the Porter Hypothesis (M. Porter 1996; M. E. Porter and Linde 1995), these and other findings (Lu et al. 2010) suggest that firms tend to develop alternative production methods by changing or upgrading technology, thereby reducing CO emissions without sacrificing GDP or employment in the long run. This study estimates the short- and long-term effects of environmental control policies on the economic growth of OECD countries. The paper by Ciccarelli and Marotta 2024 provides a significant contribution to the analysis of the macroeconomic effects of physical and transition climate risks, using a Bayesian VAR model on a panel of 24 OECD countries with annual data covering the period 1990–2019. The study shows that climate shocks tend to reduce output, while mitigation policies and technological innovation generate positive effects in the medium term. The findings highlight the importance of country-specific policy strategies and the need for coordinated climate action, particularly within monetary unions, to mitigate asymmetric impacts on macroeconomic and financial stability. In summary, previous research has extensively explored the links between demography, climate change, health, and the economy, though often addressing these aspects separately. Empirical evidence jointly examining demographic, health, and macroeconomic channels remains limited. This study contributes to this line of inquiry by employing a Panel Bayesian Vector Error Correction Model (VECM) to assess the effects of two types of climate shocks — a brown shock, associated with higher emissions, and a mitigation shock, reflecting tighter environmental policies — on demographic, health, and macro-fiscal variables. The aim is to provide a more integrated empirical perspective on how climate policy actions may influence economic and demographic dynamics over time, complementing existing findings in the literature.

3 Data

3.0.1 Macro-fiscal variables

In this study, we employ a comprehensive set of variables to analyze the macroeconomic, fiscal, and demographic dimensions in an integrated framework. Specifically, the model includes four macroeconomic variables — gross domestic product (GDP), wages, employment, and consumption —, six fiscal variables — total public expenditure, tax revenues, transfers, pensions, public debt, and interest rates —, and five demographic variables — mortality and morbidity attributable to pollution, age-specific mortality (under 65 and over 65), dependency ratio, and life expectancy. The analysis is based on an unbalanced annual panel dataset covering 21 European countries — Austria, Belgium, Czech Republic, Denmark, Finland, Germany, Greece, Ireland, Italy, Luxembourg, the Netherlands, Poland, Spain, Sweden, Estonia, Hungary, Portugal, Slovakia, Slovenia, Iceland, and Norway — over the period 1995–2019. Data are drawn from the EUROSTAT and OECD databases.

3.0.2 Carbon Intensity

Per capita carbon intensity. This variable measures the amount of carbon dioxide (CO_2) emissions generated per unit of economic output and per person, providing an indicator of the environmental efficiency of production relative to the population's economic well-being. It is defined as the ratio between per capita CO_2 emissions (in metric tons per person) and real GDP per capita:

$$CI_{i,t} = \frac{\frac{E_{i,t}}{P_{i,t}}}{\frac{Y_{i,t}}{P_{i,t}}} = \frac{E_{i,t}}{Y_{i,t}} \tag{1}$$

A higher value indicates greater carbon intensity—that is, more emissions per unit of economic output per individual—whereas a decline reflects improved energy efficiency or a transition toward cleaner energy sources.

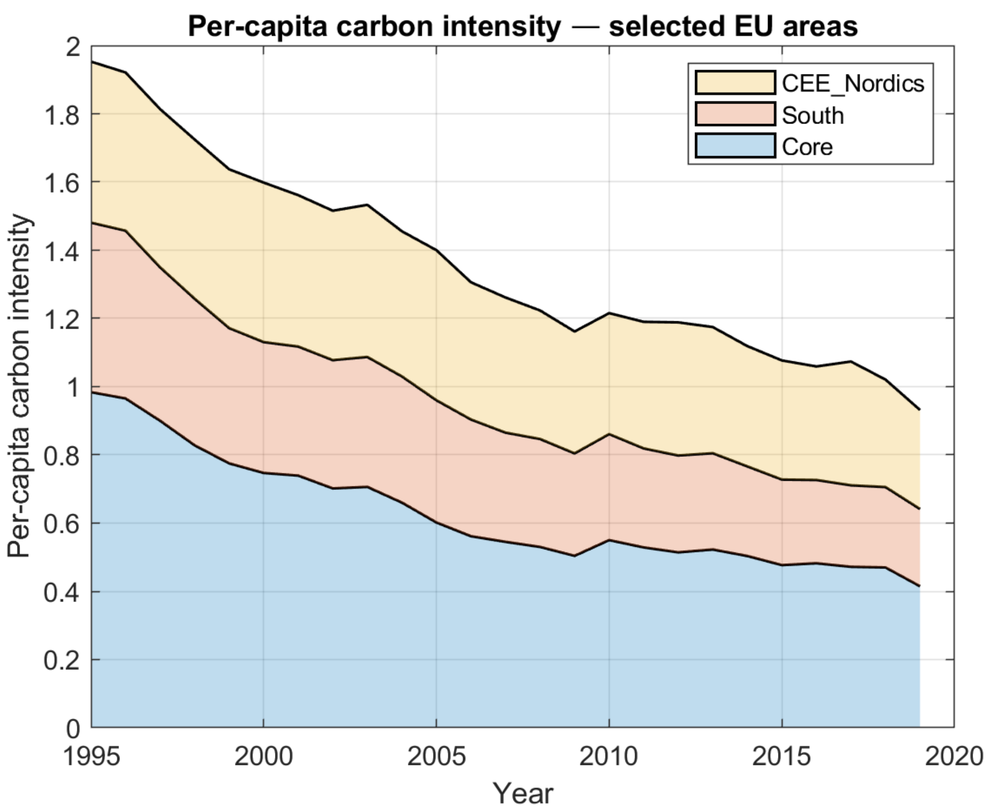

Figure 1: Per-capita carbon intensity across groups of European countries (1995–2019). The figure shows the evolution of average per-capita carbon intensity, divided into three regional groups: **Core** (Austria, Belgium, Germany, the Netherlands, Luxembourg, and Ireland); **South** (Italy, Portugal, Greece, and Spain); **North & East** (Sweden, Finland, Slovakia, Poland, Hungary, Estonia, Norway, Iceland, and Slovenia). Values are expressed as CO_2 emissions per unit of GDP per capita.

3.1 Environmental Policy Stringency

The OECD Environmental Policy Stringency (EPS) Index is a composite indicator designed to measure the degree of strictness of environmental policies across countries and over time. It quantifies how strongly governments impose environmental regulations and price mechanisms that encourage the reduction of pollution and greenhouse gas emissions.

The EPS combines multiple policy instruments — including market-based measures (such as carbon taxes, emissions trading systems, and pollution charges), non-market instruments (such as emission and performance standards), and technology support policies (such as *RD* subsidies or feed-in tariffs). Each component is normalized and aggregated to create a comparable measure of policy stringency on a scale from 0 (least stringent) to 6 (most stringent).

Originally developed by Botta and Koźluk 2014, and recently updated to EPS21 (OECD, 2021) (Kruse et al. 2022) , the index covers around 40 countries from 1990 to 2020. It allows for cross-country and temporal comparisons of environmental policy efforts, and is widely used in empirical research to assess the impact of stricter environmental policies on economic, social, and environmental outcomes.As shown in Figure 3, once the EPS is broken down into its components, the scores associated with non-market-based policies have been consistently higher than those of the other sub-indices since the 1990s.

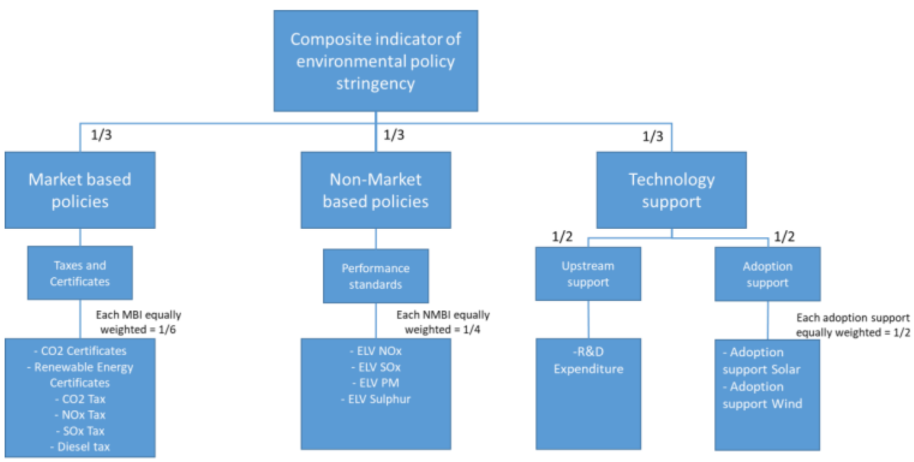

Figure 2: The figure shows the aggregation structure of the revised EPS index (referred to as "EPS21"). Source: OECD

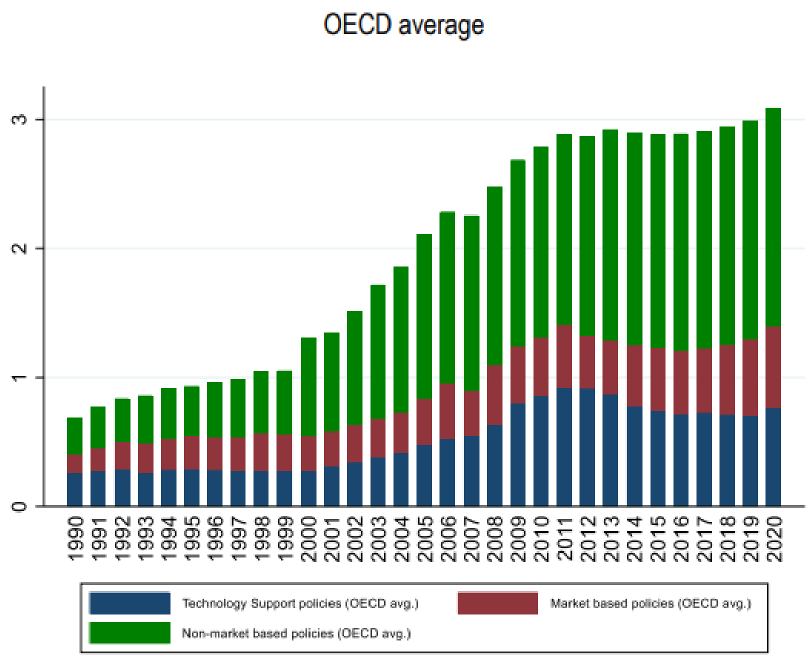

Figure 3: The figure shows the composition of the EPS over time for the OECD average. Blue bars show the contribution of technology support policies in the overall EPS. Red bars show the contribution of market based policies. Green bars show contribution of in non-market based policies. The OECD average is computed for 34 member countries. Data for Colombia, Costa Rica, Latvia and Lithuania was not available. Source: OECD.

3.2 Market Based Instruments

The Market-Based Instruments (MBI) sub-index captures environmental policies that assign an explicit price to pollution, thereby creating economic incentives to reduce emissions. These instruments include:

CO_2 Trading Schemes, which cap total emissions and allow firms to trade emission permits; stringency is measured by the average permit price in USD per tonne of CO_2.

Renewable Energy Trading Schemes, which require utilities to obtain a minimum share of electricity from renewable sources; the higher the mandated share, the stricter the policy.

CO_2 Taxes, NOx Taxes, and SOx Taxes, the stringency of which is defined by the tax rate per ton of emitted pollutant, converted into USD for comparability.

Fuel Taxes (Diesel), measured as the ratio between the tax per liter of diesel and its pre-tax price, reflect the fiscal burden of fossil fuel use.

In all cases, a higher price signal indicates a more stringent policy stance, as it raises the cost of polluting activities and strengthens the incentive to adopt cleaner technologies.The diesel tax (figure 4)remained stable over time and was the main market-based instrument until the mid-2000s. With the introduction of the EU ETS, the stringency of market-based policies increased, but with significant volatility due to fluctuations in the price of emission allowances: prices were very low in the early phases and again between 2012 and 2017, followed by a strong increase between 2018 and 2020.

Panel B: Market based policies

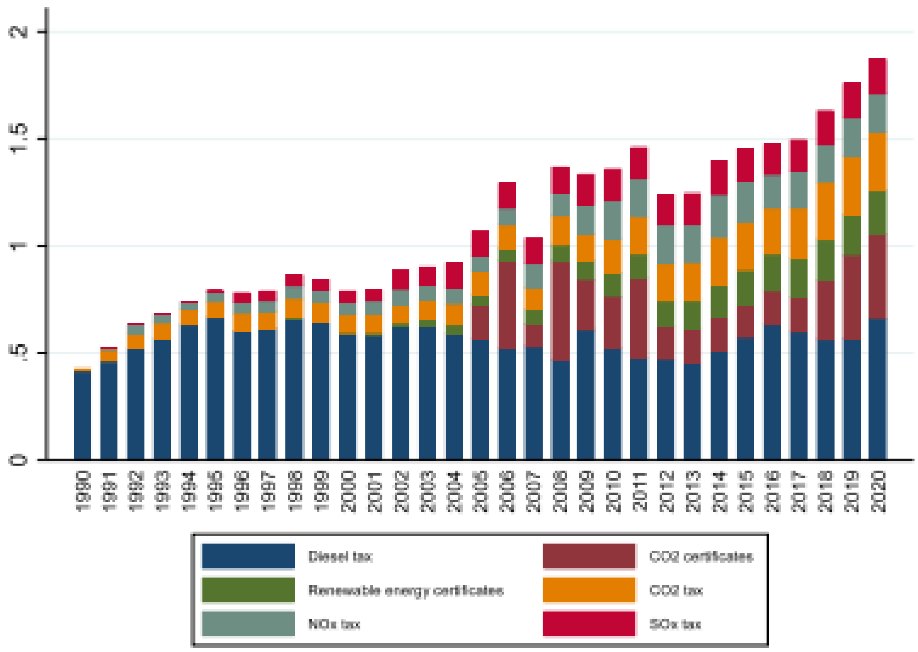

Figure 4: : The figure shows the composition of the three main components of the EPS and the relative stringency of each policy within

3.3 Non-Market Based instruments

The Non-Market-Based Instruments (NMBI) sub-index includes policies that regulate pollution through emission limits and technical standards rather than by pricing emissions.

Specifically, it encompasses:

Emission Limit Values (ELVs) for nitrogen oxides (NOx), sulfur oxides (SOx), and particulate matter (PM) are defined as the maximum concentrations of pollutants allowed for large, newly built coal-fired power plants. Lower permitted concentrations indicate higher policy stringency.

Sulfur content limits in diesel fuel set the maximum allowable sulfur concentration in diesel, acting as a measure of fuel quality standards.

These indicators capture the degree to which governments impose direct regulatory constraints on pollutant emissions. Unlike market-based instruments, they rely on command-and-control approaches that mandate compliance with specific performance thresholds.The stringency of renewable energy certificates and of NOx, SOx, and CO_2 taxes has gradually increased over the last decade, especially in a limited group of countries. However, in most countries there is still considerable scope to expand emission pricing.

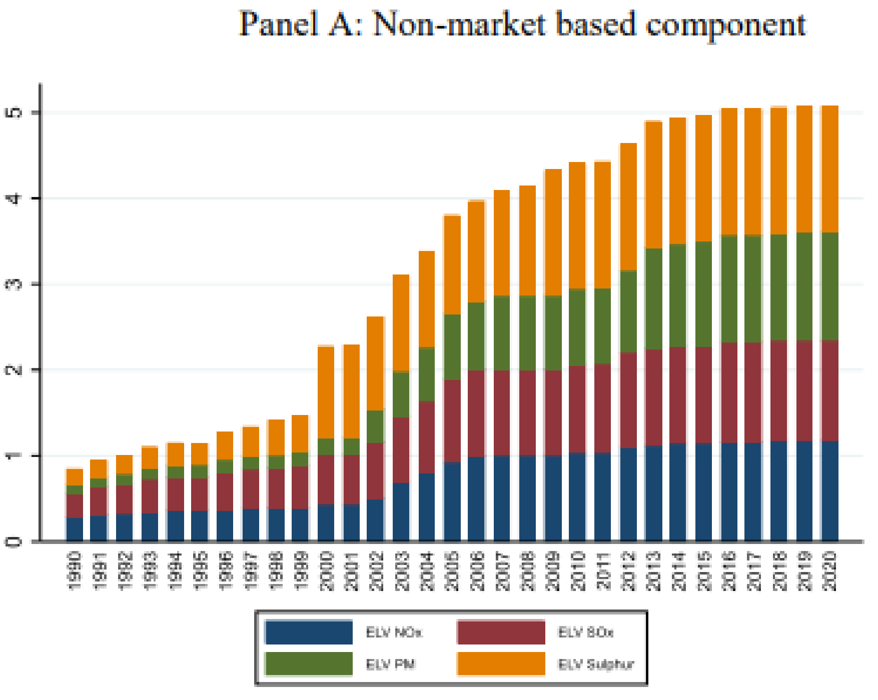

Figure 5: : The figure shows the composition of the three main components of the EPS and the relative stringency of each policy within

3.4 Technology Support (TS) Policies

The Technology Support (TS) sub-index captures policies that promote the innovation, development, and adoption of clean energy technologies. These measures aim to accelerate the energy transition by reducing technological and financial barriers to low-carbon solutions.

It includes two main components:

Public *RD* expenditure measures government spending on low-carbon energy research relative to nominal GDP. This encompasses renewable energy, energy efficiency, carbon capture and storage (CCS), nuclear, hydrogen and fuel cells, and other cross-cutting technologies.

Renewable energy price support for solar and wind reflects the relative level of subsidies or guaranteed prices provided through feed-in tariffs (FITs) or renewable energy auctions. The indicator normalizes the support level by the global levelized cost of electricity (LCOE) to account for technological cost declines.

Overall, higher values of this sub-index indicate a stronger governmental commitment to fostering technological innovation and deployment in the clean energy sector.After 2011 (figure 6), the stringency of technology support policies declined mainly because public *RD* subsidies for low-carbon technologies fell as a share of GDP. This decrease may also be linked to fiscal consolidation pressures following the Global Financial Crisis, when governments reduced public spending. This trend raises concerns, as support for clean innovation is weakening precisely when it is most needed.

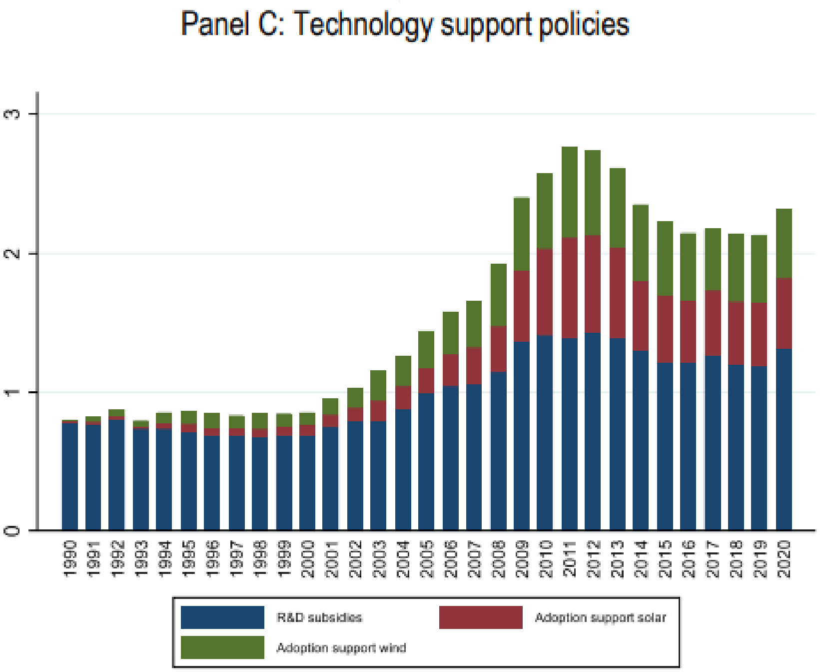

Figure 6: : The figure shows the composition of the three main components of the EPS and the relative stringency of each policy within

4 Econometric Framework: Bayesian Panel VECM

4.1 Methodological Overview: Bayesian Panel VECM

This section estimates the joint dynamics of environmental, demographic-health, and macro-fiscal variables using a Bayesian Panel Vector Error-Correction Model (BVECM) on an unbalanced panel of European countries.

Identification. The empirical framework assumes the existence of a single long-run equilibrium relationship linking emissions, economic activity, labour market conditions, public expenditure, and climate-related mortality. Emissions are used as the normalisation variable, anchoring the long-run relation and ensuring identification of the cointegration space.

Deviations from this equilibrium are corrected through heterogeneous adjustment dynamics, captured by the error-correction coefficients. This implies that variables respond differently to long-run imbalances depending on their structural role in the system.

Structural shocks are identified using a recursive (Cholesky) ordering. The ordering reflects a causal hierarchy in which climate policy and emissions affect demographic-health outcomes, which in turn propagate to macro-fiscal variables.

Estimation. The empirical analysis proceeds in four steps. First, the panel VECM is specified including lagged differences, the error-correction term, and two-way fixed effects. Second, the cointegration structure is imposed with a single long-run relation among structural variables. Third, Bayesian shrinkage is introduced through a Minnesota prior on the coefficients and an Inverse Wishart prior on the covariance matrix, stabilising estimation in a high-dimensional setting. Finally, posterior distributions are obtained via Monte Carlo simulation, and impulse response functions are computed from the VECM representation.

Impulse responses are derived from the posterior distribution using a recursive identification scheme. Point estimates correspond to posterior medians, while uncertainty is summarised by 68% credible intervals.

This framework allows us to jointly capture short-run dynamics and long-run equilibrium adjustment, while accounting for cross-country heterogeneity and parameter uncertainty.

4.2 Model Panel BVECM

We estimate a Bayesian Panel Vector Error-Correction Model (BVECM) for an unbalanced annual panel of $N = 21$ European countries over 1995–2019. The specification integrates (i) two-way fixed effects, (ii) a single cointegration relation linking environmental, demographic-health, and macro-fiscal variables, and (iii) Bayesian shrinkage to regularise the high-dimensional parameter space.

Let $y_{i,t}$ denote the K-dimensional vector of endogenous variables for country i. The estimated model is:

$$\Delta y_{i,t} = \alpha\beta' y_{i,t-1} + \sum_{p=1}^{P} \Gamma_p \Delta y_{i,t-p} + \mu_i + \tau_t + \varepsilon_{i,t}, \qquad i = 1, \dots, N,\ t = 1, \dots, T, \tag{2}$$

where $\alpha\beta'$ is the long-run adjustment term, following standard cointegration theory (Engle and Granger 1987; Johansen 1991), Γ_p captures short-run dynamics, μ_i and τ_t are country- and time-fixed effects, and $\varepsilon_{i,t} \sim (0, \Sigma)$ is the vector of reduced-form innovations. We set $P = 2$ to match annual frequency and avoid overspecification (see Appendix B for test cointegration and Grange test).

4.3 Cointegration Structure

A unique long-run equilibrium relation is imposed, with emissions used as the normalization variable to ensure proper identification of the system. This condition implies that the adjustment coefficient associated with emissions is negative ($\alpha_{\text{emiss}} < 0$), ensuring a stable convergence mechanism for the environmental block. Formally, the normalization removes the scalar indeterminacy of the cointegration space and provides an interpretable reference point for long-run comparisons across variables.

The remaining adjustment coefficients α, associated with macroeconomic and demographic-health variables, are not normalised and are instead freely estimated. They measure the speed and intensity with which each variable corrects deviations from the long-run equilibrium. Negative coefficients indicate convergence and reabsorption of imbalances, values close to zero suggest marginal participation in the adjustment mechanism, and positive coefficients reflect divergence or a response not aligned with the equilibrium correction process. In this sense, α constitutes a vector of heterogeneous adjustment speeds across the system, with emissions anchoring the long-run dynamics and the other variables reacting according to their structural role within the model.

The long-run relation is restricted to structural variables, namely emissions, real economic activity, labour-market capacity, public expenditure, and climate-related mortality. These elements define the structural state of the system and are expected to share a common equilibrium path:

$$\beta' y_{i,t} = \beta_{\text{emiss}}\text{emiss}_{i,t} + \beta_{\text{gdp}}\text{gdp}_{i,t} + \beta_{\text{empl}}\text{empl}_{i,t} + \beta_{\text{gov}}\text{gov}_{i,t} + \beta_{\text{cdi}}\text{climate\_deaths\_index}_{i,t}. \quad (3)$$

Emissions serve as the normalisation variable for identification of the cointegration relation, while the remaining coefficients capture the co-movement of macro-fiscal and health dynamics with environmental pressure. Policy-dependent variables such as transfers, pensions, tax revenues, public debt, interest rates, and life expectancy are instead included in first differences to avoid over-identification and to preserve a clear distinction between the structural equilibrium and short-run adjustment mechanisms.

Long-run variables included in β:

emiss: CO_2 emissions per capita
gdp: real GDP
empl: employment rate
gov: public expenditure
cdi: climate-related mortality index

4.4 Bayesian Estimation and Posterior Simulation

The panel VECM is estimated in a Bayesian framework that combines a Minnesota prior on the autoregressive coefficients with an Inverse Wishart prior on the covariance matrix of reduced-form innovations. Let B denote the stacked coefficient matrix of lagged differences and error-correction terms, and let Σ be the $K \times K$ covariance matrix of structural disturbances.

Prior structure. Following standard practice in Bayesian VARs (Kadiyala and Karlsson 1997; Karlsson 2013; Koop, Korobilis, et al. 2010; Litterman 1986; Sims and Zha 1998), the prior is specified as:

$$B \mid \Sigma \sim \mathcal{N}\big(\bar{B},\ \Sigma \otimes V_{\text{Minn}}\big), \quad (3)$$
$$\Sigma \sim IW(\bar{S}, \bar{\nu}), \quad (4)$$

where V_{Minn} encodes: (i) overall shrinkage towards a parsimonious AR structure, (ii) cross-equation shrinkage to limit excessive feedback among variables, and (iii) lag decay to penalize higher-order autoregressive terms. The parameters $(\bar{S}, \bar{\nu})$ control the informational tightness of the Inverse Wishart prior and ensure that Σ remains positive definite during posterior simulation.

Posterior sampling. Given the conjugate structure of the priors, the posterior distributions admit closed-form updates. Estimation proceeds by drawing $N_{\text{draws}} = 5000$ Monte Carlo samples from the joint posterior:

$$\Sigma^{(d)} \sim IW(S_n, \nu_n), \tag{5}$$

$$B^{(d)} \sim \mathcal{N}\big(B_n,\ \Sigma^{(d)} \otimes V_n\big), \qquad d = 1, \ldots, 5000, \tag{6}$$

where (B_n, V_n, S_n, ν_n) are the posterior hyperparameters implied by the conjugate update. In practice, the draws are generated through the MATLAB routines `iwishrnd` and `mvnrnd`, which implement the conditional sampling steps for (B, Σ), matching the recursive structure of the model.

Posterior impulse responses. For each posterior draw d, the matrices $(\Gamma^{(d)}, \Pi^{(d)}, \Sigma^{(d)})$ are mapped into impulse response functions using the VECM companion form. Structural shocks are identified via a recursive ordering and the lower-triangular Cholesky factor $P^{(d)}$ of $\Sigma^{(d)}$. The resulting posterior IRFs are defined as:

$$\mathrm{IRF}^{(d)}(h) = f\big(\Gamma^{(d)}, \Pi^{(d)}, P^{(d)}\big), \qquad h = 0, \ldots, H, \tag{7}$$

and summarised by median trajectories and percentile bands (16th–84th) to characterise posterior uncertainty.

This procedure preserves the cointegrated structure of the VECM at each draw and allows impulse responses to reflect joint uncertainty on both short-run dynamics and long-run equilibrium adjustment mechanisms (see Appendix B,C,D,E,F,G).

4.5 Shock Identification

Five structural shocks are identified through a Cholesky decomposition of Σ, with ordering depending on the shock type:

Brown shock: emiss $\rightarrow$ health/demography $\rightarrow$ macro-fiscal,

EPS shocks (total, MB, NMB, technology): EPS $\rightarrow$ emiss $\rightarrow$ health/demography $\rightarrow$ macro-fiscal.

This ordering reflects the hierarchy whereby climate policy affects emissions, which propagate to health-demographic channels and subsequently to macro-fiscal outcomes (Ciccarelli and Marotta 2024) (see Appendix B).

IRFs are obtained from the VECM implied dynamics and reported with Bayesian credible intervals.

5 Main Results

In this section we analyze of both brown shocks and mitigation shocks

5.1 Brown Shock: Carbon Intensity

The structural shock used in the IRFs is a one-standard-deviation impulse to the change in carbon intensity Δci, interpreted as a brown shock, i.e., an unexpected deterioration in the emissions-to-output ratio (see Appendix C).

Innovations in carbon intensity should not be interpreted as pure policy shocks. Rather, we consider them as composite shocks capturing changes in the carbon content of economic activity, driven by a combination of factors including shifts in the energy mix (e.g. fossil versus renewable energy), fluctuations in relative energy prices, and, to a lesser extent, policy interventions.

This interpretation allows us to identify "brown transition shocks", defined as adverse movements toward more carbon-intensive production structures. Such shocks are particularly relevant in the context of climate transition risks, as they capture the macroeconomic and fiscal consequences of delayed or insufficient de-carbonization (Bolton and Kacperczyk 2021; Van der Ploeg and Withagen 2015).

While this approach does not isolate a clean exogenous policy variation, it provides a more realistic representation of the joint dynamics linking energy systems, macroeconomic conditions, and environmental outcomes.

Carbon intensity (per capita) is defined as:

$$\mathrm{ci}_t \equiv \log(\mathrm{emiss}_{pc,t}) - \log(\mathrm{gdp}_{pc,t}),$$

where $\mathrm{emiss}_{pc,t}$ denotes per capita emissions and $\mathrm{gdp}_{pc,t}$ denotes real GDP per capita. The change over time,

$$\Delta \mathrm{ci}_t \approx \%\Delta(\mathrm{emiss}_{pc,t}) - \%\Delta(\mathrm{gdp}_{pc,t}),$$

measures the approximate percentage change in carbon intensity.

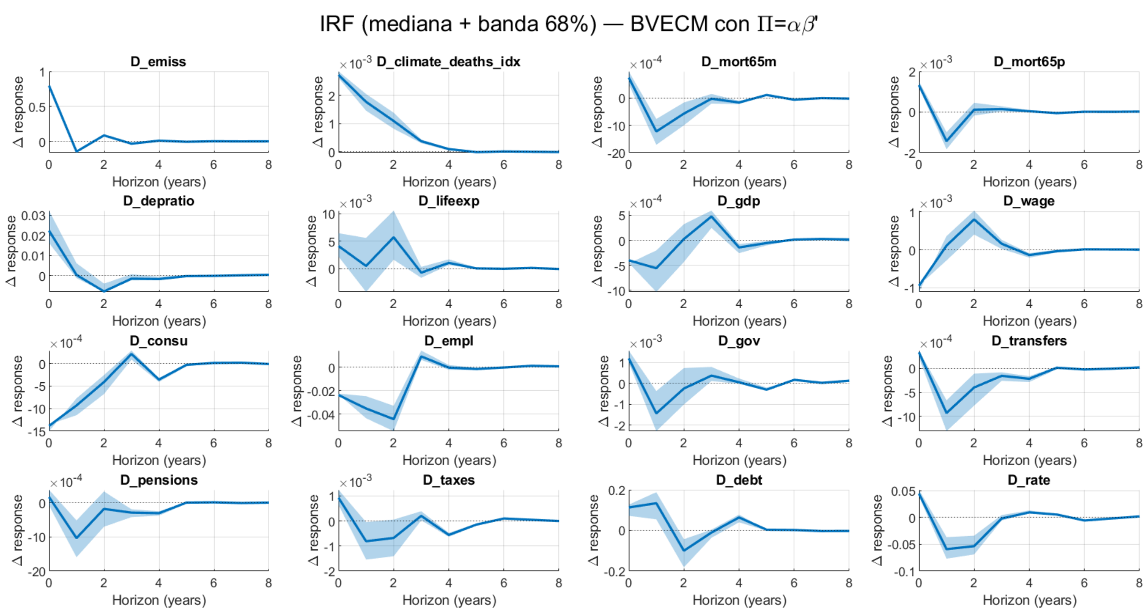

Figure 7: : The figure shows IRFs shock on emission

IRF Interpretation. The positive emissions shock leads to an increase in climate-related mortality, particularly among older cohorts, resulting in a temporary rise in the dependency ratio ($\Delta depratio$). However, as the most vulnerable segment of the elderly population is disproportionately affected, the dependency ratio declines in the medium run, reflecting a contraction in the size of the older-age cohort. Importantly, this adjustment should not be interpreted as an improvement in demographic or fiscal conditions, but rather as the outcome of adverse mortality dynamics.

Consistently, pension expenditures and social transfers increase on impact, as the system responds to heightened health and welfare needs. In subsequent years, these expenditures decline as the number of beneficiaries shrinks. This reflects a demographic adjustment that mechanically reduces the pension burden in the medium term, not due to improved system efficiency, but because of a smaller recipient base.

On the macroeconomic side, the shock has a recessionary effect: GDP and employment fall (Δgdp, $\Delta empl$), while household consumption contracts sharply ($\Delta consu$). Real wages decline during the first two years ($\Delta wage$), consistent with a weakening labour market. The contraction in economic activity results in lower tax revenues ($\Delta taxes$), while public expenditure (Δgov) follows a counter-cyclical pattern.

Public debt increases initially, reflecting higher transfers and social spending. In the medium run, however, the reduction in the number of beneficiaries eases fiscal pressures, allowing debt to gradually decline as economic conditions stabilise. This apparent improvement in fiscal indicators is therefore driven by adverse demographic developments rather than structural fiscal adjustment.

Overall, these findings highlight that climate-related shocks may generate short-run recessionary dynamics and fiscal stress, while producing medium-term adjustments through socially undesirable channels. This underscores the importance of preventive mitigation policies and the role of climate-sensitive automatic stabilisers to protect vulnerable populations and avoid welfare-reducing adjustment mechanisms.

5.2 EPS Total -Shock

The structural shock used in the IRFs is a one standard deviation impulse to the change in environmental policy stringency, Δeps_t, interpreted as a green policy shock, i.e., an unexpected tightening in policy stringency (see Appendix D).

Environmental policy stringency is measured by the total EPS index. In our dataset, EPS enters as a percentage rate:

$$eps_t \equiv \%\Delta(\mathrm{EPS}_t),$$

where EPS_t denotes the Environmental Policy Stringency (total) index at time t.

The change in the rate is

$$\Delta eps_t \equiv eps_t - eps_{t-1},$$

which measures the acceleration (or deceleration) in policy stringency. A unit structural innovation to Δeps_t is therefore interpreted as an unexpected tightening of green policy.

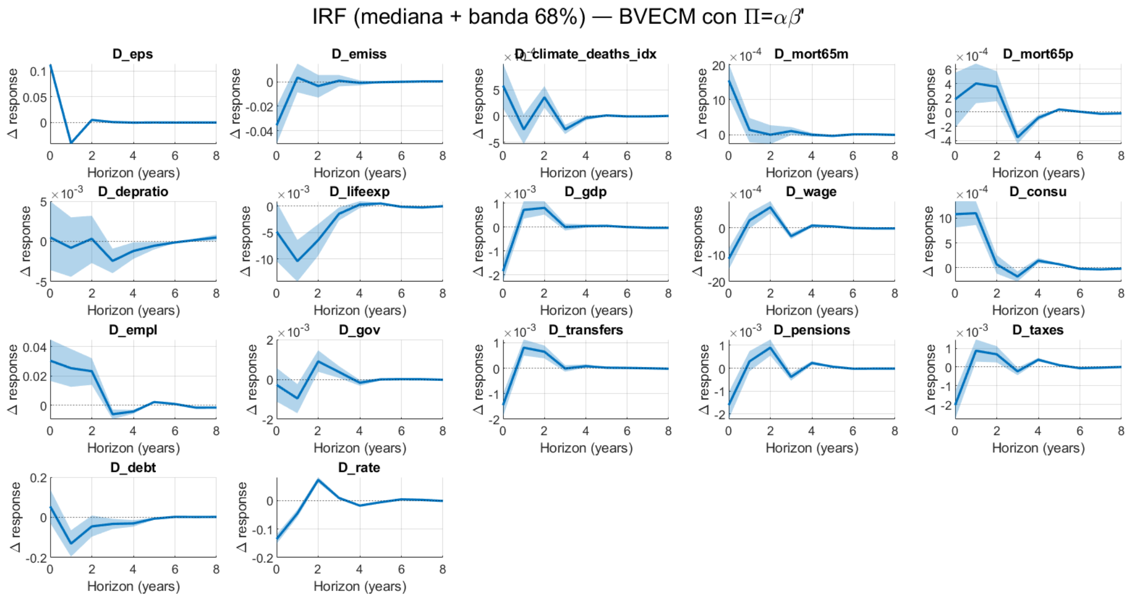

Figure 8: : The figure shows IRFs shock on EPS-Total

IRF Interpretation. Following a positive shock to Δeps_t, interpreted as an unexpected tightening of environmental policy stringency, emissions decline immediately and remain persistently below baseline levels, indicating that regulatory-based mitigation policies are effective in reducing carbon intensity in the short run.

However, the adjustment in health and demographic outcomes is considerably slower. Both mortality and climate-related morbidity ($\Delta climatedeaths$) respond with a lag, consistent with the persistence of mortality dynamics across age cohorts ($\Delta mort65p$, $\Delta mort65m$). As a result, improvements in life expectancy ($\Delta lifexp$) materialize only gradually. This temporal gap highlights a key intergenerational trade-off: while the costs of mitigation policies are borne in the short run, their benefits accrue progressively over time, particularly for future cohorts.

On the macroeconomic side, output and wages decline moderately after the shock (Δgdp, $\Delta wage$), reflecting transitional adjustment costs and sectoral reallocation. At the same time, consumption and employment increase in the short run ($\Delta consu$, $\Delta empl$), suggesting that aggregate demand remains resilient and that labour market adjustment occurs primarily through reallocation rather than net job destruction. These dynamics indicate that regulatory-based mitigation policies may entail limited short-run macroeconomic costs, but still generate distributional frictions across sectors and households. On the macroeconomic side, output and wages decline moderately after the shock (Δgdp, $\Delta wage$), reflecting transitional adjustment costs and sectoral reallocation. At the same time, consumption and employment increase in the short run ($\Delta consu$, $\Delta empl$), suggesting that aggregate demand remains resilient and that labour market adjustment occurs primarily through reallocation rather than net job destruction. These dynamics indicate that regulatory-based mitigation policies may entail limited short-run macroeconomic costs, but still generate distributional frictions across sectors and households.

This evidence is consistent with recent findings showing that green policies tend to be more labor-intensive than conventional forms of expenditure, thereby supporting employment during the transition phase shah2025effective.

The fiscal response exhibits a two-phase pattern. Transfers and pensions initially decline following the policy shock, but subsequently increase over the medium term ($\Delta transfers$, $\Delta pensions$), reflecting the activation of compensatory redistribution mechanisms aimed at smoothing adjustment costs. The relatively modest response of total public expenditure (Δgov) suggests that, in the absence of additional fiscal instruments, the redistributive capacity of the system remains limited.

Overall, these findings have direct implications for the design of climate mitigation strategies and long-term fiscal planning. First, while regulatory policies are effective in reducing emissions, they do not generate fiscal revenues, limiting the scope for automatic compensation. This highlights the importance of complementing regulatory measures with environmental taxation, such as carbon pricing, in order to create fiscal space for redistribution and green investment.

Second, the presence of transitional adjustment costs and sectoral reallocation frictions points to the need for targeted green subsidies and industrial policies to support affected sectors and facilitate labour reallocation. Without such instruments, the burden of adjustment may fall disproportionately on specific groups, undermining the political sustainability of the transition.

Third, the delayed improvement in health and demographic outcomes underscores the intergenerational dimension of climate policy. Mitigation strategies involve short-run costs borne by current cohorts, while benefits materialise over the long run. This calls for a fiscal framework that explicitly incorporates intergenerational equity, for instance through the use of targeted transfers, long-term public investment, and revenue recycling mechanisms (van der Ploeg 2023).

Taken together, these results suggest that effective climate mitigation requires an integrated policy mix in which regulatory instruments, environmental taxation, and fiscal redistribution are jointly designed to ensure macroeconomic stability, social equity, and long-term sustainability.

5.3 EPS Market Based -Shock

The structural shock used in the IRFs is a one standard deviation to the change in market-based environmental policy stringency, Δeps_t^{MB}, interpreted as a *market-based green policy shock*, i.e., an unexpected tightening in market-driven environmental regulation (see Appendix E).

Market-based environmental policy stringency is measured by the Market-Based component of the EPS index. In our dataset, this component enters as a percentage rate:

$$eps_t^{MB} \equiv \%\Delta(EPS_t^{MB}),$$

where EPS_t^{MB} denotes the market-based environmental policy stringency index at time t (e.g., carbon taxes, emissions trading systems, and pricing-based instruments).

The change in the rate is defined as:

$$\Delta eps_t^{MB} \equiv eps_t^{MB} - eps_{t-1}^{MB},$$

which measures the acceleration (or deceleration) in the tightening of market-based environmental regulation. A unit structural innovation to Δeps_t^{MB} is therefore interpreted as an *unexpected* tightening in market-based green policy.

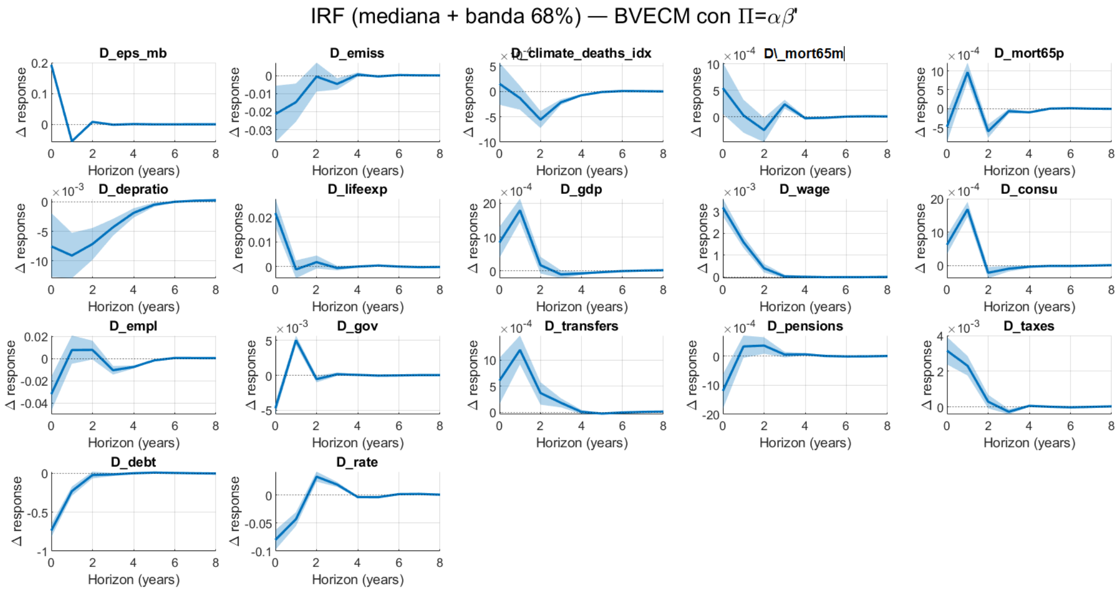

Figure 9: : The figure shows IRFs shock on EPS-Market Based

IRF Interpretation. Following a market-based environmental policy shock, defined as a unit innovation in Δeps_t^{MB}, emissions decline immediately and remain persistently below baseline levels, indicating a sustained reduction in carbon intensity. This confirms the effectiveness of price-based instruments in altering relative prices and inducing long-run behavioural and technological adjustments (Guo et al., 2021).

Demographic and health responses unfold more gradually. Environment-related mortality declines over time, with reductions in $\Delta mort65p$ and $\Delta mort65$, alongside a decrease in $\Delta climate\_deaths\_idx$. The effect is more pronounced for older cohorts, reflecting their greater exposure to environmental risks. These dynamics highlight that the benefits of mitigation policies materialise with a lag, implying an intertemporal trade-off between short-run adjustment costs and long-run welfare gains.

On the macroeconomic side, output, consumption, and wages increase following the shock, while employment declines moderately. This configuration is consistent with an adjustment along the intensive margin: carbon pricing triggers a reallocation of resources toward cleaner and more productive sectors, raising labour productivity and supporting income growth. At the same time, short-run frictions, including skill mismatches and sectoral rigidities, generate temporary employment losses (De Angelis et al. 2019). The positive response of GDP is consistent with existing evidence on the macroeconomic effects of carbon taxation (Metcalf and Stock 2020).

The fiscal response exhibits a clear two-phase pattern. In the short run, carbon pricing generates additional revenues that expand fiscal space, contributing to a reduction in public debt and allowing for a temporary decline in government expenditure. However, this initial consolidation is followed by a gradual increase in public spending, as governments implement compensatory transfers and adaptation measures to address distributional and transitional costs. The increase in $\Delta transfers$, alongside the initial decline in $\Delta pensions$, suggests a shift in the composition of public expenditure toward targeted redistributive mechanisms.

Overall, the results point to a transition path characterized by persistent environmental improvements, productivity-enhancing structural change, and dynamic fiscal adjustment. Crucially, market-based instruments generate a double dividend—environmental and fiscal—creating room for active fiscal design. In particular, the presence of additional fiscal revenues opens the possibility for revenue recycling strategies, such as reducing distortionary taxation, financing green public investment, or supporting vulnerable households through targeted transfers (van der Ploeg 2023) .

From a policy perspective, these findings suggest that carbon pricing should not be interpreted as a stand-alone instrument, but rather as the core component of a broader fiscal framework. Combining environmental taxation with green subsidies and redistributive policies is essential to mitigate short-run adjustment costs, ensure political acceptability, and align the transition with intergenerational equity objectives.

5.4 EPS Non Market Based Shock

The structural shock used in the IRFs is a one standard deviation impulse to the change in non-market-based environmental policy stringency, Δeps_t^{NMB}, interpreted as a *non-market-based green policy shock*, i.e., an unexpected tightening in regulatory environmental standards and emission limits (see Appendix F).

Non-market-based environmental policy stringency is measured by the Non-Market Based (NMB) component of the EPS index. In our dataset, this component enters as a percentage rate:

$$eps_t^{NMB} \equiv \%\Delta(\mathrm{EPS}_t^{NMB}),$$

where EPS_t^{NMB} denotes the regulatory stringency index at time t and captures measures such as emission limit values (ELVs), fuel quality standards, and technology mandates.

Change over time. The change in the rate is defined as:

$$\Delta eps_t^{NMB} \equiv eps_t^{NMB} - eps_{t-1}^{NMB},$$

which measures the acceleration (or deceleration) in the tightening of regulation-based environmental policy. A unit structural innovation to Δeps_t^{NMB} is therefore interpreted as an *unexpected* regulatory tightening in non-market-based green policy.

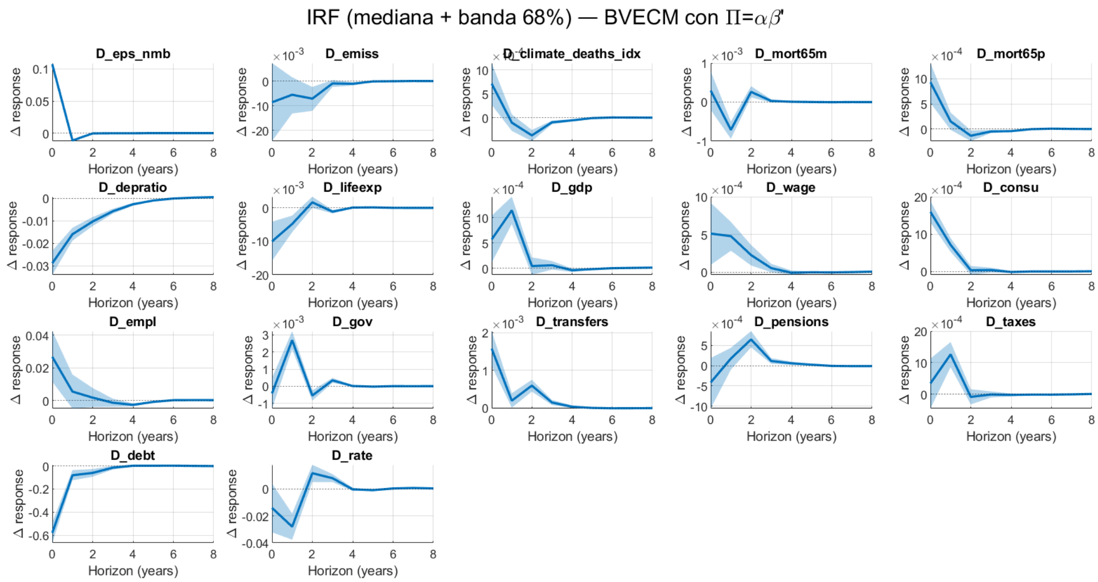

Figure 10: : The figure shows IRFs shock on EPS-Non Market Based

IRF Interpretation (Non-Market Based Policy Shock). Following a positive shock to Δeps_t^{NMB}, interpreted as an unexpected tightening of non-market-based environmental regulation (e.g., emission limits and technology standards), we observe a reduction in emissions. However, the response of $\Delta emiss$ is not statistically significant over the medium horizon. This result is consistent with the nature of NMB policies, which primarily target local pollutants (NOx, SOx, PM) rather than CO_2, and require time for technological adjustment in production processes.

The demographic and health block displays gradual improvements. Climate-related premature mortality ($\Delta climate\_deaths\_idx$) declines over time. The response is stronger for the population under 65 ($\Delta mort65m$), while mortality among the elderly ($\Delta mort65p$) decreases more slowly, reflecting their greater vulnerability. Life expectancy ($\Delta lifeexp$) decreases at impact but returns to its equilibrium level after approximately two years. The dependency ratio ($\Delta depratio$) declines persistently and returns to zero only after about six years, indicating a temporary demographic rebalancing driven by reduced premature mortality.

On the macroeconomic side, the shock generates moderately expansionary short-run effects. Output (Δgdp), wages ($\Delta wage$), consumption ($\Delta consu$), and employment ($\Delta empl$) increase in the first periods,the short-run increase in employment following non-market-based environmental regulation may reflect a substitution away from energy- and capital-intensive inputs toward more labor-intensive production processes, before technological upgrading materializes.This result suggests the presence of short-run adjustment mechanisms that warrant further investigation in future analyses.

The fiscal block exhibits a compensatory adjustment pattern. Government spending (Δgov) increases on impact, reflecting public expenditures for compliance and monitoring. Transfers ($\Delta transfers$) also rise, indicating targeted support measures during the adjustment phase (De Angelis et al. 2019) . Pension spending ($\Delta pensions$) shows no immediate reaction, increases moderately in the second year, and returns to its baseline level by the third year. Tax revenues ($\Delta taxes$) increase temporarily, helping to stabilize the fiscal balance. As a result, the public debt ($\Delta debt$) remains broadly stable over the medium horizon.

5.5 EPS Technological Shock

The structural shock used in this specification is one standard deviation to the change in the technological component of environmental policy stringency, Δeps_t^{Tech}, interpreted as an unexpected tightening in technology-oriented environmental regulation (see Appendix G).

The technological pillar of the EPS index captures policies that promote or mandate the adoption of cleaner production processes, green R&D, and low-emission technologies. In our dataset, this variable is expressed as a percentage rate:

$$eps_t^{Tech} \equiv \%\Delta(\mathrm{EPS}_t^{Tech}),$$

where EPS_t^{Tech} denotes the technological stringency sub-index at time t.

The acceleration (or deceleration) in technological policy stringency is defined as:

$$\Delta eps_t^{Tech} \equiv eps_t^{Tech} - eps_{t-1}^{Tech}.$$

A unit structural shock to Δeps_t^{Tech} is therefore interpreted as an unexpected tightening of regulations that incentivize or require the transition toward cleaner technologies.

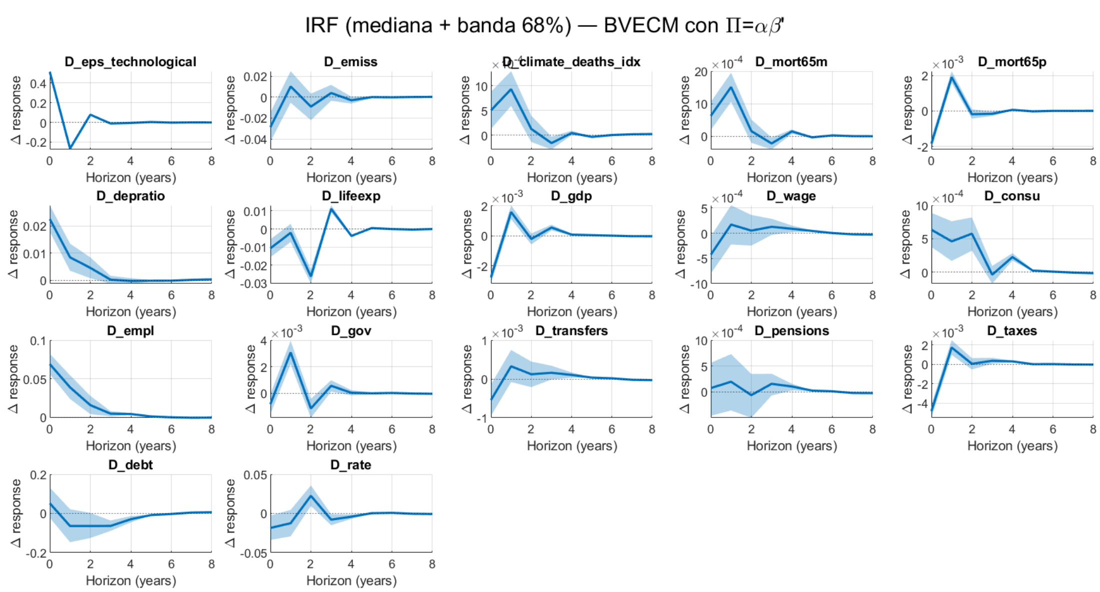

Figure 11: : The figure shows IRFs shock on EPS-Technological

IRF Interpretation (Technological Policy Shock). Following a positive shock to $\Delta eps_{technological}$, interpreted as an unexpected tightening of environmental policies aimed at promoting the adoption of cleaner production technologies, the response of emissions ($\Delta emiss$) is negative on impact, but the effect does not persist and becomes statistically insignificant over the medium horizon. This contrasts with the *market-based* shock, for which the reduction in emissions is more durable and stable over time.

In the demographic and health block, $\Delta climate\_deaths\_idx$ increases on impact and in the short run, indicating short-term transitional environmental stress. Mortality among older age groups

($\Delta mort65p$, $\Delta mort65m$) gradually declines, suggesting health improvements that emerge only over the medium term. Meanwhile, life expectancy ($\Delta lifeexp$) decreases slightly, consistent with the idea that the positive health effects of technological environmental policies require time to materialize. As mortality among older individuals declines, the dependency ratio ($\Delta depratio$) **increases**, reflecting a growing demographic weight of the over-65 population.

On the macroeconomic side, the shock generates initially recessionary effects: Δgdp decreases on impact, a result that is consistent with empirical evidence showing that accelerated technological transition entails short-run adjustment costs (Andersson et al. 2020; Ciccarelli and Marotta 2024). Wages ($\Delta wage$) display no significant response, while consumption ($\Delta consu$) increases and employment ($\Delta empl$) rises during the first two years. This suggests that sectoral reallocation toward technologically advanced industries supports labor demand in the short run, despite the temporary output loss.

The fiscal block reflects dynamics consistent with investment-driven policy interventions. Government spending (Δgov) increases on impact, in line with innovation support programs, while transfers ($\Delta transfers$) decrease as employment rises. Pension expenditures ($\Delta pensions$) and public debt ($\Delta debt$) do not show statistically significant responses, indicating a fiscally neutral effect in the short term.

Overall, the technological policy shock generates: (i) non-persistent reductions in emissions, (ii) limited health benefits concentrated among older cohorts, (iii) a temporary decline in output consistent with technological transition costs documented in the literature, and (iv) an active role for public spending in supporting the transition without creating fiscal (Ahmed 2020; Chakraborty and Chatterjee 2017; Robbins 2016). Non-market and technological policies appear less immediately effective and more dependent on public support, pointing to the need for coordinated policy mixes combining regulation, public investment, and price-based instruments.

6 Conclusion

This paper shows that incorporating demographic and health dimensions into the analysis of climate policy shocks significantly alters macroeconomic transmission mechanisms. The originality of the contribution lies in demonstrating that population structure, mortality, and pollution-related morbidity do not merely adjust passively to environmental shocks, but actively influence the sign, magnitude, and persistence of macroeconomic responses.

Under a brown shock, the deterioration in carbon intensity generates recessionary effects, which become less pro-cyclical once demographic and health channels are considered. In contrast, mitigation shocks yield more favorable outcomes. Market-based instruments produce persistent reductions in emissions and positive macro-fiscal adjustments; technological policies also reduce emissions but with more gradual effects on the demographic-health block; non–market-based regulatory measures primarily affect pollution-related mortality, with more moderate macroeconomic impacts.

These results show that climate policy instruments are not equivalent and differ in their environmental, macroeconomic, and demographic implications. Consistent with recent literature, the findings point to the need for a policy mix (Aziz et al. 2022; Ciccarelli and Marotta 2024). Combining carbon pricing with targeted technological support can help limit short-run adjustment costs while fostering long-run structural transformation. Without adequate price incentives, green technological development may generate heterogeneous outcomes across countries and sectors, with implications for cyclical dynamics. An effective climate strategy therefore requires a coordinated and coherent design of policy instruments.

The demographic responses highlight that climate policies have non-trivial intergenerational implications, affecting dependency ratios, pension systems, and the distribution of welfare across age cohorts. This calls for integrating climate policy into long-term fiscal planning frameworks that explicitly account for intergenerational equity. In this perspective, the intergenerational dimension of climate policy can be further addressed through the recycling of carbon tax revenues. As emphasized by van der Ploeg 2023, using environmental tax revenues to reduce distortionary taxes on labour can mitigate the short-run burden on current generations while preserving long-run environmental benefits, thereby improving both efficiency and intergenerational fairness.

From a fiscal policy perspective, these findings imply that climate mitigation strategies must rely on a combination of environmental taxation and targeted green public spending. Carbon pricing not only provides incentives for emissions reduction, but also generates fiscal revenues that can be used to finance green subsidies and compensate vulnerable households. At the same time, the effectiveness of these instruments depends on their integration within a credible long-term fiscal framework, ensuring debt sustainability while supporting the transition.

Overall, the results suggest that climate policy cannot be designed in isolation. Effective mitigation requires a coherent fiscal framework that integrates environmental taxation, targeted redistribution, and long-term debt sustainability considerations. In this perspective, fiscal policy plays a dual role: it supports the transition in the short run and shapes its distributional and intergenerational consequences over time.

7 Appendix A Data

Table 1: Data sources and variable definitions

Category	Variables / Definition	Source
Macroeconomic and fiscal variables		
Output, public expenditure, revenues, other macro aggregates	Nominal series from national accounts and government finance statistics. All variables are deflated using each country's GDP deflator to ensure temporal comparability and remove the influence of price dynamics from aggregate quantities.	Eurostat
Demographic variables		
Mortality under 65, mortality over 65, life expectancy, dependency ratio	Demographic indicators obtained from the corresponding population and mortality series. They capture age-specific mortality, overall longevity, and the demographic burden of non-working-age cohorts.	Eurostat
Environmental policy and distributional channels		
Environmental Policy Stringency (EPS) indices	Aggregate EPS index and sectoral components (e.g. market-based, non-market, technology-support) used to proxy climate and environmental policy effort across countries and over time.	OECD (Environmental Policy Stringency database)
Social transfers and pensions	Government social transfers (including pensions) and related items from the sector accounts and social protection statistics, used to characterise redistributive channels of fiscal policy.	Eurostat
Wages and labour income	Wage and compensation indicators (e.g. average wages, compensation of employees, labour income measures) used to proxy the labour-market distributional channel.	OECD (earnings / labour compensation statistics)
Climate-related health and emissions		
Climate-related mortality and morbidity indicators	Harmonised cross-country measures of environmental health exposure, including indicators of mortality and morbidity attributable to climate- and environment-related risks.	OECD (environmental health / climate exposure indicators)
Greenhouse gas emissions	Total and disaggregated greenhouse gas emissions, including CO_2, N_2O (in CO_2-equivalent), CH_4 (in CO_2-equivalent), HFCs (in CO_2-equivalent), PFCs (in CO_2-equivalent), SF_6 (in CO_2-equivalent), NF_3 (in CO_2-equivalent).	Eurostat (greenhouse gas emissions)

8 Appendix B. Bayesian panel VECM, identification and impulse responses

8.1 Panel structure and VECM specification

We consider an unbalanced annual panel of N European countries over the period 1995–2019. Let $y_{i,t}$ be the $K \times 1$ vector of endogenous variables for country $i = 1, \dots, N$ in year $t = 1, \dots, T_i$, including environmental, macro–fiscal and demographic–health indicators (see Appendix A for the list of variables).

To control for unobserved heterogeneity, country and time fixed effects are removed through a two–way within transformation before estimation. We remove country and time fixed effects through a two-way within transformation, in order to isolate the common short- and long-run dynamics. The model is then estimated as a pooled VECM on the transformed variables, exploiting exclusively within-country variation over time like Ciccarelli and Marotta 2024 :

$$\Delta y_t = \alpha\beta' y_{t-1} + \sum_{\ell=1}^{p-1} \Gamma_\ell \, \Delta y_{t-\ell} + u_t, \qquad u_t \sim \mathcal{N}(0, \Sigma) \tag{8}$$

where:

- $\Pi = \alpha\beta'$ is the $K \times K$ error-correction matrix;
- β is a $K \times r$ matrix of cointegration vectors ($r = 1$ in the baseline), capturing the long-run equilibrium relation among levels;

- α is the $K \times r$ loading matrix, governing the speed and sign of adjustment to long-run deviations;
- Γ_ℓ are $K \times K$ short-run coefficient matrices on $\Delta y_{t-\ell}$, $\ell = 1, \dots, p-1$;
- Σ is the $K \times K$ covariance matrix of reduced-form innovations.

In the empirical application, the cointegration space is restricted to the structural block

$$\{\text{emissions, real GDP, employment, public expenditure, climate-related mortality}\},$$

and the rank is set to $r = 1$. Emissions enter the cointegration vector as the normalisation variable, so that the corresponding loading coefficient in α is constrained to be negative, ensuring convergence of the environmental block towards the long-run equilibrium.

8.2 Cointegration estimation and construction of Π

The long-run relation is estimated in two steps. First, for each country we extract the levels of the variables included in the cointegrating set and estimate a Johansen-type VECM with rank $r = 1$, obtaining country-specific estimates $\hat{\beta}_i$. These vectors are then aligned across countries and averaged to obtain a pooled panel cointegration vector

$$\beta = \frac{1}{N} \sum_{i=1}^{N} \hat{\beta}_i,$$

after normalisation on the emissions coefficient so that $\beta_{\text{emiss}} = 1$.

Second, an error-correction term is constructed as

$$EC_t = \beta' y_{t-1},$$

standardised to have zero mean and unit variance. The standardised term EC_t enters each differenced equation in (8) as an additional regressor. Let the corresponding coefficient vector be $\tilde{\alpha}$. Since EC_t is standardised prior to estimation, the economically meaningful loading coefficients are obtained by de-standardising:

$$\alpha = \frac{\tilde{\alpha}}{\sigma_{EC}},$$

where σ_{EC} is the (pooled) standard deviation of EC_t before standardisation. The sign of α_{emiss} is aligned such that $\alpha_{\text{emiss}} < 0$ by flipping the sign of EC_t if necessary.

The long-run error-correction matrix is then constructed as

$$\Pi = \alpha \beta', \tag{9}$$

and, for numerical stability, rescaled when its Frobenius norm exceeds a small threshold τ:

$$\Pi \leftarrow \Pi \cdot \min \left\{ 1, \frac{\tau}{\|\Pi\|_F} \right\}.$$

This guarantees that the implied long-run dynamics remain stable and avoids explosive responses in the subsequent impulse-response simulations.

8.3 Bayesian prior structure

For estimation, the VECM is written in its stacked linear regression form. Let ΔY be the $T \times K$ matrix of dependent variables and X the $T \times M$ matrix of regressors,

$$X = \left[\Delta y_{t-1}, \ldots, \Delta y_{t-p+1},\, EC_t\right],$$

so that

$$\Delta Y = XB' + U, \qquad U \sim \mathcal{MN}(0,\ I_T,\ \Sigma), \tag{10}$$

where B is the $K \times M$ coefficient matrix collecting the rows of $\Gamma_1, \ldots, \Gamma_{p-1}$ and $\tilde{\alpha}$.

Following the standard Bayesian VAR literature (Doan et al. 1984; Karlsson 2013; Koop, Korobilis, et al. 2010; Litterman 1986; Sims and Zha 1998), a conjugate Normal–Inverse Wishart prior is imposed on (B, Σ):

$$\operatorname{vec}(B) \mid \Sigma \sim \mathcal{N}\big(\operatorname{vec}(B_0),\ \Sigma \otimes V_0\big), \tag{10}$$

$$\Sigma \sim \mathcal{IW}(S_0, \nu_0), \tag{11}$$

where V_0 has a Minnesota-type structure:

$$V_0 = V_{\text{Minn}}(\lambda_{\text{overall}}, \lambda_{\text{cross}}, \delta, \sigma^2_{\text{const}}, \sigma^2_{\text{exo}}).$$

The Minnesota prior encodes three dimensions of shrinkage:

1. *Overall shrinkage* λ_{overall}, which reduces the variance of all coefficients towards a parsimonious autoregressive structure.

2. *Cross-variable shrinkage* λ_{cross}, which downweights coefficients on lags of other variables relative to own-lags, limiting excessive cross-equation feedback.

3. *Lag decay* parameter δ, which multiplies the prior variance by $1/\ell^{2\delta}$ for the ℓ-th lag, penalising higher-order dynamics at annual frequency.

The hyperparameters (S_0, ν_0) in (11) determine the tightness and scale of the Inverse Wishart prior for Σ, ensuring positive definiteness of the covariance matrix for every posterior draw and controlling the dispersion of the residual variance across variables.

In the empirical implementation, the prior means B_0 are centred on a conservative dynamic specification, while (V_0, S_0, ν_0) are calibrated to deliver weakly informative but stabilising shrinkage, in line with the relatively short time dimension of the panel.

8.4 Posterior distribution and Monte Carlo sampling

Given the conjugate prior structure in (10)–(11), the posterior distribution of (B, Σ) is also Normal–Inverse Wishart:

$$\Sigma \mid \Delta Y, X \sim \mathcal{IW}(S_n, \nu_n), \tag{12}$$

$$\operatorname{vec}(B) \mid \Sigma, \Delta Y, X \sim \mathcal{N}\big(\operatorname{vec}(B_n),\ \Sigma \otimes V_n\big), \tag{13}$$

where (B_n, V_n, S_n, ν_n) are obtained through standard NIW updating formulas:

$$\begin{aligned}
V_n^{-1} &= V_0^{-1} + X'X, \\
B_n &= V_n\big(V_0^{-1}B_0 + X'\Delta Y\big), \\
\nu_n &= \nu_0 + T, \\
S_n &= S_0 + (\Delta Y - XB_n')'(\Delta Y - XB_n') + (B_n - B_0)V_0^{-1}(B_n - B_0)'.
\end{aligned}$$

Inference and impulse-response analysis are based on Monte Carlo integration. We draw $N_{\text{draws}} = 5000$ samples from the joint posterior as follows:

$$\Sigma^{(d)} \sim \mathcal{IW}(S_n, \nu_n), \tag{14}$$

$$\text{vec}(B)^{(d)} \sim \mathcal{N}\big(\text{vec}(B_n),\ \Sigma^{(d)} \otimes V_n\big), \qquad d = 1, \ldots, N_{\text{draws}}. \tag{15}$$

In practice, these draws are implemented using the MATLAB routines `iwishrnd` and `mvnrnd`, exploiting the Kronecker structure of the covariance matrix for $\text{vec}(B)$.

Each draw d yields a set of short-run matrices $\{\Gamma_1^{(d)}, \ldots, \Gamma_{p-1}^{(d)}\}$ and a loading vector $\tilde{\alpha}^{(d)}$ on the standardised error-correction term. The de-standardised loading vector $\alpha^{(d)}$ is obtained as described in Section B.2, and combined with the pooled β to form

$$\Pi^{(d)} = \alpha^{(d)}\beta',$$

which preserves the cointegrated structure at each posterior draw. For numerical robustness, the implied VAR in differences is stabilised by rescaling the companion matrix if its spectral radius exceeds 0.98, and $\Pi^{(d)}$ is shrunk when $\|\Pi^{(d)}\|_F$ is excessively large. These adjustments ensure that all simulated paths remain in the neighbourhood of the estimated stationary dynamics.

8.5 Short-run identification via Cholesky decomposition

Structural shocks are identified by imposing a recursive structure on the reduced-form innovations. For each posterior draw, the covariance matrix $\Sigma^{(d)}$ is decomposed as

$$\Sigma^{(d)} = P^{(d)}\big(P^{(d)}\big)', \tag{16}$$

where $P^{(d)}$ is lower triangular and obtained through a Cholesky factorisation (with minimal jitter added only when necessary to restore positive definiteness).

Let $\varepsilon_t^{(d)}$ denote the $K \times 1$ vector of structural shocks. The relationship between reduced-form innovations and structural shocks is:

$$u_t^{(d)} = P^{(d)}\varepsilon_t^{(d)}, \qquad \varepsilon_t^{(d)} = \big(P^{(d)}\big)^{-1}u_t^{(d)}.$$

The ordering of the variables in y_t is chosen to reflect the climate-policy transmission mechanism. In particular, the recursive ordering places the environmental policy stringency index (EPS) first, followed by emissions and the remaining macro-fiscal and demographic variables:

$$\{\text{EPS},\ \text{Emissions},\ \text{Climate-health},\ \text{Macro–fiscal}\}.$$

This implies that an unexpected tightening in climate policy is contemporaneously exogenous with respect to emissions and the macroeconomy, while feedback from emissions and macro-fiscal variables to the policy shock operates only with a lag, through the dynamic structure of the VECM.

8.6 Companion form and impulse-response computation

To obtain impulse responses, the BVECM is a in (8) written in companion form. Define the $(Kp + K) \times 1$ state vector:

$$s_t = \begin{bmatrix} \Delta y_t \\ \Delta y_{t-1} \\ \vdots \\ \Delta y_{t-p+1} \\ y_{t-1} \end{bmatrix}. \tag{17}$$

For each posterior draw d, the transition and shock-impact matrices $F^{(d)}$ and $G^{(d)}$ are given by

$$s_{t+1} = F^{(d)} s_t + G^{(d)} \varepsilon_{t+1}^{(d)}, \tag{18}$$

where

$$F^{(d)} = \begin{bmatrix} \Gamma_1^{(d)} & \Gamma_2^{(d)} & \cdots & \Gamma_{p-1}^{(d)} & \Pi^{(d)} \\ I_K & 0 & \cdots & 0 & 0 \\ 0 & I_K & \ddots & \vdots & \vdots \\ \vdots & \ddots & \ddots & 0 & 0 \\ \Gamma_1^{(d)} & \Gamma_2^{(d)} & \cdots & \Gamma_{p-1}^{(d)} & I_K + \Pi^{(d)} \end{bmatrix},$$

and

$$G^{(d)} = \begin{bmatrix} P^{(d)} \\ 0 \\ \vdots \\ 0 \\ P^{(d)} \end{bmatrix}.$$

Let e_j be the $K \times 1$ selection vector corresponding to the structural shock of interest (e.g. the EPS shock). The initial impact of a one-standard deviation shock in component j is

$$s_0^{(d)} = G^{(d)} e_j.$$

The impulse responses for horizons $h = 0, \ldots, H$ are then obtained recursively as

$$s_h^{(d)} = \left(F^{(d)}\right)^h s_0^{(d)}, \qquad h = 0, \ldots, H, \tag{19}$$

$$\mathrm{IRF}^{(d)}(h) = \text{first } K \text{ elements of } s_h^{(d)}, \tag{20}$$

which correspond to the responses of Δy_t at each horizon. For interpretation, the impulse responses are reported in terms of changes in the variables (first differences of logs or levels) and can be cumulated when appropriate (e.g. to obtain level responses for log variables).

8.7 Posterior summarisation and uncertainty quantification

The procedure above delivers, for each horizon h and variable k, a collection of posterior draws $\{\mathrm{IRF}_k^{(d)}(h)\}_{d=1}^{N_{\text{draws}}}$. Posterior impulse responses are summarised by:

- the posterior median at each horizon,

$$\widehat{\mathrm{IRF}}_k(h) = \mathrm{median}_d\big\{\mathrm{IRF}_k^{(d)}(h)\big\},$$

- and pointwise credible intervals given by the empirical τ_1 and τ_2 percentiles (typically 16$^{\text{th}}$ and 84$^{\text{th}}$),

$$\big[\mathrm{IRF}_k^{\text{low}}(h),\ \mathrm{IRF}_k^{\text{high}}(h)\big] = \big[q_{\tau_1}\{\mathrm{IRF}_k^{(d)}(h)\}, q_{\tau_2}\{\mathrm{IRF}_k^{(d)}(h)\}\big].$$

To avoid spurious persistence induced by finite-horizon truncation, a simple bias-correction is applied by subtracting the average response over the last few horizons from the entire path, ensuring that impulse responses converge to zero at long horizons.

In summary, this procedure:

1. preserves the cointegrated structure of the VECM at each posterior draw through $\Pi^{(d)} = \alpha^{(d)}\beta'$,

2. identifies structural shocks via a recursive scheme consistent with the climate-policy transmission mechanism,
3. and propagates joint uncertainty on $(\Gamma^{(d)}, \Pi^{(d)}, \Sigma^{(d)})$ into the posterior distribution of the impulse-response functions.

8.8 Cointegration Test

Table 2: Pooled Johansen trace tests between emissions and selected variables (panel)

Variable x	Effective T	Trace stat ($r = 0$)	5% crit. value	p-value	Cointegration (5%)
gdp	523	79.294	15.495	0.001	Yes
empl	498	79.017	15.495	0.001	Yes

Note: The table reports Johansen trace tests for the null of no cointegration ($r = 0$) in a two-variable system including log emissions and the variable x. Country fixed effects are removed by regression on country dummies prior to estimation. "Yes" indicates rejection of the null of no cointegration at the 5% level.

The panel cointegration tests indicate the presence of stable long-run relationships between emissions and all macroeconomic variables considered. GDP and employment exhibit strong pooled Johansen cointegration with emissions, while government expenditure and climate-related mortality show significant residual-based Engle–Granger cointegration. Overall, the results imply that emissions, economic activity, public spending and climate-related health outcomes move together in the long run, supporting the use of error-correction specifications in the empirical analysis.

Table 3: Panel Engle–Granger residual-based cointegration between emissions and selected variables (1995–2019)

Variable	**ADF stat (residuals)**	**p-value**	**Cointegration (5%)**
Climate-deaths index	−9.211	0.001	Yes
Employment	−8.796	0.001	Yes
GDP	−9.126	0.001	Yes
Government expenditure	−8.965	0.001	Yes
	All variables exhibit panel cointegration with emissions.		

The panel Engle–Granger tests provide strong evidence of cointegration between emissions and all selected variables. The highly negative ADF statistics and very small p-values indicate that the pooled residuals are stationary, confirming the presence of a shared long-run equilibrium relationship across EU countries. This result is fully consistent with estimating a panel VECM.

8.9 Test Granger

The panel Granger tests reveal three key patterns. First, GDP and climate-related mortality display a bidirectional relationship: climate-mortality shocks predict subsequent movements in economic activity, while GDP dynamics also anticipate changes in the climate-mortality index. This points to a feedback mechanism linking environmental conditions and macroeconomic performance.

Table 4: Panel Granger causality tests (pooled VAR with country fixed effects, 2 lags)

Dependent y	Predictor x	F-stat	p-value	Granger causality (1% level)
climate_deaths_idx → see rows				
gdp	*climate_deaths_idx*	11.59	0.000	Yes ($x \to y$)
climate_deaths_idx	*gdp*	35.90	0.000	Yes ($x \to y$)
climate_deaths_idx	*emiss*	36.76	0.000	Yes ($x \to y$)
emiss	*climate_deaths_idx*	0.38	0.683	No ($x \to y$)
gdp	*emiss*	10.77	0.000	Yes ($x \to y$)
emiss	*gdp*	0.54	0.583	No ($x \to y$)

Note: Each row tests whether the predictor x Granger-causes the dependent variable y in a pooled VAR with country fixed effects and two lags. "Yes" indicates rejection of the null of no Granger causality at the 1% level.

Second, the relationship between emissions and climate-related mortality is unidirectional. Emissions significantly predict the climate-mortality index, whereas climate-mortality shocks do not explain future emission dynamics. This suggests that climatic and health impacts do not trigger immediate or systematic emission adjustments in the short run.

Third, the link between emissions and GDP is also asymmetric. Emissions anticipate GDP movements, but GDP does not predict future emissions, a result consistent with the ongoing decoupling between economic growth and carbon intensity in many European countries.

Overall, the evidence points to (i) a climate–economy feedback loop and (ii) predominantly one-way relationships involving emissions, in line with the structural transition and decarbonization processes underway in the European region.

9 Appendix C-Model Diagnostics: Brown Shock (Panel-VECM)

The estimated panel-VECM is dynamically stable. The spectral radius of the companion matrix of the differenced system is:

$$\rho(\mathcal{C}_{\Delta y}) = 0.7511 < 1,$$

implying mean reversion. The implied half-life of shocks is approximately:

$$\text{half-life} = \frac{\ln(0.5)}{\ln(0.7511)} \approx 2.4 \text{ periods.}$$

The long-run matrix $\Pi = \alpha\beta'$ exhibits a relatively high initial norm ($\|\Pi\| = 0.567$) and is therefore rescaled to 0.25 to improve numerical conditioning. This renormalization does not affect the direction of adjustment or the shape of the impulse responses.

The adjustment matrix displays moderate speed:

$$\|\alpha\| = 0.2024,$$

and the emission equation shows a negative loading coefficient:

$$\alpha_{\text{emiss}} = -0.042162 \quad \text{(unscaled)},$$

indicating correction toward the long-run equilibrium: when emissions exceed their equilibrium value, subsequent changes in emissions are negative.

The cointegration vector is well identified, as indicated by $\|\beta\| = 2.519$.

The panel-VECM is estimated under a Bayesian prior structure calibrated as follows:

$$\lambda_{\text{overall}} = 1.8, \quad \lambda_{\text{cross}} = 1.0, \quad \text{decay} = 0.5, \quad \sigma^2_{\text{exo}} = 6, \quad \sigma^2_{\text{const}} = 20,$$

$$\nu_0 = 10, \quad S_0 = 0.25.$$

The estimated adjustment coefficients $\hat{\alpha}$ are predominantly negative, with two notable loadings of larger magnitude:

$$\alpha_{\text{emiss}} \approx -0.1503, \qquad \alpha_{\text{health}} \approx -0.1261,$$

while the remaining coefficients are small in absolute value (between -0.04 and $+0.01$), indicating a **selective and economically interpretable adjustment**. Sectors linked to emissions and health display the primary correction mechanism toward the long-run equilibrium.

The cointegration vector $\hat{\beta}$ components are:

Table 5: Interpretation of the estimated cointegration vector $\hat{\beta}$

Component	Sign	Interpretation
6.0155 (emiss)	+	Normalisation variable. The long-run equilibrium is anchored on emissions; the magnitude is not interpreted, only its role as reference for identifying the cointegration space.
32.5691 (gdp)	+	Co-movement with emissions in the long run. When the equilibrium emissions path rises, real GDP moves in the same direction; this is not an elasticity but a directional relation along the equilibrium trajectory.
−0.6089 (empl)	−	Compensatory component. Employment tends to adjust in the opposite direction when the system deviates from the emissions–economy equilibrium, indicating a corrective dynamic.
−11.2374 (gov)	−	Public expenditure behaves as a corrective force: it moves contrary to emissions in the long run, consistent with policy responses to disequilibria in the system.
4.7324 (cdi)	+	Climate-related mortality co-moves with emissions, indicating a structural long-run alignment between environmental pressure and climate-related health risks.

Note: Coefficients are identified up to a scaling constant. Absolute magnitudes are not interpreted as elasticities; information is conveyed by the sign and the relative relation of variables within the equilibrium structure defined by $\hat{\beta}$.

The error correction term (ECM) is statistically significant. In the emission equation, the ECM t-statistic is large and negative:

$$t(\text{ECM}_{\text{emiss}}) = -10.14,$$

confirming **active and strong mean reversion**: when emissions deviate above their long-run equilibrium, subsequent adjustments reduce emissions.

Other ECM loadings are smaller in magnitude (approximately between -1.8 and 0.9), consistent with **heterogeneous adjustment speeds across variables**, but all signs remain economically coherent.

Appendix D. Model Diagnostics for the EPS Policy Shock

The BVECM estimated for the EPS policy shock exhibits stable short-run dynamics. The spectral radius of the companion matrix of the differenced system is:

$$\rho(\mathcal{C}_{\Delta y}) = 0.7159 < 1,$$

indicating dynamic stability and mean reversion of the system.

The long-run matrix is constructed as $\Pi = \alpha\beta'$. The posterior estimate of the adjustment vector α (OLS-based) has moderate magnitude:

$$\|\alpha_{\text{OLS}}\| = 0.1858,$$

while the cointegration vector β estimated at the panel level satisfies:

$$\|\beta\| = 2.519.$$

The implied long-run matrix Π has norm $\|\Pi\| = 0.519$, which exceeds the stability threshold; therefore, following standard practice in Bayesian VECM estimation, Π is rescaled to:

$$\Pi \leftarrow \Pi \cdot \frac{0.25}{\|\Pi\|},$$

ensuring numerical conditioning without altering long-run direction.

The adjustment coefficient associated with emissions is negative:

$$\alpha_{\text{emiss}} = -0.053683 \quad \text{(unscaled)},$$

indicating that when emissions lie above their long-run equilibrium, subsequent changes in emissions adjust downward. This confirms a **stable and economically interpretable error-correction mechanism** consistent with policy-driven reductions in carbon intensity.

Overall, the EPS shock model satisfies the standard requirements of (i) dynamic stability, (ii) identifiable long-run equilibrium, and (iii) economically coherent adjustment dynamics.

The estimated error-correction term in the BVECM for the EPS policy shock yields an adjustment vector $\hat{\alpha}$ with generally small coefficients across most equations, and more pronounced loadings for variables directly linked to environmental and fiscal dynamics. In particular, the key coefficients are:

$$\alpha_{\text{emiss}} = -0.0484, \qquad \alpha_{\text{pensions}} = -0.1243, \qquad \alpha_{\text{rate}} = -0.1012,$$

while the remaining coefficients are close to zero. The negative value of α_{emiss} indicates that when emissions deviate above their long-run equilibrium level, subsequent adjustments are directed downwards, confirming a stable and economically meaningful error-correction mechanism.

The significance of the long-run adjustment is confirmed by the associated ECM t-statistics. In the emissions equation:

$$t(\text{ECM}_{\text{emiss}}) = -10.14,$$

indicating a strong and statistically robust reversion toward the long-run equilibrium. The remaining t-statistics fall in the range between approximately -1.8 and $+1.5$, reflecting heterogeneous but moderate adjustment dynamics across equations.

Overall, the results indicate: (i) a stable and economically coherent long-run equilibrium, (ii) a well-identified cointegrating relationship, and (iii) a rapid and significant adjustment in emissions, while demographic and pension-related adjustments unfold more gradually over time.

We adopt moderately tight Minnesota-style priors to improve numerical conditioning and to curb high-frequency oscillations in the IRFs. The overall shrinkage is set to $\lambda_{\text{overall}} = 0.8$, which pulls autoregressive coefficients toward zero without eliminating meaningful persistence. Cross-equation spillovers are further compressed with $\lambda_{\text{cross}} = 0.5$, limiting feedback loops across variables that typically generate zig–zag dynamics in small samples. Higher-order lags are penalised more heavily via a steeper decay, decay $= 1.5$, which downweights remote lags and promotes smoother responses.

Priors on non-dynamic regressors are also informative: $\text{var}_{\text{exo}} = 3$ for exogenous terms and $\text{var}_{\text{const}} = 8$ for the intercept, preventing the constant and exogenous controls from absorbing short-run variation and thereby stabilising the ECM channel. For the innovation covariance, we use a conjugate inverse–Wishart prior with $\nu_0 = 20$ degrees of freedom and scale factor S_0 set via S0_scale = 0.15. This combination yields a moderately concentrated prior on Σ_u, producing tighter posterior bands and reducing overshooting in the IRFs, while preserving the sign and timing of economically relevant effects.

Overall, this prior configuration strikes a balance between smoothness and flexibility: it discourages implausible high-frequency dynamics, stabilises long-run adjustment through the ECM, and leaves room for heterogeneous short-run responses across macro, fiscal, and demographic blocks. Results are qualitatively robust to reasonable relaxations of these hyperparameters.

9.1 Model Diagnostics for the Market-Based EPS Shock (BVECM)

The BVECM estimated on the market-based EPS shock exhibits stable short-run dynamics. The spectral radius of the companion matrix of the differenced system is:

$$\rho(\mathcal{C}_{\Delta y}) = 0.5566 < 1,$$

indicating dynamic stability and mean reversion. The implied half-life of a shock is approximately:

$$\text{half-life} = \frac{\ln(0.5)}{\ln(0.5566)} \approx 1.18 \text{ periods.}$$

The long-run matrix is constructed as $\Pi = \alpha\beta'$. The adjustment vector has moderate magnitude,

$$\|\alpha_{\text{OLS}}\| = 0.308,$$

and the panel cointegration vector satisfies:

$$\|\beta\| = 2.519.$$

The implied long-run matrix has Frobenius norm $\|\Pi\| = 0.862$, which is above the stability threshold; therefore, in line with standard BVECM practice, we rescale:

$$\Pi \leftarrow \Pi \cdot \frac{0.25}{\|\Pi\|} \quad \Rightarrow \quad \|\Pi\| = 0.25,$$

to improve numerical conditioning without altering the long-run direction.

The emissions equation displays a negative loading:

$$\alpha_{\text{emiss}} = -0.018030 \quad \text{(unscaled)},$$

indicating that positive deviations of emissions from their long-run equilibrium induce subsequent downward adjustments. This confirms a **stable and economically meaningful error-correction mechanism** consistent with policy-driven reductions in carbon intensity.

Overall, the market-based EPS specification satisfies (i) dynamic stability, (ii) an identifiable long-run equilibrium, and (iii) coherent adjustment dynamics.

Prior specification. Minnesota-style shrinkage with tighter cross-equation and higher-lag penalisation:

$$\lambda_{\text{overall}} = 0.6, \quad \lambda_{\text{cross}} = 0.3, \quad \text{decay} = 2.0, \quad \text{var}_{\text{exo}} = 2, \quad \text{var}_{\text{const}} = 5, \quad \nu_0 = 25, \quad \text{S0\_scale} = 0.10.$$

Adjustment (error-correction) coefficients. The estimated adjustment vector $\hat{\alpha}$ (aligned with the ordering above) is:

$$\hat{\alpha} = \begin{pmatrix} \underbrace{-0.0219}_{\Delta emiss} \\ 0.0162 \\ 0.0023 \\ 0.0012 \\ 0.0009 \\ 0.0019 \\ \underbrace{-0.0123}_{\Delta transfers} \\ -0.00036 \\ -0.00138 \\ -0.00129 \\ \underbrace{-0.0230}_{\Delta rate} \\ 0.00068 \\ -0.00298 \\ -0.00422 \\ 0.00029 \\ \underbrace{-0.2862}_{\Delta mort65p} \\ 0.1072 \end{pmatrix}.$$

Key loadings are economically interpretable: $\alpha_{\Delta emiss} < 0$ implies downward correction in emissions when the long-run error is positive; $\alpha_{\Delta rate} < 0$ indicates that rate dynamics also help restore equilibrium; the sizeable negative $\alpha_{\Delta mort65p}$ signals a strong mean-reverting adjustment in mortality among the over-65 cohort. Other coefficients are small in magnitude, consistent with a selective correction mechanism.

supporting a stable long-run relation linking environmental, macroeconomic, and demographic blocks.

Reported t-statistics for the ECM term lie broadly in the interval $\left[-1.81,\ 1.55\right]$ across equations in this specification, indicating heterogeneous—but mostly moderate—adjustment speeds, with the most pronounced adjustment in the over-65 mortality equation (consistent with the large negative $\alpha_{\Delta mort65p}$).[1]

Taken together, these estimates indicate (i) a stable and economically coherent error-correction mechanism with clear adjustment in emissions and interest rates, (ii) a strong mean-reverting component in $\Delta mort65p$ consistent with gradual health improvements following market-based policy tightening, and (iii) broadly modest adjustment elsewhere, in line with the tighter prior and the reallocation-driven transmission of market-based shocks.

9.2 Model Diagnostics: Non– Market Based EPS Shock

The BVECM for the NMB shock is estimated following the same specification as in the main text. The short-run dynamics of the system in differences are stable: after stabilization, the spectral radius of the Δy companion matrix is

$$\rho(\mathcal{C}_{\Delta y}) = 0.5579 \ < \ 1,$$

indicating non-explosive trajectories and mean-reverting behavior.

[1] Vector of reported ECM t values available upon request; see main text for inference standards and stability diagnostics.

The long-run matrix is constructed as $\Pi = \alpha\beta'$. The Frobenius norm of the unnormalized Π is relatively large,

$$\|\Pi\| = 1.57,$$

so, following standard practice in panel BVECM estimation, we rescale the matrix to improve numerical conditioning without altering the long-run equilibrium direction:

$$\Pi \leftarrow \Pi \cdot \frac{0.25}{\|\Pi\|} \quad \Rightarrow \quad \|\Pi\| = 0.25.$$

The estimated adjustment magnitude is moderate,

$$\|\alpha_{\text{OLS}}\| = 0.5627, \qquad \|\beta\| = 2.519,$$

while the adjustment coefficient associated with the emissions equation is negative and economically meaningful:

$$\alpha_{\text{emiss}} = -0.067911 \text{ (unscaled)}.$$

This implies that positive deviations of emissions from the long-run equilibrium induce a downward correction in their short-run dynamics, confirming the presence of an operative error-correction mechanism.

Summary. The diagnostic results indicate that: (i) the differenced system is dynamically stable; (ii) the cointegration structure is well identified and supported by a negative adjustment in emissions; (iii) the rescaling of Π ensures well-behaved IRFs without modifying the economic interpretation of long-run relationships.

Prior specification (same as Market-Based). We adopt the same Minnesota-style priors as in the market-based specification:

Adjustment vector $\hat{\alpha}$. Aligned with the IRF ordering, the estimated adjustment (error-correction) coefficients are:

$$\hat{\alpha} = \begin{pmatrix} 0.00314 \\ -0.06129 \\ -0.00051 \\ -0.00056 \\ 0.00118 \\ 0.02647 \\ 0.00612 \\ -0.00183 \\ -0.00077 \\ 0.00091 \\ 0.04592 \\ 0.00686 \\ 0.00061 \\ -0.00149 \\ -0.00199 \\ 0.55150 \\ -0.07643 \end{pmatrix}.$$

Note. The loading in the emissions equation is small and positive, $\alpha_{\text{emiss}} \approx 0.00314$, indicating a near-zero speed of correction in $\Delta emiss$ under the current ECM scaling; magnitudes for several fiscal/demographic equations are larger (e.g. α on $\Delta mort65p$).

ECM t–statistics. Reported t–statistics for the ECM term (contemporaneous) include:

$$t_{ECM} = \begin{pmatrix} 0.1373 \\ 0.8677 \\ -1.5282 \\ -1.8110 \\ -0.9314 \\ -0.0540 \\ 0.4621 \\ 0.6945 \\ 0.4304 \\ -0.3320 \\ -0.5210 \\ 1.0309 \\ \vdots \end{pmatrix}$$

with analogous values for the lagged ECM:

$$t_{ECM,-1} = \begin{pmatrix} -0.1373 \\ 0.8677 \\ -1.5282 \\ -1.8110 \\ -0.9314 \\ -0.0540 \\ 0.4621 \\ 0.6945 \\ 0.4304 \\ -0.3320 \\ -0.5210 \\ 1.0309 \\ 1.5547 \end{pmatrix}.$$

Interpretation (brief). The near-zero α_{emiss} suggests limited short-run error-correction in emissions under NMB shocks, while non-trivial loadings in demographic/fiscal blocks point to a stronger adjustment operating through those channels. The cointegration vector indicates a stable long-run relation consistent with the regulatory (command-and-control) transmission mechanism.

9.3 Model Diagnostics: EPS Technological Shock

The BVECM is estimated following the same specification described in Section 3. The estimated companion matrix for the VAR in differences is stable. After stabilization, the spectral radius of the Δy companion matrix is equal to 0.5591, indicating that the dynamic system lies well within the unit circle and that the model does not display explosive trajectories.

The long-run adjustment matrix $\Pi = \alpha\beta'$ is constructed by combining the estimated speed-of-adjustment coefficients (α) and the average panel cointegrating vector (β). The Frobenius norm of the unconstrained Π matrix is relatively large ($\|\Pi\| = 1.05$), which is typical in systems where cointegration is driven by slow-moving structural processes. Following the standard practice in panel cointegrated BVARs, Π is rescaled to ensure numerical stability:

$$\Pi \leftarrow \Pi \cdot \frac{0.25}{\|\Pi\|}.$$

A warning is issued in the estimation code to document this normalization step.

The estimated speed of adjustment coefficient on emissions is negative and economically meaningful ($\alpha_{\text{emiss}} = -0.1128$, unscaled), indicating that deviations of emissions from their long-run equilibrium correction path are gradually reversed over time. The magnitude of $\|\alpha_{OLS}\| = 0.3609$ and $\|\beta\| = 2.675$ is consistent with a cointegrating relation where emissions adjust more strongly than output-related variables to restore equilibrium.

Overall, the diagnostic results confirm that: (i) the dynamic system is stable, (ii) the long-run adjustment mechanism is active, and (iii) the normalization applied to Π ensures well-behaved impulse responses without altering the economic interpretation of the cointegration structure.

The shock is estimated using the same prior hyperparameters adopted in the *market-based* specification:

$$\lambda_{\text{overall}} = 0.6, \quad \lambda_{\text{cross}} = 0.3, \quad \text{decay} = 2.0, \quad \text{var}_{exo} = 2, \quad \text{var}_{const} = 5, \quad \nu_0 = 25, \quad \text{S0\_scale} = 0.10.$$

Adjustment vector $\hat{\alpha}$.

$$\hat{\alpha} = \begin{pmatrix} -0.0408 \\ 0.1040 \\ 0.00049 \\ 0.00135 \\ -0.00255 \\ -0.00897 \\ -0.00895 \\ -0.00149 \\ 0.00041 \\ -0.00029 \\ -0.01782 \\ -0.00878 \\ -0.00067 \\ 0.00053 \\ -0.00308 \\ -0.33251 \\ 0.08133 \end{pmatrix}$$

The adjustment coefficient associated with the emissions equation is negative:

$$\alpha_{\text{emiss}} = -0.0408,$$

indicating a gradual correction mechanism that drives emissions back toward their long-run equilibrium when they deviate from it.

ECM t-statistics.

$$t_{ECM} = \begin{pmatrix} 0.9076 \\ -0.1475 \\ -1.1024 \\ 2.4347 \\ -0.0223 \\ -0.1081 \\ 0.0604 \\ -1.2807 \\ -0.9405 \\ -0.6214 \\ 0.7287 \\ 0.5701 \\ \vdots \end{pmatrix}$$

with similar dynamics for the lagged ECM term:

$$t_{ECM,-1} = \begin{pmatrix} -0.9076 \\ -0.1475 \\ -1.1024 \\ 2.4347 \\ -0.0223 \\ -0.1081 \\ 0.0604 \\ -1.2807 \\ -0.9405 \\ -0.6214 \\ 0.7287 \\ 0.5701 \\ -0.4785 \end{pmatrix}$$

Interpretation. The negative value of α_{emiss} confirms a downward adjustment of emissions when they deviate from the long-run equilibrium relationship. The large negative adjustment coefficient in the equation for $\Delta mort65p$ ($\alpha = -0.3325$) suggests that demographic dynamics in the elderly population play an important role in the long-run re-equilibration mechanism. The estimated cointegrating relationship reflects a stable link between environmental, demographic, and production dynamics, consistent with the transmission of the technological policy shock through the structural channel of cleaner technology adoption.

References

Abdul-Nabi, S. S., Al Karaki, V., Khalil, A., & El Zahran, T. (2025). Climate change and its environmental and health effects from 2015 to 2022: A scoping review. *Heliyon*, *11*(3).

Ahmed, K. (2020). Environmental policy stringency, related technological change and emissions inventory in 20 oecd countries. *Journal of environmental Management*, *274*, 111209.

Andersson, M., Baccianti, C., & Morgan, J. (2020). *Climate change and the macro economy.* ECB Occasional Paper.

Aziz, N., Hossain, B., & Lamb, L. (2022). Does green policy pay dividends? *Environmental Economics and Policy Studies*, *24*(2), 147–172.

Bekun, F. V., Adedoyin, F. F., Etokakpan, M. U., & Gyamfi, B. A. (2022). Exploring the tourism-co2 emissions-real income nexus in e7 countries: Accounting for the role of institutional quality. *Journal of Policy Research in Tourism, Leisure and Events*, *14*(1), 1–19.

Bhattacharya, M., Paramati, S. R., Ozturk, I., & Bhattacharya, S. (2016). The effect of renewable energy consumption on economic growth: Evidence from top 38 countries. *Applied energy*, *162*, 733–741.

Bolton, P., & Kacperczyk, M. (2021). Do investors care about carbon risk? *Journal of financial economics*, *142*(2), 517–549.

Boserup, M. (1965). Agrarian structure and take-off. In *The economics of take-off into sustained growth* (pp. 201–224). Springer.

Botta, E., & Koźluk, T. (2014). Measuring environmental policy stringency in oecd countries: A composite index approach.

Caglar, A. E., Guloglu, B., & Gedikli, A. (2022). Moving towards sustainable environmental development for brics: Investigating the asymmetric effect of natural resources on co2. *Sustainable Development*, *30*(5), 1313–1325.

Chakraborty, P., & Chatterjee, C. (2017). Does environmental regulation indirectly induce upstream innovation? new evidence from india. *Research Policy*, *46*(5), 939–955.

Ciccarelli, M., & Marotta, F. (2024). Demand or supply? an empirical exploration of the effects of climate change on the macroeconomy. *Energy Economics*, *129*, 107163.

Cohen, G., Jalles, J. T., Loungani, P., & Marto, R. (2018). The long-run decoupling of emissions and output: Evidence from the largest emitters. *Energy Policy*, *118*, 58–68.

Coole, D. (2013). Too many bodies? the return and disavowal of the population question. *Environmental Politics*, *22*(2), 195–215.

Crist, E., Ripple, W. J., Ehrlich, P. R., Rees, W. E., & Wolf, C. (2022). Scientists' warning on population. *Science of the Total Environment*, *845*, 157166.

De Angelis, E. M., Di Giacomo, M., & Vannoni, D. (2019). Climate change and economic growth: The role of environmental policy stringency. *Sustainability*, *11*(8), 2273.

Doan, T., Litterman, R., & Sims, C. (1984). Forecasting and conditional projection using realistic prior distributions. *Econometric reviews*, *3*(1), 1–100.

Dorling, D. (2020). *Slowdown: The end of the great acceleration—and why it's good for the planet, the economy, and our lives.* Yale University Press.

Ehrlich, P. R., & Ehrlich, A. H. (2009). The population bomb revisited. *The electronic journal of sustainable development*, *1*(3), 63–71.

Ehrlich, P. R., & Ehrlich, A. H. (2013). Can a collapse of global civilization be avoided? *Proceedings of the Royal Society B: Biological Sciences*, *280*(1754), 20122845.

Elgin, C., & Tumen, S. (2012). Can sustained economic growth and declining population coexist? *Economic Modelling*, *29*(5), 1899–1908.

Engle, R. F., & Granger, C. W. (1987). Co-integration and error correction: Representation, estimation, and testing. *Econometrica: journal of the Econometric Society*, 251–276.

Espoir, D. K., Sunge, R., & Bannor, F. (2021). Economic growth and co emissions: Evidence from heterogeneous panel of african countries using bootstrap granger causality.

Friedl, B., & Getzner, M. (2003). Determinants of co2 emissions in a small open economy. *Ecological economics*, *45*(1), 133–148.

Halkos, G., & Psarianos, I. (2016). Exploring the effect of including the environment in the neoclassical growth model. *Environmental economics and policy studies*, *18*(3), 339–358.

Henderson, J. V., Jang, B. Y., Storeygard, A., & Weil, D. N. (2024). *Climate change, population growth, and population pressure* (tech. rep.). National Bureau of Economic Research.

Jacobson, M. Z. (2008). On the causal link between carbon dioxide and air pollution mortality. *Geophysical Research Letters*, *35*(3).

Jia, L., Chang, T., & Wang, M.-C. (2023). Revisit economic growth and co2 emission nexus in g7 countries: Mixed frequency var model. *Environmental Science and Pollution Research*, *30*(3), 5540–5579.

Johansen, S. (1991). Estimation and hypothesis testing of cointegration vectors in gaussian vector autoregressive models. *Econometrica: journal of the Econometric Society*, 1551–1580.

Jones, C. I. (2022). The end of economic growth? unintended consequences of a declining population. *American Economic Review*, *112*(11), 3489–3527.

Kadiyala, K. R., & Karlsson, S. (1997). Numerical methods for estimation and inference in bayesian var-models. *Journal of Applied Econometrics*, *12*(2), 99–132.

Karlsson, S. (2013). Forecasting with bayesian vector autoregression. *Handbook of economic forecasting*, *2*, 791–897.

Koop, G., Korobilis, D., et al. (2010). Bayesian multivariate time series methods for empirical macroeconomics. *Foundations and Trends® in Econometrics*, *3*(4), 267–358.

Kruse, T., Dechezleprêtre, A., Saffar, R., & Robert, L. (2022). Measuring environmental policy stringency in oecd countries: An update of the oecd composite eps indicator. *OECD Economic Department Working Papers*, (1703), 0_1–56.

Kuznets, S. (1967). Population and economic growth. *Proceedings of the American philosophical Society*, *111*(3), 170–193.

Le Quéré, C., Andrew, R. M., Friedlingstein, P., Sitch, S., Hauck, J., Pongratz, J., Pickers, P. A., Korsbakken, J. I., Peters, G. P., Canadell, J. G., et al. (2018). Global carbon budget 2018.

Litterman, R. B. (1986). Forecasting with bayesian vector autoregressions—five years of experience. *Journal of Business & Economic Statistics*, *4*(1), 25–38.

Lu, C., Tong, Q., & Liu, X. (2010). The impacts of carbon tax and complementary policies on chinese economy. *Energy policy*, *38*(11), 7278–7285.

Lupi, V., & Marsiglio, S. (2021). Population growth and climate change: A dynamic integrated climate-economy-demography model. *Ecological Economics*, *184*, 107011.

Maestas, N., Mullen, K. J., & Powell, D. (2023). The effect of population aging on economic growth, the labor force, and productivity. *American Economic Journal: Macroeconomics*, *15*(2), 306–332.

Maji, I. K. (2015). Does clean energy contribute to economic growth? evidence from nigeria. *Energy Reports*, *1*, 145–150.

Metcalf, G. E., & Stock, J. H. (2020). Measuring the macroeconomic impact of carbon taxes. *AEA papers and Proceedings*, *110*, 101–106.

Nordhaus, W. (2018). Projections and uncertainties about climate change in an era of minimal climate policies. *American economic journal: economic policy*, *10*(3), 333–360.

Porter, M. (1996). America's green strategy. *Business and the environment: a reader*, *33*, 1072.

Porter, M. E., & Linde, C. v. d. (1995). Toward a new conception of the environment-competitiveness relationship. *Journal of economic perspectives*, *9*(4), 97–118.

Rasoulinezhad, E., Taghizadeh-Hesary, F., & Taghizadeh-Hesary, F. (2020). How is mortality affected by fossil fuel consumption, co2 emissions and economic factors in cis region? *Energies*, *13*(9), 2255.

Ricci, F. (2007). Channels of transmission of environmental policy to economic growth: A survey of the theory. *Ecological Economics*, *60*(4), 688–699.

Ripple, W. J., Wolf, C., Newsome, T. M., Barnard, P., & Moomaw, W. R. (2020). World scientists' warning of a climate emergency. *BioScience*, *70*(1), 8–100.

Robbins, A. (2016). How to understand the results of the climate change summit: Conference of parties21 (cop21) paris 2015. *Journal of public health policy*, *37*(2), 129–132.

Roca, J., Padilla, E., Farré, M., & Galletto, V. (2001). Economic growth and atmospheric pollution in spain: Discussing the environmental kuznets curve hypothesis. *Ecological Economics*, *39*(1), 85–99.

Rubashkina, Y., Galeotti, M., & Verdolini, E. (2015). Environmental regulation and competitiveness: Empirical evidence on the porter hypothesis from european manufacturing sectors. *Energy policy*, *83*, 288–300.

Simon, J. L. (2019). *The economics of population growth*. Princeton university press.

Sims, C. A., & Zha, T. (1998). Bayesian methods for dynamic multivariate models. *International Economic Review*, 949–968.

Skare, M., Streimikiene, D., & Skare, D. (2021). Measuring carbon emission sensitivity to economic shocks: A panel structural vector autoregression 1870–2016. *Environmental Science and Pollution Research*, *28*(32), 44505–44521.

Soytas, U., & Sari, R. (2009). Energy consumption, economic growth, and carbon emissions: Challenges faced by an eu candidate member. *Ecological economics*, *68*(6), 1667–1675.

Strulik, H. (2024). Long-run economic growth despite population decline. *Journal of Economic Dynamics and Control*, *168*, 104943.

Thakoor, M. V. V., & Kara, E. (2022). *Macroeconomic effects of climate change in an aging world*. International Monetary Fund.

Van der Ploeg, F., & Withagen, C. (2015). Global warming and the green paradox: A review of adverse effects of climate policies. *Review of Environmental Economics and Policy*.

van der Ploeg, F. (2023). Fiscal costs of climate policies: Role of tax, political, and behavioural distortions. *De Economist*, *171*(2), 119–137.

Conclusions

This thesis is situated within the macroeconomic literature examining the interactions between climate change, mitigation policies, and macroeconomic dynamics, building on a growing body of work that studies the effects of physical climate shocks and environmental policies using VAR and panel approaches . Relative to these contributions, the three essays adopt an empirical perspective that places particular emphasis on the role of the measures used to capture climate stress, the macro-fiscal context, and demographic and health channels in shaping the transmission of climate-related shocks.

The first contribution relates to the literature that uses temperature-based indicators as proxies for physical climate shocks, by considering wet-bulb temperature (WBT) as an alternative and complementary measure to the widely used 2-meter air temperature. Since WBT combines temperature and humidity, it allows for a closer representation of heat stress in terms of physiological constraints on labour supply and human well-being, which have been extensively discussed in the climatological and health literature. The results show that using this measure is associated with persistent and seasonally asymmetric macroeconomic responses, suggesting that the choice of the climate indicator may affect both the identification and the interpretation of the macroeconomic effects of physical climate shocks, particularly in regions characterized by high humidity and thermal stress.

The second contribution connects to the literature on fiscal multipliers and fiscal policy under debt constraints, extending it to the context of the green transition. Existing empirical evidence on green fiscal multipliers remains relatively limited and often does not explicitly account for the interaction between expenditure composition and fiscal conditions. The analysis shows that the multipliers associated with green public spending tend to differ from those of aggregate expenditure and that these differences are sensitive to fiscal space and debt regimes. In this sense, the results contribute to the ongoing discussion on the macroeconomic sustainability of green investments, indicating that the effectiveness of climate-related fiscal policy depends importantly on the macro-fiscal environment in which it is implemented.

The third contribution relates to the literature analyzing the health and demographic consequences of pollution and climate change, by explicitly integrating these dimensions into a dynamic macroeconomic framework. While many studies treat mortality, morbidity, and population structure as parallel or secondary outcomes of environmental shocks, the empirical evidence shows that these factors interact with macroeconomic dynamics and influence both the magnitude and persistence of policy effects. In particular, carbon-intensive ("brown") shocks are associated with a joint deterioration of health, demographic, and macroeconomic indicators, whereas mitigation shocks are compatible with more favourable long-run adjustments. The analysis also indicates that different climate policy instruments operate through distinct transmission channels, leading to heterogeneous effects on the real economy and on the demographic-health block.

Overall, the three essays suggest that the macroeconomic analysis of climate change can benefit from an approach that jointly considers the choice of climate stress indicators, the fiscal context, and socio-demographic channels, in line with recent developments in the literature. The empirical evidence indicates that these elements can have non-negligible implications for estimated dynamics and their interpretation, providing useful insights for empirical analysis and for the assessment of climate policies over the medium and long run.